Untersuchungen zur Rolle von Histon-ähnlichen Proteinen bei der Genregulation im Uropathogenen *Escherichia coli* Isolat 536

Studies on the Role of Histone-like Proteins in Gene Regulation in Uropathogenic *Escherichia coli* Isolate 536

Dissertation

zur Erlangung des naturwissenschaftlichen Doktorgrades

der Bayerischen Julius-Maximilians-Universität

Würzburg

vorgelegt von

Claudia Maria Müller

aus Sonthofen

Würzburg, Dezember 2005

Eingereicht am:

Mitglieder der Promotionskomission:

Vorsitzender:	.....
1. Gutachter:	Professor Dr. Dr. h.c. mult. J Hacker
2. Gutachter:	Professor B. E. Uhlin
3. Gutachter:	Dr. U. Dobrindt

Tag des Promotionskolloquiums:

Doktorurkunde ausgehändigt am:

Erklärung

Gemäß § 4 Abs. 3 Ziff. 3, 5 und 8 der Promotionsordnung der Fakultät für Biologie der Bayerischen Julius-Maximilians-Universität Würzburg.

Ich versichere hiermit, dass ich die vorliegende Arbeit selbständig und nur unter Verwendung der angegebenen Quellen und Hilfsmittel verfasst habe.

Weiterhin versichere ich, dass die Dissertation bisher nicht in gleicher oder ähnlicher Form in einem anderen Prüfungsverfahren vorgelegen hat und ich bisher keine akademischen Grade erworben oder zu erweben versucht habe.

Würzburg, im Dezember 2005

(Claudia Müller)

DANKSAGUNG

Die vorliegende Arbeit wurde im Zeitraum von Januar 2003 bis Oktober 2005 am Institut für Molekulare Infektionsbiologie der Universität Würzburg, sowie am Lehrstuhl für Molekularbiologie der Universität Umeå, Schweden, durchgeführt.

Für die Unterstützung dabei möchte ich mich bei folgenden Personen bedanken:

- An erster Stelle bei Herrn Prof. Jörg Hacker für die Bereitstellung des Themas und des Arbeitsplatzes, sowie für die stete Unterstützung und Förderung meiner Arbeit.
- Bei Prof. Bernt Eric Uhlin für seine Diskussionsbereitschaft, die fruchtbaren Aufenthalte in seinem Labor, die Bereitstellung von Stämmen, Plasmiden und Seren, sowie die Übernahme des Zweitgutachtens (Tack så mycket för allting)
- Bei Prof. Levente Emődy an der Pècs Medical School für die Nutzung der dort etablierten Tierversuchs-Modelle, sowie bei seinen Mitarbeitern, Gábor Nagy und György Schneider, die ich als nette Kollegen in Würzburg erleben durfte, für die Durchführung der Tierversuche bzw. der Hilfestellung bezüglich „Kapsel“-Fragen.
- Bei Prof. Otto Holst vom Leibnitz Zentrum für Medizin und Biowissenschaften in Borstel für die Lipopolysaccharid-Analyse.
- Bei Dr. Uli Dobrindt für seine kompetente Anleitung und Betreuung dieser Arbeit.
- Bei meinen Box-Nachbarn Stefan, Karin, Mella, und Caroline, sowie den übrigen „Colis“ und anderen Institutsmitarbeitern für ihre Unterstützung in allen wissenschaftlichen und nicht-wissenschaftlichen Problemen und die gute Atmosphäre.
- To all current and former members of the BEU lab in Umeå, especially to Monica, Stina, Annika, Anna, Jurate and Carlos, for their hospitality and for making me feel like home even in dark winter days in northern Sweden.
- To all members of the International Graduate College for the extra amount of fun.

Schließlich möchte ich mich nochmals ausdrücklich bei meinem „Soziale-Kompetenz“-Team (ihr wisst schon) bedanken für alle Kaffe- und Mittagspausen, Kinobesuche, Film- und Spieleabende..... Ohne euch wäre es nur halb so schön gewesen! Danke Suse!

Für ihre langjährige Freundschaft bei Susanne, Geli, Annette und Adelheid.

Und meiner Familie für ihre bedingungslose Unterstützung in allen Lebenslagen.

TABLE OF CONTENT

1. Summary 13

1. Zusammenfassung 15

2. Introduction 17

2.1. Regulation of gene expression 17

2.2. Histone-like proteins 19

2.2.1. Histone-like proteins of Escherichia coli 19

2.2.2. Gene regulation by histone-like proteins 21

2.2.3. Histone-like nucleoid structuring protein (H-NS) 24

2.2.4. The H-NS paralog StpA 31

2.2.5. Interactions between H-NS and StpA 32

2.2.6. Other H-NS-like proteins 32

2.3. Uropathogenic Escherichia coli 36

2.4. Pathogenicity islands 38

2.5. Aims of this study 39

3. Material 40

3.1. Strains 40

3.2. Plasmids 40

3.3. Oligonucleotides 41

3.4. Chemicals and enzymes 43

3.5. Antibodies 44

3.6. Media, Agar-plates and antibiotics 45

3.6.1. Media 45

3.6.2. Agar plates 46

3.6.3. Antibiotics 48

3.7. DNA and Protein Markers 48

3.8. Technical Equipment 49

4. Methods 50

4.1. Manipulation of DNA 50
4.1.1. Small scale isolation of plasmids 50
4.1.2. Isolation of chromosomal DNA 50
4.1.3. Precipitation of DNA with alcohol 51
4.1.4. Determination of nucleic acid concentrations 51
4.1.5. Polymerase chain reaction (PCR) 51
4.1.6. Enzymatic digest of DNA with restriction endonucleases 53
4.1.7. Horizontal Gel Electrophoresis 53
4.1.8. Isolation of DNA fragments from agarose gels 54
4.1.9. Ligation of DNA fragments 54
4.1.10. Transformation of bacterial cells 54
4.1.11. Gene inactivation by λ Red recombinase-mediated mutagenesis using linear DNA fragments 55
4.1.12. Southern Blot analysis 57
4.1.13. Sequence analysis 58

4.2. Manipulation of RNA 59
4.2.1. Isolation of total RNA with hot phenol 59
4.2.2. Removal of contaminating DNA by DNase treatment and RNA cleanup 60
4.2.3. Enrichment of bacterial mRNA 60
4.2.4. Reverse transcription (RT) for cDNA synthesis 61
4.2.5. Semi-quantitative reverse-transcription PCR (RT-PCR) 62
4.2.6. Northern hybridization 63
4.2.7. Identification of the *hlp* transcription start site by primer extension 64

4.3. Expression profiling using DNA arrays 65
4.3.1. Membrane Layout 65
4.3.2. RNA isolation and cDNA labeling 65
4.3.3. Hybridization an detection 67
4.3.4. Intensity reading 67
4.3.5. Data analysis 68

4.4. Working with Protein 69
4.4.1. Denaturing polyacrylamide gel electrophoresis (PAGE) 69
4.4.2. Visualization of proteins in acrylamide gels by Coomassie staining 70
4.4.3. Immunoblotting 71
4.4.4. Purification of His-tagged protein 72
4.4.5. Determination of protein concentrations 73
4.4.6. Chemical crosslinking 73
4.4.7. Electrophoretic mobility shift assay (EMSA) 73
4.4.8. *in vivo* protein stability assay 74

4.5. Analysis of lipopolysaccharides (LPS) 74
4.5.1 Isolation of LPS 74
4.5.2 Electrophoresis and staining with silver nitrate 75

4.6. Phenotypic assays 76
4.6.1. Measurement of ß-galactosidase activity 76
4.6.2. Detection of secreted α-hemolysin 77
4.6.3. Detection of siderophores in culture supernatants 77

4.6.4. Detection of autoaggregation 78
4.6.5. Detection of biofilm forming abilities 78
4.6.6. Survival at high osmolarity 79
4.6.7. Serum resistance 79
4.6.8. *In vivo* virulence assay 79

4.7. In silico analysis 80

5. Results 81

5.1. Impact of H-NS and StpA on expression pattern of UPEC strain 536 81
5.1.1. Construction of *hns* and *stpA* mutants 81
5.1.2. Expression profiling using DNA macroarrays 82
5.1.3. Effect of H-NS on expression of virulence-associated genes 87

5.2. Characterization of the novel H-NS-homolog Hlp 89
5.2.1. Identification of a novel H-NS-like protein in UPEC strain 536 89
5.2.2. Screening for the presence of the hlp *gene in other* E. coli *isolates* 91
5.2.3. Chromosomal location of the gene encoding for Hlp 91
5.2.4. Analysis of hlp transcription 93
5.2.5. Overexpression and purification of HLP 96
5.2.6. Analysis of Hlp stability 99
5.2.7. Hlp has in vivo *activity* 101

5.3. Role of the H-NS paralogs 104
5.3.1. Construction of *hlp* mutants 104
5.3.2. Role of H-NS and its paralogs on expression of virulence-associated genes 105
5.3.3 Effect of H-NS on in vivo *virulence* 121
5.3.4. Role of H-NS and its paralogs at different temperatures 122
5.3.5. Summary – phenotypic characterization 124

6. Discussion 125

6.1. H-NS and virulence 125

6.2. Identification of H-NS and H-NS/StpA dependent regulons 131

6.3. Characteristics of the novel H-NS-like protein Hlp 132
6.3.1. The hlp *gene* 132
6.3.2. The Hlp protein 133
6.3.3. Hlp activity 134

6.4. Biological function of the H-NS paralogs 136
6.4.1. Fine-tuning of fimbrial gene expression 136
6.4.2. Alteration in surface structure and extracellular substances 137
6.4.3. Effect on growth rates 138

6.5. Temperature-dependent expression of histone-like proteins 139

6.6. Implications and Outlook 141

7. References *144*

8. Appendix *155*

8.1. Legends to figures and tables: **155**

8.2. Nucleotide and amino-acid sequence of histone-like proteins in UPEC strain 536 ..... **157**

8.3. Expression profile of hns and hns/stpA mutants **158**

8.4. Expression ratios of major virulence-associated genes **163**

8.5. Supplementary material (tables and figures) **166**

8.6. Curriculum vitae **174**

8.7. Publikationen **175**

8.8. Abbreviations **176**

1. Summary

In this study, the role of histone-like proteins in gene regulation in uropathogenic *Escherichia coli* isolate 536 was monitored. The histone-like nucleoid structuring protein H-NS is a global regulator in *Escherichia coli* that has been intensively studied in non-pathogenic strains. No comprehensive study on the role of H-NS and its homolog StpA on gene expression in a pathogenic *E. coli* strain has been carried out so far. Moreover, we identified a third, so far uncharacterized member of the H-NS-like protein family in uropathogenic *E. coli* isolate 536, which was designated Hlp (H-NS-like protein).

Hlp is a 134-amino acid protein, which shares 58 % sequence identity with H-NS. The gene coding for the Hlp protein, *hlp*, was found in several uropathogenic *E. coli* variants, but not in non-pathogenic *E. coli* K-12. In UPEC strains 536 and CFT073, Hlp is encoded on a possibly horizontally acquired 23-kb genomic region inserted into the *serU* locus. Studies on *hlp* transcription revealed that the gene is transcribed monocistronically from a single promoter and that expression is repressed by H-NS. Purified Hlp protein was binding to its own and to the *hns* promoter, thereby mediating negative auto- and crossregulation. Furthermore, Hlp and H-NS were directly interacting, resulting in the formation of stable heteromers. Complementation studies with *hns* mutant strains in a K-12 background revealed that the Hlp protein had *in vivo* activity, being able to complement the lack of H-NS in terms of motility, growth, and repression of the *proU*, *bgl*, and *clyA* genes.

When analyzing the role of the histone-like proteins in expression of virulence-associated genes by using DNA arrays and classical phenotypic assays, most of the observed effects were mediated by the H-NS protein alone. Expression profiling revealed that transcript level of more than 500 genes was affected by an *hns* mutation, resulting in increased expression of α-hemolysin, fimbriae and iron-uptake systems, as well as genes involved in stress adaptation. Furthermore, several other putative virulence factors were found to be part of the H-NS regulon. On the other hand, no effect of StpA alone was observed. An *hns stpA* double mutant, however, exhibited a distinct gene expression pattern that differed in great parts from that of the *hns* single mutant. This suggests a direct interaction between the two homologs and the existence of distinct regulons of H-NS and an H-NS/StpA heteromeric complex.

Although the H-NS protein has – either as homomer or in complex with StpA – a marked impact on gene expression in pathogenic *E. coli* strains, its effect on urovirulence is ambiguous. At a high infection dose, *hns* mutants accelerated lethality in murine UTI and sepsis models relative to the wild type, probably due to increased production of α-hemolysin. At lower infectious dose, however, mutants lacking H-NS were attenuated through their impaired growth rate, which can only partially be compensated by the higher expression of numerous virulence factors.

As seen with StpA, an *hlp* single mutant did not exhibit a notable phenotype under standard growth conditions. A severe growth defect of *hns hlp* double mutants at low temperatures, however, suggests a biological relevance of H-NS/Hlp heteromers under certain circumstances. Furthermore, these mutants expressed more capsular polysaccharide and curli fimbriae, thereby indicating a distinct role of H-NS and Hlp in regulation of these surface structures. The H-NS paralogs Hlp and StpA also modulated H-NS-mediated regulation of fimbrial adhesins, and are oppositely required for normal growth at low or high temperatures, respectively.

Finally, expression levels of the three histone-like proteins H-NS, StpA and Hlp itself varied with different temperatures, thereby suggesting a flexible composition of the nucleoid-associated protein pool. Hence, we propose a similar biological role of Hlp and StpA, which does not rely on a distinct function of the single protein, but rather on their interaction with the global regulator H-NS.

1. Zusammenfassung

In dieser Studie wurde die Rolle von Histon-ähnlichen Proteinen bei der Genregulation im uropathogenen *Escherichia coli* (UPEC) Isolat 536 untersucht. Das Histon-ähnliche Protein H-NS (*engl.* histone-like nucleoid structuring protein) ist ein globaler Regulator in *E. coli*, der in apathogenen Stämmen eingehend untersucht worden ist. Im Gegensatz dazu liegen noch keine umfassenden Studien zur Rolle von H-NS und des homologen Proteins StpA in einem pathogenen *E. coli* Stamm vor. Zudem konnten wir ein drittes, bis jetzt noch nicht charakterisiertes Mitglied der Familie von H-NS-ähnlichen Protein im uropathogenen *E. coli* Isolat 536 identifizieren, das Hlp benannt wurde (für H-NS-like protein).

Hlp ist ein aus 134 Aminosäuren bestehendes Protein, dessen Sequenz zu 58 % identisch mit der des H-NS Proteins ist. Das Gen, das für das Hlp Protein kodiert, *hlp*, konnte in zahlreichen uropathogenen und Fäkalisolaten nachgewiesen werden, jedoch nicht im apathogenen *E. coli* K-12. In den UPEC Isolaten 536 und CFT073 ist das *hlp* Gen auf einer 23-kb großen genomischen Insel lokalisiert, die in den *serU* Lokus inseriert ist und möglicherweise über horizontalen Gentransfer erworben wurde. Untersuchungen zur Transkription des *hlp* Gens ergaben, dass das Gen monocistronisch von einem einzigen Promotor transkribiert, und dessen Expression durch H-NS reprimiert wird. Rekombinantes Hlp Protein war befähigt, sowohl an seinen eigenen, als auch an den *hns* Promotor zu binden, was zu negativer Auto- und Kreuzregulation führte. Zudem konnte gezeigt werden, dass Hlp und H-NS direkt miteinander interagieren, was zu stabilen Heteromeren führte. Komplementierungsstudien in *hns* Mutanten einiger K-12 Stämme ergaben, dass das Hlp Protein über *in vivo* Aktivität verfügt, was es befähigte, die Abwesenheit von H-NS bei zahlreichen Phänotypen wie z.B. Motilität, Wachstum, und Repression der *proU*, *bgl* und *clyA* Gene zu komplementieren.

Die Rolle der Histon-ähnlichen Proteine bei der Expression von Virulenz-assoziierten Genen wurde mittels DNA Array Technologie, sowie klassischen phänotypischen Tests analysiert. Dabei wurden die meisten der beobachteten Effekte einzig durch das H-NS Protein bedingt. Die Expressionsstudien ergaben, dass über 500 Gene von einer *hns* Mutation beeinflusst wurden, was eine verstärkte Expression des α-Hämolysins, mehrerer Fimbrien und Eisenaufnahmesysteme sowie von Genen, die in Stress-Antworten involviert sind, bedingte.

Des Weiteren konnten zahlreiche putative Virulenzfaktoren dem H-NS-Regulon zugeordnet werden. Andererseits konnten keine Effekt durch StpA beobachtet werden. Eine *hns stpA* Doppelmutante wies jedoch ein eindeutiges Expressionsmuster auf, das in großen Teilen von dem der *hns* Einzelmutante abwich. Dies legt nahe, dass beide Proteine direkt miteinander interagieren, was das Auftreten von unterschiedlichen Regulons zur Folge hat, die entweder durch H-NS oder einem heteromeren H-NS/StpA Komplex beeinflusst werden.

Obwohl das H-NS Protein – entweder als Homomer oder als Komplex mit StpA – einen sehr starken Einfluss auf die Genexpression pathogener *E. coli* Stämme nimmt, bleiben dessen Effekte auf die tatsächliche Virulenz im Urogenitaltrakt unklar. In einem experimentellen Mausmodell der aufsteigenden Harnwegsinfektion bewirken *hns* Mutanten, in hoher Dosis verabreicht, eine rasch eintretende Lethalität, was vermutlich der verstärkten Produktion von α-Hämolysin zuzuschreiben ist. In verringerter Dosis verabreicht, sind diese Mutanten durch ihre langsameren Wachstumsraten jedoch attenuiert, was nur teilweise durch die vestärkte Expression zahlreicher Virulenzfaktoren kompensiert werden kann.

Wie schon bei StpA beobachtet, besitzt eine *hlp* Mutante keinen offensichtlichen Phänotyp, zumindest unter Standard-Wachstumsbedingungen. Jedoch macht sich in *hns hlp* Doppelmutanten ein starker Wachstumsdefekt bei erniedrigten Temperaturen bemerkbar, was eine biologische Relevanz von H-NS/Hlp Heteromeren unter bestimmten Bedingungen nahe legt. Des Weiteren exprimierten diese Mutanten erhöhte Mengen an Kapsel-Polysacchariden und Curli-Adhesin, was als Indiz für eine besondere Rolle für H-NS und Hlp bei der Regulation dieser Oberflächenstrukturen dienen kann. Zudem hatten beide H-NS-Paraloge Hlp und StpA einen modulierenden Effekt bei der H-NS-vermittelten Regulation weiterer Fimbrien-Adhesine und waren in gegenläufigen Maßen für normales Wachstum bei erhöhten bzw. erniedrigten Temperaturen notwendig.

Zuletzt variierte das Expressionsniveau der drei Histon-ähnlichen Proteine H-NS, StpA und Hlp bei unterschiedlichen Temperaturen, was auf eine flexible Zusammensetzung verfügbarer Nucleoid-assoziierter Proteine hindeutet. Dies alles impliziert, dass Hlp eine ähnliche biologische Relevanz wie StpA aufweist, die nicht auf gesonderten Funktionen des einzelnen Proteins beruht, sondern vielmehr auf deren Interaktionen mit dem globalen Regulatorprotein H-NS.

2. Introduction

2.1. Regulation of gene expression

Like all organisms, bacteria are facing the problem of high energetic costs for biosynthesis of every single protein. In order to minimize these costs, only those proteins that are required under a certain condition are produced. Therefore, bacteria possess highly developed sensory systems to detect environmental conditions and cellular response systems in order to adapt their protein synthesis pattern to the stimulus. This is of special importance for pathogenic bacteria, which have to express additional traits, the so-called virulence factors, during colonization of their host. Since these virulence factors impose high energetic costs upon the cell, virulence-associated genes are only expressed when bacteria are in contact with their host and not in the environmental reservoir [for reviews see Gross (1993) or Finlay and Falkow (1997)]. Thus, studies on regulation of virulence-associated genes are an important prerequisite for understanding infection processes, and might also provide targets for new anti-infective treatments by inhibiting expression of virulence factors in the host.

The amount of a given protein can be regulated at various steps, such as transcription, translation, or stability of both mRNA and the protein itself. Transcriptional regulation is the most economic mechanism for the cell, since it automatically prevents all later stages, and it is also the most rapid way of adaptation to a new stimulus. Furthermore, it allows simultaneous regulation of several genes at a time, reflected in the operon concept (Dorman, 1994). In this context, one has to distinguish between regulation of transcription initiation and of transcription elongation/termination. Here, we will focus on regulation of transcription initiation.

Transcription begins with binding of RNA polymerase holoenzyme (R = ßß'$\alpha_2\sigma$) to the -35 promoter site (P), which is recognized by a specific σ-factor. This results in the formation of the initial closed complex RP_{c1} and, after further interactions of the RNA polymerase with extended regions of the promoter, of closed complex RP_{c2}. Reversible opening of 10- to 15-bp of the DNA helix driven by binding of free energy then results in open complexes RP_{o1} and RP_{o2}. Thus, the initial ribonucleotide can bind at the opened +1 site, then called ternary initiated complex, followed by promoter clearance and dissociation of the σ-factor after synthesis of the first 7 to 12 bases of messenger-RNA.

The ternary transcribing complex consisting of the core RNA-polymerase then continues with elongation of transcription (Record *et al.*, 1996).

Several factors influence this process: First, the sequence at the initiation site determines the promoter strength, i.e. initiation velocity, via σ-factor recruitment. Each σ-factor recognizes a specific consensus sequence. For instance, a typical σ^{70}-site is TTGACA at -35 and TATAAT at –10, with a 17-bp spacer region inbetween. Therefore, the strength of a promoter correlates with its homology to this consensus sequence (Record *et al.*, 1996).

Second, more than one σ-factor exist, each with their own consensus sequence. These alternative σ-factors compete for the RNA polymerase, and are themselves regulated by environmental signals. For instance, mRNA of the heat-shock sigma factor, σ^{32}, exhibits enhanced stability at elevated temperatures, thereby outcompeting the standard sigma factor σ^{70} under heat-shock conditions and thus resulting in transcription of the heat-shock genes (Straus *et al.*, 1987).

Moreover, transcription is affected by DNA supercoiling. Supercoiling can occur in circular DNA, when the free ends of the strands are rotated with respect to each other before covalently closing the circle. Depending on the direction of rotation, either new helical turns will be introduced, which is referred to as overwound DNA (or positive supercoiling), or existing turns are removed, which is then called underwound DNA (or negative supercoiling). This also introduces torsional strain into the DNA molecule, resulting in changes in the number of base pairs per helix turn (Travers and Muskhelishvili, 2005). In nature, most DNA is negatively supercoiled.

Supercoiled molecules possess free energy, which can facilitate open complex formation at the promoter. Furthermore, it might help to realign the –35 and –10 sites of the promoter when the spacer length is suboptimal. Supercoiling can also indirectly affect transcription by stabilizing DNA looping or bending. Changes in superhelicity can both have positive and negative effects on transcription [for reviews see Dai and Rothman-Denes (1999) or Perez-Martin *et al*. (1994)]. In *Shigella flexneri*, stress induced changes in supercoiling have been reported to affect transcription of some virulence-associated genes such as porins or type 1 fimbriae (Dorman *et al.*, 1990).

Finally, there are additional transcription factors that either induce or repress transcription initiation. The concept of inducers/repressors is known since more than 40 years, when it was first described for the *lac* operon by Jacob and Monod (1961), and will not be discussed further. However, there are other activating proteins, which do not bind to an operator sequence, but instead interact with the RNA polymerase, e.g. via the σ-factor or via the carboxyterminal domain of its α-subunit (α-CTD), thereby enhancing transcription. Prominent examples are the cyclic AMP receptor protein CRP, the osmoregulator OmpR of the EnvZ/OmpR two-component system, or the oxidative stress regulator OxyR (Ishihama, 1993).

These are just a few examples for the variety of transcriptional regulation mechanisms, and most of them do not work separately, but rather in highly complex regulatory networks. In this study, however, the focus was set on a more global regulation of gene expression mediated by histone-like proteins, which will be presented in the next section.

2.2. Histone-like proteins

2.2.1. Histone-like proteins of Escherichia coli

Histones in eukaryotic cells are positively-charged proteins, thus being able to bind negatively charged DNA and resulting in the formation of nucleosomes. This way, the degree of negative supercoiling of DNA is increased, mediating compactation of the chromosomes by a factor of up to 10,000 during mitosis (Lewin, 2002).

Prokaryotic cells are facing the same problem: the linear chromosome of the bacterium *Escherichia coli* has a length of 1.6 mm, which has to fit into a cell of 2 x 1 µm in size (Dame, 2005). In contrast to the eukaryotic chromosome, half of the DNA supercoils are protein free, i.e. unconstrained, and formed by the action of the DNA topoisomerases (Hardy and Cozzarelli, 2005). The other half of supercoils is found in unstable complexes with proteins that have similarities to eukaryotic histones. However, this similarity is not based on amino acid identities, but rather on protein function. Bacterial histone-like proteins are characterized by their DNA-binding activity, by a relatively low molecular mass, and by their usually high abundance (Dorman and Deighan, 2003). In *E. coli*, there are twelve major species of nucleoid-associated proteins, which are listed in Table 1.

Table 1: Molecular properties of *E. coli* histone-like proteins. Adapted after Talukder and Ishihama (1999) and Talukder *et al*. (1999)

Protein	Name	MW (kDa)	DNA-binding specificity	Maximal expression (monomers/cell)	Native protomer
CbpA	Curved DNA-binding protein A	33.4	curved DNA	late stationary phase (15,000)	homodimer
CbpB	Curved DNA-binding protein B; also: Rob	33.0	curved DNA	exponential phase (10,000)	monomer
DnaA	DNA-binding protein A	53.0	sequence specific	mid-exponential phase (900-2,700)	monomer
Dps	DNA-binding protein from starved cells	19.0	non-sequence specific	late stationary phase (180,000)	dodecamer
Fis	Factor for inversion stimulation	11.2	+/- sequence specific	exponential phase (60,000)	homodimer
Hfq	Host factor for phage $Q_{ß}$	11.2	curved DNA	exponential phase (55,000)	monomer/hexamer
H-NS	Histone-like nucleoid structuring protein	15.4	curved DNA	constant expression (20,000)	homodimer/heterodimer tetramer
HU	Heat-unstable nucleoid protein	9.2+9.2	non-sequence specific (kinked DNA, junctions)	exponential phase (60,000)	heterodimer
IciA	Inhibitor of chromosome initiation A	33.5	sequence specific	exponential phase (800)	homodimer
IHF	Integration host factor	11.2+10.7	sequence specific	early stationary phase (55,000)	heterodimer
Lrp	Leucine-responsive regulatory protein	19.0	sequence specific	exponential phase (2,600)	homodimer
StpA	Suppressor of *td*⁻ phenotype A	15.3	curved DNA	exponential phase (200)	homodimer/heterodimer, multimers

DNA-binding either requires a specific binding sequence, as observed for IHF, Lrp, or Fis, or happens in a non-sequence specific manner, e.g. with HU, H-NS, or Dps (Talukder and Ishihama, 1999). Binding of histone-like proteins can either result in DNA compactation by affecting superhelicity, in bridging of adjacent DNA stretches, or in introduction of sharp bends into the DNA (Dame, 2005).

Another difference between the nucleoid-associated proteins is their abundance in the cell. For instance, Dps is expressed at high levels in stationary phase only, whereas HU is most abundant during exponential growth (Talukder *et al.*, 1999). Furthermore, many histone-like proteins are regulated by environmental stimuli. To mention a few examples, Dps is induced upon starvation and stress situations, Lrp levels are elevated in minmal medium, and H-NS is cold-shock induced. Thus, the protein composition of the bacterial nucleoid is highly flexible, depending on many factors such as growth phase. As a result, the nucleoid becomes more compact during stationary phase, due to a decrease in superhelicity (Talukder *et al.*, 1999). These changes in the status of the bacterial chromosome affect many other DNA processes such as replication, recombination, repair, and regulation of transcription (Dorman, 1994).

2.2.2. Gene regulation by histone-like proteins

Nucleoid proteins have been shown to be global regulators, affecting expression of many genes simultaneously. Regulated genes include those that are necessary for cell viability, such as genes involved in protein synthesis and metabolism. Moreover, histone-like proteins often mediate changes in the expression pattern in response to environmental signals (McLeod and Johnson, 2001).

Regulation by histone-like proteins can be both negative and positive, and relies on several distinct mechanisms: Repression can be the result of protein binding within the –35 to -10 regions, thereby occluding the RNA polymerase from the promoter and inhibiting transcription. This mechanism is quite common for histone-like proteins with specific binding sites. An example is the Fis protein, which binds to extended regions between –16 and –68 bp of the *gyrA* promoter (Finkel and Johnson, 1992). Moreover, repression can also be the result of competition of histone-like proteins and a specific activator for the same binding site, as it was observed for Fis and cAMP-CRP at the *bglG* promoter (Caramel and Schnetz, 2000).

In contrast to this more or less specific repression, histone-like proteins can also inhibit transcription by a mechanism called transcriptional silencing (Rine, 1999). During this process, the regulatory protein binds to a so-called silencer region, which is often AT-rich and can be remotely located from the promoter. The silencer region serves as nucleation site, from which more proteins bind in a cooperative manner along the DNA, resulting in sequestration of DNA and preventing binding of other proteins, such as transcriptional activators or the RNA polymerase itself (Yarmolinsky, 2000). Again, the *bgl* operon encoding the enzymes for utilization of ß-D-glucosides can serve as an example. The histone-like protein H-NS is binding to a ~100-bp AT-rich silencer region upstream of the CRP binding site and polymerizes along the DNA, probably involving high order multimerization, as proposed by Williams and Rimsky (1997). This process does not require direct interactions with the RNA polymerase, and neither point mutations, small insertion, nor shifting of the silencer region resulted in relieved repression (McLeod and Johnson, 2001; Yarmolinsky, 2000). However, other DNA-binding proteins like CRP can act as anti-silencers by binding between the silencer region and the promoter, functioning as a roadblock to H-NS polymerization (Mukerji and Mahadevan, 1997).

On the other hand, there are also many examples for an activation of transcription by histone-like proteins. The first mechanism requires direct interactions with the RNA polymerase, as seen for Fis-mediated activation of the ribosomal operon *rrnB* (Bokal *et al.*, 1997). Fis was shown to assist both in the recruitment of the RNA polymerase and in closed complex formation. This activation of *rrnB* transcription is counteracted by H-NS binding to the –25 promoter region (Afflerbach *et al.*, 1998).

In contrast to the previous example, where Fis functions as direct activator of transcription, activation by histone-like proteins can also result from an architectural role. Since some histone-like proteins are able to introduce sharp bends into the DNA, regulatory effects result from a local change in DNA topology. For instance, after bending the *Pseudomonas putida Pu* promoter, IHF was shown to facilitate the recruitment of the RNA polymerase by bringing an upstream α-CTD binding site into the correct position (Bertoni *et al.*, 1998). The ability of many proteins such as H-NS to constrain negative supercoils also has to be taken into account due to the influence of superhelicity on transcription, as mentioned before.

Moreover, many histone-like proteins possess, in addition to the DNA-binding domain, an oligomerization domain. Therefore, two proteins bound to different sites of the chromosome can interact via their oligomerization domain, resulting in bridging of adjacent DNA stretches (Dame *et al.*, 2005; Esposito *et al.*, 2002).

The combined effects of DNA-bending and DNA-bridging proteins and the consequences for a dynamic bacterial chromosome are depicted in Fig. 1.

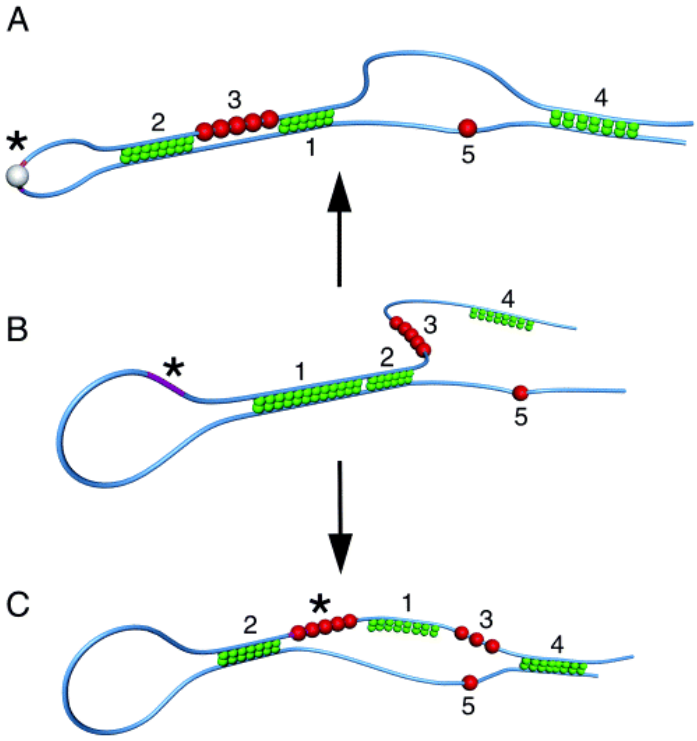

Fig. 1: Schematic representation of the bacterial nucleoid. The organization of the supercoiled loops and the relative orientation of sites within are affected by the binding of nucleoid-associated proteins such as HU, H-NS, IHF and Fis. The organization within loops is important for DNA compaction and can also play a role in the modulation of transcription. DNA is depicted in cyan. Green spheres correspond to H-NS; red spheres correspond to HU; the grey sphere corresponds to a DNA bending protein, such as IHF, Fis or HU. (B) starting configuration: H-NS bridging and HU ridgifying DNA. (A) and (C) binding of other proteins in the vicinity results in reconfiguration of the loop. In the first example (A), this loop is bound by a protein that bends DNA (e.g. IHF), which imposes relocation of the bound protein to the tip of the loop. In parallel, other bound proteins within the loop will become relocated. In the second example (C), HU becomes co-operatively bound to the binding site. It is energetically unfavourable for a rigid tract of DNA to find itself located within the tip of a loop and therefore it moves away into the stem. From Dame (2005).

Thus, histone-like proteins modulate the function of the bacterial chromosome by strongly modifying its structure. A more detailed introduction to the mechanism of generegulation by histone-like proteins will be presented in the next section about the histone-like nucleoid structuring protein H-NS.

2.2.3. Histone-like nucleoid structuring protein (H-NS)

The H-NS protein The H-NS protein was originally identified as a major component of the bacterial nucleoid (Varshavsky *et al.*, 1977), and therefore was termed histone-like nucleoid structuring protein (Lammi *et al.*, 1984). H-NS is a 137-amino acid protein with a molecular weight of 15.4 kDa. Three isoforms with around neutral pI values do exist in the cell (Spassky *et al.*, 1984), which is the result of post-translational modifications.

The protein consists of two domains: an N-terminal oligomerization domain and a C-terminal DNA-binding domain connected by a flexible linker (Renzoni *et al.*, 2001; Ueguchi *et al.*, 1997). Fig. 2 depicts the two-domain structure and the functions assigned to each domain or specific residue, as well as the predicted secondary structure.

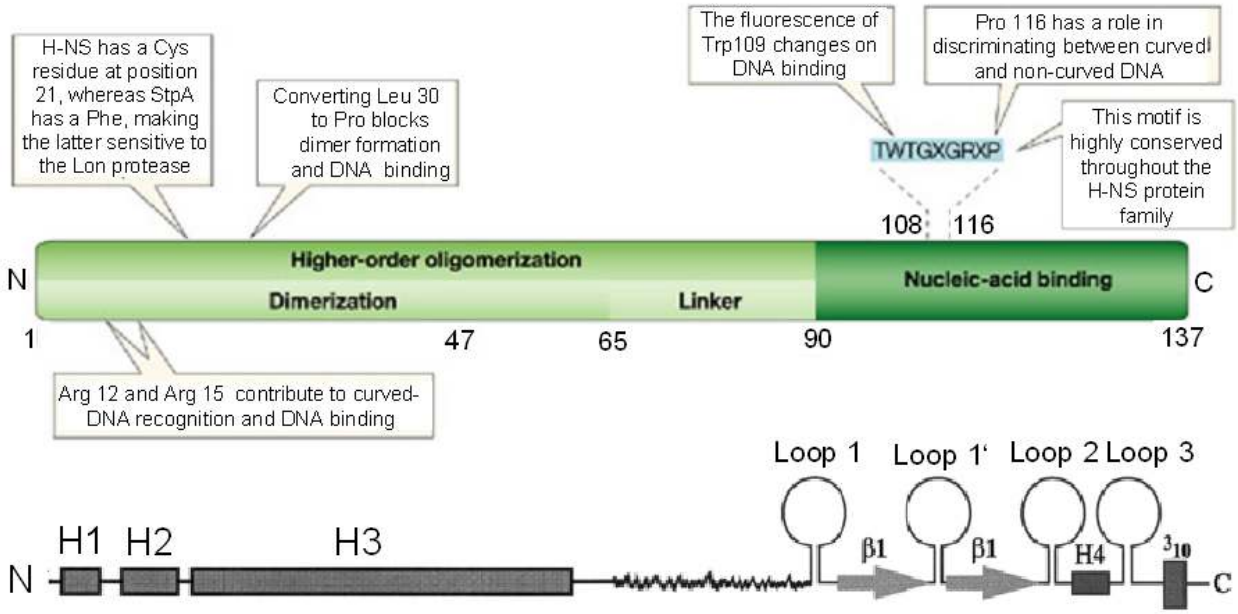

Fig. 2: Predicted structure of the H-NS protein. Numbers designate the amino acid residues of the 137-amino acid protein. Upper panel: Two-domain structure after Dorman (2004); Lower panel: predicted secondary structure after Schroder&Wagner (2002). See text for further details.

The DNA-binding domain encompasses residues 90 to 137, and is highly conserved in all H-NS-like proteins (Dorman *et al.*, 1999). Sequence alignments of these proteins gave the degenerate consensus motif TWTGXGRXP. The three-dimensional structure of the domain has been solved by NMR measurements, and results from an antiparallel ß-sheet structure composed of two short ß-strands, ß1 and ß2, reaching from residues 96-100 and 105-108 (Shindo *et al.*, 1995).

After a loop structure, an α-helix, H4, stretching from residue 116-124, and a very short 3_{10}-helix from residues 129-132 follows the structure. The DNA-binding motif is located in loop 2, and most loss-of-function mutations are also mapping this loop structure (Williams and Rimsky, 1997). This indicates, that the structurally variable loop structures of H-NS-like proteins confer DNA-binding, whereas the rigid ß-sheet and α-helices mainly have an architectural role (Schroder and Wagner, 2002; Shindo *et al.*, 1999).

The minimal dimerization domain stretches from residues 1-64 and consists of three α-helices, H1 to H3, comprising residues 1-8, 12-20, and 22-53, respectively (Renzoni *et al.*, 2001). The longest helix H3 is predicted to form the core of a coiled-coil structure in a homotrimer, whereas the other two helices have stabilizing functions.

The two domains are connected by a protease-sensitive linker region, encompassing residues 65 to 90 (Cusick and Belfort, 1998). Recent studies revealed, that the flexible linker is required for higher-order oligomerization (Stella *et al.*, 2005). However, the amino acid composition of the region is very divergent among H-NS-like proteins, and so far, no loss-of-function mutation has been isolated.

Several studies suggest that H-NS monomers predominantly oligomerize into tetramers and, to a lesser extend, into homodimers (Ceschini *et al.*, 2000; Stella *et al.*, 2005). However, oligomerization states up to 20-mers have been reported (Smyth *et al.*, 2000). A proposed mechanism for oligomerization is depicted in Fig. 3. For the *S. typhimurium* H-NS protein, the α-helices of the N-terminus were found in an antiparallel configuration with the helices of the corresponding molecule in the dimer (Esposito *et al*., 2002), whereas in *E. coli*, the helices of the same molecule interacted in a “handshake” manner (Bloch *et al*., 2003). In the schematic model, dimerization requires interactions between the N-terminus and the linker region, and serves as basis for formation of tetramers via dimer-dimer interactions. The process of tetramerization depends on interactions between two C-terminal domains (and the linker) of each dimer, as well as linker-linker interactions (Stella *et al*., 2005). However, data on H-NS oligomerization is a much disputed topic and the answer still remains unclear.

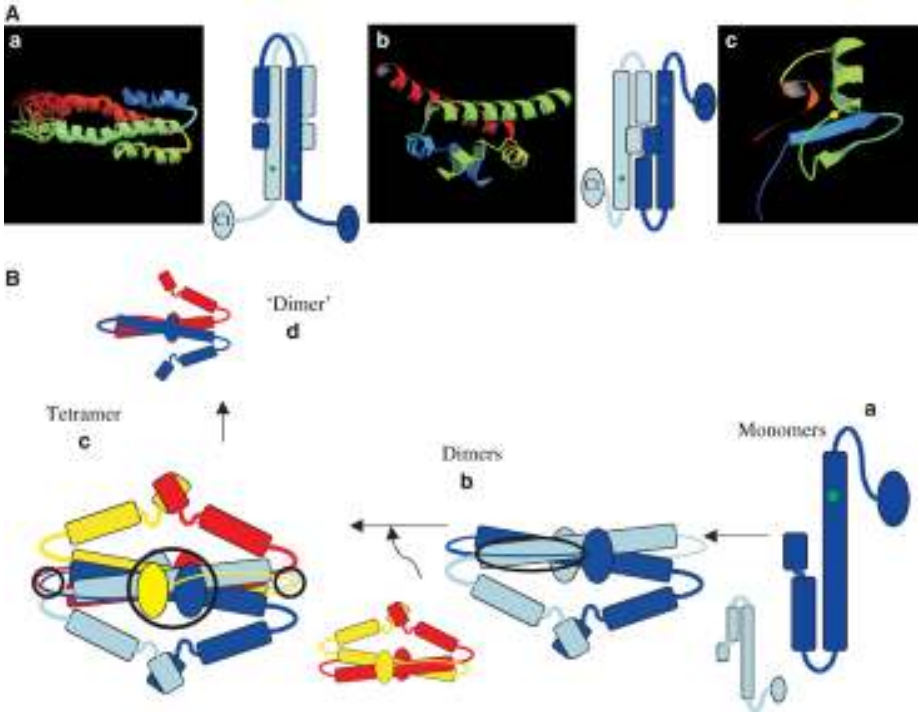

Fig. 3: Schematic models for H-NS dimerization and tetramerization. (A) 3D-structures of isolated H-NS domains: dimeric N-domain of *S. typhimurium* (a) and *E. coli* (b); monomeric C-domain of *E. coli* (c). A schematic representation of the two N-domains is shown to the right of the structures from which they are derived; spheres represent the C-terminus Ct, rectangles represent the three α-helices of the N-terminus. (B) Hypothetical, schematic models of the H-NS structures: (a) monomer; (b) dimer; (c) tetramer and (d) an alternative 'dimer' generated by removing a monomer from each dimer of the tetramer. In the scheme, the protein−protein interactions found to be important for oligomerization are highlighted: in 'b', a black oval encircles the linker−N-domain interaction contributing to dimerization and in 'c', the large black circle encompasses the C-domain−C-domain (with a contribution of the linker) and the small black circles indicate the linker−linker interactions contributing to tetramerization. [Stella *et al.* (2005)].

Nevertheless, it is evident that the state of oligomerization affects the regulatory activity of H-NS. Truncated proteins consisting of the C-terminus only are able to bind DNA, but with much lower affinities than the native protein (Shindo *et al.*, 1995), and inhibition of oligomerization abolishes repression of some target genes such as *proU* and *bgl* (Ueguchi *et al.*, 1996; Ueguchi *et al.*, 1997; Williams *et al.*, 1996).

H-NS binds to DNA in a non-sequence-specific manner, but with a preference for intrinsically curved, double-stranded DNA, which is generally AT-rich (Spurio *et al.*, 1992; Yamada *et al.*, 1991). This might also explain the the tendency to form oligomers, since inside the DNA bend, the monomers are more likely to find interaction partners (Dame *et al.*, 2001).However, H-NS was also shown to bind RNA, resulting in post-transcriptional regulation of certain genes (Deighan *et al.*, 2000; Yamashino *et al.*, 1995).

Binding is either specific for AT-rich nucleation sites, which requires only low protein concentrations and promotes cooperative binding to lower affinity sites, resulting in transcriptional silencing (see section 2.3.2.). At high protein concentrations, non-specific binding can be observed, which results in polymerization of H-NS at the DNA (Rimsky *et al.*, 2001). However, a physiological role of such unspecific binding is improbable.

H-NS binding results in compactation of the chromosome (Spassky *et al.*, 1984) and therefore, overexpression of H-NS even has a lethal outcome (Spurio *et al.*, 1992). Moreover, subsequent interactions of the oligomerization domains of two bound H-NS molecules result in bridging or looping of DNA as depicted in Fig. 4.(Dame *et al.*, 2005; Dorman, 2004).

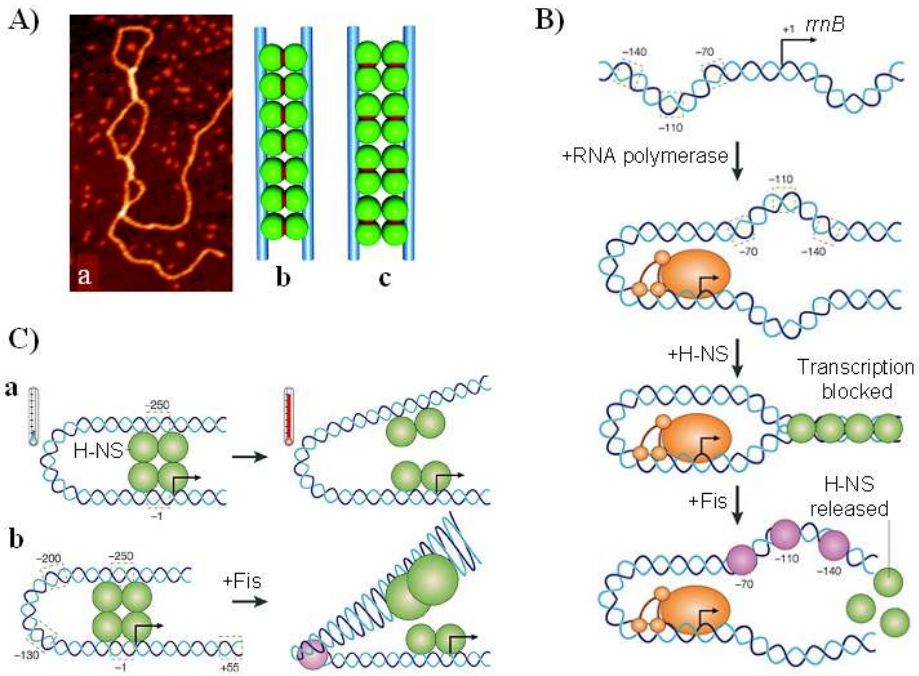

Fig. 4: Schematic models for repression -mechanisms by H-NS.
(A) DNA bridging via oligomerization; SFM micrographs of H-NS-DNA samples (a), two possible mechanisms assuming binding of H-NS dimers to different DNA-strands (b) or to the same strand (c) prior to oligomerization. [Dame (2005)].
(B) H-NS-mediated trapping of RNA polymerase at the *rrnB* promoter and antagonism by Fis. H-NS 'zips up' the DNA flanking the promoter, producing an H-NS−polymerase−DNA ternary complex that prevents the escape of RNA polymerase into the elongation phase of transcription. Fis disrupts this complex.
(C) H-NS-mediated repression of the *virF* virulence gene promoter in *S. flexneri*. Formation of a repressive complex at low temperatures after DNA looping is antagonized at higher temperatures (a), or after Fis-mediated destabilization of the complex due to DNA bending. [Dorman (2004)].

This DNA binding and reorganization activity of H-NS certainly has consequences for any DNA-depending process. Therefore, the two-domain structure of the H-NS protein accounts for its unique and global regulation mechanisms.

The hns *gene*

The *hns* gene, also known as *osmZ, drdX* or *bglY*, was initially isolated by Pon *et al.* (1988) and maps at 27 min of the *E. coli* chromosome between the *galU* and *tdk* genes. It is transcribed monocistronically from a single promoter (La Teana *et al.*, 1989).

Expression of *hns* is activated by the Fis protein and repressed by autoregulation. The binding sites for Fis and H-NS at the *hns* promoter are overlapping, and therefore, Fis is stimulating *hns* transcription both directly and indirectly via counteracting autorepression (Falconi *et al.*, 1993). Furthermore, autoregulation is coupled to DNA synthesis, resulting in a constant ratio of H-NS to DNA in the cell (Free and Dorman, 1995). Finally, *hns* expression is 2-4 fold increased at low temperatures mediated by the major cold shock protein CspA (La Teana *et al.*, 1991). This correlates with the finding that H-NS is required for adaptation to a cold environment (Dersch *et al.*, 1994). Some studies also report that expression of *hns* increases after entering stationary phase; however, other studies could not confirm this result.

The H-NS regulon

The effects of H-NS have been studied in detail in non-pathogenic *E. coli*, where it is considered a global regulator of gene expression (Atlung and Ingmer, 1997; Hommais *et al.*, 2001; Ussery *et al.*, 1994). Mutation in the *hns* gene affect several cellular processes including recombination, transposition and deletion events (Falconi *et al.*, 1991; Kawula and Orndorff, 1991; Rouquette *et al.*, 2004; Shiga *et al.*, 2001) and leads to a highly pleiotropic phenotype. In general, *hns* mutants grow more slowly than the wild type, especially at lower temperatures (Barth *et al.*, 1995), exhibit a mucoid phenotype, and are non-motile and serine-sensitive.

Two-dimensional gelelectrophoresis revealed, that more than 30 proteins are affected in *E. col*i K-12 by a mutation in the *hns* gene (Barth *et al.*, 1995; Bertin *et al.*, 1990; Laurent-Winter *et al.*, 1995; Yamada *et al.*, 1991). Later on, more data was obtained from expression profiling using DNA arrays. This approach confirmed the global effects of H-NS on the gene expression pattern, since ~ 5 % of all genes in *E. coli* K-12, i.e. about 250 genes, were directly or indirectly altered in an *hns* mutant (Hommais *et al.*, 2001), with increased expression of more than 80 % of all deregulated genes [for a complete list of deregulated genes see Table 1 of the original publication].

To summarize, 21 % of the deregulated genes were involved in transcription and translation, 30 % encoded components of the cell envelope, and about the same number of genes were of yet unknown function. The affected cell envelope components included genes involved in motility (*fli* genes), in adhesion (type 1 fimbriae, *fim*, and the curli adhesin, *csgA*), or the outer membrane porin *ompX*, all of which exhibited an upregulated expression in the *hns* mutant.

Moreover, H-NS was found to predominantly affect genes whose encoded products are involved in adaptation to a changing environment, such as osmolarity, pH and anaerobiosis, thereby indicating a central role of H-NS for adaptability of bacterial cells. For instance, many genes normally induced by oxygen starvation (e.g. cytochrome oxidases), by carbon starvation (e.g. *gnd*, *slp*), or in minimal medium (e.g. the DNA-binding protein Lrp) were induced in the absence of H-NS. The same result was obtained for genes induced by acid stress, such as the lysine decarboxylase *cadBA*, the arginine decarboxylase *adiA*, and the glutamate decarboxylases *gadAB*, which resulted in increased viability of the *hns* mutant at low pH compared to the wild type.

Other examples are osmoregulated genes, such as the outer membrane porin-encoding genes *ompC* and *ompF*, or the *proU* operon, which were also upregulated in strains lacking H-NS. Effects of H-NS on *proU* expression have been intensively studied. The operon encodes a glycine-betaine/proline transport system, that is up to 100-times induced at high osmolarity (Lucht and Bremer, 1994), probably due to an increase in intracellular potassium glutamate concentration and/or an increase in DNA supercoiling (Higgins *et al.*, 1988). Mutations in *hns* lead to a moderately increased *proU* expression even at low osmolarity, thereby indicating that H-NS is able to represses *proU* transcription. Indeed, H-NS was found to bind upstream of the *proU* promoter, as well as to a curved downstream regulatory element (DRE) (Lucht *et al.*, 1994). However, osmoregulation of *proU* is not abolished in an *hns* mutant, which suggests, that a combination of direct effects of supercoiling, and an indirect effect of osmolarity on H-NS mediated repression is involved in osmoregulation of *proU*.

Another group of H-NS-regulated genes codes for components of the transcription and translation apparatus defining growth phase or growth rates. The mechanism of H-NS mediated repression of the ribosomal RNA operon *rrnB* has been described before (see also Fig 4B).

However, most of these studies have been performed in non-pathogenic *E. coli* K-12 strains. The overall effect of H-NS for virulence of pathogenic bacteria was so far only studied in some strains.

Beloin and Dorman (2003) and Falconi *et al*. (1998) report, that H-NS mainly affects invasiveness of *Shigella flexneri* and enteroinvasive *E. coli* by repressing the expression of the plasmid-encoded regulators VirF and VirB, which are required for expression of the invasion-associated genes *ipa* (Dagberg and Uhlin, 1992). The mechanism for H-NS-mediated thermoregulation and repression at the *virF* promoter can be seen in Fig. 4c. VirF is required for activation of VirB, which then activates the *ipa* genes. In *Salmonella enterica*, H-NS was found to repress the *spv* virulence locus, which is required for intracellular survival (O'Byrne and Dorman, 1994). H-NS also affects the transcriptional regulator *hilA*, which activates the type III secretion system encoded on the *Salmonella* pathogenicity island 1, under low osmolarity conditions (Schechter *et al.*, 2003). In enteropathogenic *E. coli*, H-NS mediates thermoregulation of heat-labile enterotoxin (LT) synthesis by interacting with the DRE of the gene encoding the LT subunit A at low temperatures, thereby resulting in maximum expression of LT at 37 °C, i.e. body temperature (Trachman and Maas, 1998).

For other pathogenic *E. coli* strains, only some selected virulence-associated genes were tested for H-NS-regulated expression, such as P-, K88-, and K99 pili, as well as toxins HlyA and ClyA (Westermark *et al.*, 2000; White-Ziegler *et al.*, 2000). For most of these virulence factors, H-NS was found to mediate temperature-regulated expression. For instance, the di-galactoside binding pyelonephritis-associated pili encoded by the *pap* operon are only produced at 37 °C, but not at lower temperatures (Göransson *et al.*, 1990). This is the result of H-NS binding to the *papBA* promoter region, where it inhibits both transcription and DNA methylation at two sites involved in phase-variation of the pili (Blomfield, 2001). The same temperature-dependent expression is described for the α-hemolysin determinant *hly*, which is more effectively repressed by H-NS at low temperatures due to increased affinity of H-NS for the promoter region at 25 °C compared to 37 °C (Madrid *et al.*, 2002).

However, not all pathogenic variants do produce the same virulence factors. For instance, the uropathogenic *E. coli* isolate strain 536 used in this study, does not express K88-, and K99-pili at all, but instead possesses several other fimbrial determinants such as the *pix* cluster, where no transcriptional studies have been carried out so far.

2.2.4. The H-NS paralog StpA

In addition to H-NS, *Escherichia coli* cells express an intraspecies homolog, i.e. a paralog, called StpA, which was first discovered as a multicopy suppressor of a thymidilate synthase-negative phenotype in a T4 phage (Zhang and Belfort, 1992; Zhang *et al.*, 1996).

StpA is a 133-amino acid protein, which shares 58 % sequence identity to the H-NS protein and has a similar domain structure (Cusick and Belfort, 1998). Identity to H-NS is greater in the C-terminus (73 %) than in the N-terminus (51 %). StpA can bind DNA with even higher affinity than H-NS (Sonnenfield *et al.*, 2001), where it is able to constrain supercoils. However, StpA also displays an additional RNA chaperone activity (Zhang *et al.*, 1996) and is able to stimulate complementary RNA strand annealing and *in vitro* trans-splicing of a model intron (Cusick and Belfort, 1998; Zhang *et al.*, 1995).

Like H-NS, StpA is able to form homodimers, as well as higher order oligomers (Johansson *et al.*, 2001). Overexpression of StpA can in some parts complement the lack of H-NS, as shown for the regulatory effect on the arginine decarboxylase gene *adi*, as well as on *proU* and *pap* genes, and the *hns* gene itself (Shi and Bennett, 1994; Sonden and Uhlin, 1996; Zhang *et al.*, 1996). Mutations in the *stpA* gene, however, do not result in a notable phenotype under standard growth conditions.

The lack of phenotype can be partly explained by the low level of *stpA* expression in wild type cells, yielding in approximately 200 monomers of the StpA protein per cell, whereas H-NS is usually present in 20,000 monomers per cell (Spassky *et al.*, 1984). Transcription of *stpA* is negatively regulated by StpA itself and by H-NS (Zhang *et al.*, 1996). However, the level of StpA increases during growth in minimal media due to the action of Lrp, or after temperature upshift and increase in osmolarity, whereas carbon starvation results in repression of *stpA* transcription (Free and Dorman, 1997; Sonden and Uhlin, 1996). Thus, StpA is strongly regulated by environmental conditions.

2.2.5. Interactions between H-NS and StpA

H-NS and its paralog StpA are interacting at several levels. At the transcriptional level, interactions include cross-regulation between H-NS and StpA, as already described before. Therefore, StpA levels are increased in a *hns* mutant, and, to a lesser extend, higher H-NS amounts are found in strains lacking StpA. In the first case, derepression of StpA in the *hns* mutant can compensate some of the effects of the mutation (Sonden and Uhlin, 1996), therefore StpA is considered as a molecular backup for H-NS.

Moreover, interactions occur at the protein level, since both proteins were found to form heteromers (Johansson *et al.*, 2001; Williams *et al.*, 1996). Heteromerization involves the middle portions as well as the C-terminus of H-NS and seems to rely on a different mechanism to H-NS homodimerization. As part of this heteromeric complex, StpA is protected from degradation by the Lon protease (Johansson and Uhlin, 1999), which depends on a phenylalanine residue at position 21 of the StpA protein (see Fig. 2). This suggests, that the biologically relevant form of StpA is the heteromer with H-NS. Indeed, Free *et al*. (1998) reported, that StpA can act as molecular adaptor for truncated H-NS protein lacking the C-terminus. Via heteromerization, intact StpA can direct truncated H-NS to DNA, resulting in repression of the *bgl* operon. In this way, StpA was shown to take part in the regulatory network of DNA-binding proteins.

2.2.6. Other H-NS-like proteins

The H-NS protein can be found among many *Enterobacteriaceae*, such as *E. coli*, *Shigella flexneri*, *Salmonella typhimurium*, *Serratia marcescens*, or *Proteus vulgaris* (see Fig. 5), but also in the related *Haemophilus* genus (Atlung and Ingmer, 1997). Many of those species also possess the StpA protein, which is thought to result from gene duplication.

H-NS-like proteins with lower homology were identified outside the *Pasteurella* group of γ-proteobacteria, like in *Vibrio cholerae*, *Yersinia pestis*, or *Photorhabdus luminescens* [for a review see Table 1 of Tendeng and Bertin (2003)]. Even some intracellular symbionts such as *Buchnera aphidicola* and *Wigglesworthia glossinidia*, which are characterized by their reduced genome size, encode an H-NS protein, thereby suggesting that it has a necessary function in the cell.

Interestingly, *Pseudomonas* species do not have any proteins with amino acid sequence similarity to H-NS. However, there is a family of MvaT proteins, which exhibit structural similarity to H-NS, thereby being able to complement some *hns* phenotypes, and also to bridge stretches of DNA (Dame *et al.*, 2005; Tendeng *et al.*, 2003b).

H-NS proteins are not restricted to γ-proteobacteria. Some representatives of the group of ß-proteobacteria, such as *Ralstonia* spp. or *Bordetella pertussis* also encode H-NS-related proteins. In the latter, the protein is termed BpH3, and has been shown to restore *hns* phenotypes such as motility, mucoidity, or serine susceptibility. The same is true for the HvrA protein of the α-proteobacterium *Rhodobacter capsulatus*, which is involved in regulation of the photosystems (Bertin *et al.*, 1999). These two proteins share only 30 % amino acid identity to H-NS, and especially the N-terminus is not well conserved. Nevertheless, the secondary structure still is predicted to be mainly α-helical, thereby being able to oligomerize via coiled-coil formation. The C-terminus, including the DNA-binding motif, is quite conserved, resulting in DNA-binding activity of both HvrA and BpH3.

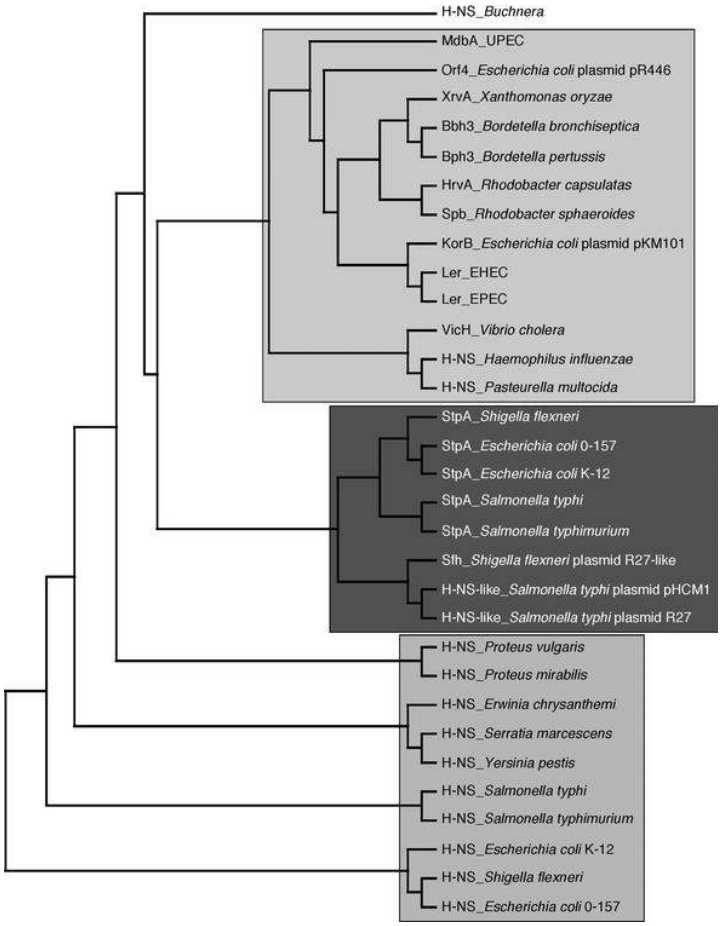

Fig. 5: Cladogram of H-NS-homologs in various bacterial species.
From Beloin *et al* (2003)

Proteins with 40 % amino acid identity to HvrA were also found in a psychrotrophic *Actinobacter* spp. isolated in Siberia, and a psychrophilic *Psychrobacter* spp. from Antarctica (Tendeng *et al.*, 2003a). In the latter, H-NS-related functions were only observed at temperatures below 30 °C, due to thermal instability of the α-helical conformation of the N-terminus at 37 °C.

Moreover, there are proteins with homology to the C-terminus of H-NS only, thereby being able to bind to DNA, but lacking oligomerization ability. Examples are a transcription factor of *Rhodobacter sphaeroides*, SPB, the virulence regulator of *Xanthomonas oryzae*, XvrA, or the pleitropic regulator of *Vibrio cholerae*, VicH (Bertin *et al.*, 1999). Interestingly, many of these homologs are encoded on plasmids, such as the KorB protein encoded on plasmid pKM101 of *E. coli*, or ORF4 of the IncM plasmid R446 of *E. coli* (Dorman *et al.*, 1999).

There are also proteins with homology only to the N-terminus of H-NS. The most prominent example is the Hha protein, which mediates thermoregulation of hemolysin expression in *E. coli* (Nieto *et al.*, 2000). The 8-kDa protein is able to form heteromers with H-NS, and can be considered as an independent oligomerization domain of H-NS (Nieto *et al.*, 2002). An Hha homolog, YmoA, can be found in *Yersinia enterocolitica*, where it acts as a repressor of the virulence-associated *yop* genes (Cornelis *et al.*, 1991). *E. coli* encodes a recently discovered Hha homolog, YdgT, which also interacts with H-NS (Paytubi *et al.*, 2004), and even more Hha homologs can be found on conjugative plasmids (Madrid *et al.*, 2002).

The fact that many H-NS homologs are encoded on plasmids, suggests, that they might have been acquired by horizontal gene transfer. Beloin and co-workers (2003) discovered a third member of the H-NS-like protein family in *Shigella flexneri*, the Sfh protein. Sfh shares about 60 % amino acid homology with H-NS and StpA, and it has DNA-binding activity. Sfh is able to interact with both H-NS and StpA, forming heteromeric complexes (Deighan *et al.*, 2003). Furthermore, it is able to complement an *hns* mutation and affects virulence gene expression when overexpressed (Beloin *et al.*, 2003). The same authors reported, that the protein is encoded on a high-molecular-weight plasmid similar to the self-transmissable plasmid R27 of *Salmonella typhi*, and is only found in *S. flexneri* strain 2a 2457T, but not in strains 5a, 2a Sf301, or any other serotype. This suggests, that the protein has been acquired only recently.

The same situation might have occurred in uropathogenic *E. coli* strains. Plasmid p24-2 encodes a protein termed MdbA, which exhibits full-length homology to H-NS after a mutational frameshift (Dorman *et al.*, 1999). Another example for horizontal gene transfer is the H-NS-like protein Ler. This Ler protein is encoded on the LEE pathogenicity island of enteropathogenic *E. coli*, where it activates the expression of virulence genes (Haack *et al.*, 2003). This situation can serve as an example of a piece of extragenetic material that encode its own regulatory proteins.

Recently, Williamson and Free (2005) described a truncated H-NS-homolog in enteropathogenic *E. coli*. The protein termed H-NST is lacking the C-terminal DNA-binding domain. However, due to the homology to the N-terminus of H-NS, both proteins are able to interact. This interaction interferes with the repressive function of H-NS on transcription of some genes. Therefore, H-NST might be considered as an anti-H-NS factor. Like the Ler protein mentioned before, H-NST is encoded on a genomic island only present in the pathogenic variants.

As a result, many strains express several H-NS-like proteins at a time, with up to 5 copies as seen in *Shigella flexneri* or *Pseudomonas putida* (Tendeng and Bertin, 2003), which then are able to interact with each other and modulate their function. Due to variation in the N-terminus, the specificity and affinity of the interaction might vary between the homologs, which leads to a complex network of histone-like proteins. With progress in genome sequencing, the multitude of identified H-NS homologs and possible ways of interactions will be further increased. Thus, acquisition of H-NS-like proteins, which are able to interact with H-NS and modulate its activity, might be an important step in fine tuning the regulatory network during evolution of a pathogen.

Finally, it is worthwhile mentioning that the occurrence of H-NS-like proteins seems to be restricted to Gram-negative bacteria, since up to now, no H-NS-like protein has been identified in a Gram-positive organism.

2.3. Uropathogenic *Escherichia coli*

The urinary tract is the most common site of bacterial infection in industrialized countries (Warren, 1996), and urinary tract infection (UTI) is also the leading nosocomial disease. UTI can be caused by several microbial pathogens. The most common agent for urinary tract infections, however, are uropathogenic *E. coli* (UPEC), which cause UTI in about 80% of all cases (Hooton and Stamm, 1997; Svanborg and Godaly, 1997)

The urinary tract represents an usually sterile compartment, which is protected from bacterial infections by various mechanisms such as urine flow and immune responses. Furthermore, the urinary tract is a hostile environment in terms of supporting bacterial growth. The chemical composition, osmolarity, and pH of urine determine the rate of bacterial growth and the maximum population that can be supported, and can be very variable, depending on the diet. Normal urine constituents include amino acids and glucose, which are usually present at sufficient concentrations to support rapid bacterial growth. However, other components of urine, such as urea and organic acids, may inhibit growth, mainly by affecting pH and osmolarity (Asscher *et al.*, 1966). Therefore, the ability of some pathogens to overcome these mechanisms and colonize the urinary tract is linked to the presence of virulence factors encoded by horizontally acquired genes not present in their non-pathogenic relatives. These factors include *adhesins*, *cytotoxins*, *iron-uptake systems* and extracellular polysaccharides such as *lipopolysaccharide* and *capsules*. For comprehensive reviews on virulence factors of uropathogenic *E. coli* see Emödy *et al.* (2003), Johnson (1991), Mühldorfer *et al*. (2001), or Oelschlaeger (2002).

UPEC strain 536 (O6:K15:H31), a clinical isolate from acute pyelonephritis, expresses one or several types of each of the virulence factors mentionend above. Interestingly, most of those virulence factors are encoded on large, unstable regions of the chromosome, so-called pathogenicity islands (PAIs), which will be introduced in the next section. Table 2 lists all relevant virulence factors of UPEC strain 536.

Table 2: Virulence and fitness factors of uropathogenic *E. coli* isolate 536.

Virulence factor	Function during infection	Localization	Genes	Encoded on	Regulators	Refs *
Adhesins						
Type 1 fimbriae	Adhesion to glycoproteins with N-linked oligomannose chains on mucosal epithelium and tissue matrix; invasion; biofilm formation	surface	*fim*	chromosome	phase variation by FimB and FimE recombinases, Lrp, IHF, H-NS, $tRNA_5^{Leu}$; upregulated during UTI	1
P-related fimbriae	Adhesion to α-D-Gal-(1-4)-ß-D-Gal receptors on mucosal epithelium and tissue matrix; cytokine induction	surface	*prf*	PAI II_{536}	PrfB, PrfI, PrfX (SfaB, SfaC)	2
S fimbriae	Adhesion to α-Sialyl-(2-3)-ß-Gal receptors on mucosal and endothelial cells, and tissue matrix	surface	*sfa*	PAI III_{536}	SfaB, SfaC, (PrfB, PrfI), H-NS	2, 3
thin aggregative fimbriae (curli)	Adhesion to unknown structures on fibrinonectin, laminin, and plasminogen of mucosal cells and matrix; biofilm formation	surface	*csg*	chromosome	CsgD, Crl, RpoS, H-NS; thermoregulation	4, 5
Toxins						
α-hemolysin	Cytotoxicity, hemolysis; involved in renal failure	secreted	*hly*	PAI $I\&II_{536}$	RfaH, $tRNA_5^{Leu}$, Hha, H-NS, thermoregulation	6, 7, 8
Iron-uptake systems						
Yersiniabactin	Iron acquisition; fitness; (phenolate type)	secreted	*ybt*	PAI IV_{536}	YbtA, Fur; induced under iron limitation	9
Salmochelin	Iron acquisition; fitness; urovirulence (catecholat type)	secreted	*iro*	PAI III_{536}	Fur; induced under iron limitation	10
Hemin receptor	Iron acquisition; fitness	secreted	*chuA*	genomic islet	RfaH; Fur; induced under iron limitation	11, 12
Enterobactin	Iron acquisition; fitness; (catecholat type)	secreted	*fep*	chromosome	Fur, induced under iron limitation	13, 14
Ferrichrome	Iron acquisition; fitness; (hydroxamat type)	secreted	*fhu*	chromosome	Fur, induced under iron limitation	15
Extracellular polysaccharides						
O6-antigen (LPS)	Cytokine induction; serum resistance; immunoadjuvant	surface	*wa*,wb**	genomic islet	RfaH	6
K15-antigen (capsule)	Antiphagocytic anticomplement effect; serum resistance; evasion of immune recognition	surface	*kps*	PAI V_{536}	RfaH, H-NS, IHF, BipA; thermoregulation (for K5 capsules)	6, 16
M-antigen (colanic acid)	Protection of cells under conditions of membrane perturbations; adhesion; biofilm formation	surface	*cps*	chromosome	RcsA, RcsB, RcsF, RcsC, Lon, H-NS (indirectly); thermoregulation	17
Others						
Flagella	Motility; adaptation; fitness	surface	*fli, flg*	chromosome	Crp, H-NS, OmpR	18
Ag43	Autotransporter mediating cell-cell interactions; autoaggregation; biofilm formation	surface	*agn43*	PAI $III\&V_{536}$	phase variation by OxyR and Dam, RfaH (indirectly)	19

* *Selected references on regulation*: 1=Blomfield (2001), 2=Morschhäuser *et. al*. (1994); 3=Morschhäuser *et al*. (1993); 4=Gerstel *et al.* (2003); 5=Olsen *et al*. (1993a); 6=Nagy *et al.* (2002); 7=Nieto *et al*. (2000); 8=Dobrindt *et al.* (2002b); 9=Carniel (2001); 10=Russo *et al*. (2002); 11=Nagy *et al*. (2001); 12=Torres&Payne (1997); 13=Ozenberger *et al*. (1987); 14=Escolar *et al*. (1998); 15=Mademidis&Koster (1998); 16=Rowe *et al*. (2000); 16=Schneider *et al*. (2004); 17=Gottesman&Stout (1991); 18=Soutourina&Bertin (2003); 19=Schembri *et al*. (2003)

2.4. Pathogenicity islands

Pathogenicity islands have been first described in UPEC strain 536 (Blum *et al.*, 1994; Hacker *et al.*, 1997; Knapp *et al.*, 1986), but afterwards have been found in the genomes of many human, animal, and plant pathogens. The characteristics of a pathogenicity island are reviewed by Hacker and Kaper (2000). Similarly, there are DNA regions that do not contain virulence-associated genes, but nevertheless contribute to the fitness of the bacterium. These so-called genomic islands (GEIs) or fitness islands help microorganisms to live in the environment (Hacker and Carniel, 2001). Genomic islands represent (formerly) mobile DNA elements and are considered to have been acquired by horizontal gene transfer, thereby contributing to the evolutionary potential of bacteria (Dobrindt *et al.*, 2004; Hacker *et al.*, 2003). Therefore, the bacterial chromosome can be divided into two gene pools: the "flexible gene pool" including the majority of horizontally acquired DNA, and the conserved "core gene pool", which mainly represents essential genetic information for basic cellular processes such as DNA replication, protein synthesis, and key metabolic pathways (Dobrindt and Hacker, 2001).

So far, six pathogenicity islands, as well as several smaller genomic islets encoding the hemin receptor (*chu*) or the O6-specific Lipopolysaccharide (*wa**, *wb**), have been identified in UPEC strain 536. Fig. 6 depicts the localization of those islands in the chromosome, as well as the encoded virulence factors.

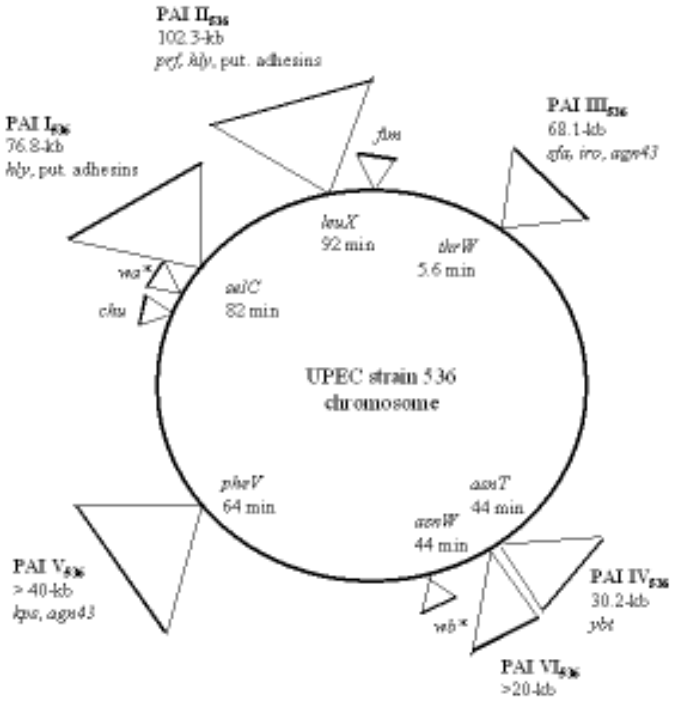

Fig. 6: Chromosomal map of uropathogenic *E. coli* strain 536. The map is based on the chromosomal map of *E. coli* K-12 strain MG1655, and depicts the chromosomal localization of the known PAIs and some other virulence-associated genes. [(Schneider, 2005)]

2.5. Aims of this study

Although the effect of the histone-like proteins H-NS and StpA are well characterized in non-pathogenic *E. coli* K-12 strains, their role in pathogenic strains has only been studied for some selected virulence traits. Using DNA macroarrays, RT-PCR and different phenotypic tests, we monitored the effects of histone-like proteins in an uropathogenic *E. coli* isolate on a larger scale and assessed their role for overall virulence in experimental murine models of ascending urinary tract infection and sepsis.

Uropathogenic *E. coli* strain 536 can serve as a model organisms due to different reasons. The genome of strain 536 was sequenced recently, thereby enabling both genetic manipulations and bioinformatic analyzes. Moreover, most virulence factors are encoded on extragenetic material, the pathogenicity islands. This imposes the question, whether PAI-encoded genes are part of the “normal” regulatory network of the host cell, mediated by global regulators such as H-NS. Furthermore, many PAIs themselves encode known or putative regulators. We could also identify an H-NS homolog (Hlp) that is encoded on a putative genomic island. Therefore, another aim of this study was to assess, whether such a regulator only affects PAI-encoded genes or also gene expression of the core genome.

In summary, the aim of this study was to answer the central question, whether there is regulatory cross-talk between pathogenicity islands and the chromosome mediated by histone-like proteins.

3. Material

3.1. Strains

All bacterial strains used in this study and their relevant genotype are listed in Table 3.

Table 3: Bacterial strains used in this study.

Strain	Relevant properties	Reference
UPEC 536	clinical isolate from pyelonephritis; serotype O6:K15:H31	(Berger *et al.*, 1982)
536 *ΔstpA*	chromosomal deletion of CDS	This study
536 *Δhns*	chromosomal deletion of CDS	This study
536 *Δhlp*	chromosomal deletion of CDS	This study
536 *ΔstpA Δhns*	chromosomal deletions of CDS	This study
536 *ΔstpA Δhlp*	chromosomal deletions of CDS	This study
536 *Δhns Δhlp*	chromosomal deletions of CDS	This study
536 *ΔstpAΔhnsΔhlp*	chromosomal deletions of CDS	This study
Nissle 1917 (DSM6601)	Probiotic *Escherichia coli* strain; O6:K5:H1	Ardeypharm GmbH, Herdecke (Germany)
E. coli MG1655	F^-, λ^-, *ilvG*, *rfb*-50 *rph*-1	(Blattner *et al.*, 1997)
BEU740 *	MG1655 *hns::cat*	Uhlin; unpublished
BEU693 *	GM37, *trp*::Tn 10. *proU-lac Z*	(Sonden and Uhlin, 1996)
BEU694 *	BEU693 *Δhns*	(Sonden and Uhlin, 1996)
E. coli DH5α	F^-, *end*A1, *hsd*R17 (r_k^-, m_k^-), *sup*E44, *thi*-1, *rec*A1, *GyrA*96, *rel*A1, λ^-, Δ(*argF-lac*)U169, Φ80*dlac*Z ΔM15	BRL, Bethesda Research Laboratories 1986
E. coli Rosetta™	*E. coli* K-12	Novagen
E. coli BL21 *Δhns* *	F^- *ompT hsd*S_B (r_B^- m_B^-) *gal dcm* (DE3)	(Zhang *et al.*, 1996)
JGJ152 *	MC4100 *stpA60::*Km^R, *hns::*Cm^R	(Johansson and Uhlin, 1999)
MC4100	F^- *araD139* Δ(*argF-lac*)*U169 rpsL150* (Str^r) *relA1 flbB5301 deoC1 ptsF25 rbsR*	(Silhavy *et al.*, 1984)
MC4100 *Δhns ΔstpA*	chromosomal deletions of (partial) CDS	This study
MC4100 *Δhns Δlon*	chromosomal deletions of CDS	This study
MC4100*ΔhnsΔstpAΔlon*	chromosomal deletions of (partial) CDS	This study

* kind gifts from B. E. Uhlin

3.2. Plasmids

All plasmids used and constructed during this study are listed in Table 4. Maps of the newly constructed plasmids are found in the appendix (Fig. 54).

Table 4: Plasmids used in this study.

Plasmid	Relevant properties	Reference
pKD46	*repA101* (ts), *araBp-gam-bet-exo* (λ red recombinase under the contol of *araB* promotor), Ap^R (*bla*)	(Datsenko and Wanner, 2000)
pKD3	oriRγ, Ap^R, *cat*-gene flanked by FRT sites	(Datsenko and Wanner, 2000)
pKD4	oriRγ, Ap^R, *npt*-gene flanked by FRT sites	(Datsenko and Wanner, 2000)
pCP20	Yeast Flp recombinase gene (FLP, aka exo) *ts-rep*, Ap^R, Cm^R	(Datsenko and Wanner, 2000)
pASK75	expression vestor with aTc-inducible tet $^{p/o}$ promoter	(Skerra, 1994)
pASK75-HIS*hlp*	His_6-tagged *hlp* subcloned in pASK75	This study
pWKS30	low copy number cloning vector; *bla*	(Wang and Kushner, 1991)
pWKS30-*hlp*	750-nt subclone of the *hlp* locus in pWKS30	This study
pYMZ80 *	1.6-kb subclone of the *clyA* locus in pUC18	(Westermark *et al.*, 2000)
pBSN2 *	translational fusion *hns* in pMW156 (translational *lacZ* fusion vector, Km^R)	(Sonden and Uhlin, 1996)
pGEM®-T_{easy}	Ap^R, *ori*f1, *lacZ*	Promega, 1997

* kind gifts from B. E. Uhlin

3.3. Oligonucleotides

The oligonucleotides used for gene disruption using the λRed-based method (Datsenko and Wanner, 2000), as well as the IRD_{800} labelled oligonucleotides were purchased from MWG-Biotech (Ebersberg, Germany). All other oligonucleotides used for PCR verification of the mutants and RT-PCR were purchased from Sigma-Genosys (Steinheim, Germany). The sequences and the application of all oligonucleotides are listed in Table 5.

Table 5: Oligonucleotides used in this study.

Name	Length	Sequence (5'→3')	Application
hns-1	69-mer	AAA TCC CGC CGC TGG CGG GAT TTT AAG CAA GTG CAA TCT ACA AAA GAT TAG TGT AGG CTG GAG CTG CTT	disruption of *hns* gene
hns-2	76-mer	ATT ATT ACC TCA ACA AAC CAC CCC AAT ATA AGT TTG AGA TTA CTA CAA TGC ATA TGA ATA TCC TCC TTA GTT CCT A	
hns-3	20-mer	TTC GTC ATA ACA CCC TTG GC	confirmation of *hns*
hns-4	20-mer	GTC AGC CTA CGA TAA TCT CC	genotype
stpA-1	69-mer	AGA AGC GAC GCC GGA CGC GCC CTA GCA GCG ACA TCC GGC CTC AGT AAT TAG TGT AGG CTG GAG CTG CTT	disruption of *stpA* gene (complete CDS)
stpA-2	76-mer	GCG ACG AAA TAC TTT TTT TGT TTT GGC GTT AAA AGG TTT TCT TTA TTA TGC ATA TGA ATA TCC TCC TTA GTT CCT A	
stpA-1B	64-mer	GAT CAG GAA ATC GTC GAG AGA TTT ACC TTC TGC CAG CGC CTG AGC GTG TAG GCT GGA GCT GCT T	disruption of *stpA* gene (partial deletion)
stpA-2B	71-mer	GTC CGT AAT GTT ACA AAG TTT AAA TAA CAT TCG CAC CCT CCG TGC CAT ATG AAT ATC CTC CTT AGT TCC TA	
stpA-3	20-mer	GGA ATC AGC GGT TTT TGT GG	confirmation of *stpA*
stpA-4	20-mer	GGA ATT AGC GAG CAG AGA GC	genotype

Table 5 - continued

Name	Length	Sequence (5'→3')	Application
hlpII-1	69-mer	GCA TT A TTT TTA TTA ATC GCC TAT TTT AAA ACA CCG GAT GAC ATA CTA TGG TGT AAG CTG GAG CTG CTT	disruption of *hlp* gene
hlpII-2	71-mer	CTG TTA TCT TGA GAA CAG TGA AGC CCG GAT ATG CTG TAG CGG TTA CAT ATG AAT ATC CTC CTT AGT TCC TA	
hlp-3	20-mer	CCA TCA AAC CAA AAG CGC AG	confirmation of *hlp*
hlp-4	20-mer	GCT GCG TAT CAT TGG TGG CG	genotype
lon-1	64-mer	GTC ATC TGA TTA CCT GGC GGA AAT TAA ACT AAG AGA GAG CTC TAT GGT GTA GGC TGG AGC TGC T	disruption of *lon* gene
lon-2	71-mer	CCT GCC AGC CCT GTT TTT ATT AGT GCA TTT TGC GCG AGG TCA CTA CAT ATG AAT ATC CTC CTT AGT TCC TA	
lon-3	20-mer	CTC GGC GTT GAA TGT GGG GG	confirmation of *lon*
lon-4	20-mer	CCG CCA TCT AAC TTA GCG AG	genotype
hlp-primext	20-mer	GCC TGT GCG CGA AGT GTA CG	5'IRD$_{800}$-labeled oligo for primer extension
XhoI-His-hlp	83-mer	TGC TCT AGA TAG TAA AGG AAA AAC T ATG CAT CAC CAT CAC CAT CAC ATC GAG GGC AGG ATG AGT GAA GCT CTT AAG GCA CTG	amplification of 6xHis-*hlp* fragment for cloning into pASK75
hlp-HindIII	30-mer	TGC AAG CTT TTA GAT AGC AAA GTC TTC CAG	
hlp-fwHindIII	26-mer	GCG AAG CCT CCA TCA AAC CAA AAG CG	amplification of native *hlp* fragment for cloning into pWKS30
hlp-rv-XbaI	27-mer	GCG TCT AGA GCT GCG TAT CAT TGG TGG	
pASK75seq	23-mer	CGA ATG GCC AGA TGA TTA ATT TCC	sequencing primer for pASK75 constructs
16S-I	19-mer	TCT CCT GAG AAC TCC GGC A	standardization of RT-
16S-II	19-mer	CAG CGT TCA ATC TGA GCC A	PCR reactions
hns-RT1	20-mer	CAG CTG GAG TAC GGC CTT GG	Amplification of *hns*-
hns-RT2	20-mer	CGT ACT CTT CGT GCG CAG GC	transcript by RT-PCR
stpA-RT1	20-mer	GCA ATT GGC TTC GGT GTA CG	Amplification of *stpA*-
stpA-RT2	20-mer	TCG CGA ATT CTC CAT TGA CG	transcript by RT-PCR
hlp-RT1	20-mer	CGT ACA CTT CGC GCA CAG GC	Amplification of *hlp*-
hlp-RT2	20-mer	CCA GTG TCT TAC CAG CTT CG	transcript by RT-PCR
c2410-fw	21-mer	CAG ACA ACA GTG ATT TAA TCG	Amplification of orf upstream of *hlp* by RT-PCR
c2410-rv	20-mer	CTG CGC TTT TGG TTT GAT GG	
fimA-RT1	20-mer	GTT GTT CTG TCG GCT CTG TC	Amplification of *fimA*-
fimA-RT2	20-mer	TCT GAA CTA AAT GTC GCA CC	transcript by RT-PCR
prfA-RT1	20-mer	CCC CTC TTT TAC ATG GTT GC	Amplification of *prfA*-
prfA-RT2	20-mer	GGC AGT GGT GTC TTT TGG TG	transcript by RT-PCR
sfaA-RT1	20-mer	GGT TAA TGG TGG TAC AGT TC	Amplification of *sfaA*-
sfaA-RT2	20-mer	CCT ACA TTT GTT GCA CTA CC	transcript by RT-PCR
hlyA-RT1	20-mer	GCA CAC TGC AGT CTG CAA AG	Amplification of *hlyA*-
hlyA-RT2	20-mer	GTG TCC ACG AGT TGG TTG AT	transcript by RT-PCR
crp-RT1	20-mer	GAG CAC GCT TAT TCA CCA GG	Amplification of *crp*-
crp-RT2	20-mer	CCG GGT GAG TCA TAG CAT CC	transcript by RT-PCR

Table 5 - continued

Name	Length	Sequence (5'→3')	Application
fepA-RT1	20-mer	CCT TCC AGA CCT TCA ACC AC	Amplification of *fepA*-
fepA-RT2	20-mer	CGT AGC CCG TAT TCA AAA GC	transcript by RT-PCR
fyuA-RT1	20-mer	CGA CGT TTT ATA CCC ACA CC	Amplification of *fyuA*-
fyuA-RT2	20-mer	CCA TAG GTA CGG TAA CGA CG	transcript by RT-PCR
chuA-RT1	20-mer	CCT GCT GCC CTT GAT AAC TG	Amplification of *chuA*-
chuA-RT2	20-mer	CCA AAC CCG AAC TTA CGT CC	transcript by RT-PCR
iroN-RT1	20-mer	CCT GGT TGG GGT TGA ATA GCC	Amplification of *iroN*-
iroN-RT2	20-mer	CGC CCT CTT CGC TAC TTT CC	transcript by RT-PCR
csgA-RT1	20-mer	GCT CTG GCA GGT GTT GTT CC	Amplification of *csgA*-
csgA-RT2	20-mer	CCA AAG CCA ACC TGA GTG AC	transcript by RT-PCR
kpsE-RT1	20-mer	CGT ATC TGC GTG AGG ACG CT	Amplification of *kpsE*-
kpsE-RT2	21-mer	CGA TTC CTG CGG CAA CTG TGG	transcript by RT-PCR
orf70-RT1	20-mer	CCA AGT CAT AAC CGA GTG GG	Amplification of *orf70*-
orf70-RT2	21-mer	GCA CTG TCA GCT TCA GCA ACC	transcript by RT-PCR
kpsM-RT1	20-mer	GAA AGC CGC CGT TCA TGC TC	Amplification of *kpsM*-
kpsM-RT2	20-mer	GCC CCT ATA GAC CGC GTA GC	transcript by RT-PCR
hns-prom1	20-mer	CCC TGC TCT TAT TGC GAC TG	Amplification of *hns*
hns-prom2	20-mer	CAC GAA GAG TAC GGA TGT TG	promoter region for gel shift (~350bp)
stpA-prom1	20-mer	GAC AGC AGA AAG CAC CAG TG	Amplification of *stpA*
stpA-prom2	20-mer	ACG GAG GGT GCG AAT GTT AT	promoter region for gel shift (~350bp)
hlp-prom1	20-mer	GCG ATG AAG AAA TAG TAG CC	Amplification of *hlp*
hlp-prom2	20-mer	CGC GAA GTG TAC GAA TAT TG	promoter region for gel shift (~350bp)
kpsF-prom1	19-mer	CAT CAC CAT TAT TTG CGT G	Amplification of *kpsF*
kpsF-prom2	20-mer	GTA CTG CTC TGG TCA TCA GG	promoter region for gel shift (~350bp)
kpsM-prom1	20-mer	GTT GGT AAT CAA TCG CGT GC	Amplification of *kpsM*
kpsM-prom2	20-mer	GCA TGA ACG GCG GCT TTC TG	promoter region for gel shift (~350bp)
ORF72-prom1	22-mer	CCA GAT AGT TGC GAT TAC ATT G	Amplification of ORF72
ORF72-prom2	24-mer	CTT TAC ATT CGT ACT CAT TAC ATG	promoter region for gel shift (~350bp)

3.4. Chemicals and enzymes

All chemicals and enzymes used in this study were purchased from the following companies: New England Biolabs (Frankfurt am Main), Invitrogen (Karlsruhe), MBI Fermentas (St. Leon-Roth), Roche Diagnostics (Mannheim), Gibco BRL (Eggenstein), Dianova (Hamburg), Difco (Augsburg), Merck (Darmstadt), Oxoid (Wesel), GE Healthcare/Amersham Biosciences (Freiburg), Roth (Karlsruhe), Serva and Sigma-Aldrich (Taufkirchen).

Radionucleotides were purchased from Amersham Biosciences (Freiburg).

The following commercial kits were used:

- Plasmid Mini and Midi kit, QIAGEN, Hilden
- PCR purification kit, QIAGEN, Hilden
- Gel extraction kit, QIAGEN, Hilden
- RNeasy kit, QIAGEN, Hilden
- MICROBExpress kit, Ambion, Huntingdon (UK)
- Omniscript Reverse Transcriptase, OIAGEN, Hilden
- Superscript III Reverse Transcriptase, Invitrogen, Karlsruhe
- pGEM®-T_{easy} Vector System, Promega, Mannhein
- SequiTherm EXCELL II DNA Sequencing Kit-LC, Epicentre, Oldendorf
- ABI Prism BigDye Terminator Cycle Sequencing Ready Reaction kit, Applied Biosystems, Foster City (USA)
- ECL™ Direct Acid Labeling and Detection System, and ECL™ advance system, Amersham Biosciences, Freiburg
- Protino Ni-1000 protein purification kit, Macherey-Nagel, Düren
- Gelfiltration LMW calibration kit, Amersham Biosciences, Freiburg
- Roti-Nanoquant, Roth, Karslruhe

3.5. Antibodies

The following antibodies were used for Immunoblotting:

- polyclonal antibody against purified P-related fimbriae from rabbit (Dr. Salam Kahn)
- polyclonal antibody against purified S fimbriae from rabbit (Dr. Salam Kahn)
- polyclonal antibody against H-NS from rabbit (kind gift from B. E. Uhlin)
- polyclonal anitbody against StpA/Hlp from rabbit (kind gift from B. E. Uhlin)
- polyclonal anti-rabbit antiserum from donkey; HRP conjugated (Dianova)

3.6. Media, Agar-plates and antibiotics

All media were autoclaved for 20 min at 120 °C, if not stated otherwise. Supplements for media and plates were sterile filtered through a 0.22 µm pore-filter and added after cooling down the media to <50 °C.

3.6.1. Media

LB medium (Luria-Bertani): (Sambrook *et al.*, 1989)

10 g	tryptone from casein	
5 g	yeast extract	
5 g	NaCl	ad 1 l dH_2O

MM9 minimal medium: (Kalinowski *et al.*, 2000)

100 ml	10 x MM9 salts	3 g l^{-1} KH_2PO_4
		5 g l^{-1} NaCl
		10 g l^{-1} NH_4Cl
100 ml	0.5 M Tris (pH 6.8)	
100 ml	10 % (w/v) casamino acids	
20 ml	20 % (w/v) glucose	
2 ml	1 M $MgSO_4$	
0.1 ml	1 M $CaCl_2$	
0.3 ml	10 mM thiamine	ad 1 l dH_2O; sterile filtered

M63B1 minimal medium:

10 ml	20 % (w/v) $(NH_4)_2SO_4$ solution	
13.6 g	KH_2PO_4	
1 ml	10 % (w/v) $MgSO_4$ solution	
1 ml	0.1 % (w/v) $FeSO_4$ solution	ad 978 ml dH_2O

pH adjusted to 7 with KOH and autoclaved; then addition of

2 ml	0.05 % (w/v) thiamine (sterile filtered)
20 ml	20 % (w/v) glucose (sterile filtered)

MMA minimal medium: (Silhavy *et al.*, 1984)

10.5 g	K_2HPO_4	
5.5 g	KH_2PO_4	
1 g	$(NH_4)_2SO_4$	
0.5 g	sodium-citrate x $2H_2O$	
1 g	casamino acids	
20 ml	20 % (w/v) glucose	
1 ml	1 M $MgSO_4$	
5 ml	0.4 % (w/v) tryptophane	
60 ml	5 M NaCl	ad 1 l dH_2O; sterile filtered

3.6.2. Agar plates

LB agar plates:

LB medium + 1.5 % (w/v) agar (Difco Laboratories, Detroit, USA)

Motility agar plates:

LB medium + 0.3 % (w/v) agar

Blood agar plates:

LB plates containing 5 % (v/v) washed sheep erythrocytes
(Elocin Lab, Mühlheim a. d. Ruhr)

***bgl* agar plates:** (Free *et al.*, 1998)

10 g	tryptone from casein	
5 g	yeast extract	
5 g	NaCl	
15 g	agar	ad 735 ml dH_2O

autoclaved and cooled to 50 °C, then addition of

200 ml	2.5 % (w/v) salicin solution (sterile filtered)		
5 ml	indicator solution (sterile filtered):	12.5 ml	EtOH
		0.5 g	bromophenol blue
		0.5 ml	10 N NaOH
		12 ml	dH_2O

Congo Red agar plates:

1 l autoclaved LB agar without salt

1 ml 0.4 mg ml^{-1} Congo Red dye solution

1 ml 0.2 mg ml^{-1} Coomassie brilliant blue R-250

dye solutions were stirred for 1h at 50 °C and sterile filtered

Fluostain agar plates: (Solano *et al.*, 2002)

LB agar without salt

200 µg ml^{-1} Fluostain 1 (Sigma)

CAS agar plates: (Schwyn and Neilands, 1987)

I) *Basal agar medium*:

30.24 g PIPES; dissolved in 250 ml dH_2O + 12 ml 50 % NaOH

100 ml 10 x MM9 salts 3 g l^{-1} KH_2PO_4

5 g l^{-1} NaCl

10 g l^{-1} NH_4Cl

autoclaved and cooled to 50 °C;

15 g agar dissolved in 500 ml dH_2O

autoclaved, cooled to 50 °C and mixed with first solution; then addition of

30 ml 10 % (w/v) casamino acids solution (sterile filtered)

10 ml 20 % (w/v) glucose solution (sterile filtered)

II) *CAS indicator solution*: (100 ml)

60.5 mg Chrome azurole S (CAS; Sigma) dissolved in 50 ml dH_2O

10 ml iron ^{III} solution: 27 mg $FeCl_3$ x 6 H_2O

83.3 µl 37 % HCl

ad 100 ml dH_2O

To the above solution, 72.9 mg hexadecyltrimethyl ammonium bromide (HDTMA) dissolved in 40 ml distilled water was added slowly under stirring. The resultant dark blue solution was sterile filtered, heated to 50 °C and added very slowly along the glass walls to the basal agar medium before pouring approximately 25 ml into each plate.

3.6.3. Antibiotics

When appropriate, media and plates were supplemented with the antibiotics listed in Table 6 in the indicated concentrations. Stock solutions were sterile filtered and stored at –20 °C until usage.

Table 6: Antibiotic substances used in this study.

Antibiotic	Stock concentration	Solvent	Working concentration
Chloramphenicol (Cm)	50 mg ml^{-1}	EtOH	20 µg ml^{-1}
Ampicillin (Ap)	100 mg ml^{-1}	dH_2O	100 µg ml^{-1}
Kanamycin (Km)	50 mg ml^{-1}	dH_2O	50 µg ml^{-1}
anhydro-Tetracycline (aTc)	2 mg ml^{-1}	EtOH	0.2 µg ml^{-1}
Spectinomycin (Spec)	100 mg ml^{-1}	dH_2O	100 µg ml^{-1}

3.7. DNA and Protein Markers

To determine the size of DNA fragments in agarose gels, the "Generuler^{TM}" 1-kb DNA ladder, purchased from MBI Fermentas, was used (Fig 7 A). As a reference in denaturing agarose gels for Northern blotting, both the low-range RNA marker from Peqlab, as well as the 0.24-9.5-kb RNA ladder from Invitrogen were used (Fig 7 B and C, respectively). To determine the molecular weight of protein fractions separated by polyacrylamide gel electrophoresis, "Rainbowmarker" (RPN800) purchased from Amersham Biosciences was used (Fig 7 D).

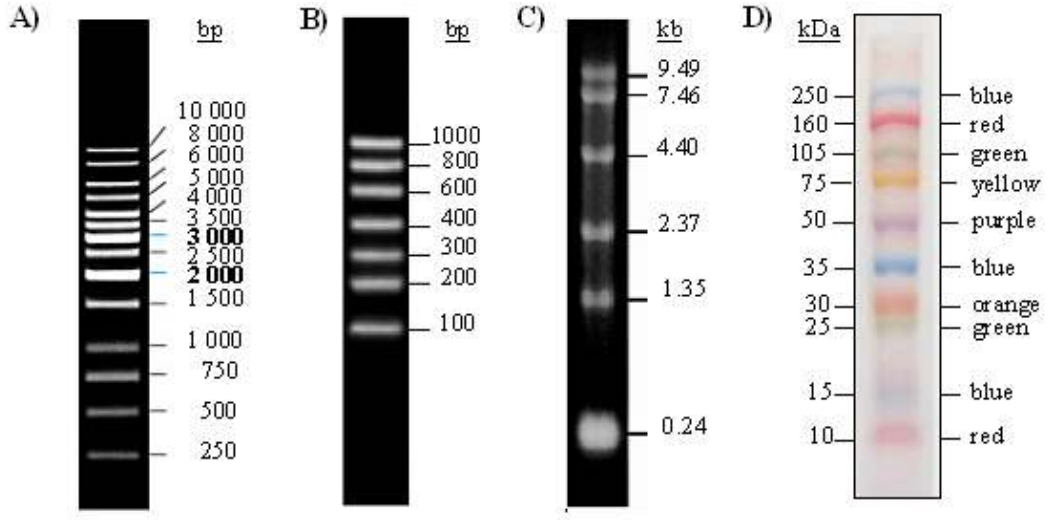

Fig. 7: DNA and protein markers used for electrophoresis. (A) Generuler 1-kb DNA ladder (Fermentas); (B) Low range RNA ladder (Peqlab); (C) 0.24-9.49-kb RNA ladder (Invitrogen); (D) Rainbowmarker (Amersham Biosciences).

3.8. Technical Equipment

Balances	IL-180, Chyo Balance Corp
	Kern 470
	Ohaus Navigator
Autoclaves	Integra Bioscience, H+P Varoclav
Incubators	Memmert Tv40b (30°C, 43°C) Heraeus B5050E (37°C)
Clean bench	NUAIRE, Class II, type A/B3
Electrophoresis systems	BioRad
Electroporator	Gene Pulser, BioRad
FPLC	Amersham Pharmacia
Hybridization oven	HybAid Mini 10
Centrifuges (cooled)	Beckmann J2-HC → JA10 and JA20 rotors
	Haraeus Sepatech Megafuge1.OR Haraeus Sepatech Biofuge 13R
Centrifuges (table top)	Eppendorf 5415C Hettich Mikro20
Magnetic stirrer	Heidolf MR3001K
Micropipettes	Eppendorf Research 0.5-10 µl
	Gilson pipetman 20 µl, 200 µl, 1000 µl
Microwave	AEG Micromat
Power supplies	BioRad Power Pac 300
PCR-Thermocycler	Biometra T3
pH-meter	WTW pH 525
Documentation	BioRad GelDoc2000 + MultiAnalyst Software V1.1
Developer	Agfa Curix 60
Photometer	Pharmacia Biotech Ultrospec 3000
Phosphoimager	Amersham Biosciences, Typhoon 4600
Shakers	Bühler TH30 SM-30 (37°C, 150 rpm)
	Innova 4300, New Brunswick Scientific (37°C, 220 rpm)
	Innova 4230, New Brunswick Scientific (30°C, 220rpm)
Sonicator	Bandelin Sonoplus HD70; Tip UW70
Speedvac	Savant SC110
Thermoblocks	Liebisch
Vacuum Blotter	Pharmacia + LKD Vacu Gene Pump
Videoprinter	Mitsubishi Hitachi, Cybertech Cb1
Vortexer	Vortex-Genie 2^{TM} Scientific Industries
UV-Crosslinker	BioRad
Waterbath	GFL 1083, Memmert

4. Methods

If not stated otherwise, all methods followed the instructions described in the CSH Laboratory Manual (Sambrook 1989). Centrifugations with no other indications were carried out in a table top centrifuge at 13,000 rpm.

4.1. Manipulation of DNA

4.1.1. Small scale isolation of plasmids

While using the QIAGEN Plasmid Midi and Mini Kit, bacteria were collected from 100 ml over night cultures by centrifugation (6,000 rpm, 4 °C, 15 min) and resuspended in 4 ml buffer P1, according to the manufacturer's recommendations. After 5 min incubation at room temperature, 4 ml buffer P2 were added for lysis of the cells. After clearing of the suspension, 4 ml neutralization buffer P3 were added and samples were incubated for 10 min on ice. Cell debris and genomic DNA was removed by centrifugation (11,000 rpm, 4 °C, 30 min). Plasmid DNA containing supernatant was loaded on equilibrated columns by gravity flow. Columns were washed with buffer QC. Subsequently, plasmid DNA was eluted with 3.5 ml buffer QF and precipitated by addition of 0.7 vol isopropanol. After centrifugation (13,000 rpm, 4 °C, 20 min), DNA pellets were washed with 70 % (v/v) ethanol, air-dried and resuspended in water.

Plasmid isolation using the QIAspin mini kit were performed similarly with some modifications: bacteria were harvested from 1-10 ml over night cultures, buffer N3 containing guanidine hydrochloride was used for neutralization, and plasmid DNA was purified from the supernatant by using small spin columns, which were centrifuged at 13,000 rpm for 1 min DNA was eluted in a small volume of dH_2O and directly used for further experiments.

4.1.2. Isolation of chromosomal DNA

Bacteria from 1 ml of an over night culture were harvested by centrifugation for 4 min in a 1.5 ml reaction tube. After washing with 1 ml TNE buffer, cells were centrifuged for 4 min and resuspended in 270 µl TNE-X solution. 30 µl lysozyme (5 mg ml^{-1}) were added and samples were incubated for 20 min at 37 °C. Afterwards, 15 µl proteinase K (20 mg ml^{-1}) were added and further incubated for up to 2 h at 65 °C until the solution became clear. The genomic DNA was precipitated by addition of 0.05 vol 5 M NaCl (15 µl) and 500 µl ice-cold ethanol and then collected by centrifugation for 15 min. After washing two times with 1 ml

70 % (v/v) ethanol, DNA pellets were air-dried and redissolved in 100 µl sterile dH_2O. (after Grimberg *et al*. (1989))

TNE:	10 mM	Tris	
	10 mM	NaCl	
	10 mM	EDTA	pH 8.0
TNE-X:	TNE + 1 % Triton X-100		

4.1.3. Precipitation of DNA with alcohol

DNA was either precipitated with ethanol or with isopropanol. In the first case, 0.1 vol 3 M Na-acetate (pH 4.8) were added to the samples before the addition of 2.5 vol ice-cold 100 % (v/v) ethanol. For the precipitation with isopropanol, 0.7 vol were used. Samples were incubated for at least 1 h at –80 °C before centrifugation (13,000 rpm, 4 °C, >20 min). The DNA pellet was washed with 70 % (v/v) ethanol, dried in a Speedvac for 10 min and resuspended in dH_2O.

4.1.4. Determination of nucleic acid concentrations

Nucleic acid concentrations were measured at 260 nm in quartz cuvettes with a diameter of 1 cm. An absorption at 260 nm of 1.0 corresponds to 50 µg ml^{-1} double-stranded DNA or 40 µg ml^{-1} RNA. The purity of the preparations was determined by measuring the absorption of the sample at 280 nm. DNA and RNA was considered sufficiently pure when the ratio A260 / A280 was higher than 1.8 or 2.0, respectively.

4.1.5. Polymerase chain reaction (PCR)

This method allows the exponential amplification of DNA regions *in vitro* by using a heat-stable DNA polymerase from *Thermophilus aquaticus* (*Taq*). This way, even small amounts of template DNA can be amplified to high copy numbers and easily visualized during screening assays. Another application of PCR is site-directed mutagenesis by using oligonucleotides with adapted sequences, e.g. restriction sites.

Standart PCR

For routine PCR-amplification, *Taq* DNA polymerase kits of different suppliers (QIAGEN, Sigma) were used. Usually, the reaction was performed in a final volume of 20 µl.

Mix for one sample:

2 µl	10 × reaction buffer (QIAGEN)
2 µl	20mM dNTP mix (Sigma)
0.6 µl	25 mM $MgCl_2$
0.2 µl	100 pM primer solution 1
0.2 µl	100 pM primer solution 2
1 µl	100 ng μl^{-1} template DNA or boiled cells
0.05 µl	*Taq* DNA polymerase (QIAGEN)
14 µl	dH_2O

For the Sigma Red *Taq* polymerase kit, both primers and template DNA were added to 8.6 µl dH_2O and 10 µl 2x Red *Taq* ready mix (see the manufacturer's instructions).

The thermal profile was designed according to the annealing temperature of the individual primers and the length of the expected amplification product:

Initial denaturation	2 min, 95 °C	
1. Denaturation	45 sec, 95 °C	25-35 cycles
2. Annealing	45 sec (54-60 °C)	
3. Elongation	30 sec 0.5-5 min, 72 °C	
Final elongation	2 min, 72 °C	

PCR with proof-reading polymerases

For site-directed mutagenesis using PCR products, a different polymerase with 3'→5' proof-reading activity had to be used in order to prevent misincorporations during extension. The composition of a typical PCR mix for the λRed-Mutagenesis (see section 4.1.11) is given below:

Mix for 1 sample:

5 µl	10 × Opti buffer (Eurogentec)
5 µl	20mM dNTP mix (Sigma)
3.5 µl /kb	50 mM $MgCl_2$
1 µl	100 pM primer solution 1
1 µl	100 pM primer solution 2
1 µl	100 ng μl^{-1} template plasmid DNA
0.5 µl	DAP Goldstar polymerase (Eurogentec)
	ad 50 µl dH_2O

After amplification, PCR products were eventually purified using a commercial PCR purification kit (QIAGEN). For this purpose, 5 vol buffer PB were added to the PCR samples and the mixture was loaded onto the spin columns. Washing and elution was performed as described for the gel extraction kit (see section 4.1.8.).

4.1.6. Enzymatic digest of DNA with restriction endonucleases

The DNA was dissolved in dH_2O and mixed with 0.2 vol 10 × reaction buffer and 1 U of restriction enzyme per µg DNA, so that the final volume of the sample was 15 µl for plasmid DNA and 50 µl for genomic DNA. The mixture was incubated at 37 °C, depending of the specific requirements of the enzyme indicated on the product sheets. Whereas plasmid DNA was digested for one to two hours, digestion of genomic DNA was carried out over night. The reaction was stopped by adding 0.2 vol stop-mix (see following section 4.1.7.). When appropriate, inactivation of the restriction enzyme was carried out by heating the samples for 20 min at 65 °C.

4.1.7. Horizontal Gel Electrophoresis

For routine analytical and preparative separation of DNA fragments, horizontal gel electrophoresis was performed using agarose gels under non-denaturing conditions. Depending on the size of the DNA fragments to be separated, the agarose concentration varied between 1 and 2 % (w/v) in running buffer (1 × TAE). In order to have a visible running front and to prevent diffusion of the DNA, 0.2 vol loading dye was added to the samples before loading. The electrophoresis was carried out at a voltage in the range between 16-120 V. The gels were stained in an ethidium bromide solution (10 mg ml^{-1}), washed with water and photographed under a UV-transilluminator.

50x TAE buffer:	2 M	Tris
	6 % (v/v)	acetic acid (99.7 %)
	50 mM	EDTA (pH 8.0)
		ad 1 l dH_2O
6x loading dye:	0.25 %	bromophenol blue
	0.25 %	xylenecyanol FF
	15 %	Ficoll (Type 400, Pharmacia)
	30 %	glycerol
		ad 50 ml dH_2O

4.1.8. Isolation of DNA fragments from agarose gels

DNA was purified from agarose gels using the QIAquick Gel Extraction Kit (QIAGEN). Agarose pieces containing the DNA fragment of interest were cut out of the gel and subsequently melted for 10 min at 50 °C in QG buffer (supplied by the manufacturer). The DNA was separated from the rest of the solution by applying the mixture to QIAquick spin columns followed by centrifugation for 1 min. The columns were then washed with 750 µl PE buffer (supplemented with ethanol). Residual PE buffer was removed by centrifugation (2 × 1 min). Finally, the DNA was by eluted from the column with 20-50 µl sterile dH_2O.

4.1.9. Ligation of DNA fragments

Linearized vector and insert DNA after restriction digest can be ligated either due to the presence of sticky ends or by blunt-end ligation. The modifying enzyme for ligation process was a T4-DNA ligase (New England Biolabs). Best efficiencies were obtained using a insert/vector ratio of 3/1. Reactions were performed over night at 16 °C in a final volume of 15 µl containing 1.5 µl 10 x ligation buffer and 50 U T4 ligase.

4.1.10. Transformation of bacterial cells

Preparation of $CaCl_2$ competent bacterial cells and heat-shock transformation

A 100 ml LB culture was inoculated with 1 ml of an over night culture. Cells were grown to an OD_{600} of 0.6-0.8 and cooled on ice. The culture was centrifuged for 5 min at 3,500 × g at 4 °C and the pellet was resuspended in 50 ml ice-cold 0.1 M $CaCl_2$ and incubated on ice for 30 min. After a second centrifugation, the cells were resuspended in 2 ml ice-cold 0.1 M $CaCl_2$ and either used immediately for transformation, or prepared for freezing at –80 °C by addition of 50 % (v/v) glycerol to a final concentration of 15 %. 200 µl of competent cells were thawed on ice and ~ 100 ng of plasmid DNA were added for transformation. After incubation on ice for 30 min, the cells were incubated at 42 °C for 90 sec and then again placed immediately on ice for 5 min. 1 ml LB was added and the cells were incubated at 37 °C for 1 h, allowing the expression of the selection marker before the mixture was plated on selective LB agar plates.

Preparation of electrocompetent cells and electroporation

50 ml LB medium were inoculated with 500 µl of an over night culture of the strain of interest and grown OD_{600} of 0.6-0.8. The cells were collected by centrifugation for 10 min at

2,000 × g at 4 °C. The pellet was left on ice for 30 min and then washed with 50 ml ice-cold dH_2O. After a second centrifugation step at the same conditions, the pellet was resuspended in 25 ml 10 % (v/v) glycerol, centrifuged again and finally resuspended in 600 µl 10 % glycerol. The cells were stored as 40 µl aliquots at -80 °C. For electroporation, one aliquot was thawed on ice and mixed with ~ 0.5 µg DNA. The mixture was applied into a "Gene pulser" cuvette (BioRad) with a distance between the electrodes of 0.1 cm and incubated for 10 min on ice. The cells were electroporated using a Gene pulser transfection apparatus (BioRad) at the following conditions: 2.5 kV, 25 µF, and 600 Ω for linear fragments or 200 Ω for plasmids. Immediately after electroporation, 1 ml LB medium was added to the cuvettes. The mixture was transferred into a new tube and incubated at 37 °C (or 30 °C for temperature-sensitive plasmids) for 1 h before the cells were plated on selective agar plates.

4.1.11. Gene inactivation by λ Red recombinase-mediated mutagenesis using linear DNA fragments

The construction of the mutants was performed using linear DNA for recombination, as described by Wanner and Datsenko (2000). This method relies on the replacement of a chromosomal sequence with an antibiotic marker that is generated by PCR using primers with homology extensions to the flanking regions of the target sequence. Recombination is mediated by the Red recombinase derived from the λ phage. This recombination system consists of three genes (*γ, β, exo*), which encode the phage recombinases and an inhibitor of the host RecBCD exonnuclease V, which normally mediates degradation of linear DNA in the cell. A schematic overview of the procedure is depicted in Figure 8.

Briefly, a linear DNA fragment containing an antibiotic marker cassette flanked by FRT sites and 45-nt homologous extensions to the target genes (up- and downstream of *hns*, *hlp*, and *stpA*, respectively) was amplified by PCR as described in section 4.1.5.2.. The proof-reading Dap Goldstar polymerase (Eurogentec) was used for amplification of the linear fragments with plasmids pKD3 (harboring a cassette) or pKD4 (harboring a kanamycin resistance cassette) as template in a total volume of 400 µl. The annealing temperature for all primers was 54 °C using 30 cycles of amplification. PCR products were purified using the QIAquick PCR purification kit, ethanol precipitated and resuspended in 10 µl dH_2O.

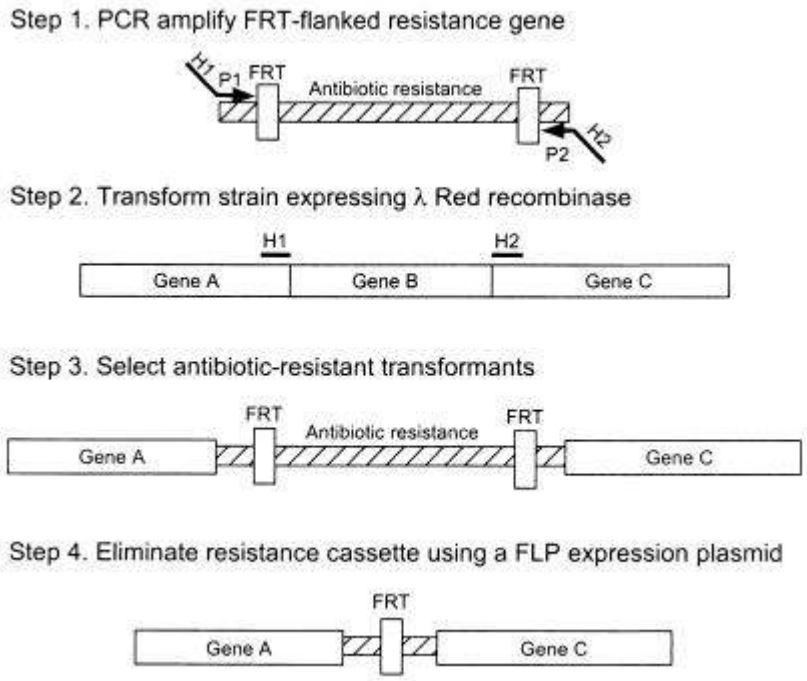

Fig. 8: Strategy for inactivation of chromosomal genes using PCR products
(Datsenko and Wanner, 2000)

Meanwhile, 536 wild type cells were first transformed with the pKD46 helper plasmid by electroporation (see section 4.1.10.2.). Transformants were selected at 30 °C on agar plates containing 100 µg ml^{-1} ampicillin. Of these transformants, electrocompetent cells were prepared from 50 ml LB cultures supplemented with ampicillin and 3 ml of an 0.1 M arabinose solution to induce the Red recombinase on the helper plasmid. 40 µl competent cells were transformed with 5 µl of the linear PCR fragment by electroporation. After the addition of 1 ml LB medium to the cuvette, cells were allowed to recover by incubation for 2 h at 30 °C with aeration. In contrast to normal electroporation, the cultures were then taken out of the incubator and left standing on the bench top over night at room temperature. In the next morning, cells were spun down, resuspended in 300 µl LB medium and distributed onto three agar plates supplemented with the appropriate antibiotic (Cm or Km, respectively). Transformants with confirmed allelic exchange were also re-streaked onto ampicillin-containing agar plates at 37 °C to confirm loss of the temperature-sensitive helper plasmid pKD46.

The antibiotic marker could be removed with the help of the FLP recombinase (encoded on plasmid pCP20), which mediates recombination between the two FRT sites flanking the antibiotic cassette, thus leaving behind a complete deletion of the open reading frame.

Electroporation was performed as described in section 4.1.10.2.. Transformants were first selected on ampicillin-containing agar plates at 30 °C, and then re-streaked onto LB agar plates with no antibiotic. These plates were incubated at 37 °C in order to induce the loss of the second helper plasmid pCP20. The deletion mutants now could be used to introduce a second or third mutation by starting the whole procedure from the beginning. All mutations were confirmed by both PCR and Southern hybridization.

4.1.12. Southern Blot analysis

Vacuum blotting

For Southern blot analysis, 10 µg chromosomal DNA were restricted with an appropriate endonuclease, harboring 1 to 5-kb DNA fragments containing the target gene. The DNA fragments were separated by horizontal gelelectrophoresis (see section 4.1.7.). Meanwhile, a nylon membrane (Nytran Super Charge; pore size 0.45 µm; Schleicher&Schuell, Dassel, Germany) of appropriate size was shortly preincubated in dH_2O and then soaked for 10 min in 20 × SSC. Afterwards, DNA was transferred from the agarose gel to the membrane using a vacuum blotter (Amersham-Pharmacia) by applying a 50 mbar vacuum. The following solutions were applied on the surface of the agarose gel during the blotting procedure:

Depurinization solution (0.25 N HCl)	8 min
Denaturation solution (0.5 N NaOH; 1.5 M NaCl)	8 min
Neutralization solution (0.5 M Tris-HCl, pH 7.5; 1.5M NaCl)	8 min
20 × SSC (0.3 M Na-citrate, pH 7.0; 3 M NaCl)	>50min

After DNA transfer, the nylon membrane was incubated for 1 min in 0.4 N NaOH and 1 min in 0.25 M Tris-HCl, pH 7.5 for neutralization. The membrane was then shortly dried and the DNA was crosslinkd to the membrane by exposure to UV light.

Probe labelling (ECL™ Kit, Amersham Biosciences)

For labelling of DNA probes, the ECL™-Kit (enhanced chemoluminescence) was used. The binding of a DNA probe to the complementary sequence on the nylon membrane was detected by chemoluminescence. Positively charged horseradish peroxidase molecules were mixed with the negatively charged DNA probe. Addition of glutaraldehyd covalently linked the horseradish peroxidase molecules with the DNA probes. Reduction of H_2O_2 by the peroxidase

requires the oxidation of luminol which results in light emission, which can be detected by suitable light-sensitive films, e.g. the Hyperfilm ECL.

For labeling of the probe, 100 ng DNA per ml hybridization buffer in a final volume of 10 µl in dH_2O were denatured for 10 min at 90 °C and cooled for 5 min on ice. Subsequently, 10 µl labelling reagent and 10 µl glutaraldehyd were added. The mixture was incubated for 10 min at 37 °C and then added to the hybridization reaction.

Hybridization and detection of the membrane

Hybridization of the membrane was carried out over night at 42 °C in hybridization solution (10-15 ml), after the nylon membrane had been pre-incubated at 42 °C in the hybridization solution for 1 h. The next day, the membrane was washed twice for 20 min at 55 °C with wash solution I and two times for 10 min at RT with wash solution II. The membrane was placed on Whatman paper to remove the rest of the wash solution, and then incubated for 5 min in 5-10 ml detection solution I and detection solution II provided with the kit and mixed immediately (1:1) before application to the membrane. The membrane was superficially dried on Whatman paper and packed in saran wrap avoiding air bubbles on the top surface of the membrane. Chemoluminescence was detected by exposure of the membrane to Hyperfilm ECL. The exposure time depended on the signal intensity.

Wash solution 1: 0.5 × SSC; 0.4 % (w/v) SDS

Wash solution 2: 2 × SSC

4.1.13. Sequence analysis

The nucleotide sequences of mutagenized chromosomal genes or plasmid constructs was determined using fluorescent dye terminators (ABI prism BigDye terminator kit, Applied Biosystems). The sequencing-PCR mix for one sample was:

30 ng	PCR product (or: 0.5 µg plasmid DNA)	
1.5 µl	10 pM primer	
2 µl	5 x buffer (kit component)	
2 µl	premix (kit component)	ad 10 µl ABI-H_2O

The thermal profile for the PCR reaction was: 40 cycles of denaturation at 96 °C for 30 sec, annealing at ≤ 60 °C for 15 sec, and extension at 60 °C for 4 min, followed by final extension at 60 °C for 2 min. Sequencing products were purified by ethanol precipitation (see section 4.1.3.) and analyzed in a ABI prism sequencer (Perkin Elmer).

4.2. Manipulation of RNA

For working with RNA, special care had to be taken in order to prevent contamination of the samples with exogenous RNases. Gloves were worn throughout the experiment and double autoclaved pipette tips and reaction tubes were used. For all buffers and solutions, water was pre-treated over night with 0.1 % (v/v) diethylpyrocarbonate (DEPC) at 37 °C.

4.2.1. Isolation of total RNA with hot phenol

20 ml LB cultures were grown to mid-log phase, i.e. to an optical density at 600 nm of 0.6. Cells were harvested by centrifugation (4,000 rpm, 4 °C, 10 min) and then resuspended in 1 ml ice-cold KMT buffer. 600 µl each of the suspension were tranferred to two 2 ml safe-lock caps containing a mixture of 200 µl acid phenol (pH 4) and 400µl NEMST buffer pre-heated to 90 °C. For cell lysis, samples were incubated at 90 °C for 5 min, and then chilled on ice for another 5 min. After centrifugation in a table top centrifuge for 2 min at 13,000 rpm, phase separation occurred, resulting in an RNA containing aqueous phase and an acid phenol phase containing cell debris, proteins and DNA. The upper aqueous phase was carefully transferred to fresh tubes. Two additional phenol extractions and three chloroform extractions were performed before precipitation of total RNA with 0.7 vol isopropanol over night at – 20 °C. After centrifugation, the RNA pellet was washed with 70 % (v/v) ethanol and resuspended in 100 µl nuclease-free water. RNA preparation were stored at – 80 °C. [Chuang *et al*. (1993)]

KMT buffer: 10 mM KCl
5 mM $MgCl_2$
10 mM Tris
ad 200 ml DEPC-H_2O

adjust pH to 7.4 and autoclave

NEMST buffer: 0.4 M NaCl
40 mM EDTA
20 mM Tris
ad 190 ml DEPC-H_2O

adjust pH to 7.4 and autoclave

+ 8 ml 25 % SDS solution
+ 2 ml ß-mercaptoethanol

4.2.2. Removal of contaminating DNA by DNase treatment and RNA cleanup

Contaminating DNA was removed from total RNA preparations by DNase I digestion. 15 µg RNA in a final volume of 85 µl were mixed with 10 µl 10 x OnePhorAll plus buffer (Amersham Biosciences) and 5 µl RNase free DNase I (Roche Diagnostics). Samples were incubated for 1 h at 37 °C, followed by RNA cleanup using the RNeasy Mini kit (QIAGEN). According to the manufacturer's instructions, 350 µl RLT buffer supplemented with 10 µl ml^{-1} ß-mercaptoethanol and 250 µl 100 % (v/v) ethanol were added to the DNase treated RNA samples, before loading them onto the purification columns. After brief centrifugation, the columns were transferred to fresh collection tubes and washed twice with 500 µl RPE buffer. Finally, RNA was eluted from the column in 60 µl nuclease-free water.

As a control for successful removal of all DNA from the samples, 2 µl of the DNase treated RNA or 1 µl DNA as positive control were used as template in a PCR reaction with primers binding within the coding sequence of the α-hemolysin gene *hlyA*. The DNase digest was considered as complete if no product could be amplified from the RNA samples.

4.2.3. Enrichment of bacterial mRNA

Total RNA preparations consist of a mixture of ribosomal RNA (23 S, 16 S, and 5 S rRNA), transfer RNAs (tRNA), messenger RNA (mRNA), and small RNAs. The most abundant components are both the 23 S and 16 S rRNA, which therefore might interfere with downstream applications such as transcription studies.

Commercial kits like the MICROBExpress kit from Ambion are available, which can be used to remove rRNA from total RNA samples, thereby resulting in an enrichment of the messenger RNA. The principle of this method is a so called sandwich capture hybridization. Capture-oligonucleotides are used that can hybridize to the 16 S and 23 S rRNA molecules due to short complementary sequences. The other end of the capture oligo is complementary

to short oligonucleotide sequences coupled to a magnetic bead (so called Oligo MagBeads), which then binds the capture-oligo/rRNA hybrid molecules. The beads can then be retained in a magnetic stand, leaving only mRNAs, tRNA, 5 S rRNA and small RNAs in the supernatant.

The procedure was performed following the manufacturer's instructions. 10 µg of DNase-treated RNA in a final volume of 12 µl in nuclease-free water were mixed with 3 µl 10 mM EDTA in order to chelate divalent cations, which might cause hydrolysis of RNA. Subsequently, 200 µl binding buffer and 4 µl of the capture-oligo mix were added to the RNA samples with vortexing and brief centrifugation. The samples were then incubated at 70 °C for 10 min to denature the secondary structure of the RNA. Annealing of the capture-oligos to rRNA was performed for 1 h at 37 °C. In the meantime, 50 µl Oligo MagBeads per sample were prepared by washing them with water and resuspending them in binding buffer. After the annealing reaction was completed, 50 µl Oligo MagBeads, which have been pre-warmed to 37 °C, were added to the RNA samples and incubated for 15 min at 37 °C for binding of the beads to the oligo/rRNA hybrids. Removal of the magnetic beads was performed by placing the reaction tubes into a magnetic stand for > 3 min, during which time the beads were pulled to the side of the tubes. The clear supernatant containing the enriched mRNA was then transferred to a new tube and stored at –20 °C.

10 µg total RNA typically yielded in 2-3 µg enriched mRNA, which then was used for expression profiling (see section 4.3.).

4.2.4. Reverse transcription (RT) for cDNA synthesis

For cDNA synthesis, the Superscript III reverse transcription kit (Invitrogen) was used. 4 µg of total RNA in a final volume of 10 µl were mixed with 1 µg of random hexamer primers (Amersham Biosciences). Primer annealing was carried out at 65 °C for 5 min. After brief cooling, 9 µl of a reverse transcription mixture were added to the samples. The composition of the RT-mix for 1 sample was:

2 µl	25 mM deoxynucleotide mix
1 µl	0.1 M dithiothreitol (DTT; kit component)
4 µl	5 x first strand buffer (kit component)
1 µl	40U μl^{-1} RNase OUT recombinant RNase inhibitor (Invitrogen)
1 µl	200U μl^{-1} Superscript III reverse transcriptase (kit component)

cDNA synthesis was performed at 52 °C for 60 min, followed by heat inactivation of the transcriptase at 70 °C for 15 min.

4.2.5. Semi-quantitative reverse-transcription PCR (RT-PCR)

cDNA samples derived from reverse transcription were 20x diluted in water and directly used for PCR amplification. As a control for DNA contaminations, a second PCR reaction was performed using total RNA without any reverse transcription reaction. DNA served as positive control for the PCR reaction. For adjustment of cDNA amounts, 16 S rRNA (*rrsA*) was used as internal standard using 35 cycles of amplification. The RT-PCR primers were selected with the FastPCR software version 3.6.28 (Ruslan Kalendar, Institute for Biotechnology, University of Helsinki, Finland) with the following primer options: product length range from 350 – 400-nt; annealing temperature range from 57 - 59 °C. The sequences of all oligonucleotides used are listed in Table 5.

For the PCR reaction, Red *Taq* polymerase ready mix (Sigma) was used (see section 4.1.5.1.). The 2 x concentrated mix contained all necessary components for PCR, thereby minimizing pipetting errors. 10 µl of the ready mix were mixed with 4.6 µl water and 0.2 µl of each 100 pM RT-primer. This mixture was then added to the adjusted cDNA in a final volume of 5 µl and placed into the thermal cycler.

Thermal profile:	Initial denaturation	2 min, 95 °C	
	1. Denaturation	30 sec, 95 °C	25-35 cycles
	2. Annealing	30 sec, 57-59 °C	
	3. Elongation	30 sec, 72 °C	
	Final elongation	2 min, 72 °C	

Since the PCR ready mix already contained a loading dye for gelelectrophoresis, 10 µl of the PCR samples were directly loaded on a 2 % agarose gel and analyzed after ethidium bromide staining. To keep the PCR amplification in linear range, i.e. to prevent over-saturation of the PCR products, the cycle number of amplification was altered, whereas the template amount was always kept constant.

4.2.6. Northern hybridization

For Northern blotting, RNA was separated by denaturing electrophoresis. A 1.2 % agarose/ formaldehyde gel was prepared by mixing 1.95 g agarose and 96 ml DEPC-treated H_2O. The agarose was dissolved by heating in a microwave, mixed well, and cooled to 60 °C. In a fume hood, 11.05 ml of 37 % formaldehyde, and 13.3 ml freshly prepared 10 x MOPS buffer were added, mixed well and poured into the gel casting device.

20 µg DNase-treated RNA in a final volume of 10 µl were mixed with an equal volume of 2 x RNA loading buffer and denaturated at 55 °C for 15 min. The RNA samples were then loaded onto the formaldehyde gel and separated in 1 x MOPS running buffer at 4 V / cm electrode distance for 4-5 hours, until the Bromophenol blue dye had migrated three-quarters of the way down the gel. After electrophoresis was completed, the gel was stained with ethidium bromide and photographed to record the electrophoretic separation of the loaded RNA.

RNA was transferred to a nylon membrane by vacuum blotting as described earlier for Southern hybridization (see section 4.1.12.), with minor modifications: RNA transfer does not need depurinization, and the composition of the denaturation- and neutralization buffers differed slightly. Transfer was performed at 50 mbar for 4 - 5 h. The nylon membrane was prepared for hybridization as described for Southern hybridization analysis.

DNA probes were amplified by PCR using the same primers as for RT-PCR, followed by ECL-labeling, and hybridization to the membrane over night at 42 °C. After washing with 0.4 x SSC/0.1 % SDS, transcripts were detected using the ECL advance nucleic acid detection kit (Amersham Biosciences) following the manufacturer's recommendations.

10 x MOPS buffer:	200 mM	MOPS (pH 7.0)
	50 mM	Na-Acetate
	10 mM	EDTA
		ad 1 l DEPC-H_2O

2 x RNA loading buffer:	6.5 ml	Formamide
	1.2 ml	Formaldehyde
	2 ml	10 x MOPS
	0.4 ml	50 % sucrose
	0.02 g	Bromophenol blue
	0.02 g	Xylene cyanol

Denaturation solution: 0.05 N NaOH; 0.01 M NaCl

Neutralization solution: 0.1 M Tris-HCl, pH 7.5

4.2.7. Identification of the *hlp* transcription start site by primer extension

To determine the transcription start site of *hlp*, primer extension was performed, using an IRD_{800}-labeled primer (hlp-primext) binding 35 bp downstream of the translational start codon of Hlp. 2 pM primer was annealed to 20 or 40 µg DNase-treated RNA isolated from the 536 *hns/stpA* mutant (see sections 4.2.1 and 4.2.2.) in a total volume of 15 µl, using a stepwise decrease in temperature.

Thermal profile for primer annealing:	90 °C – 2 min
	80 °C – 7 min
	65 °C – 7 min
	45 °C – 7 min
	30 °C – 7 min

Subsequently to primer annealing, reverse transcription to cDNA was performed for 90 min at 54 °C using the Superscript III reverse transcription kit (Invitrogen) as described in section 4.2.4. Specifically, 15 µl of the following mixture were added:

RT-mix for 1 sample:	4 µl	20 mM dNTP mix
	6 µl	5 x first strand buffer
	1.5 µl	0.1 M DTT
	1.5 µl	RNase OUT ribonuclease inhibitor (Invitrogen)
	2 µl	Superscript III reverse transcriptase

After reverse transcription, residual RNA was removed by RNaseA digest for 20 min at 37 °C in RNase buffer (3 ng μl^{-1} RNaseA in 0.2 M EDTA, pH 8). Subsequently, cDNA was ethanol-precipitated and resuspended in 3 µl loading dye (Epicenter). Of each sample, 0.5 µl and 1.5 µl were loaded onto the sequencing gel.

Simultaneously, a sequencing reaction with UPEC 536 wild type chromosomal DNA was performed using the same primer and the Seqitherm Excel II sequencing kit (Epicenter). 200 ng DNA was mixed with 2 pM IRD_{800}-labeled primer, 7.2 µl 3.5x sequencing buffer and 1 µl polymerase in a final volume of 17 µl. 4 µl of this mixture were added to four independent PCR caps containing 2 µl of either A-, C-, G-, or T- termination nucleotides, and the caps were overlayed with one drop of light mineral oil. Amplification was carried out using a thermal profile consisting of an initial denaturation step at 95 °C for 5 min followed by 30 cycles of denaturation at 95 °C for 30 sec, annealing at 57 °C for 15 sec, and extension at 70 °C for 1 min. After thermocycling has been completed, 3 µl loading dye were added, and 1.5 µl of each reaction were loaded on the fluorescent sequencing gel.

Sequencing and extension products were separated by electrophoresis through 6 % polyacrylamide-7.5M urea gels and analyzed by a LiCor DNA sequencer Model 2400 (MWG-Biotech).

4.3. Expression profiling using DNA arrays

Expression profiling is a technique to study the relative amounts of all transcripts at a given time of sample collection, thereby allowing to monitor the expression level of every single gene spotted on the array membrane.

4.3.1. Membrane Layout

For expression profiling, an *E. coli* K12-specific array (Panorama *E. coli* gene arrays from Sigma-Genosys, Cambridge, United Kingdom) and the *E. coli* "pathoarray" (Dobrindt *et al.*, 2003) were used in combination. Therefore, by using both types of arrays, it was possible to measure expression levels of all housekeeping genes as well as most of the known virulence-associated genes of UPEC strain 536.

4.3.2. RNA isolation and cDNA labeling

Total RNA was prepared from mid-log phase cultures grown in LB at 37 °C followed by DNase treatment and enrichment of mRNA, as described in sections 4.2.1.-4.2.3.

Reverse transcription was performed similarly as described for RT-PCR (see section 4.2.4.), but with using the Omniscript reverse transcriptase (QIAGEN) and a radionucleotide for labelling of the cDNA. Primer annealing was performed for 5 min at 93 °C using the following mixture:

1.5 µg	enriched mRNA
3 µl	0.5 µg µl^{-1} random hexamer primers (Amersham)
ad 26 µl	nuclease-free water

After primer annealing, samples were briefly chilled on ice and 12 µl of the reverse transcription mixture were added.

RT mix for 1 sample:	4 µl	5 mM dCTP-, dGTP-, dTTP-mix (Sigma)
	2 µl	10µCi µl^{-1} [α-^{33}P]-dATP (Amersham Biosciences)
	4 µl	10 x reverse transcription buffer (kit component)
	0.5 µl	40U µl^{-1} RNase OUT ribonuclease inhibitor (Invitrogen)
	2 µl	4 U µl^{-1} Omniscript reverse transcriptase (kit component)

Reverse transcription was performed at 42 °C for 2 h. Subsequently, unincorporated nucleotides were removed from labeled cDNA using Microspin G-50 columns (Amersham Biosciences). Samples passed through the gel-filtration column by centrifugation at 4,000 rpm for 4 min, leaving salts and unincoporated nucleotides in the matrix, whereas the labelled cDNA was found in the eluate.

Incorporation rates of labelled nucleotides were determined by measuring radioactivity of the cDNA in the eluate (equals incorporated radionucleotides) and of the radioactivity retained in the column (equals unincorporated radionucleotides).

$$Incorporation\,rate = \frac{radioactive\ count\,(eluate)}{radioactive\ count\ \ (column + eluate)}\ \text{x}\ 100$$

The obtained value can be used as a marker for the quality of reverse transcription and should be > 50 %. In our cases, the incorporation rates used to range from 58 – 65 %.

4.3.3. Hybridization an detection

Hybridization of the labelled cDNA to the membranes was performed as recommended in the technical protocol for the Panorama *E. coli* K-12 array (Sigma Genosys). After 10 min denaturation at 93 °C in hybridization buffer, labelled cDNA from step 4.3.2. was added to the pre-hybridized membranes and incubated for 16 h at 65 °C in a hybridization oven. Membranes were washed three times for 3 min in washing solution at room temperature, followed by three additional washing steps for 20 min at 65 °C. After washing, the membranes were sealed in plastic bags and exposed to a PhosphoImager screen (Molecular Dynamics) for 48 h. Membranes could be re-used up to 10 times after stripping (see Panorama-Array manual).

Hybridization buffer:	5 x	SSPE
	2 %	SDS
	1 x	Denhardt's reagent
	100 µg ml^{-1}	sonicated, denatured salmon testes DNA
Washing solution:	0.5 x	SSPE
	0.2 %	SDS
20 x SSPE:	3.6 M	NaCl
	0.2 M	$NaH_2(PO_4)$; pH 7.7
	20 mM	EDTA
100 x Denhardt's reagent:	2 %	Ficoll (MW 400,000)
	2 %	polyvinylpyrrolidone (PVP; MW 40,000)
	2 %	BSA

4.3.4. Intensity reading

Exposed PhosphoImager screens were scanned on a Typhoon 8600 variable mode imager (Molecular Dynamics) at 50 µm resolution. Spot intensities were measured with the ArrayVision software (Imaging Research, St. Catharines, Canada) using the overall spot normalization function of the program.

The exact settings are listed in Table 7.

Table 7: Parameters of the Arrayvision pre-set protocols (Wizard) used for reading intensity values.

Parameter	***E. coli* K-12 array:**	***E. coli* pathoarray**
Array type	Radio-isotopic array	Radio-isotopic array
Analysis type	Expression	Expression
# of arrays	4	4
# of extra channels	1	1
Measure type	MTM density	MTM density
Array organization	3 levels (18432 total spots)	2 levels (1536 total spots)
Level 1 (Spots)	4 x 4	4 x 4
Level 2 (Spot groups)	16 x 24	8 x 12
Level 3 (sub-arrays)	3 x 1	-
Spot shape	Circle	Circle
Start position	Defined	Not defined
Alignment	Not aligned	Not aligned
Labels	Custom	Custom
Replication	On	On
Background	Corners between spots (average)	Corners between spots (average)
Reference	All spots	All spots
Segmentation:	Off	Off
Anchors:	None	None

Mean values were calculated from the duplicate spots of each gene. Only values with 2-fold higher intensities than the background were included into the analysis.

4.3.5. Data analysis

For each mutant, four independent hybridizations were performed, each in pair with the wild type. For the calculation of intensity ratios, spot intensities in the mutants were directly compared to the intensities in the wild type of the corresponding co-hybridization experiment. As indicator for the reproducibility of the procedure, the four wild type experiments from each set of data were compared to each other during analysis in order to validate the quality of the hybridizations.

Statistical analysis was performed using the SAM software (Statistical analysis of microarrays; Stanford university). Data sets were composed as two-class, unpaired data in four blocks for each experiment. Two-class unpaired groups are two sets of measurements, in which the experiment units are all different in the two groups. For example, control and

treatment groups, with samples from different patients, or in our case, wild type and mutant from different rounds of hybridization, which were defined as separate blocks. This allow permutations of the samples within each of the blocks, but not across the different data sets, in order to correct for hybridization differences.

After running the analysis, all genes which were significantly deregulated were listed by the program. The output is hereby depending on two variables: the fold-change and the false discovery rate. The False Discovery Rate (FDR) is computed as median (or 90 th percentile) of the number of falsely called genes divided by the number of genes called significant. Here, we chose a fold change of ± 2. Deregulation was considered significant, if the false discovery rate was at least <10 % for each gene.

Further statistical analysis was performed using the SPSS software Version 11.5 or the GeneData Expressionist software.

4.4. Working with Protein

4.4.1. Denaturing polyacrylamide gel electrophoresis (PAGE)

Protein samples were separated and analyzed in denaturing polyacrylamide gels as described by Laemmli (1970). This is done using the detergent sodium dodecylsulfate (SDS), which binds to proteins and leaves them unfolded and negatively charged. Therefore, the protein mixture can be separated in the meshwork of the polyacrylamide gel due to variable migration speed depending on the size of the protein. Since most of the proteins of interest in this study were about 15 kDa in size, a 15 % resolution polyacrylamide gel was used. The size of the gels was 10 × 10 × 0.5 cm, and electrophoresis was performed at room temperature at 16 mA per gel in 1 x electrophoresis buffer. The samples were loaded onto the gel after heating for 10 min at 90 °C in 1 × loading buffer.

The acrylamide gel consists of two parts: a lower part mediating the separation of the proteins, and an upper part, which is used for concentration of the sample in a single running front after entering the gel. The mixture sufficient for 4 mini gels was:

15 % separation gel:	15 ml	30 % acrylamyde:bis-acrylamide (37.5:1)
	5 ml	1.5 M Tris-HCl, pH 8.8
	10 ml	dH_2O
	300 µl	10 % (w/v) SDS
	250 µl	10 % (w/v) ammonium persulfate (APS)
	8 µl	TEMED
5 % collecting gel:	1.96 ml	30 % acrylamyde:bis-acrylamide (37.5:1)
	2.8 ml	0.5 M Tris-HCl, pH 6.8
	4.6 ml	dH_2O
	112 µl	10 % (w/v) SDS
	32 µl	10 % (w/v) APS
	16 µl	TEMED
10 x running buffer:	30 g	Tris
	144 g	glycine
	10 g	solid SDS
		ad 1 l dH_2O
4 x SDS-loading buffer:	2.5 ml	1 M Tris-HCl, pH 6.8
	4ml	50 % (v/v) glycerol
	0.8 g	solid SDS
	0.1 ml	ß-mercaptoethanol
	0.02 g	bromophenol blue
		ad 10 ml dH_2O

4.4.2. Visualization of proteins in acrylamide gels by Coomassie staining

After electrophoresis, the polyacrylamide gels were incubated for 15 min in Coomassie staining solution. Protein bands were visualized after removing unbound Coomassie dye by incubating the gel in destaining solution I for 30 min, followed by incubation in destaining solution II for > 2h.

Staining solution:	1 g	Coomassie Brilliant Blue R-250
	0.25 g	Coomassie Brilliant Blue G-250
	238 ml	ethanol
	50 ml	acetic acid
		ad 500 ml dH_2O

Destaining solution I: 10 % (v/v) acetic acid; 50 % (v/v) ethanol

Destaining solution II: 7.5 % (v/v) acetic acid; 5 % (v/v) ethanol

4.4.3. Immunoblotting

For the preparation of crude cell extracts, 800 µl bacterial culture were centrifuged for 2 min at 13,000 rpm in a table top centrifuge and the pellet was resuspended in ¼ vol of the measured optical density of the culture in 1 x Laemmli buffer (e.g. 250 µl for a sample with OD_{600nm} = 1). After heating the samples for 10 min at 90 °C, 15 µl were used for PAGE (see section 4.4.1.). After PAGE, separated proteins were transferred to a nitrocellulose membrane (Optitran BA-S85 Reinforced NC; pore size 0.45 µm; Schleicher&Schuell). The transfer of the proteins was carried out between two graphite plates in a semi-dry western blotting apparatus, using 12 Whatman paper slices, soaked with Anode buffer I, II or Cathode buffer. The membrane was incubated for 5 min in Anode buffer II. The lower graphite plate (anode) was moistened with water and covered with 6 slices of Whatman paper soaked with Anode buffer I, followed by 3 slices of Whatman papers soaked with Anode buffer II. The nitrocellulose membrane was laid on top of the Whatman papers, followed by the polyacrylamide gel and 3 slices of Whatman paper soaked in Cathode buffer. Air bubbles were carefully removed before laying the second graphite plate at the top (cathode). The transfer was carried out by applying an electric current of 0.8 mA cm^{-2} for 1 h.

Anode buffer I:	0.3 M Tris, 20 % methanol
Anode buffer II:	25 mM Tris, 20 % methanol
Cathode buffer:	25 mM Tris, 40 mM ε-amino-n-capronic acid, 20 % methanol

After transfer of the proteins, the membrane was incubated over night at 4 °C (or 1 h at room temperature) in TBS-T solution (0.05 M Tris-HCl, pH 7.5; 0.15 M NaCl; 0.1 % Tween 20) supplemented with 5 % fat-free dry milk. Subsequently, the blot was incubated with the primary antibody for 1 h at room temperature. The concentration of the primary antibody depended on the titre, but the dilution usually ranged between 1:1000 to 1:5000 in TBS-T supplemented with 5 % dry milk. After washing the membrane with TBS-T three times for 5 min, the secondary peroxidase-conjugated antibody (1:5000 diluted in TBS-T) was added and incubated for 1 h at room temperature. Finally, the membrane was washed three times for 10 min with TBS-T at room temperature. Signal detection using the ECL kit (Amersham Biosciences) was performed as described before (see section 4.1.12.3.).

4.4.4. Purification of His-tagged protein

Overexpression of recombinant protein

Escherichia coli strain BL21(DE3) *Δhns* was used for overexpression of recombinant Hlp protein from plasmid pASK75-His*hlp*. 800 ml LB-cultures were grown at 37 °C with aeration to OD_{600nm} =0.2, before adding the inducer anhydro-tetracycline at a final concentration of 0.2 µg ml^{-1}. Protein synthesis was carried out for 6 h.

Preparation of cleared lysate

Cells were pelleted by centrifugation (6,000 rpm, 4 °C, 20 min) and resuspended in 10 ml of LEW buffer (50 mM NaH_2PO_4, 300 mM NaCl, pH 8) containing protease inhibitor cocktail (Complete Mini, Roche). Cells were lysed by sonication for 10x 20 sec pulses with 20 sec cooling periods in between. Cell debris was then removed by two rounds of centrifugation at 18,000 *g* for 20 min at 4 °C. The cleared lysate was stored on ice until further use.

Affinity chromatography

His-tagged proteins can easily be purified by immobilized metal ion affinity chromatography due to the interactions of the polyhistidine tag and immobilized Ni^{2+} ions in the columns. After loading onto the prepacked column, retained recombinant protein can be eluted from the column in a buffer containing imidazole. We were using Protino Ni 1000 columns (Macherey-Nagel), following the manufacturer's recommendations. The cleared lysate was loaded onto the equilibrated columns by gravity flow. After two washes in 1x LEW buffer, bound protein was eluted with elution buffer (i.e. 1x LEW buffer containing 250 mM imidazole) in 3 x 1.5 ml fractions.

Eluted protein was dialysed into storage buffer [150 mM NaCl, 50 mM Tris-HCl (pH 8), 1 mM EDTA, 0.5 mM DTT, 20 % glycerol] and concentrated using Vivaspin 10,000 columns (Vivascience, Hannover, Germany). Eventually, the His-tag was removed by factor XA digest (New England Biolabs, Frankfurt, Germany) over night at room temperature prior to dialysis.

Size-exclusion chromatography

After factor XA treatment, the protease should be removed from the samples by size-exclusion chromatography. This procedure is based on differences of the proteins of a mixture in their migration speed through a gel matrix depending on the size of the protein.

Small proteins have to pass through the pores of the matrix, whereas big proteins are excluded from the pores and only have to migrate though the interstitial spaces, thereby traveling faster.

Concentrated protein samples in a total volume of 1 ml were loaded onto a HiLoad Superdex 75 prep grade column (Amersham Biosciences) and eluted with a buffer containing 150 mM NaCl, 50 mM Tris-HCl (pH 7.5) in 2 ml fractions. A commercial gelfiltration calibration kit (Amersham Biosciences) was used to estimate the approximate sizes of the proteins in the various fractions.

4.4.5. Determination of protein concentrations

Protein concentrations were determined using Roti-Nanoquant solution (Roth) following the manufacturer's instructions. 200 µl protein samples were mixed with 800 µl 1 x assay solution, and absorbance was measured at 590 nm and 450 nm. Protein concentrations were then calculated using the following formula (based on a BSA calibration curve):

$$\mu g \text{ protein} = \frac{A_{590nm} / A_{450nm} - 0.4475}{0.1132}$$

4.4.6. Chemical crosslinking

Homomeric and heteromeric interactions between Hlp, H-NS and StpA were analyzed by chemical crosslinking for 20 min at room temperature using glutaraldehyde in a final concentration of 2.5 mM. Crosslinked products were analyzed by Western immunoblotting.

4.4.7. Electrophoretic mobility shift assay (EMSA)

DNA-protein interactions were studied by a gel retardation assay using recombinant His-Hlp protein purified from *E. coli* BL21 *Δhns*. As substrate for binding, 350-bp PCR products containing the promoter regions of *hlp*, *hns*, and *stpA* were used. poly(dIdC) was used as non-specific competitor DNA.

Mix per sample:	2 µl	5 x binding buffer	
	1 µl	1 µg µl^{-1} poly(dIdC)	
	0.5 µl	1 M KCl	
	100 ng	target DNA fragment	
	4 µl	protein dilution	ad 10 µl dH_2O

Samples were incubated for 20 min at room temperature and then loaded onto a 6 % Tris-glycine gel. DNA was visualized by ethidium bromide staining.

5 x binding buffer:	125 mM	HEPES acid, pH 7.3
	0.5 mM	EDTA
	25 mM	DTT
	50 %	glycerol
5 x Tris-glycine buffer:	125 mM	Tris, pH 8.5
	0.5 mM	glycine

4.4.8. *in vivo* protein stability assay

To determine the intracellular stability of Hlp, the recombinant protein from pASK75-His*hlp* and pWKS30-*hlp*, respectively, was expressed in an *stpA* background in the presence or absence of H-NS and/or the Lon protease. The assay was performed as described by Johansson and Uhlin (Johansson and Uhlin, 1999). Briefly, 20 ml cultures were grown to OD_{600nm} = 0.4 in LB medium (for strains harbouring the pASK75-His*hlp* plasmid, medium was supplemented with the inducer anhydro-tetracycline). Further protein synthesis was inhibited by the addition of 100 µg ml^{-1} spectinomycin. Samples for Western blotting were taken before and 160 min after the addition of spectinomycin.

4.5. Analysis of lipopolysaccharides (LPS)

4.5.1 Isolation of LPS

For analysis of the LPS composition, cells from agar plate or pellets of liquid cultures were used. After weight measurement, the cells were resuspended in an adequate amount of water so that the concentration was 1 mg cells per 30 µl suspension. 30 µl sample (i.e. 1 mg cells) were mixed with 10 µl 4 x SDS-sample buffer (see section 4.4.1.) and incubated at 100 °C for 10 min. After brief cooling, 20 µl 1 x SDS-sample buffer supplemented with 100 µg proteinase K were added to the samples, which then were incubated at 60 °C for 1 h for removal of proteins. 30 µl of the LPS preparations were used for electrophoresis.

4.5.2 Electrophoresis and staining with silver nitrate

Separation of the LPS components was performed by denaturing polyacrylamide gelelectrophoresis as described earlier for proteins (see section 4.4.1.). 15 % separation gels were used in a format of 20 x 20 cm, and electrophoresis was carried out over night at 8 mA at room temperature.

After electrophoresis, the polyacrylamide gels were stained with $AgNO_3$. All used devices were carefully washed with double destilled water, and gloves were worn throughout the experiment. The gels were fixed over night in 100 ml 1 × fixation solution. The next day, the solution was replaced by 100 ml 1 × periodate solution and the gels were incubated for 5 min for oxidation. Subsequently, the gels were washed three times for 30 min with dH_2O, and then incubated for 10 min in silver nitrate solution. After three more washes for 10 min with dH_2O, the gels were developed in developing solution preheated to 60 °C. As soon as the intensity of the appearing bands was satisfying, the reaction was stopped by incubation in 50 mM EDTA solution for 10 min. [Tsai and Frasch (1982)]

2 × fixation solution:	250 ml	Isopropanol
	70 ml	acetic acid
		ad 500 ml in dH_2O
Periodate solution:	0.87 g	Na-m-periodate ($NaIO_4$)
	100 ml	1 × fixation solution
Silver nitrate solution:	1.4 ml	1 M NaOH
	1 ml	NH_3 (33 %)
	70 ml	dH_2O
	1.25 ml	20 % (w/v) $AgNO_3$
Developing solution:	100 ml	2.5 % (w/v) Na_2CO_3
	27 µl	formaldehyde (40 %)

4.6. Phenotypic assays

4.6.1. Measurement of ß-galactosidase activity

The ß-galactosidase activity of *lacZ* reporter strains was determined as described by Miller (1972). Samples were taken from mid-log phase cultures, i.e. after reaching an optical density between 0.4 and 0.5. Experiments were performed in triplicate from independent cultures, with three separate measurements for each sample. Strains containing the *hns-lacZ* (pBSN2) fusion were grown in LB medium supplemented with 50 µg ml^{-1} kanamycin and 100 µg ml^{-1} ampicillin. For the assay of ß-galactosidase activity in the chromosomal *proU-lacZ* strains (BEU693 and BEU694) cultures were grown in minimal medium A supplemented with 20 ng ml^{-1} tryptophane, 0.3 M NaCI and 100 µg ml^{-1} ampicillin.

In brief, samples were incubated on ice for 20 minutes. In the meantime, assay solutions were prepared by adding 2.7 µl ß-mercaptoethanol per ml Z-buffer, and by dissolving 4 mg ml^{-1} o-Nitrophenyl-ß-galactopyranoside (ONPG) in this ready-to-use Z-buffer.

If the expected expression levels were high, 0.1 ml of the samples were mixed with the 0.9 ml Z-buffer using autoclaved glass tubes; in case of low expression levels, 0.5 ml sample and buffer were used. Cells were lysed by the addition of 15 µl toluol, followed by vigorous vortexing for 10 sec. Subsequently, open glass tubes were incubated for 40 min at 37 °C with shacking to remove the toluol, and after that placed into a 28 °C water bath. After 5 min of equilibration, 200 µl of the ONPG solution were added to each samples to start the reaction. After sufficient yellow color has developed, 500 µl stop-solution (1 M Na_2CO_3) were added to the tubes, while the time of the reaction was recorded using a stopwatch. Then, the reaction-liquids were tranfered to cuvettes, and absorption was measured at both 420 nm and 550 nm. Growth medium was used as negative control, and as blank for the absorption measurement.

ß-galactosidase activity (in Miller units) was calculated using the following formula:

$$\text{ß-galactosidase activity} = \frac{1000 \times (OD_{420nm} - 1.75 \times OD_{550nm})}{t_{(min)} \times \text{sample volume}_{(ml)} \times OD_{550nm}}$$

Z-buffer (-ß-ME): 8.51 g Na_2HPO_4
5.5 g NaH_2PO_4 xH_2O
0.75 g KCl
0.12 g $MgSO_4$ ad 1 l in dH_2O

pH adjusted to 7; stored at +4 °C

4.6.2. Detection of secreted α-hemolysin

Hemolytic activity was studied both on 5 % (v/v) blood agar plates as well as in a liquid hemolysis assay as described by Nagy *et al.* (2002), with minor modifications. Briefly, 20 ml LB cultures from late-log phase grown at 30 °C were centrifuged at 6,000 rpm for 20 min at 4 °C. The supernatant was carefully transferred to a new tube and stored on ice. Meanwhile, 1 ml fresh bovine erythrocytes was washed twice in 20 ml PBS before resuspending the cells in 15 ml of a solution containing 150 mM NaCl and 20 mM $CaCl_2$. The blood suspension was further diluted (usually 10 times) in the same solution. 1 ml of the dilution was transferred to a 1.5 ml cap to which a small amount of the detergent saponin was added for complete hemolysis. After brief centrifugation, absorbance was measured at 545 nm, which corresponds to the absorbance of hemoglobin. The obtained value should be around 0.8 (equals 100 % hemolysis), otherwise the blood had to be diluted again. For the assay, the bacterial culture supernatants were diluted in LB medium in a final volume of 500 µl per dilution. Samples were mixed with an equal volume of the adjusted erythrocytes and incubated for 30 min at 37 °C prior to centrifugation. The amount of hemoglobin released during hemolysis was measured at A_{545nm}, using erythrocytes incubated with 500 µl LB medium as blank.

Hemolytic activity is defined as the dilution at which 50 % hemolysis occurred, which means A_{545nm} equals 0.2 (due to the 2 x dilution of the samples with the blood suspension).

4.6.3. Detection of siderophores in culture supernatants

The production of siderophores was assessed in a chrome azurole S (CAS) liquid assay as described by Schwyn and Neilands (1987). Bacteria were grown over night in MM9 medium at 37 °C with aeration. The next morning, the chelator 2,2'-dipyridyl was added to the cultures in a final concentration of 0.1 mM, resulting in iron depletion during 3 h of incubation at 37 °C.

Cells were removed by centrifugation (6,000 rpm, 4 °C, 20 min) and supernatants were mixed with an equal volume of CAS assay solution. This solution contained a blue Fe-CAS complex, which turned red when siderophores are present. The degradation of the complex was monitored photometrically at A_{630nm}.

CAS assay solution I:	6 ml	10 mM HDTMA
	44 ml	dH_2O
	1.5 ml	Fe^{III} - solution
	7.5 ml	2 mM CAS solution (slowly added under stirring)

CAS assay solution II:	4.307 g	anhydrous piperazine
	40 ml	dH_2O
	6.25 ml	12 M hydrochloric acid (carefully added)

CAS assay solutions I and II were mixed and brought to a final volume of 100 ml with dH_2O. After sterile filtration, the solution could be stored for several months at 4 °C if protected from light.

4.6.4. Detection of autoaggregation

In order to study cell to cell interactions, an autoaggregation assay was performed. Cells were first grown over-day in 5 ml LB medium at 37 °C. In the evening, 100 µl of the culture were used to inoculate 5 ml M63BI medium supplemented with 0.4 % glucose. These minimal medium cultures were grown over night at 37 °C with aeration. The next day, optical densities of the cultures were measured at 600 nm, and all cultures were adjusted to OD_{600nm} = 1.5 with M63BI medium. 3 ml of the adjusted cultures were incubated statically at room temperature. Every hour, a 200 µl sample was taken 1 cm below the surface and mixed with 600 µl M63BI medium. Again, the optical density of the samples was measured at 600 nm, in order to quantitate the aggregation of cells at the bottom of the tubes.

4.6.5. Detection of biofilm forming abilities

Biofilm formation was assessed in a microtiter plate assay modified after O'Toole and Kolter (1998). Bacteria were grown over-day in 3 ml LB medium at 37 °C with aeration. In the evening, 3 ml of various minimal media were inoculated with 20 µl of the LB cultures and incubated over night at 37 °C with aeration.

The next morning, 100 µl of fresh minimal medium were distributed in a microtiter plate (8 wells per strain) and inoculated with 10 µl of the over night cultures. The plates were incubated statically at 30°C for 24 h and 48 h, respectively. Subsequently, the wells were washed trice very carefully with 1 x PBS and dried for 1 h at 80 °C. The biofilm was stained with 0.1 % crystal violet for 1 h. The staining solution was discarded and the plates were rinsed trice with water. Pictures of the biofilm were taken by cutting the front row of wells from the microtiter plate. To quantitate the biofilm, the wells were destained with 200 µl destaining solution (80 % ethanol / 20 % acetone) for 30 min. Remaining biofilm was dissolved by pipetting the solution up and down several times, before diluting the solution 10 times in dH_2O and measuring absorbance at 570 nm.

4.6.6. Survival at high osmolarity

Bacteria were grown over night in LB medium at 37 °C with aeration. The next morning, cells were diluted 1:1000 in fresh LB medium or medium supplemented with 3 M NaCl and incubated for 1 h at 37 °C before plating serial dilutions onto LB agar plates. Colony forming units (CFU) were counted after 16 h at 37 °C. Survival rates were calculated as CFU_{+NaCl} divided by CFU_{-NaCl}.

4.6.7. Serum resistance

Serum resistance of *E. coli* strains was analyzed by incubating the bacteria in 90 % human serum. Bacteria were grown in LB medium to mid-log phase and then washed in saline. The cultures were diluted 1:10 in human serum and incubated at 37 °C. Samples were taken at 0, 0.5, 1, 2, 3, and 4 h, respectively. Viable cell counts were determined by plating aliquots onto LB plates and incubating over night at 37 °C. The assay was performed both with normal and heat-inactivated (56 °C for 30 min) serum. Triplicates were used for each strain, and assays were repeated three times.

4.6.8. *In vivo* virulence assay

All *in vivo* assays were performed by Gabor Nagy and György Schneider at the Institute of Medical Microbiology and Immunology, University of Pécs Medical School, Hungary.

Lung toxicity assay

The assay was performed as described by Hacker and co-workers (Hacker *et al.*, 1986). Briefly, 3-week-old CFLP mice (Gödöllõ, Hungary) weighting 10 to 12 g were infected intranasally under superficial ether anesthesia with 50 µl of a bacterial suspension (3×10^9 CFU ml^{-1}) grown over night in LB medium. Five mice were treated for each strain. The animals were observed for 24 h and death rates were recorded.

Ascending urinary tract infection model

Intravesical infection of 3 to 4-day-old CFLP mice (Gödöllõ, Hungary) was performed as described by Allison *et al*. (1994). Bacteria were grown over night at 37 °C in LB medium, harvested by centrifugation, washed once, and normalized to the required inoculum density (10^9 or 10^8 CFU ml^{-1}) in PBS by adjusting the suspension to the appropriate optical density at 600 nm, justified by viable counts. A 25 µl aliquot of this bacterial suspension containing 0.05 % Pontamin Sky Blue dye (Searle Pharmaceuticals, High Wycombe, United Kingdom) was introduced into the bladder directly through the abdominal wall. The stain, which had no toxic or antibacterial effects, served as an indicator for successful inoculation (i.e., the stain became localized only to the bladder, which was visible through the hairless skin). Dead mice were counted every 24 h. For every strain, 10 infant mice were injected simultaneously, and assays were repeated four times.

4.7. *In silico* analysis

For standard sequence comparison and similarity searches, the Basic Local Alignment Search Tool (BLAST) at the National Center for Biotechnology Information Homepage was used. For alignments of nucleotide and amino acid sequences, the BioEdit sequence alignment editor V7.0.1 was used (Hall, 1999). Genome comparison was performed using the Artemis Comparison Tool (ACT) Release 4 of the Sanger Institute.

5. Results

5.1. Impact of H-NS and StpA on expression pattern of UPEC strain 536

Although the effect of *hns* and *stpA* mutations are well characterized in non-pathogenic *E. coli* K-12 strains (Bertin *et al.*, 2001; Hommais *et al.*, 2001), the effects in pathogenic strains have only been studied for some selected virulence traits. Using DNA macroarrays, the role of H-NS and StpA on gene expression of a pathogenic isolate was studied on a larger scale, by monitoring the expression levels of both the "core"-genome, as well as the "patho" gene-pool encoded on extragenetic material.

5.1.1. Construction of *hns* and *stpA* mutants

For expression profiling, *hns* and *stpA* single mutants, as well as an *hns/stpA* double mutant were constructed in the uropathogenic *E. coli* isolate 536. The construction of the mutants was performed using linear DNA for recombination, as described by Wanner and Datsenko (2000). This method relies on the replacement of a chromosomal sequence with an antibiotic marker that is generated by PCR using primers with homology extensions to the flanking regions of the target sequence (see method section 4.1.11.). After allelic replacement of the target gene with the antibiotic resistance marker, the marker can be eliminated using the FLP recombinase, resulting in a complete deletion of the target sequence. These recombination events lead to a shift in the fragment size, which can be visualized by both PCR amplification and by Southern hybridization (see Fig. 9).

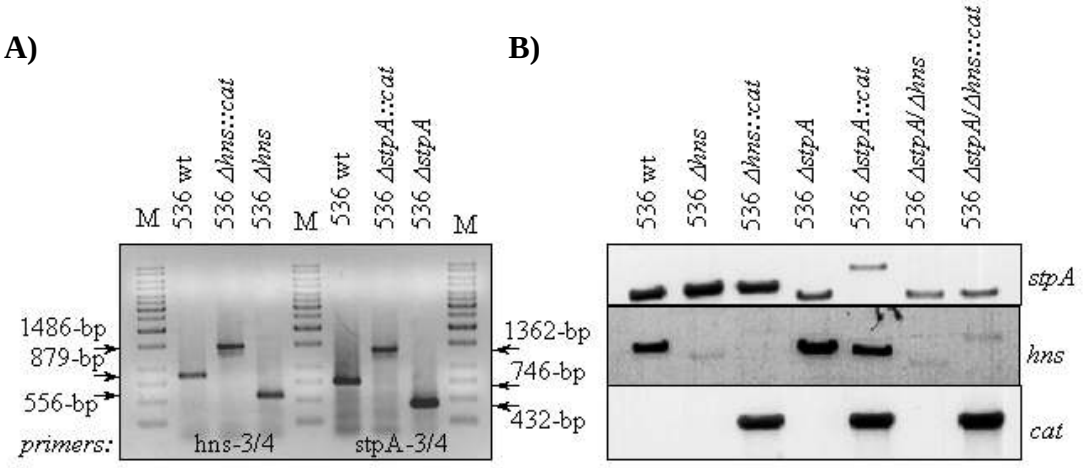

Fig. 9: Verification of the *hns* and *stpA* mutations. (A) PCR verification using primers binding outside the coding sequences of *hns* and *stpA*; (B) Southern hybridization using *Eco*RV restricted chromosomal DNA and PCR generated DNA probes specific for *stpA*, *hns*, and *cat* fragments. M = Marker ("Generuler" 1 kb).

The results of PCR verification and Southern hybridization confirm that both the *hns* and/or the *stpA* loci were successfully mutagenized in UPEC strain 536.

5.1.2. Expression profiling using DNA macroarrays

Quality of the hybridizations and expression pattern of wild type UPEC strain 536

For expression profiling, RNA was extracted from UPEC strain 536 and its isogenic *hns* and *stpA* mutants grown to mid-log phase (see method section 4.3.). After reverse transcription using radioisotopes, labelled cDNA was hybridized to a commercial *E. coli* K-12 array (Sigma-Genosys) and a *E. coli* pathoarray containing probes specific for most of the virulence factors encoded on pathogenicity islands I to IV of UPEC strain 536. Membranes were exposed to a Phosphoimager screen. An example of resulting hybridization signals can be seen in Fig. 10.

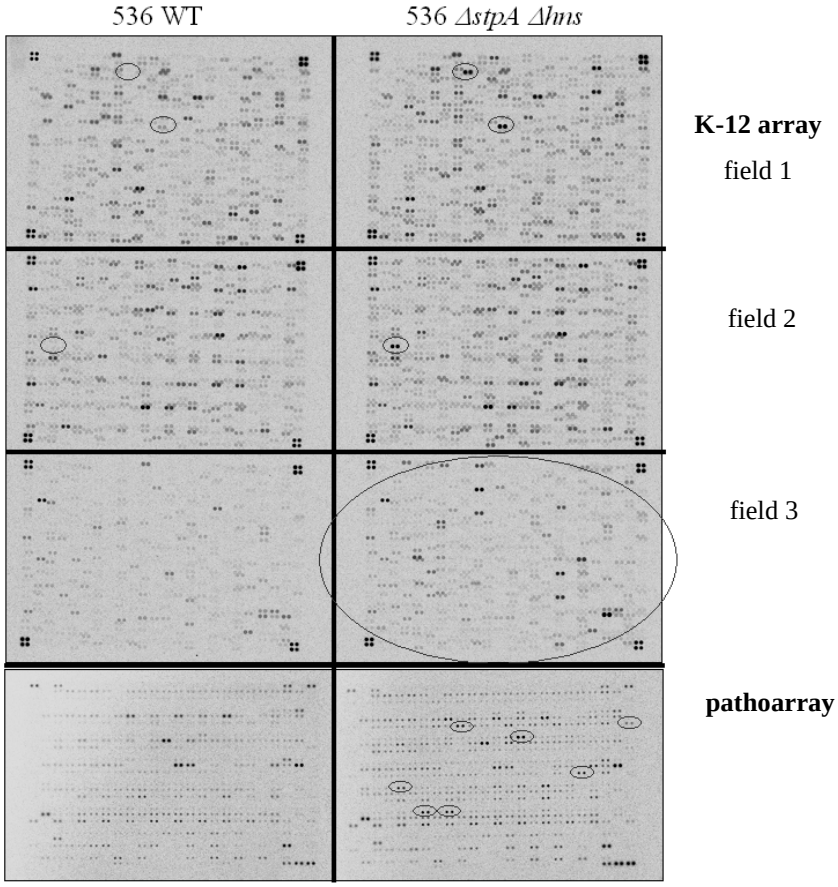

Fig. 10: Example of hybridization signals obtained with cDNA of wild type strain 536 and its isogenic *stpA/hns* mutant. Phosphoimager screens were scanned at 50 µm resolution. Spots with obvious differences in signal intensities between the *hns/stpA* mutant and the wild type, i.e. deregulated genes, are marked with circles.

For each mutant, four independent hybridizations were performed, each in pair with the wild type. As indicator for the reproducibility of the procedure, the averages of the four wild type experiments from each data set were compared to each other (see Fig. 11).

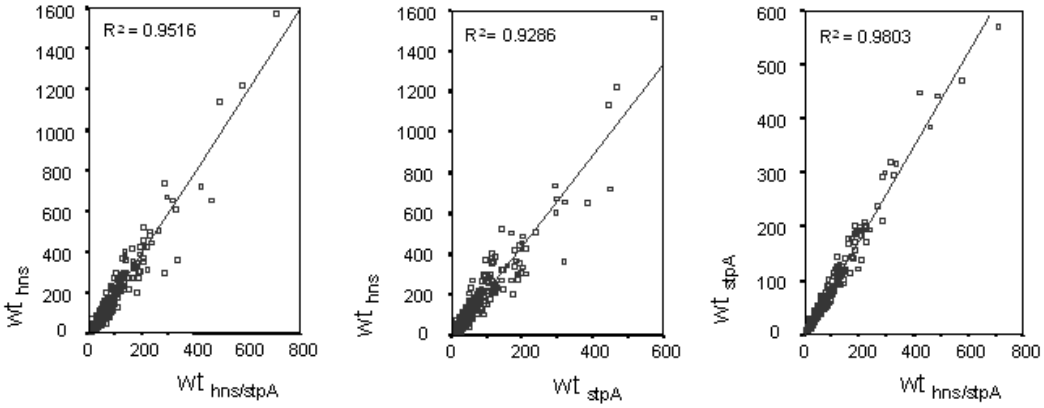

Fig. 11: Scatter plots and trendlines for linear regression between different experiments. Data sets included the averages of the signal intensities of each gene on the *E. coli* K-12 array for wild type UPEC 536 in co-hybridization with its *hns*, *stpA* and *hns/stpA* mutants.

In all three cases, the coefficient of linear regression exceeded 93 %, indicating a low level of variation between the experiments and therefore validates the quality of the hybridizations.

As a second indicator for reproducibility, the genes of the wild type data sets were sorted according to their measured signal intensities. 43 genes were found among the 50 genes with highest expression in all the wild type co-hybridizations. This again infers a good reproducibility of hybridization.

This approach also allowed to gain insight into the current gene expression status of a wild type cell under standard growth conditions (LB medium, 37 °C, mid-log phase). Therefore, average signal intensities of each gene were calculated from the three wild type data sets and sorted according to their expression level. The 50 genes with the highest signal intensities are listed in Table 17 in the appendix. The most abundant transcripts either encode proteins involved in translation, such as ribosomal proteins and elongation factors, enzymes involved in energy metabolism, or structural components of the cell wall, such as outer membrane proteins and transport proteins. These results are in good agreement with array data obtained with the uropathogenic *E. coli* isolate CFT073 (Snyder *et al.*, 2004).

Expression pattern of hns *and* stpA *mutants*

After analysis of the expression pattern of the wild type strain, those of the different mutants were studied. As expected from previous experiments with non-pathogenic *E. coli* K-12, lack of H-NS had a strong impact on the expression profile (Hommais *et al.*, 2001).

In the *hns* single mutant of UPEC strain 536, 551 of the 4290 translatable ORFs on the K-12 array were assigned to be significantly deregulated compared to the wild type, i.e. the signal intensity ratio of mutant / wild type is greater 2 (upregulation) or less than 0.5 (downregulation). Regarding the genes specific for the *E. coli* strain 536 detectable with the pathoarray, 31 of the 391 ORFs were significantly deregulated in the mutant. These results confirm the role of H-NS as a global regulator in *E. coli*, acting mostly as repressor of gene expression.

In contrast, not a single gene appeared differently regulated in the 536 *stpA* single mutant. Therefore, genes, which may be regulated by StpA alone and finally might result in a notable phenotype, remain to be identified.

In the 536 *hns/stpA* mutant, 389 genes of the K-12 genome were deregulated compared to the wild type. Like in the *hns* mutant, most of the affected genes had a higher expression level in the mutant, but there were also many downregulated genes (almost twice as many in the *hns* single mutant). The results on total numbers of deregulated genes is summarized in Table 8.

Table 8: Total numbers of deregulated genes in the 536 *hns* and *stpA* mutants.
Results were obtained using the SAM software (see method section 4.3.5.)

	***E. coli* K-12 array**		***E. coli* pathoarray**		
Mutant	upregulated	downregulated	upregulated	downregulated	**total**
536 *stpA*	0	0	0	0	**0**
536 *hns*	515	36	31	0	**582**
536 *hns/stpA*	323	66	42	0	**431**

From these results, one could speculate that all differences in gene expression in the *hns/stpA* mutant might be due to the lack of H-NS. However, when comparing the data sets of the *hns* single mutant and the *hns/stpA* mutant, only a subset of genes was commonly altered in both mutants. For the *E. coli* K-12 array, only 248 of the deregulated genes were found in both mutants, whereas 33 genes were shared on the *E. coli* pathoarray. Consequently, the obvious differences between the *hns* and the *hns/stpA* mutant were investigated in more detail.

Finally, the coefficents for linear regression between mutant and wild type data sets were calculated as before (see Fig. 11). Both the *hns* and the *hns/stpA* mutants had a lower regression coefficient (R^2 = 0.85 and R^2 = 0.56, respectively) than the *stpA* mutant (R^2 = 0.98), which also results from the different degree of deregulation in these mutants.

To analyze the number of deregulated genes as well as the level of deregulation, the data sets from the *hns* single mutant and the *hns/stpA* double mutant were sorted according to the expression ratios. A list of the 50 genes with highest upregulation, and 37 genes with highest downregulated expression can be found in the appendix (Tables 13-16). Interestingly, only 18 genes of this top-50 list of upregulated genes can be found in both mutants, and only 21 genes of 37 are commonly downregulated. Moreover, the distribution of the deregulated genes into functional groups exhibited some major differences between the *hns* and the *hns/stpA* mutant (Fig. 12).

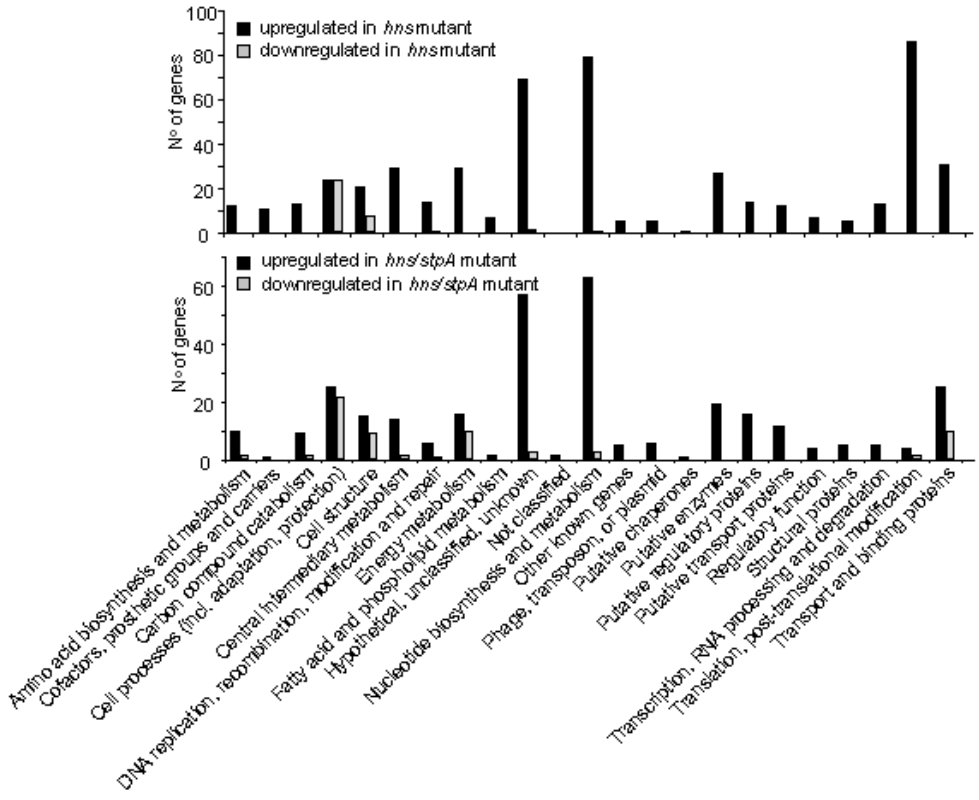

Fig. 12: Distribution of the deregulated genes of the core genome into functional groups. Upper panel: *hns* mutant of strain 536; lower panel: 536 *hns/stpA* mutant. Upregulated genes are depicted as black bars, downregulated genes are presented in grey.

The distribution of the upregulated genes was quite similar in both mutants, with one exception: significantly more genes coding for proteins involved in translation and post-translational modifications were upregulated in the *hns* mutant compared to the *hns/stpA* mutant (86 vs. 4 genes). This group included genes encoding ribosomal proteins and tRNA synthetases, thereby indicating a high level of protein synthesis in the absence of H-NS alone.

The most prominent difference in the *hns/stpA* double mutant was the occurrence of a large number of downregulated genes. Most of these genes clustered in the group of genes coding for transport and binding proteins (10 genes), as well as genes whose encoded products are involved in all kinds of metabolic processes like energy metabolism and central intermediary metabolism (12 genes). This effect on metabolism was also reflected in the reduced growth rate of the double mutant. Growth experiments with UPEC strain 536 and its mutants at 37°C in LB medium revealed an impaired growth rate in the *hns/stpA* mutant compared to the wild type and the *stpA* single mutant (see Table 12). Interestingly, despite a prolonged lag phase, the generation time of the *hns* mutant turned out to be the same as that of the wild type.

Finally, a cluster analysis was performed using the GeneData Expressionist software in order to quantify the differences in the expression patterns. As seen in Fig. 13, all wild type co-hybridizations, as well as the hybridizations of the *stpA* mutant clustered closely together, thereby indicating similar expression patterns. Furthermore, the expression patterns of the *hns* and the *hns/stpA* mutant did not fall into one cluster, but were partly unrelated.

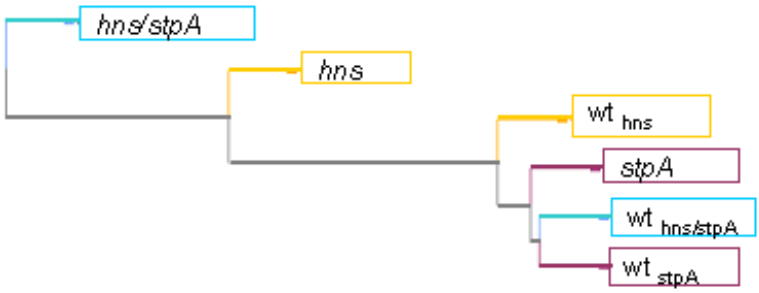

Fig. 13: Cluster analysis of expression profiles of the wild type strain 536 and its derivatives.
The cluster analysis was performed with the GeneData Expressionist software.

Taken together, a very distinct expression profile of the *hns* single mutant and the *hns/stpA* double mutant was found. This suggest the existence of two different regulons, depending on either the H-NS protein alone, or a concerted action of H-NS and StpA.

5.1.3. Effect of H-NS on expression of virulence-associated genes

Despite the differences in metabolism and translation, the *hns* and the *hns/stpA* mutants behaved very similarly concerning the expression of virulence-associated genes. The expression pattern on the *E. coli* pathoarray revealed major overlaps in both mutants: all 33 commonly affected genes on the *E. coli* pathoarray were upregulated compared to the wild type and included the major virulence factors of strain 536.

All deregulated genes whose products are involved in fitness and virulence are listed in Tables 18-24 in the appendix. A schematic view of the expression levels of some selected virulence-associated genes is given in Fig. 14. Not unexpectedly, most of the factors were only mildly expressed *in vitro* in LB, especially the iron-uptake systems. However, the expression of some genes such as the *sfa*- and the α-hemolysin gene cluster reached very high levels in the absence of H-NS.

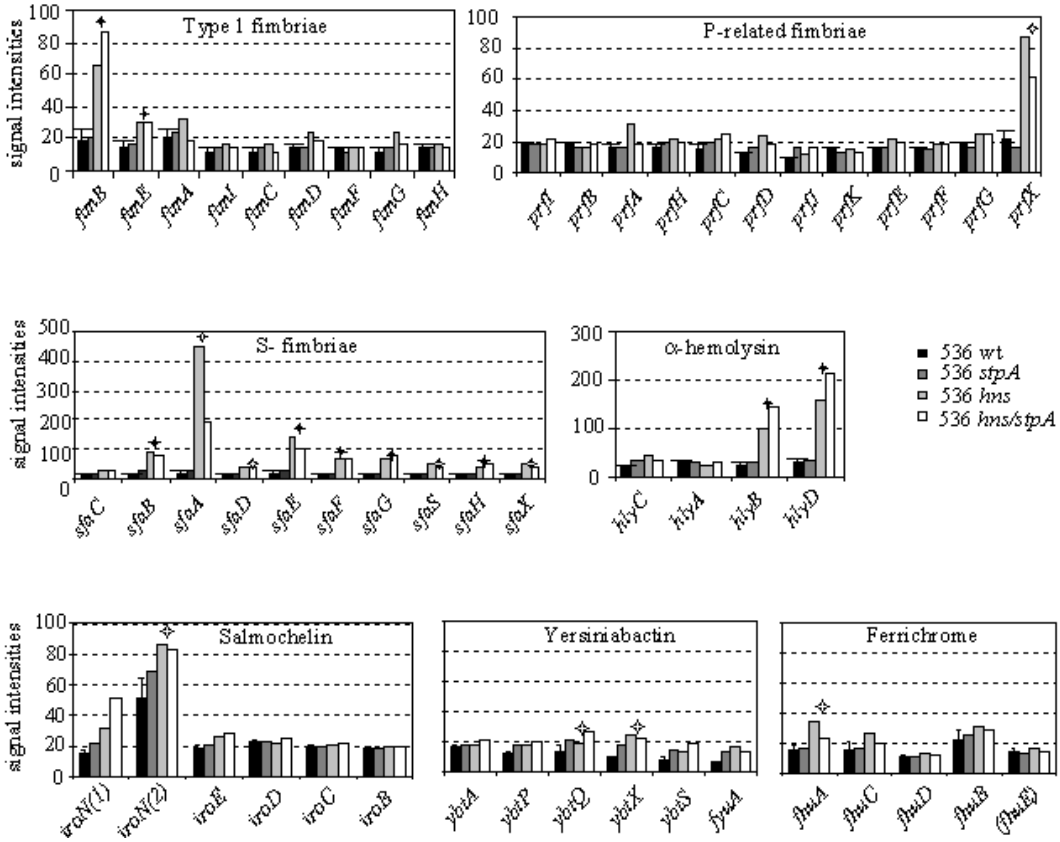

Fig. 14: Expression levels of major virulence-associated genes in UPEC 536 and isogenic mutants. Measured signal intensities on hybridized arrays of three types of fimbrial adhesins (type 1, P-related and S-fimbriae), the α-hemolysin determinant, and three types of iron-uptake systems (salmochelin, yersiniabactin, and ferrichrome receptors) encoded on the chromosome or on pathogenicity islands. Genes with significantly upregulated expression levels compared to the wild type are marked with an asterisk.

A more detailed analysis of the impact of H-NS on the expression of virulence-associated genes, and the confirmation of the array data by classical phenotypic assays and semi-quanititative RT-PCR can be found in section 5.3.2..

However, it should be mentioned, that not all differences observed are not all ascribable to H-NS-mediated regulation alone, but most likely also result from indirect effects from other regulators. From our array data, we could identify more than 20 known or putative transcriptional regulators with altered expression in the *hns* mutants, and about 50 proteins with other regulatory functions. Among them were many two-component systems such as EvgAS or the PhoPQ system, or other pleiotropic regulators like the Hha protein or the the cyclic AMP receptor protein CRP, all of which are described to have a broad spectrum of target genes. Using semi-quantitative RT-PCR, we could at least confirm lower *crp* transcript levels in strains lacking H-NS (data not shown).

To summarize, expression profiling revealed a downregulation of genes whose encoded products are involved in motility and chemotaxis, whereas the expression of many other virulence-associated genes, e.g. coding for S and P fimbriae, as well as for the α-hemolysin (transport) system and various siderophore receptors, was upregulated in both the *hns* and the *hns/stpA* mutant. This indicates, that H-NS might also contribute to the virulence of UPEC strain 536.

5.2. Characterization of the novel H-NS-homolog Hlp

5.2.1. Identification of a novel H-NS-like protein in UPEC strain 536

The sequencing project of the UPEC strain 536 genome was finished soon after the start of this thesis and therefore the genome became available for homology searches. Using the H-NS sequence of strain MG1655 (Accession No BAA36117) as query, the genome of strain 536 was searched for proteins with homologies to H-NS by a Blast analysis.

Like in the K-12 strain, UPEC strain 536 possesses both the *hns* equivalent (nucleotide sequence identity $hns_{K\text{-}12}$ / hns_{536} = 99.5 %) as well as the *stpA* homolog (nucleotide sequence identity $stpA_{K\text{-}12}$ / $stpA_{536}$ = 99.0 %). Interestingly, a third hit was obtained, annotated as a putative open reading frame (ORF) coding for a putative DNA-binding protein of 134 amino acids, which was now termed Hlp for H-NS-like protein. The nucleotide sequence identity between hlp_{536} and $hns_{K\text{-}12}$ was 57.2 %, which is about the same as the identity between hns_{536} and $stpA_{536}$. These results strongly suggested that UPEC strain 536 expresses a third, so far unknown member of H-NS-like proteins.

When comparing the amino-acid sequences of all three proteins of UPEC strain 536, the strongest homology existed between Hlp and H-NS (57.7 % amino acid identity). The homology of Hlp to StpA was slightly lower (52.2 % amino acid identity), resembling the homology of H-NS to StpA (51.1 % amino acid identity). The result of a sequence alignment of all three nucleoid-associated proteins in UPEC strain 536 is represented in Fig. 15.

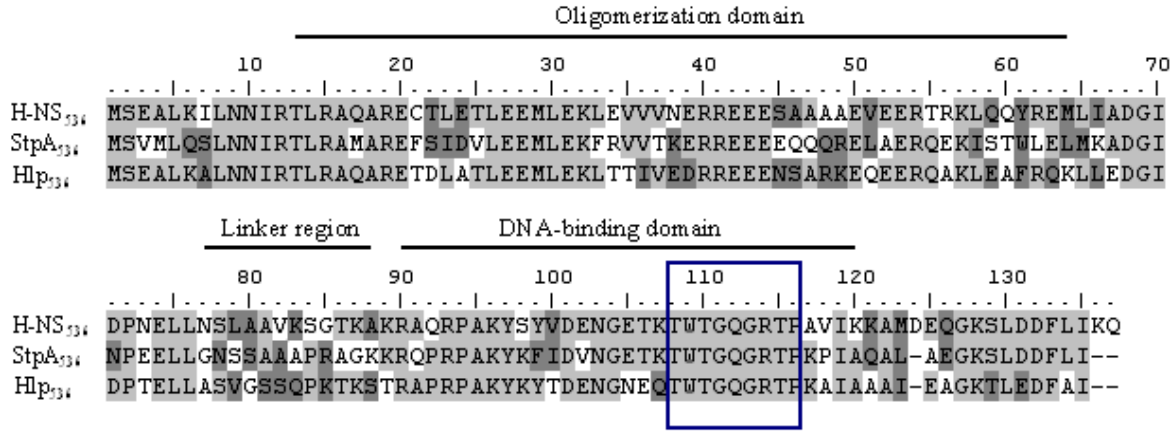

Fig. 15: **Sequence alignment of the three nucleoid-associated proteins of UPEC strain 536.**
Identical residues are depicted with light shading; dark shading shows residues with >50 % similarity. The domain structure is indicated above the sequence; blue box = core DNA-binding motif.

By using the *hlp* sequence as query in an ordinary Blast search, the sequence occurred to be 100 % identical to ORF c2411 of UPEC strain CFT073 (Accession No NP_754303), where it was termed *hnsB* by Williamson and Free (2005).

The properties of the three histone-like proteins were predicted using the Protparam Tool (http://www.expasy.org/tools/protparam.html). The results are listed in Table 9. All three proteins share very similar properties, especially with regard to their size. Only the StpA protein differs in charge and therefore has a more basic pI. The only obvious differences between H-NS and Hlp is the hydropathicity, i.e. the amino acid composition according to their hydrophobicity.

Fig. 16 depicts the outcome of a secondary structure prediction retrieved at http://npsa-pbil.ibcp.fr using consensus mode. The N-terminus of all three proteins is predicted to be mostly α-helical. The linker region (residues 63 to 79) is not conserved and shows a variable structure. The C-terminus, on the other hand, is supposed to be highly conserved between H-NS-like proteins, consisting of an antiparallel ß-sheet, an α-helix, and one 3_{10}-helical structure. All these features were also found in the predicted secondary structures of Hlp and StpA. Moreover, a tertiary structure prediction of both the H-NS and the Hlp molecule resulted in a very similar outcome (data not shown).

Table 9: Predicted protein parameters the three histone-like proteins of UPEC strain 536.

	H-NS	StpA	Hlp
Nº of amino acids	137	134	134
Molecular weight (kDa)	15.54	15.36	15.05
Theoretical pI	5.44	7.95	5.24
Neg. charged residues	25	22	25
Pos. charged residues	23	23	22
Hydropathicity (GRAVY)	-0.751	-0.755	-0.932

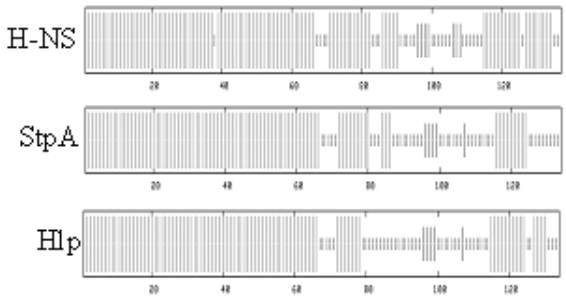

Fig. 16: Secondary structure prediction for H-NS, StpA, and Hlp (http://npsa-pbil.ibcp.fr)
bar code: full = α-helix; intermediate = ß-sheet; small = random coil

The finding that UPEC isolates 536 and CFT073 carried identical copies of the *hlp* gene, led to the further investigation of the distribution of *hlp* in other strains.

5.2.2. Screening for the presence of the **hlp** *gene in other* **E. coli** *isolates*

To study the distribution of the third H-NS-like protein-encoding gene in different *E. coli* sero- and pathotypes, 131 pathogenic and faecal isolates were tested by PCR for the presence of the *hlp* gene using primers binding within the *hlp* coding sequence. The strain collection comprised extraintestinal pathogenic *E. coli* isolates as well as intestinal pathogens and faecal isolates of healthy volunteers. The result of the screening is presented in Table 10.

Table 10: Occurrence of the *hlp* gene in other *E. coli* variants. The presence of the *hlp* gene was monitored by PCR screening using primer binding within the coding sequence. In total, 131 clinical isolates were tested. Extraintestinal pathogens (ExPEC) included uropathogenic *E. coli* isolates (n=41), strains causing sepsis (n=15), and newborn meningitis (NBM; n=10); intestinal pathogens (IPEC) included enterotoxigenic *E. coli* (ETEC; n=4), enterohemorrhagic *E. coli* (EHEC; n=12), enteropathogenic *E. coli* (EPEC; n=4), enteroinvasive *E. coli* (EIEC; n=2), and enteroaggregative *E. coli* (EAEC; n=4).

Variant	***hlp*** $^{+}$	***hlp*** $^{-}$	**% *hlp*** $^{+}$
ExPEC (n = 66)	38	28	57.6
whereof UPEC (n = 41)	32	9	78.1
Faecal isolates (n = 38)	15	23	39.5
IPEC (n = 27)	1	26	3.7
Total (n = 131)	**54**	**77**	**41.2**

A 355-bp PCR product could be amplified in 54 out of the 145 strains. Most of the *hlp*-positive strains belonged to the group of extraintestinal pathogens, with UPECs as prevalent subgroup (32 positive isolates; including strains 536, CFT073, and J96). The *hlp* gene was also present in a high number of faecal strains. A detailed list of all tested strains is provided in the appendix (Table 25). However, the presence of the *hlp* gene did not correlate with a any specific serotype of the isolates.

5.2.3. Chromosomal location of the gene encoding for Hlp

To learn more about possible ways of acquisition of *hlp*, its chromosomal location was analyzed in UPEC strain 536 and CFT073. In both strains, the *hlp* gene is located 4.6-kb upstream of the tRNA locus *asnT*. This gene is the integration site of a 32-kb pathogenicity island. The island, in strain 536 termed PAI_{IV}, represents the core of the so-called high pathogenicity island (HPI) of *Yersinia* [for exact description see Dobrindt *et al*. (2002a)].

The chromosomal sequence context (80-kb) in proximity to the *asnT* gene of UPEC strain 536 was compared to the corresponding chromosomal region of strain MG1655 (Fig. 17). The nucleotide sequence of this region in UPEC strain 536 is very homologous to the one of UPEC strain CFT073 (data not shown). The absence of the 32-kb HPI in K-12 strain MG1655 can be readily detected, depicted as white stretch of no-homology between the two sequences. Interestingly, a second white stretch is present upstream of the *serU* gene, indicating another insertion of 23,173 bases into the chromosomes of strain 536 (and CFT073). This putative genomic island has been described recently by Williamson and Free (2005) for strain CFT073.

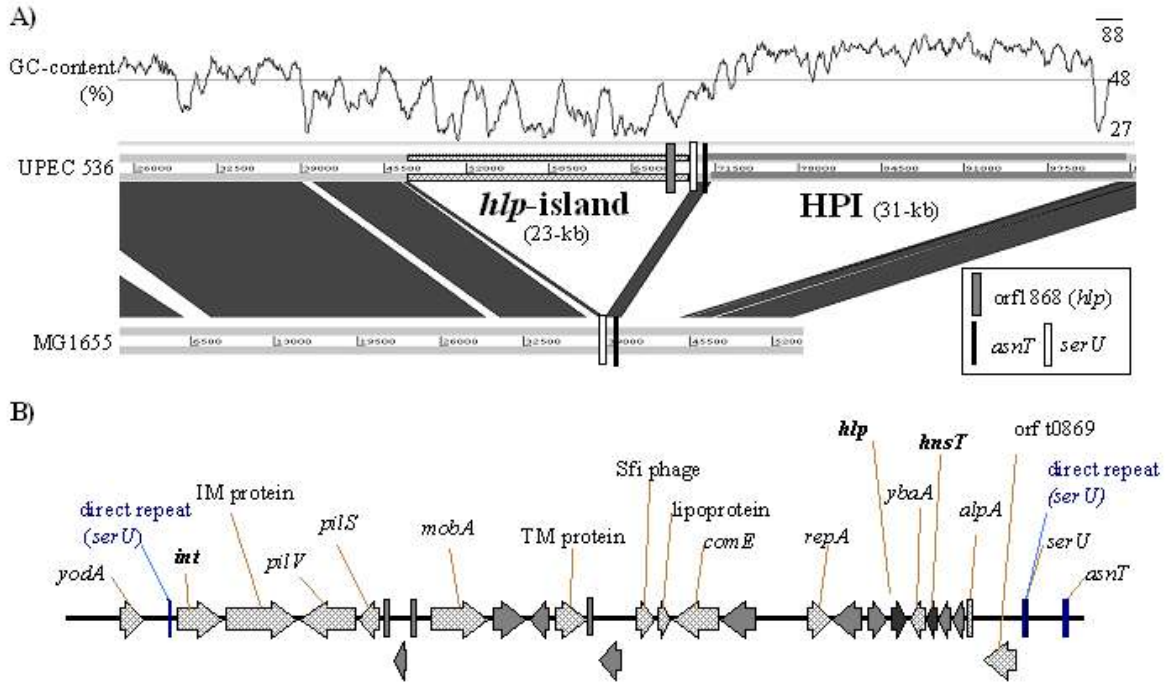

Fig. 17: Analysis of the chromosomal location of the *hlp* gene coding for Hlp. (A) Genome comparison of the *asnT*-region of UPEC strain 536 and non-pathogenic *E. coli* K-12 strain MG1655 retrieved by the ACT software (Sanger Center). Dark shading indicates regions of high homology. The location of the *hlp* gene, as well as both tRNA loci are marked within the sequences. The GC-content of the UPEC 536 sequence is depicted in a window size of 500-bp; (B) Schematic map of the *hlp* island according to the ORF annotation of Williamson and Free (2005).

The question arose, whether the inserted region represents a so far uncharacterised pathogenicity island (PAI) in strain 536. PAIs are defined as large regions in the chromosome which are often flanked by direct repeats and encode virulence-associated genes as well as mobile genetic elements such as integrases, transposases, and phages. Moreover, PAIs exhibit a different GC-content compared to the rest of the chromosome, and are often associated with tRNAs (Hacker *et al.*, 1997).

The 23-kb insertion containing the *hlp* gene was now analyzed for each of these characteristics. As already mentioned, the region is inserted at the *serU* locus. A short 14-bp duplication of the *serU* gene was found at the other end of the insertion, thereby forming a direct repeat structure. When analyzing the GC-content of the *hlp* island, it was obvious that the GC-content (37.7 % over the whole region) was much lower compared to that of the upstream chromosomal region or the downstream HPI. Furthermore, an ORF encoding a P4-like integrase (*int*), as well as a MobA-like conjugal transfer protein (*mobA*) and two phage proteins (*alpA* and Sfi 11) were found on the island. Therefore, the *hlp*-containing insertion might be considered as an additional genomic island. However, only genes with homology to *ybaA*, which encodes a conserved protein of the type 1a colicin plasmid, and *pilV* and *pilS* homologs, which are the minor subunit of type IV pili - long extracellular appendages used for attachment during conjugation - can be mentioned as possible virulence factors. Hence, the *hlp*-island can not be considered as pathogenicity island.

Nevertheless, the results suggest that UPEC strain 536, as well as other pathogenic *E. coli* strains might have acquired an *hlp* containing genomic island by horizontal gene transfer.

5.2.4. Analysis of hlp transcription

hlp *is transcribed monocistronically*

When taking a closer look at the sequence context of the *hlp* gene, a second ORF (corresponding to c2410 in CFT073) upstream of *hlp* is reading into the same direction as *hlp*. To explore, whether both ORFs are transcribed polycistronically, the transcription start point of *hlp* was identified by primer extension analysis. This revealed a single promoter starting at a thymine residue 37 bases upstream of the translation initiation codon of Hlp (see Fig. 18 A). However, no perfect consensus sequence of a typical *E coli* σ-factor could be identified.

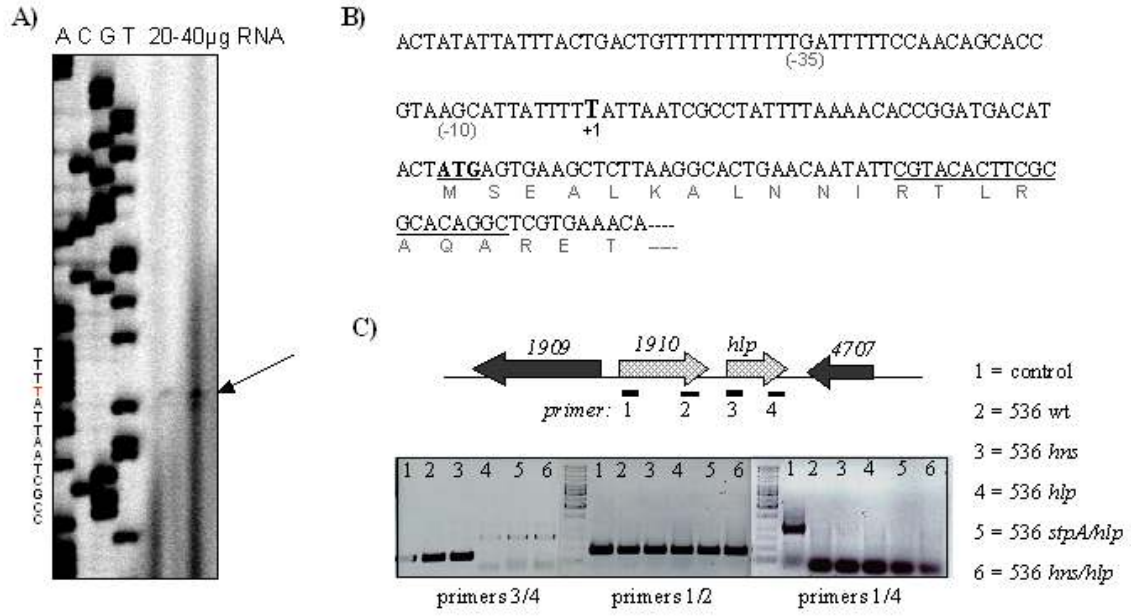

Fig. 18: Analysis of *hlp* transcription. (A) Primer extension analysis using RNA extracted from 536 wt and primer hlp-primext; (B) *hlp* promoter sequence; the transcriptional start point is indicated in bold, the primer binding site is underlined; (C) RT-PCR for amplification of the *hlp* transcript (405-nt), the orf1910 transcript (479-nt), and a putative co-transcript (1042-nt).

Transcript analysis by RT-PCR using primer combinations spanning *hlp* and/or the upstream region corroborated that *hlp* is not part of an operon with ORF1910 (Fig 18 C). Furthermore, Northern blotting revealed a transcript length of ~600 nucleotides, thereby also confirming a monocistronic *hlp* transcript (Fig. 19 A).

hlp *is subject to both auto- and crossregulation*

The expression level of *hlp* in the wild type strain 536 and its isogenic mutants was studied by semi-quantitative Northern blotting (Fig. 19 A). No transcript could be detected in the *hlp* mutants, whereas the 600-nt transcript was present in the wild type, as well as in the *stpA* and *hns* mutants. In the latter, the amount of *hlp* mRNA was increased compared to the wild type, especially in the *hns/stpA* double mutant. This suggests a repression of *hlp* expression by H-NS, and therefore in a derepression in strains lacking H-NS.

The cross-regulating activity of all three DNA-binding proteins was further assessed by semi-quantitative reverse transcription PCR (RT-PCR), using primers binding within the coding sequence of *hlp*, *hns*, and *stpA*.

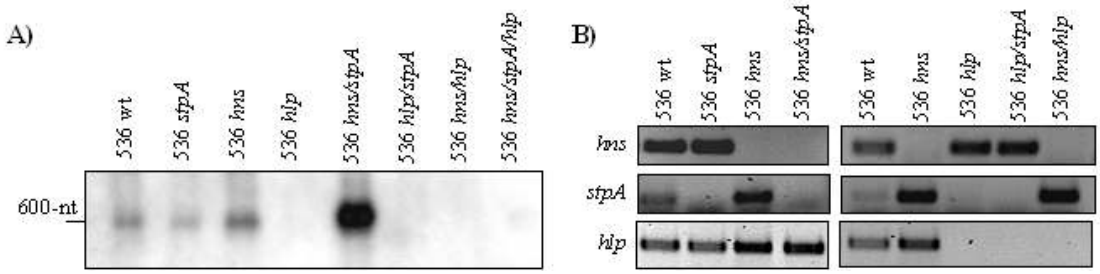

Fig. 19: Influence of histone-like proteins on *hlp*, *hns*, and *stpA* transcript amounts.
(A) Detection of *hlp* transcripts from 20 µg RNA by Northern blotting using an ECL-labelled DNA probe; (B) Semi-quantitative RT-PCR using primers binding within the coding sequence of *hns*, *stpA*, and *hlp*.

Derepression of both *hlp* and *stpA* transcription occurred in the absence of H-NS, thereby confirming its role as a repressor. A slightly higher amount of *hns* transcript could be detected in the *stpA* mutant, as it was described before in *E. coli* K-12 (Sonden and Uhlin, 1996). Lack of StpA did not affect *hlp* transcription. On the other hand, expression of *stpA* was not altered in an *hlp* mutant, whereas a derepression of *hns* transcription occurred in the absence of Hlp (Fig. 19 B). These results suggest that all three histone-like proteins are able to mediate repression of at least one of their homologs, thereby forming a cross-regulatory network.

To further confirm this cross-regulating activity, band shift assays were performed with purified Hlp, H-NS, and StpA proteins of strain 536 and K-12, respectively. For these experiments, ~350-bp PCR fragments containing the promoter regions of the *hlp*, *hns*, and *stpA* genes were used as target for protein binding.

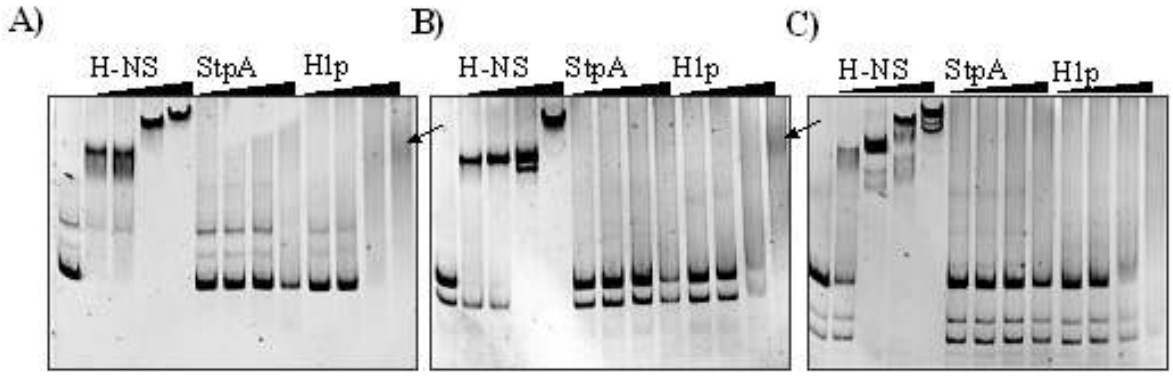

Fig. 20: Analysis of binding capacities of histone-like proteins to their own promoter regions.
Electrophoretic mobility shift assay using ~350-nt PCR fragments containing the *hlp* (A), *hns* (B), and *stpA* (C) promoter regions. Concentrations of purified H-NS, StpA, and His-Hlp was 5.3 µM, 7.1 µM, 11 µM, and 21µM.

Binding of the StpA preparation could not be observed (Fig. 20 - middle lanes). On the other hand, H-NS was binding to all three promoter fragments with equal affinities, resulting in

very specific DNA-protein complexes (Fig. 20 – left lanes). Finally, Hlp was also binding to all fragments, with the weakest affinity for the *stpA* promoter and the highest affinity for its own promoter (Fig. 20 – right lanes). The latter finding suggests, that Hlp, like H-NS and StpA, is able to mediate both cross- and auto-regulation.

Cross-regulation requires promoter regions, which are suitable for protein binding. Both H-NS and StpA have been shown to preferentially bind to AT-rich, intrinsically curved DNA sequences. Moreover, both the *hns* and the *stpA* promoter regions are predicted to have these features. Therefore, we also analyzed the *hlp* promoter region. The AT-content of the 400-bp upstream region was 63.77 %, which is even higher than for the *hns* and *stpA* promoters (AT-content 60.55 % and 63.52 %, respectively). Futhermore, the curvature prediction of the DNA fragment exhibited a strong curvature (see Fig. 52 in the appendix). This result further confirms, that the own promoter regions are possible targets for binding of histone-like proteins.

5.2.5. Overexpression and purification of HLP

For overproduction and purification of His-tagged Hlp, plasmid pASK75-His*hlp* was initially introduced into *E. coli* strain Rosetta™. However, when the 16-kDa His-Hlp protein was then enriched from the cytoplasmic fraction by Ni-affinity chromatography, a second, slightly smaller protein was co-purified (Fig. 21 A).

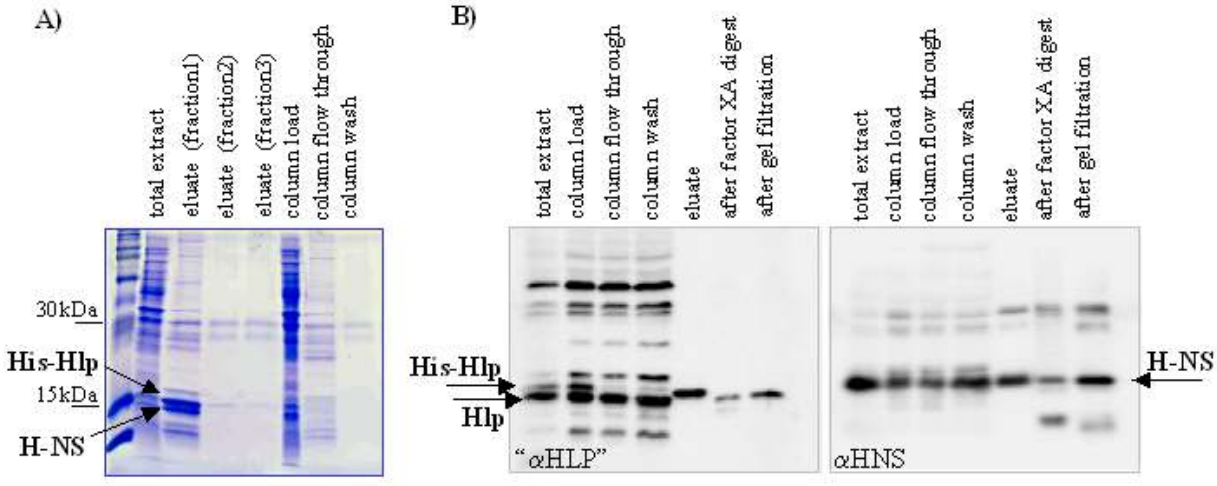

Fig. 21: Analysis of fractions during purification of His-tagged Hlp. Recombinant Hlp protein was overexpressed in *E. coli* Rosetta™ and purified using Ni-affinity chromatography. (A) Coomassie stained denaturing polyacrylamide gel of purification steps. (B) Immunoblot of the same samples with antibodies recognizing Hlp (left panel) and H-NS (right panel).

The approximate molecular weight of the second protein (~15.5 kDa) suggested that it might be native Hlp protein. Since the *hlp* gene cloned after the His-tag still had its own translation start codon, un-tagged protein could have been co-synthesized and co-purified due to dimerization with His-Hlp. N-terminal sequencing of the smaller protein, however, resulted in the sequence SEALK**I**LM, which matches the sequence of the H-NS protein. Immunoblotting with antiserum recognizing H-NS confirmed the presence of a 15.5-kDa band in all purification fractions (Fig. 21 B). When using an antiserum detecting both Hlp and StpA, both the 15.5-kDa band and a larger one corresponding to His-tagged protein appeared. This again strongly indicates, that H-NS is co-purifying with Hlp.

We also wanted to determine the nature of the interaction between H-NS and Hlp that leads to co-purification. Therefore, the Ni-column was washed with increasing salt concentrations in the wash buffer prior to elution. Even with a potassium chloride concentration of as much as 2 M, elution of H-NS due to dissociation of the complex was not observed (Fig. 22), thereby indicating hydrophobic interactions between the two proteins.

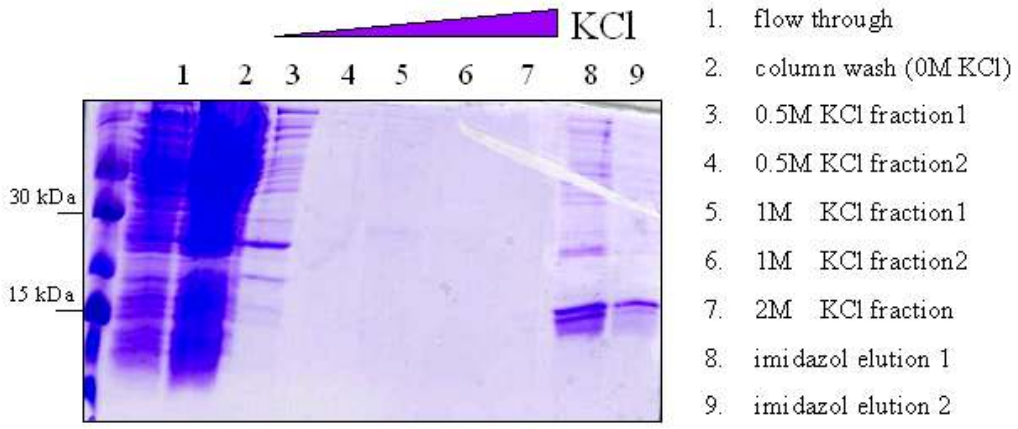

Fig. 22: Analysis of the nature of the interaction between Hlp and H-NS. Recombinant Hlp protein was expressed and purified as seen in Fig. 21 A, but here the Ni-column was washed with increasing concentrations of KCl prior to elution with imidazole.

Washing the column with up to 80 mM imidazole neither resulted in elution of any protein, thereby confirming that H-NS is not unspecifically retained in the column, but is rather bound in a specific H-NS/Hlp complex.

Another indication that the biological form of Hlp is not a monomer was derived from gel filtration chromatography. The first intention for using this technique resulted from the contamination of the protein samples with proteinase factor XA after removing the His-tag. The proteinase consists of two subunits of 30 and 50 kDa.

Therefore it should be possible to separate the subunits from the 15-kDa Hlp protein in a gel filtration column. However, all Hlp protein eluted much earlier as expected (by comparing the Hlp run with a MW calibration run), namely in fractions 20 to 25 (Fig. 23 A). In the calibration run, bovine serum albumin with a molecular weight of 67 kDa eluted in fraction 22, whereas ovalbumin with a molecular weight of 43 kDa eluted in fraction 26. This indicates, that Hlp migrated like a protein of approximately 60 kDa.

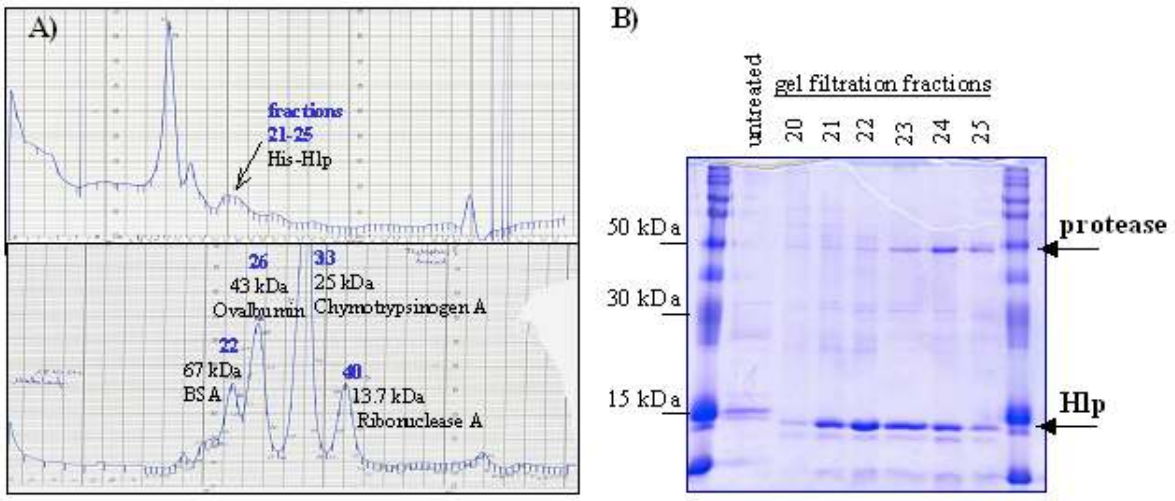

Fig. 23: Analysis of native Hlp by gel filtration (A) UV measurements of the different fractions during gel filtration. Upper panel = Hlp sample; lower panel = MW calibration samples containing four different proteins. (B) Coomassie stained denaturing acrylamide gel of gelfiltration fractions.

When analyzing the fractions by denaturing gel electrophoresis, we also found the 50-kDa subunit of the factor XA protease in the late fractions (Fig. 23 B). This result strongly suggests, that the biological form of Hlp is a tetramer – either as homomeric complex, or as heteromers with H-NS – wich adds up to a MW of 60 kDa, and therefore can not be separated from the protease by non-denaturing gel filtration chromatography.

Finally, the heteromeric complex was directly detected by chemical crosslinking of proteins in the eluate with glutaraldehyde. Immunoblotting using antisera recognizing H-NS or Hlp revealed the presence of a 30-kDa H-NS/Hlp complex, as well as higher oligomers in the crosslinked fraction (Fig. 24 B).

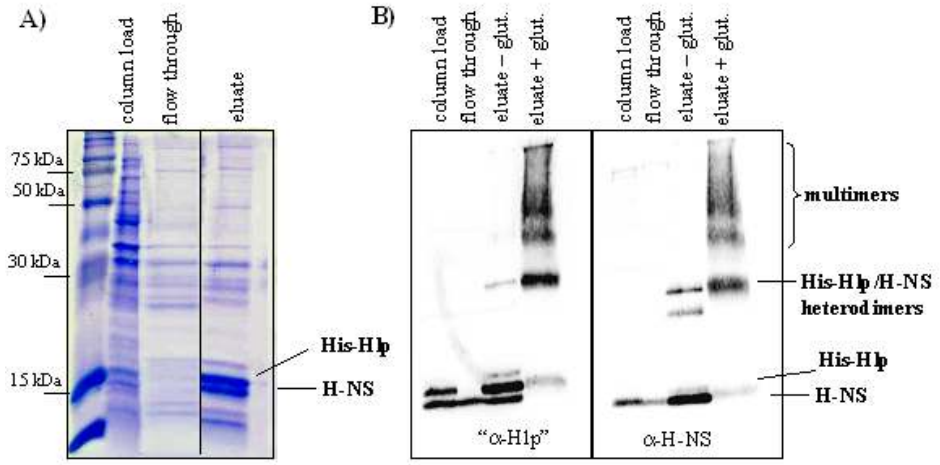

Fig. 24: Analysis of *in vitro* oligomerization by chemical crosslinking. Recombinant Hlp protein was expressed in *E. coli* Rosetta™ and purified using Ni-affinity chromatography. Proteins in the eluate were chemically crosslinked with glutaraldehyde and analyzed by denaturing polyaclyamide gelelctrophoresis (A) and immunoblotting (B)

Taken together, these results infer direct protein-protein interactions between Hlp and H-NS, resulting in the formation of a stable heteromeric complex.

5.2.6. Analysis of Hlp stability

To obtain pure Hlp protein without co-purification of H-NS or StpA, strain JGJ152 (*hns/stpA*) was transformed with the expression plasmid pASK75-His*hlp*. However, it was not possible to obtain any recombinant protein using the standard protocol for purification. Only when decreasing the period of protein synthesis induction to < 1 h (instead of 6 h), a small amount of His-Hlp could be purified (Fig. 25 A).

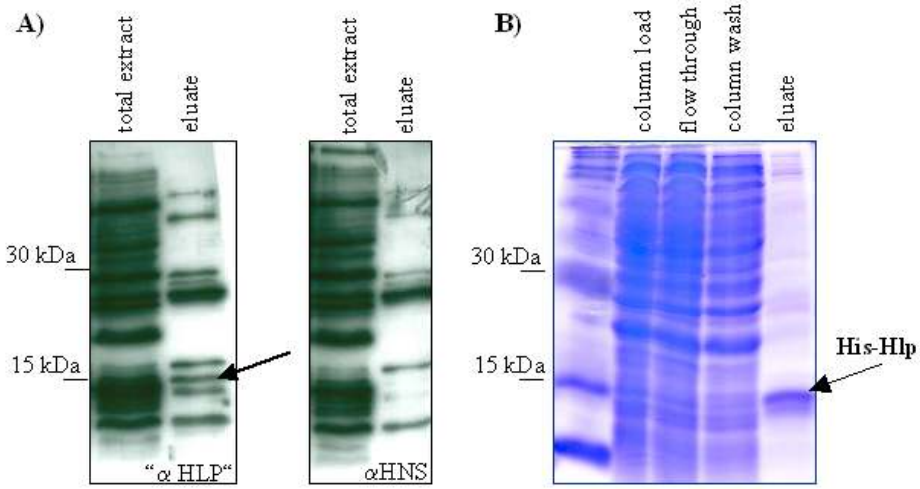

Fig. 25: Alternative strategies for purification of recombinant Hlp protein.
(A) Immunoblot of total extracts and eluted proteins after purification from strain JGJ152 (MC4100 *hns/stpA*) after 1 h induction; (B) Coomassie stain of purification fractions from protease-negative *E. coli* expression strain BL21(DE3) *hns*.

Johansson and Uhlin (1999) reported that StpA is readily degraded by the Lon protease, if not protected by H-NS. If the same were true for Hlp, it would explain the failure to purify Hlp in an *hns* mutant strain like JGJ152, since any newly synthesized Hlp protein would be degraded by a host protease during induction. On the other hand, it should then be possible to purify Hlp in a *hns* mutant lacking any protease. Therefore, the expression plasmid was transferred into an *hns* mutant of the protease-negative expression strain BL21(DE3). Indeed, using this strain, we were able to obtain high amounts of His-Hlp without any contamination by H-NS (Fig. 25 B). This result indicates, that - as in case of StpA - H-NS might protect Hlp from degradation.

To test this hypothesis, Hlp was expressed from either a low copy number plasmid (pWKS30-*hlp*) or from the inducible His-Hlp expression plasmid, and protein stability was assessed in *E. coli* MC4100 mutants lacking both StpA and H-NS, and/or the Lon protease. In case of the low copy number plasmid, no degradation of the native Hlp protein in an *hns*-negative, protease-positive strain could be observed 3 h after stopping protein synthesis by addition of spectinomycin, thereby contradicting this hypothesis (Fig 26 A).

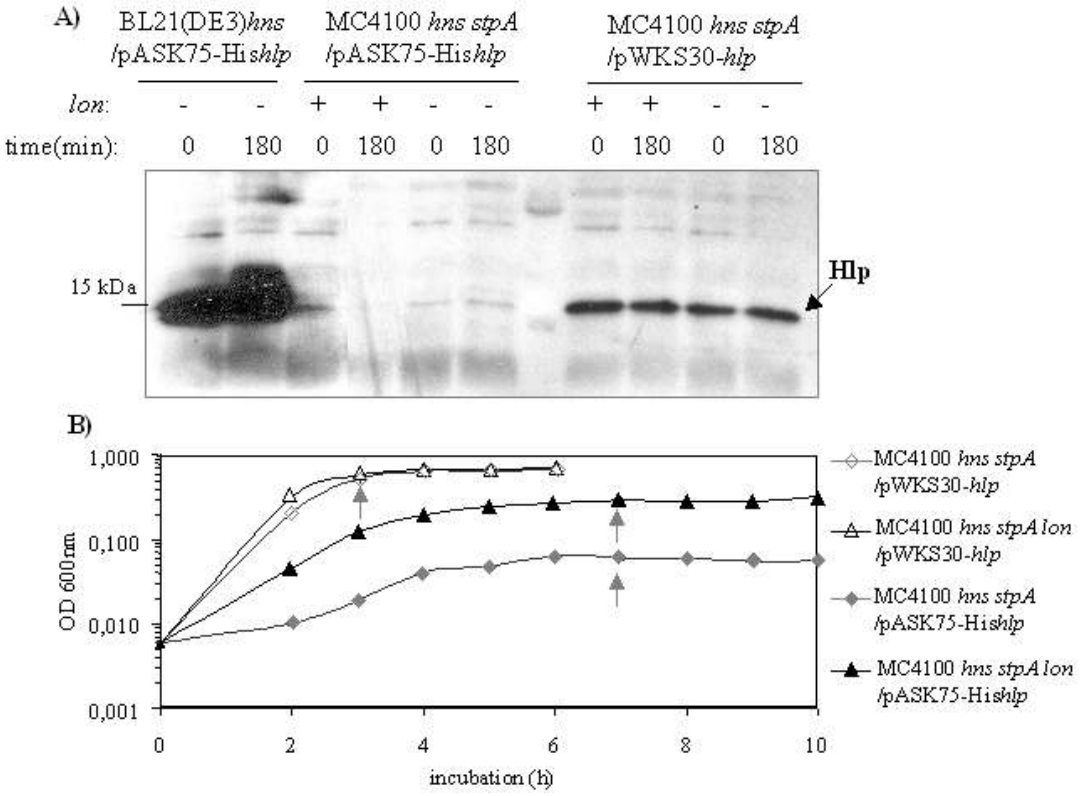

Fig. 26: Analysis of Hlp stability. (A) Immunoblot for the detection of Hlp protein before and 3 h after inhibition of protein synthesis by addition of spectinomycin. Strains transformed with pASK75-His*hlp* were grown in presence of the inducer a-Tc. (B) Growth curves of the transformants during the stability assay. Arrows indicate the time point of addition of spectinomycin (t_0).

Interestingly, no recombinant protein expressed from plasmid pASK75-His*hlp* could be detected at all in the *hns stpA* double mutants, while high amounts were synthesized in strain BL21(DE3) *hns*. Furthermore, the MC4100 mutants grew only poorly under standard growth conditions, and the growth defect was further enhanced in the presence of the inducer anhydro-tetracycline (Fig. 26 B). Therefore, this suggests that the failure to purify recombinant Hlp protein in strain JGJ152 was not a result of proteolytic degradation of Hlp, but rather caused by an insufficient expression level in the MC4100 background due to some sort of plasmid intolerance.

5.2.7. Hlp has in vivo *activity*

After successful overexpression and purification of the Hlp protein, it was tested, whether Hlp has any *in vivo* activity. Therefore, native protein was expressed from a low copy number plasmid (pWKS30-*hlp*) in *hns* mutants of the K-12 strains MG1655 and MC4100, and its ability to complement for the lack of H-NS was assessed for some well described *hns* phenotypes.

As a first test system, *E. coli* K-12 strain MG1655 and its isogenic *hns* mutant BEU740 harbouring plasmid pWKS30-*hlp* or the vector control were stabbed on swarming agar plates to assess their motility. The wild type strain with or without the plasmids exhibited swarming ability, whereas the *hns* mutant was completely non-motile. Expression of Hlp from plasmid pWK30-*hlp*, however, restored motility of the *hns* mutant to the same extent as the wild type (Fig 27 A). This indicates, that Hlp can assume activation of the flagella master operon *flhCD* in absence of the normal regulator H-NS.

Next, expression of two determinants was analyzed which are usually silent in the wild type due to repression by H-NS, namely the cytolysin-encoding gene *clyA* and the *bgl* operon, which encodes enzymes for the utilization of ß-glucosides. Because of transcriptional silencing, *E. coli* K-12 wild type cells are non-hemolytic on blood agar plates, and white on agar plates containing the ß-glucosidase substrate X-Glu, whereas *hns* mutants exhibit a hemolytic phenotype and grow as blue colonies on X-Glu plates. When introducing the *hlp*-plasmid into the *hns* mutant, it became non-hemolytic on blood agar and white on X-Glu plates, thereby resembling the wild type (Fig. 27 B and C). The same results were obtained with *hns stpA* mutants in an *E. coli* MC4100 background (data not shown). This indicates, that Hlp can silence the *clyA* and *bgl* determinants in the absence of H-NS independently of StpA.

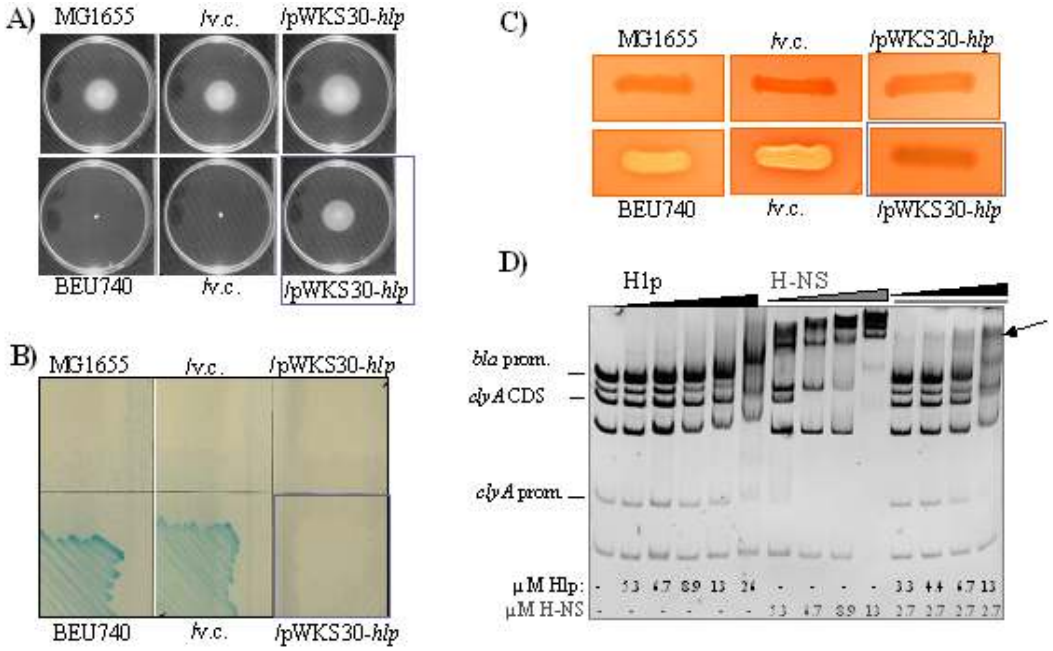

Fig. 27: Analysis of complementing activity of Hlp in strains lacking H-NS. *E. coli* K-12 strain MG1655 and its isogenic *hns* mutant BEU740 were transformed with the low copy number plasmid pWKS30-*hlp* and the vector control, and changes in typical *hns* phenotypes were monitored.
(A) Swarming ability on 0.3 % agar plates; (B) Expression of ß-glucosidases (*bgl*) on X-Glu plates; (C) Hemolytic activity on blood agar plates; (D) Electrophoretic mobility shift assay testing binding of Hlp and/or H-NS to *EcoR*I/*Dra*I restricted plasmid pYMZ80 containing the *clyA* gene.

However, when monitoring binding activity of Hlp to the *clyA* promoter by electrophoretic mobility shift assay as described by Westermark *et al.* (2000), no specific binding could be detected with the Hlp protein alone (Fig. 27 D). On the other hand, addition of small amounts of H-NS resulted in specific DNA-protein complexes, thereby suggesting possible effects of Hlp on *clyA*. However, since no functional ClyA protein is expressed in UPEC strain 536, this effect is off less significance in the wild type cells.

Another typical *hns* phenotype is derepression of the osmotically inducible glycine-betaine transport system encoded by the *proU* operon. Using chromosomal *proU-lacZ* fusion strains in both an *hns*$^{+}$ (BEU693) and *hns* $^{-}$ (BEU694) background, a higher ß-glucosidase activity was observed in the *hns* mutant transformed with the vector control than in the wild type (1040 vs. 777 Miller units, respectively). After complementation of the mutant with Hlp, *proU* transcription was reduced to wild type levels (Fig. 28 A). However, introduction of the *hlp*-containing plasmid into the wild type strain resulted in higher ß-galactosidase activity (1011 Miller units) compared to the vector control strain, thereby indicating, that Hlp might act as an anti-H-NS factor for *proU* repression in this test system.

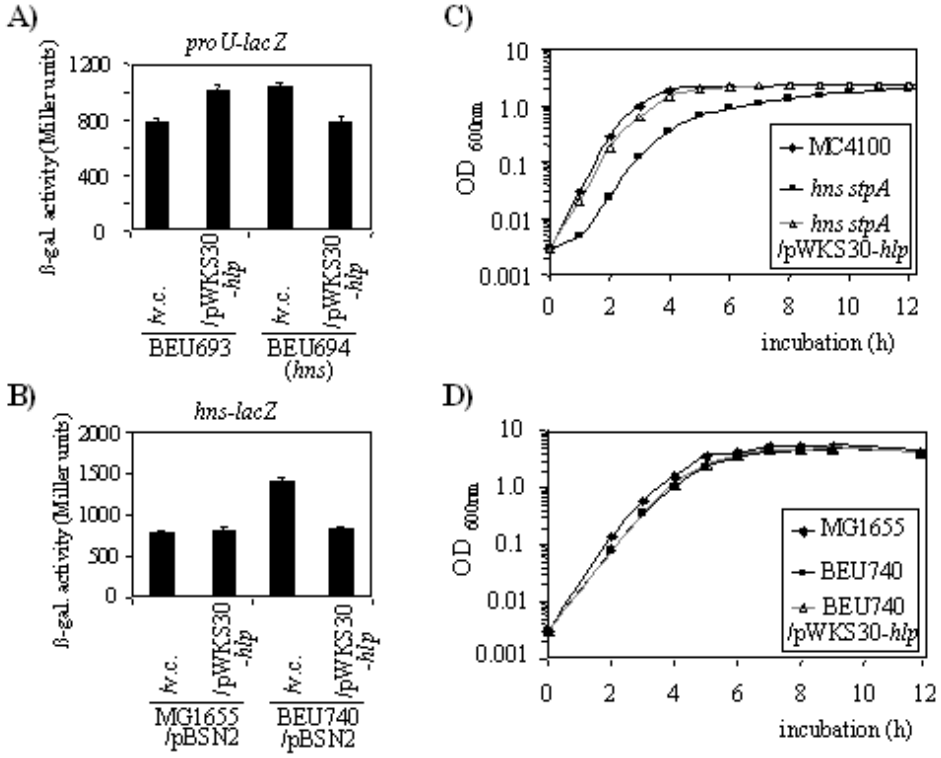

Fig. 28: Effects of Hlp on transcription levels and growth rates of *hns* mutants. (A) ß-galactosidase activity of chromosomal *proU-lacZ* reporter strains; (B) ß-galactosidase activity of plasmid-encoded (pBSN2) *hns-lacZ* reporter strains; (C) Growth curves of strain MC4100 and isogenic *hns/stpA* double mutant at 37 °C; (D) Growth curves of strain MG1655 and isogenic *hns* single mutant (BEU740) at 37 °C.

H-NS was shown to negatively affect its own transcription by autoregulation. To assess, whether expression of the Hlp protein can also mediate repression of *hns* expression, both the *hlp*-encoding plasmid and a plasmid-encoded *hns-lacZ* fusion (pBSN2) were introduced into strain MG1655 and its isogenic *hns* mutant, and ß-galactosidase activity was determined.

As expected, *hns* transcription was derepressed in the *hns* mutant transformed with the vector control, thereby confirming negative autoregulation (Fig. 28 B). This effect was abolished when the mutant was complemented with Hlp, resulting in the same *hns* expression level as in the wild type. This result indicates that the Hlp protein is able to repress *hns* transcription, and further confirms transcriptional cross-regulation of the histone-like proteins.

Strains lacking both H-NS and StpA have a growth defect even at normal growth conditions. This growth defect was partially restored after introducing the *hlp*-containing plasmid into an *hns stpA* double mutant of strain MC4100 (Fig. 28 C). Thus, Hlp can also substitute H-NS in terms of growth.

However, the growth curve of the complemented strain resembled more that of an *hns* mutant, and almost no complementation was observed in an *hns* single mutant (Fig 26 D). These results suggest that, in terms of growth, the presence of the StpA protein is of more importance than Hlp.

To summarize, we provide evidence that UPEC strain 536 and other *E.coli* variants express a third histone-like protein with high homology to H-NS. The gene coding for Hlp is located on a so far uncharacterized genomic island of 23-kb in size inserted at the *serU* locus. Due to structural similarities at the N-terminus, H-NS and Hlp are directly interacting, thereby forming stable heteromers. In contrast to StpA, the Hlp protein is not proteolytically degraded by the Lon protease in absence of H-NS. The heteromer is supposed to be the biologically relevant form of Hlp. Moreover, Hlp exhibits *in vivo* activity, since it can complement for the lack of H-NS in terms of motility, repression of the *bgl*, *clyA*, and *proU* operons, and also has an effect on growth rates. However, these experiments were performed in a K-12 background, where Hlp does not naturally occur, and therefore do not answer the question for the biological role of the H-NS paralog.

5.3. Role of the H-NS paralogs

Due to the high homology between the histone-like proteins, one might speculate about the degree of redundancy in the cell. Does a similar structure also imply similar functions, or do the H-NS paralogs play separate roles in the gene regulation process? To answer this question, mutants deficient for one or several of the histone-like proteins were constructed and searched for differences in their phenotype.

5.3.1. Construction of *hlp* mutants

The construction of the *hlp* single, double and triple mutants was performed using the λRed method, as described for the *hns* and *stpA* mutants (see section 5.1.1.). The *hns/stpA/hlp* triple mutant was constructed by introducing a linear fragment containing a chloramphenicol-resistance cassette with homology extension to *hlp* into the pre-existing *hns/stpA* mutant.

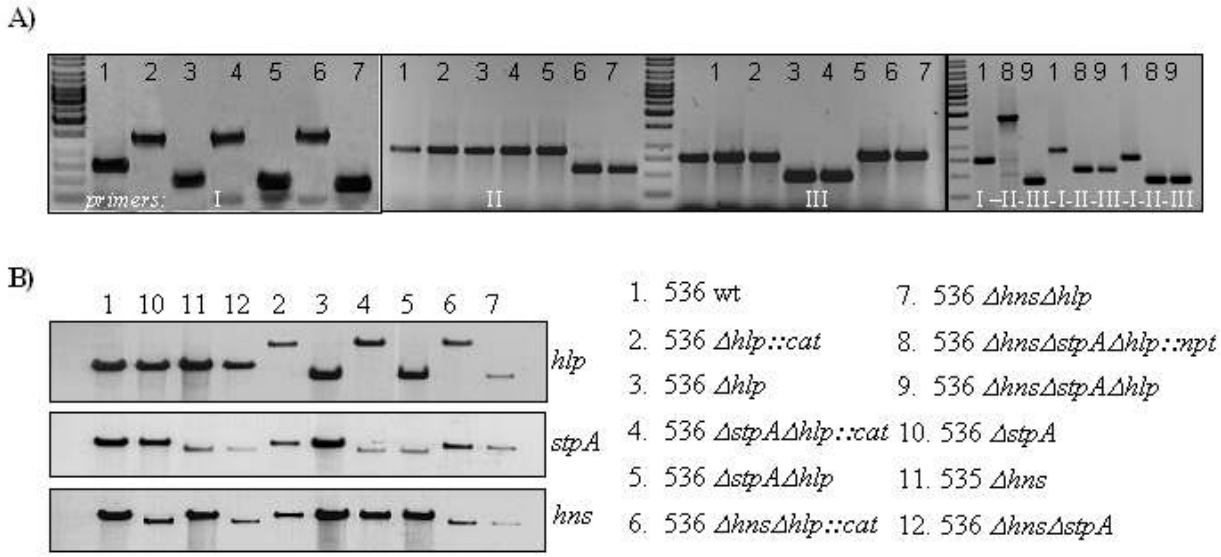

Fig. 29: Verification of the *hlp* mutations. (A) PCR amplification using primer combinations I = hlp-3/4; II = hns-3/4; and III = stpA-3/4; (B) Southern hybridization using *EcoR*V restricted DNA and PCR generated DNA probes binding to *hlp*, *hns*, or *stpA* fragments.

All mutation were confirmed by both PCR amplification of the target region and by Southern hybridization (Fig. 29).

5.3.2. Role of H-NS and its paralogs on expression of virulence-associated genes

The phenotypes of the newly constructed mutants were tested by classical physiological assays for typical virulence traits of uropathogenic *E. coli*. At the same time, these tests served to confirm the array data obtained with the *hns* and *stpA* mutants.

Motility and chemotaxis

The effect of H-NS on motility is a rare example for an activating role of H-NS and has already been described for several strains (Soutourina *et al.*, 1999). This was also true for UPEC strain 536, where all H-NS deficient mutants were completely non-motile on swarming agar plates (Fig 30).

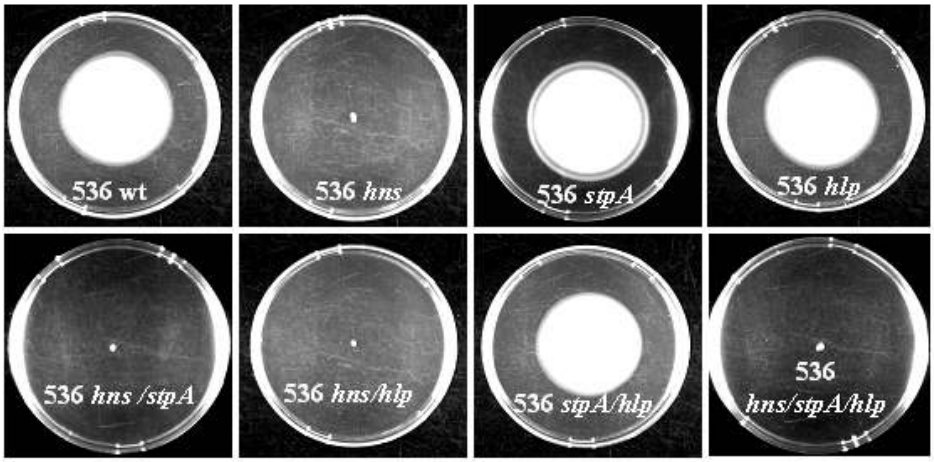

Fig. 30: Swarming ability of H-NS deficient mutants of *E. coli* 536 on swarming agar plates.

This result is supported by the array data, where the expression of almost all genes of the flagellar operons was downregulated (see appendix - Table 18). Furthermore, the lack of motility seemed to coincide with a ceased expression of genes whose encoded products are involved in chemotaxis such as *cheW*, *cheA*, *cheZ* and *cheY*. In total, 32 genes of this functional group were downregulated. The strongest effect was observed for the flagellin gene *fliC* itself, where the expression was 12.6 times lower in the *hns* mutant and 9.3 in the *hns/stpA* mutant, respectively. Taken together, our results were in good agreement with previous observations for other *E. coli* strains, including K-12, and further confirm the positive regulation of motility by H-NS.

Adhesins

Strain 536 encodes at least three types of fimbrial adhesins, namely the chromosomally encoded type 1 fimbriae (*fim*), P-related fimbriae (*prf*) encoded on PAI_{II} and S-fimbrial adhesin (*sfa*) encoded on PAI_{III}. Lack of H-NS affected expression of all three of them.

The effect of H-NS on type 1 fimbriae expression is already described in the literature, where H-NS was shown to repress the recombinases *fimB* and *fimE* (Olsen and Klemm, 1994). Both recombinases are involved in the phase variation of an invertible DNA fragment containing the *fimA* promoter, therefore mediating switching between a fimbriated and a non-fimbriated state. In UPEC strain 536, the same effect of H-NS on expression of the recombinases was observed using the DNA arrays. Lack of H-NS resulted in a significant upregulation of *fimB* by factor >4 and of *fimE* by factor >2 in both *hns* and *hns/stpA* mutants (Fig 14; section 5.1.3.).

Expression of the structural genes was not significantly altered at the transcriptional level. At least for the major fimbrial subunit *fimA*, this lack of regulation was confirmed by semi-quantitative RT-PCR (Fig. 31 B).

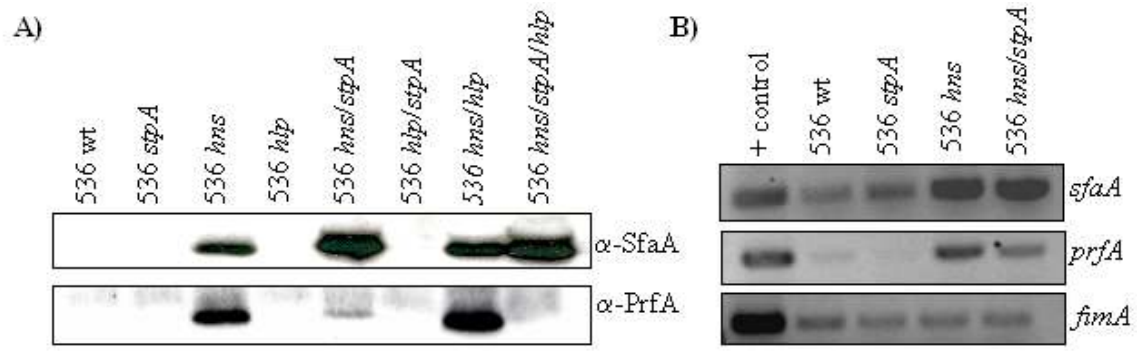

Fig. 31: Effect of histone-like proteins on production of fimbrial adhesins.
(A) Immunoblot using antisera directed against purified S- and P-fimbriae; B) semi-quantitative RT-PCR for major fimbrial subunits. Samples were taken from liquid cultures in mid-log phase.

S fimbriae are mainly found in uropathogenic *E. coli* and in strains causing newborn meningitis (Morschhäuser *et al.*, 1993). Using the *E. coli* pathoarray, the expression level for each gene of the *sfa* gene cluster in an *hns* mutant strain could be monitored. All structural genes were significantly upregulated in the mutants when compared to the wild type (Fig. 14; section 5.1.3.). The most prominent derepression could be observed for the major subunit-encoding gene *sfaA*. Expression of the *sfaA* gene was 27 times higher in the *hns* mutant compared to the wild type, and 12 times higher in the *hns/stpA* mutant, which ranked *sfaA* among the 10 most strongly affected genes sorted according to their expression levels (see appendix - Tables 13 & 14). When monitoring the expression of *sfaA* at the protein level using a specific antiserum against purified S fimbriae, or at the transcriptional level using semi-quantitative RT-PCR, we also saw a massive derepression in all *hns* mutants (Fig. 31 B), thereby confirming the results from transcriptional profiling.

UPEC strain 536 expresses another type of fimbriae with similarities to the pyelonephritis-associated P-pili. It could be shown that, like for the *pap* genes, H-NS also affects expression of those P-related fimbriae. Western blotting using PrfA specific antiserum revealed that expression of the major subunit was increased in H-NS deficient strains compared to the wild type, especially when taking samples from static cultures or from agar plates (Fig. 31 A).

When going back to the data from the *E. coli* pathoarray, derepression of *prfA* transcription was not as drastic as seen at the protein level (Fig 14; section 5.1.3.). However, when comparing signal intensities on the array, it was evident that the overall expression level of P-related fimbriae was very low under these conditions, i.e. mid-log phase samples from liquid cultures. Only the *prfX* gene encoding a putative regulator was significantly upregulated in both mutants, with expression ratios of 5.2 in the *hns* mutant and 3.7 in the double mutant. This gene encodes a 17-kDa protein, which is believed to be a putative regulator of the *prf* operon.

To verify, whether derepression of the genes for both S- and P-fimbriae at the transcriptional level also resulted in increased biogenesis of fimbriae, cells grown on agar plate were fixed onto Mica platelets and analyzed by atomic force microscopy (AFM). As seen in Fig. 32, an *hns* mutant cell is heavily fimbriated in contrast to the wild type.

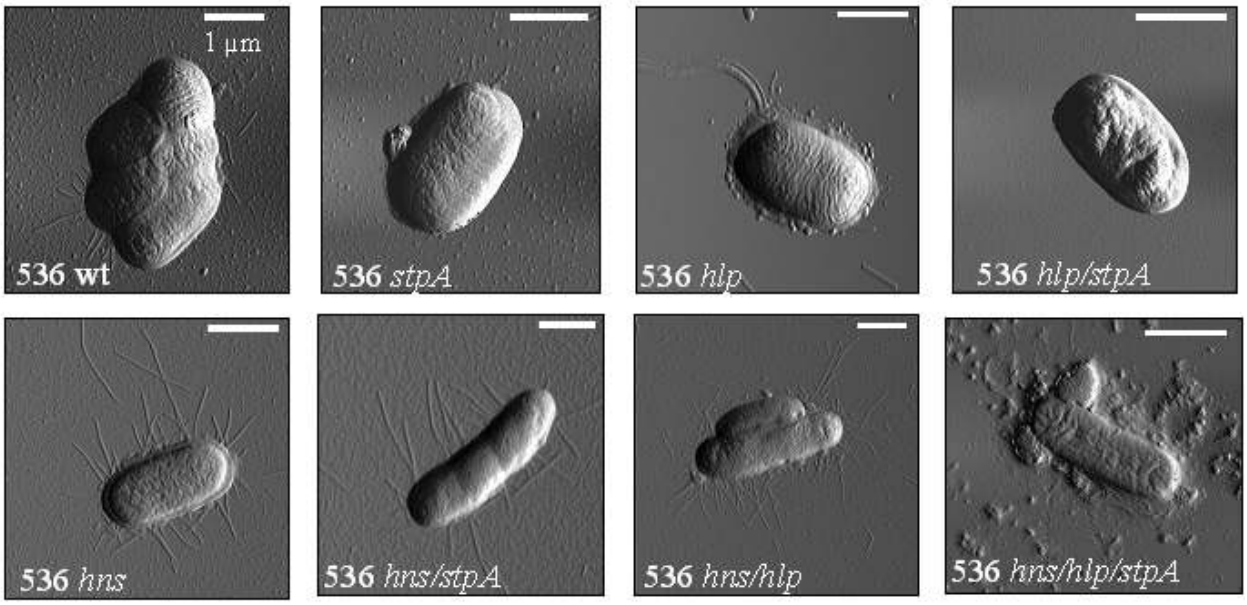

Fig. 32: Analysis of fimbriae expression of wild type strain 536 and its isogenic mutants by AFM.
(Tapping mode)

This technique also resulted in the discovery of other interesting aspects of cell morphology, such as filamentous growth of *hns* mutants, or the seemingly increased production of outer membrane vesicles in strains lacking both H-NS and Hlp. More AFM micrographs of each mutant can be found in the appendix (Fig. 51).

With regard to the hyper-fimbriated phenotype, a higher expression of S- and P-pili was also found in the *hns/hlp* double mutant and the triple mutant. However, when comparing expression levels between the *hns/stpA* and the *hns/hlp* mutant, a clear difference was observed: As determined from the immunoblot, lack of StpA resulted in a less pronounced derepression of P-pili in the absence of H-NS, whereas expression of S-pili was even higher compared to the *hns* single and *hns/hlp* double mutants.

Taken together, the results infer a major role of H-NS in regulating the expression of both P- and S-fimbriae, which are believed to be important virulence factors during urinary tract infections, whereas the H-NS paralogs Hlp and StpA do not seem to be of major importance. Nevertheless, both proteins seem to have a modulating function on the effect of H-NS, e.g. resulting in fine-tuned cross-regulation of fimbrial adhesins.

Hemolytic activity

UPEC strain 536 possesses two *hly* determinants encoding α-hemolysin. Both gene clusters are located on pathogenicity islands (PAI_I and PAI_{II}) and the biological function of having two copies of *hlyCABD* is still unknown. Both clusters encode the RTX-toxin HlyA, the activator HlyC, and proteins HlyB and HlyD, involved in toxin secretion.

On the *E. coli* pathoarray, both transport proteins HlyB and HlyD were significantly upregulated in H-NS deficient strains, and the activator HlyC showed a trend towards higher expression in the mutants (Fig 14; section 5.1.3.). When using the more sensitive method of RT-PCR, an increased amount of the *hlyA* transcript encoding the toxin itself could be detected (Fig. 33 C). Furthermore, secretion of α-hemolysin was visualized by stabbing the strains on blood agar plates and detecting the formation of halos around the colonies due to lysis of erythrocytes (Fig. 33 A). Here, the problem arose that the *hns* mutants did not grow to the same colony size as the other strains. Therefore, a quantification of hemolysis was not possible. However, when measuring hemolytic activity of culture supernatants from late-log phase cultures grown at 30 °C to ensure maximal expression of the hemolysin, the hemolytic units of all *hns* mutants were about 5 to 10 times higher compared to the wild type (Fig. 33 B; Table 12).

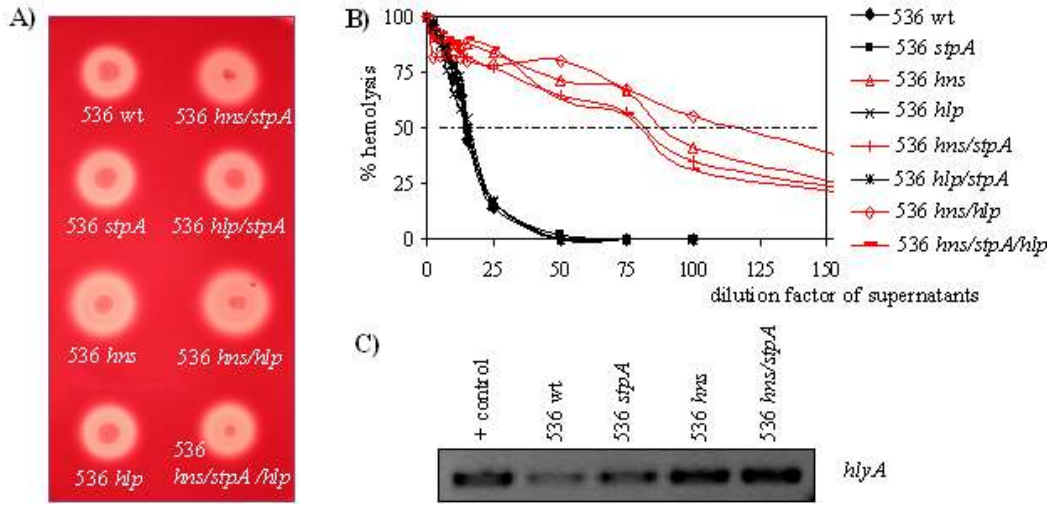

Fig. 33: Effects of histone-like proteins on hemolytic activity. (A) Phenotype on a blood agar plate containing 5 % sheep erythrocytes; (B) semi-quantitative hemolysis assay with diluted culture supernatants. Hemolytic units equal the dilution factor at which 50 % hemolysis occurred; (C) semi-quantitative RT-PCR for α-hemolysin-encoding gene *hlyA*.

This repressive effect of H-NS on hemolysin expression is consistent with earlier findings in the literature (Madrid *et al.*, 2002; Nieto *et al.*, 2000), where H-NS was shown to mediate thermoregulation by binding to the regulator Hha. In *hns* mutants of strain 536, the expression of *hha* itself was also increased by factor 4.7 (*hns*) and 2.1 (*hns/stpA*), respectively. This result confirms, that Hha requires functional H-NS protein for its activity as a repressor.

Iron uptake systems

UPEC strain 536 encodes five types of iron uptake systems. The salmochelin system (*iro*) and the yersiniabactin system (*ybt*) are both encoded on pathogenicity islands, the hemin receptor (*chuA*) locus resides on a small islet not present in *E. coli* K-12, whereas the determinants coding for the ferrichrome (*fhu)* and the enterobactin system (*fep*) are located within the *E. coli* core genome. Each system consists of proteins involved in binding of the siderophore/hemin by a receptor and distinct proteins for the transport of the complexes into the cell.

When going back to the expression levels of the various gene detectable with the DNA arrays, only genes encoding the corresponding receptors had an altered expression level in the *hns* mutants (see appendix - Table 20). In detail, the expression of the salmochelin receptor *iroN*, the ferrichrome receptor *fhuA*, and the yersiniabactin receptor *fyuA* together with three other genes of the cluster, *ybtQ ybtS* and *ybtX* were significantly upregulated. The enterobactin system and the hemin receptor were not affected by the mutations.

However, these values derive from non-inducing conditions, were the total expression levels of these genes were very low. Therefore, the more sensitive method of semi-quantitative reverse-transcription PCR (RT-PCR) was used, which enables the detection of low transcript amounts.

As already seen on the array, significant higher transcript levels of the salmochelin receptor gene *iroN* were detected by RT-PCR in the H-NS deficient strains compared to the wild type, whereas the transcript levels of the hemin receptor gene *chuA* were much lower in these strains (Fig. 34 D). Expression of the enterobactin receptor gene *fepA* was not altered by the mutations and expression of the yersiniabactin receptor gene *fyuA* was not detectable under these conditions. These results indicate that H-NS has divergent effects on the expression of the different siderophores systems, playing both an activating and a repressing role.

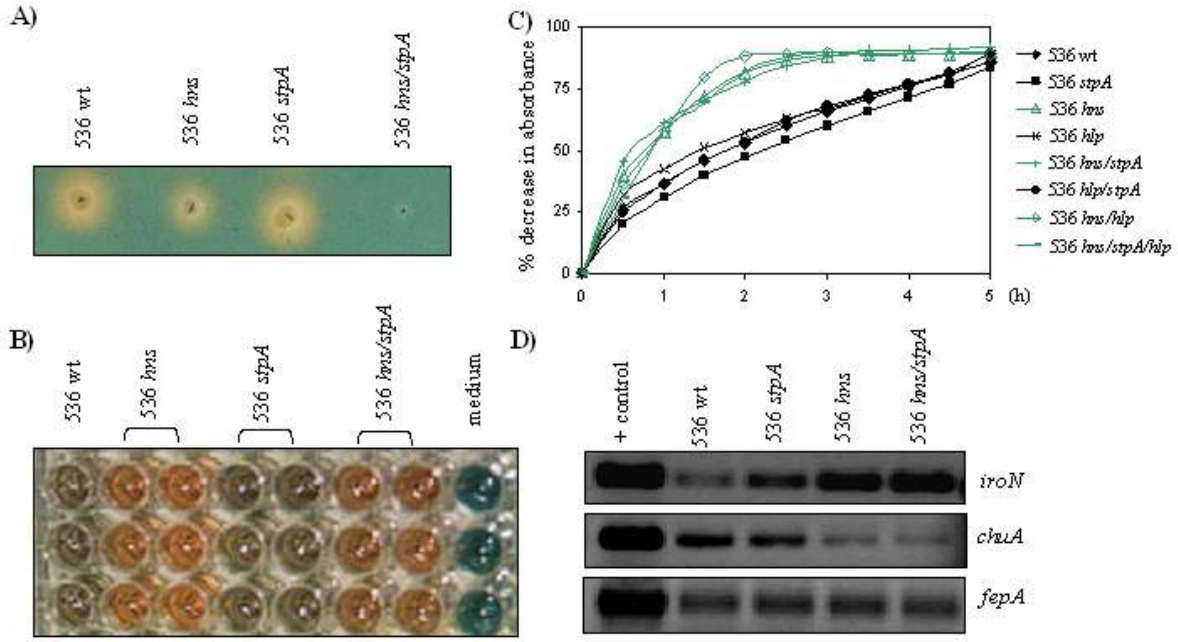

Fig. 34: Effects of histone-like proteins on the production of siderophores. (A) UPEC strain 536 and mutants stabbed onto agar plates containing chrome azurole S (CAS); yellow halos are formed in the presence of siderophores due to degradation of the blue iron complex ; (B) CAS liquid assay on microtiter plate scale; degradation of the assay solution can be measured photometrically at 630 nm; the picture was taken after 45 min; (C) CAS liquid assay quantitation; (D) semi-quantitative RT-PCR for three siderophore receptor genes.

To further study this effect, secreted siderophores were directly detected using a chrome azurole S (CAS) - based assay developed by Schwyn and Neilands (1987). First, strains were stabbed onto agar plates containing the blue CAS-iron complex. Secreted siderophores would bind the iron and result in degradation of the blue complex, thereby forming a yellow halo around the colonies (Fig. 34 A). As on the blood agar plates, quantitation was not possible due to the growth defects of the *hns* mutants.

Therefore, a chromatographic assay for the detection of siderophores was performed under iron-limiting conditions (see method section 4.6.2.). In this assay, the blue iron-complex in the assay solution is degraded gradually if siderophores are present in the supernatants and consequently, the absorbance decreases (Fig. 34 B). The quantitation of the assay is shown in Fig. 34 C. All strains reach the same absorbance at state of equilibrium, thereby indicating an equal amount of siderophores in the supernatants. However, the decrease in absorbance happens much faster in H-NS deficient strains. Taken together, our data infer a differential regulation of the iron uptake systems by H-NS.

Stress resistance

H-NS is known to be involved in adaptation to various types of stress situations (Atlung and Ingmer, 1997; Hommais *et al.*, 2001). This role was also found when analyzing the expression pattern of *hns* mutants of UPEC strain 536. Many gene whose products are involved in stress adaptation and multidrug resistance were found among the list of upregulated genes on the K-12 array (see appendix - Table 23). In particular, many of these genes were involved in acid resistance, like the determinants coding for glutamate decarboxylases/antiporters GadA, GadB, XasA, and their activators GadX (YhjX) and GadE (YhjE), the lysine decarboxylase CadA and *CadB,* as well as the acid chaperones HdeA HdeB. All these genes were among the ten most strongly upregulated genes. Furthermore, many genes within the “acid resistance cluster” like *yhiQ*, *yhiD*, and *yhjHJKL* were upregulated in the mutants. Derepressed genes whose products are involved in multidrug resistance included *mdtEF* and *emrKY*, as it was already described by Nishino *et al*. (2004).

The data obtained in this study also supported the well-known role of H-NS in osmoprotection. The genes coding for the glycine-betaine/proline transporter system *proVWX* were significantly upregulated in the *hns* mutants, with *proV* ranking on positions 4 (*hns*) and 15 (*hns/stpA*) among the 50 most strongly upregulated genes (see appendix - Tables 13 & 14). Other osmotically inducible proteins like *osmC*, *osmB* and *osmY*, as well as the chaperones *dnaKJ* exhibited increased expression levels in the mutants compared to the wild type.

To test, whether this upregulation of osmoprotection genes also resulted in increased survival rates at high osmolarity, LB cultures were incubated with 3M NaCl for 2 h and CFU was determined before and after the treatment (Hommais *et al.*, 2001).

Only 4 % (±2.3) of the wild type cells and 5 % (± 3.9) of the *stpA* mutant cells were still alive after 2 h incubation at high osmolarity, whereas the survival rates were significantly increased in both the *hns* single mutant (61 ± 17.8 %) and the *hns/stpA* double mutant (69 ± 13.7 %).

Multicellular behavior

Bacterial lifestyle is rarely single celled, but in contrary, bacteria tend to aggregate and form complex multicellular communities. The most prominent example for such a community is a biofilm, *per definitionem* a structured community of bacterial cells enclosed in a self-produced polymeric matrix and adherent to an inert or living surface (Costerton *et al.*, 1999). One prerequisite for the formation of biofilm are direct cell-to-cell interactions. In *E. coli*, these interactions can for instance be mediated by the self-recognizing surface adhesin Antigen 43. At least in *E. coli* K-12, Ag43 was found to be important for the biofilm forming process because of autoaggregation (Danese *et al.*, 2000).

Consequently autoaggregating abilities of UPEC strain 536 and its isogenic mutants were measured by a simple assay (see Methods section 4.6.3.). As seen in Fig. 35 A, all H-NS deficient strains aggregated after some time and accumulated at the bottom of the tubes.

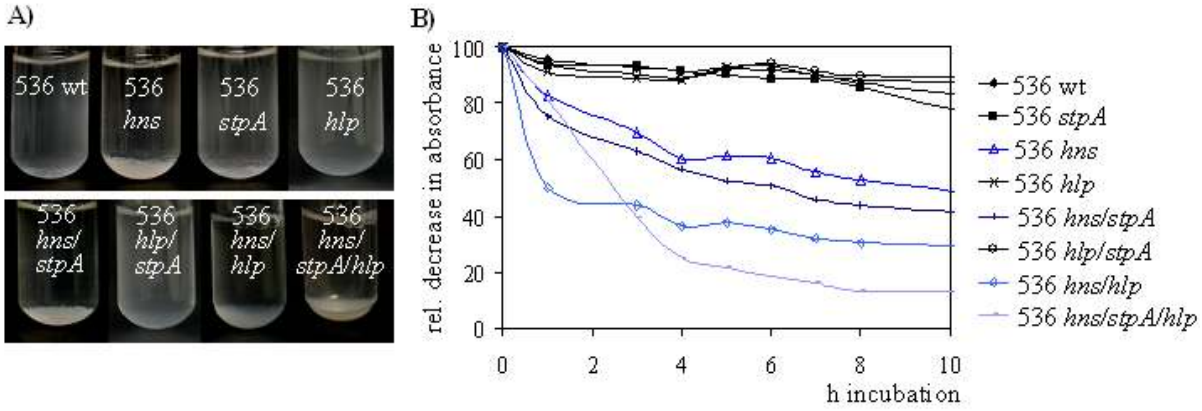

Fig. 35: Effects of histone-like proteins on autoaggregative behavior. (A) Cultures of UPEC strain 536 and isogenic mutants in M63BI minimal medium after 24 h static incubation at room temperature; (B) quantitation of autoaggregation by measuring optical densities (OD_{600nm}) from 1 cm below the surface.

Quantitation of the assay revealed some differences in the time course of aggregation. All H-NS deficient double and triple mutants settled down faster than the single mutant. Furthermore, lack of Hlp seemed to further enhance autoaggregation (Fig. 35 B).

This autoaggregative phenotype of H-NS deficient strains might also refer to an altered biofilm forming capacity. When testing biofilm formation using a microtiter plate assay, some differences were observed between the mutants and the wild type, though very much depending on the growth medium (data not shown). However, it was not possible to quantitate the assay properly, and the results were hardly reproducible. This was mostly due to the weak biofilm forming ability of *E. coli* strains in general, thereby rendering this assay a weak method.

Another approach for assessing multicellular behaviour is to study the phenotype of a strain on plates containing the dye Congo Red. Differences in the production of curli adhesin (or cellulose) result in different Congo Red-binding capacities, visualized in a red/brownish colour of the colonies. The phenotypes of UPEC strain 536 and its mutants on such Congo Red agar plates incubated at different temperatures is represented in Fig. 36.

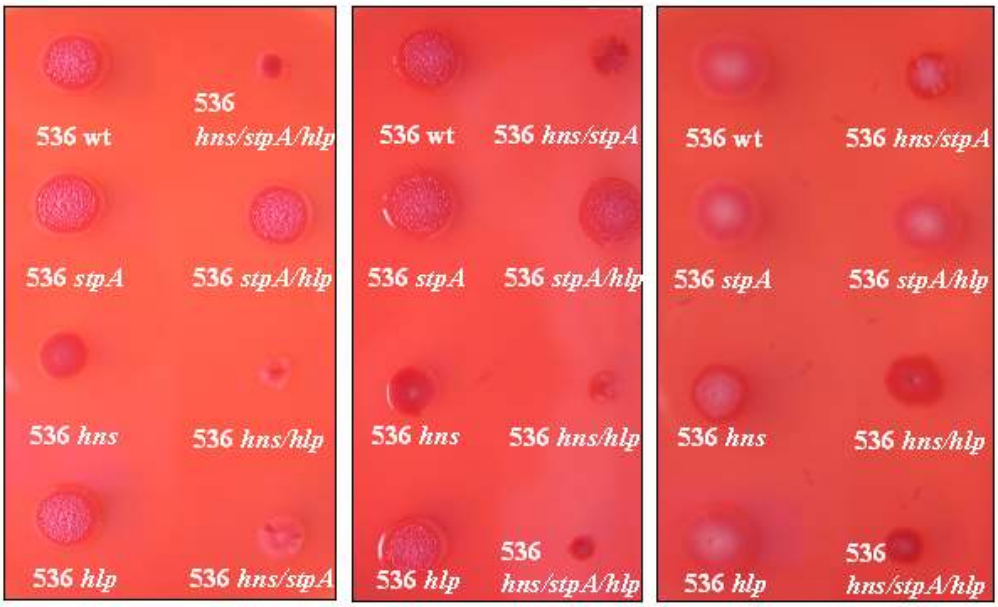

Fig. 36: Effects of histone-like proteins on multicellular behavior. Congo Red-binding assay to test for production of curli and cellulose. Plates were incubated at room temperature (left panel), 30 °C (middle panel) or 37 °C (right panel).

UPEC strain 536 does not express cellulose and curli at 37 °C, therefore growing in white, unstructured colonies. At lower temperatures on the other hand, the wild type strain exhibits a brown, structured colony morphology. The same was found for all H-NS positive mutants. H-NS deficient strains, however, differed in their phenotype. At room temperature, all *hns* mutants grew into unstructured colonies, but some of them were still able to bind Congo Red. At 37 °C on the other hand, these mutants exhibited a more structured colony morphology.

Here, especially strains lacking both H-NS and Hlp were found to bind Congo Red in high amounts. This result suggests, that the expression of curli and cellulose might be altered in the *hns/hlp* and the triple mutant. Therefore, the expression levels of the corresponding genes were monitored by semi-quantitative RT-PCR (Fig 37). Expression of the major curli subunit-encoding gene *csgA* and the gene that codes for the cellulose regulator YaiC was induced in the absence of both H-NS and Hlp, thereby confirming the hypothesis derived from the Congo Red-assay.

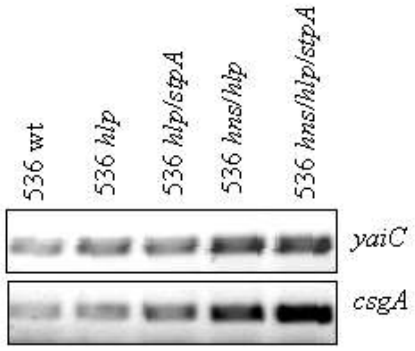

Fig. 37: Effect of H-NS and Hlp on production of curli adhesin and cellulose . Semi-quantitative RT-PCR for the cellulose regulator (*yaiC*) and the major subunit of curli fimbriae (*csgA*)

A second hint for the involvement of both H-NS and Hlp in the composition of extracellular substances is the mucoid phenotype of the *hns/hlp* mutant and the triple mutant on ordinary agar plates at 37 °C (data not shown). The best visualization of the mucoid phenotype, however, was obtained on salicin plates. These plates are normally used to test the ability of a strain to utilize ß-glucosides such as salicin. The enzymes required for this metabolic pathway are encoded in the so called *bgl* operon. In wild type cells, this operon is completely silent due to repression by H-NS (Defez and De Felice, 1981). In the absence of H-NS, transcription of the *bgl* genes is derepressed and the cells are able to utilize the substrate in the agar plate, resulting in a red color of the colonies.

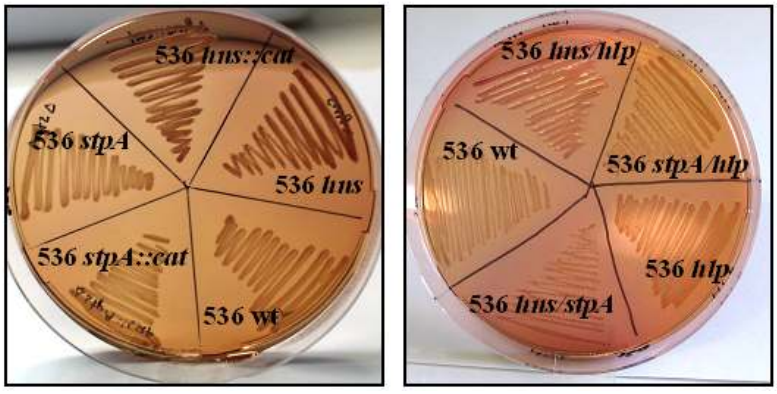

Fig. 38: Effects of histone-like proteins on utilization of ß-glucosides. The ability to utilize ß-glucosides was assessed on agar plates containing 0.4 % salicin and indicator dyes. (The mucoid/glossy phenotype of the *hns/hlp* mutant should be specially pointed out)

As seen in Fig. 38, only H-NS deficient strains grew in red colonies, thereby indicating, that the other H-NS homologs are not required / or able to silence the operon.

Speculating about the reasons for the mucoid phenotye, other factors than curli and cellulose have to be considered. This led us to also test the strains for the expression of the K15 capsule and lipopolysaccharide.

Capsules, Lipopolysaccharide, and serum resistance

UPEC strain 536 expresses a capsule of the K15 serotype, which has been recently described by Schneider and co-workers (2004). Using a K15 capsule-specific antiserum, Dr. György Schneider was now able to detect a significant higher signal intensity in the *hns/hlp* mutant compared to the wild type and all other mutants (Fig. 39 A).

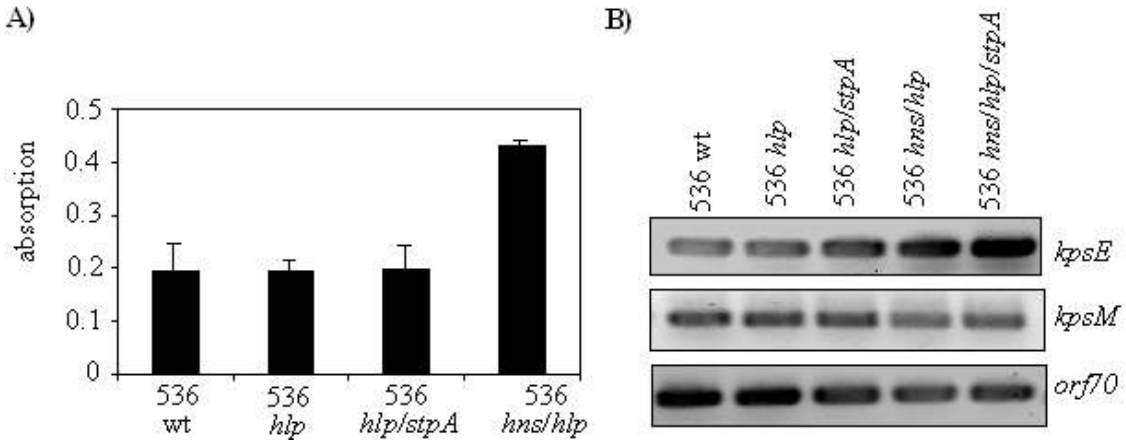

Fig. 39: Effects of H-NS and Hlp on expression of the K15 capsule determinant. (A) ELISA with polyclonal K15 serum (performed by G. Schneider in Pécs, Hungary); (B) semi-quantitative RT-PCR for capsular genes of region 1 (*kpsE*), region 2 (*orf70*), and region 3 (*kpsM*).

When analyzing transcript levels of representative genes for every region of the capsule determinant by semi-quantitative RT-PCR, divergent effects of the mutations were revealed. Expression of the *kpsE* gene of region 1, which is involved in translocation of the capsule components across the periplasm and outer membrane was upregulated in strains lacking both H-NS and Hlp, whereas the *kpsM* gene and *orf70* seemed to be downregulated in these mutants. The first gene encodes a protein involved in translocation across the cytoplasm, the latter one is part of the variable region 2 and its product has no homology to any known protein at the nucleotide level.

To further confirm a regulatory effect of histone-like proteins on the expression of the capsule determinant, binding abilities of Hlp and H-NS to the promoter regions of all three capsule regions, which are thought to form separate transcription units, were assessed by electrophoretic mobility shift assay. As seen in Fig. 40, both the H-NS and the Hlp protein were able to bind to all three promoter regions. H-NS exhibited the highest affinity to the *kpsM* (region 3) and ORF70 (region 2) promoters, whereas Hlp was binding to all promoter regions with equal affinities.

Since we were mostly interested in possible synergistic effects of H-NS and Hlp, which might explain the phenotype of the *hns/hlp* double mutant, pre-incubated mixtures of H-NS and Hlp were also analyzed in the assay. No obvious differences in the band shifts of the *kpsM*- and ORF72 promoter fragments were detected with the protein mixtures (Fig. 40 B and C, respectively). Interestingly, the *kpsF* fragment shifted at much lower protein concentrations of the protein mixture (i.e. at 5.3 µM equimolar mixture) compared to the single proteins, where no binding was observed at the same concentration (Fig. 40 A).

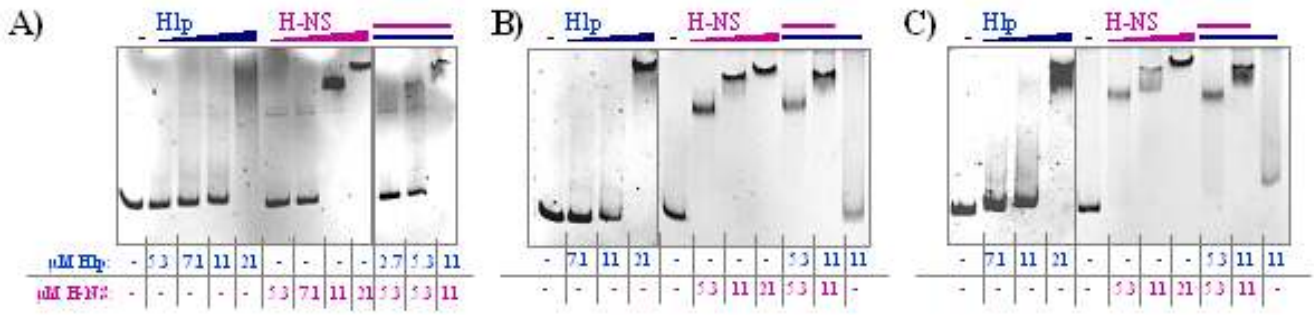

Fig. 40: Analysis of binding capacities of H-NS and Hlp to promoter regions of the K15 determinant. Electrophoretic mobility shift assay. ~400-nt fragments upstream of *kpsF* (A; region1), *kpsM* (B; region3), and ORF72 (C; region2) were amplified by PCR and incubated with purified His-Hlp and/or H-NS protein in concentrations given below each lane. Mixtures of Hlp and H-NS were pre-incubated prior to addition of the target DNA.

These results indicate that the global regulator H-NS, as well as its homolog Hlp, affect the expression of the capsule determinant. Furthermore, it suggests, that the formation of heteromeric protein complexes between the H-NS paralogs might alter their DNA-binding properties.

Some enteric bacteria produce a second type of capsule, also known as M antigen. It consists of colanic acid, a negatively charged polymer of glucose, galactose, fucose, and glucuronic acid that forms a protective capsule surrounding the bacterial cell surface (Whitfield and Roberts, 1999). Colanic acid does not seem to be involved in urovirulence, since *cps* genes are generally not expressed at temperatures above 30 °C.

Colanic acid biosynthesis is activated by the regulator RcsA, which itself is subject to repression by H-NS (Gottesman and Stout, 1991; Sledjeski and Gottesman, 1995). When screening our expression profiling data of the *hns* and *hns/stpA* mutants, however, we could not detect any derepression of the *rcsA* gene in H-NS-deficient strains.

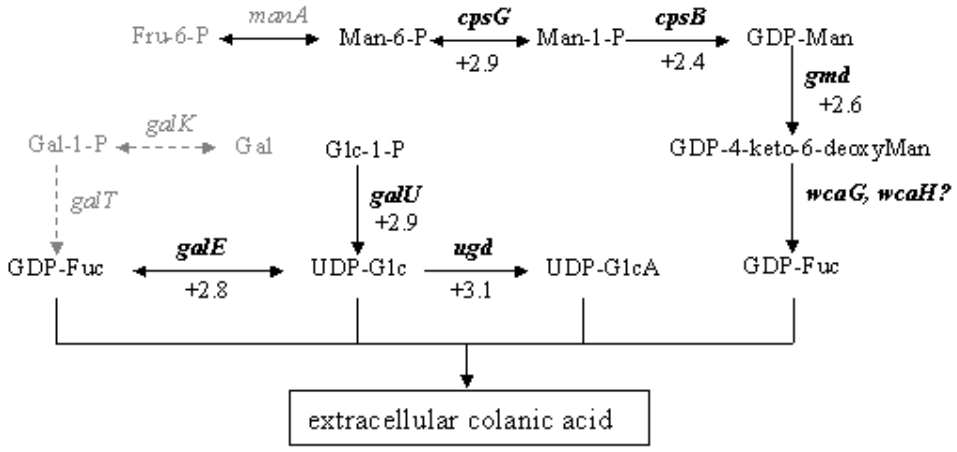

Fig. 41: Effect of lack of H-NS on expression of genes involved in colanic acid synthesis. Proposed pathway for biosynthesis of colanic acid; adapted after Stevenson *et al.* (1996). Genes with upregulated expression levels in the *hns* and *hns/stpA* mutant are depicted in bold. Fru = frucose; Fuc = L-Fucose; Gal = D-Galactose; GlcA = D-glucuronic acid; Glc = D-Glucose; Man = Mannose.

Nevertheless, many genes involved in synthesis of the four building blocks were significantly upregulated (Fig. 41). This indicates, that lack of H-NS might – in an RcsA-independent manner - result in an increased amount of colanic acid polysaccharide on the cell surface.

Finally, the effect of histone-like proteins on lipopolysaccharide (LPS) production was tested. LPS consists of immunogenic glycolipids, which, in contrast to capsular polysaccharides, are anchored in the outer membrane via the hydrophobic component lipid A, also known as endotoxin. The structure of LPS consisting of the lipid A moiety, the inner and outer core, and the O-specific side chains (O6 in UPEC strain 536), is depicted in Fig. 42 A.

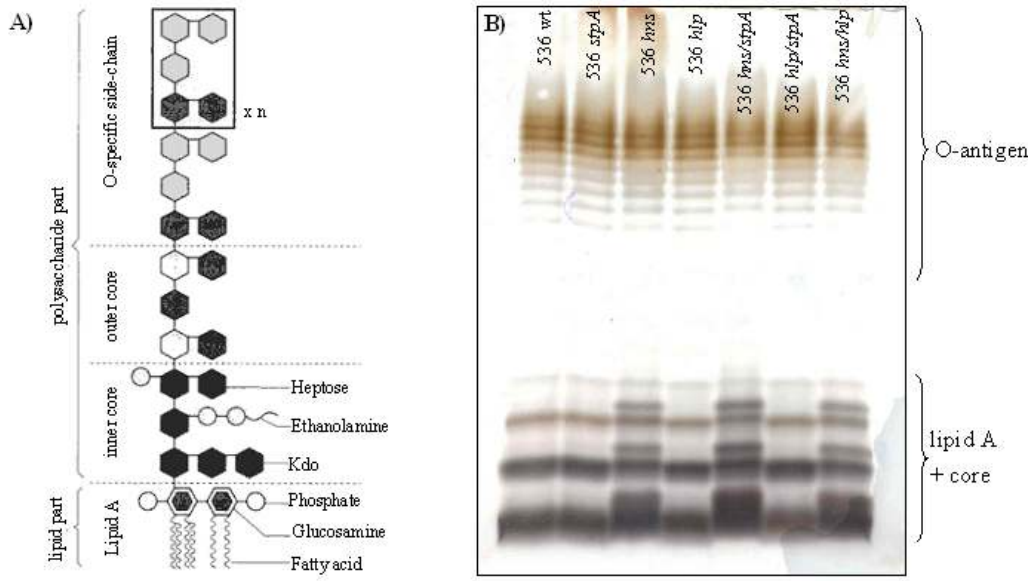

Fig. 42: Analysis of lipopolysaccharide composition in strains deficient for histone-like proteins.
(A) Schematic structure of LPS consisting of lipid A, core, and O-antigen; (B) Silver stain of LPS preparations from cells grown on plate.

LPS of UPEC strain 536 and its isogenic mutants was purified and analyzed by denaturing polyacrylamide gelelectrophoresis (Fig 42 B). All strains exhibited a smooth LPS phenotype with no obvious differences in the O-specific side chains. Also, the total amount of LPS seemed to be unaffected by the mutations. The core and lipid A part, however, was altered in all H-NS deficient strains, with additional bands of higher molecular weight appearing on the gel.

This result indicates that lipid A and the core region might be chemically modified in the absence of H-NS. The nature of these modifications was analyzed by Olga Ovchinnikova in the group of Prof. Otto Holst at the Division of Structural Biochemistry of the Leibnitz Center for Medicine and Biological Sciences in Borstel. The results are listed in Table 11.

Table 11: LPS-composition of UPEC strain 536 wild type and isogenic *hns* mutant.

	nmol component per ml		molar ration (rel. to Kdo_{AcP})	
Component	LPS -wt	LPS -*Δhns*	LPS -wt	LPS -*Δhns*
Kdo_{AcP}	156	181	1	1
Kdo_{HCl}	243	300	1.5	1.6
P	1082	911	**6.9**	**5.0**
C12:0	86	108	0.5	0.6
C14:0	88	112	0.6	0.6
3OH-C14:0	604	674	3.9	3.7
C16:0	17	39	0.1	0.2

The only difference in LPS from the wild type and the *hns* mutant was the phosphate content. Wild type LPS seem to contain 7 phosphate residues, whereas LPS of the mutant only contained 5 phosphates. All other components, as well as the O-antigen and core composition did not exhibit any significant differences, as seen by ^{1}H-NMR measurements. Nevertheless, no effect of H-NS on LPS synthesis is described in the literature to date. Therefore, the result of the ^{31}P-NMR measurements might lead to the discovery of a so far unknown aspect of H-NS regulation.

Alterations in LPS structure often result in an altered susceptibility towards chemical components, such as cationic antimicrobial peptides (Guo *et al.*, 1998). Furthermore, changes in the extracellular polysaccharide might also affect immunostimulation or immunoevasion, reflected in serum resistance.

Normally, UPEC strain 536 is resistant towards killing by human serum. Serum resistance in *E. coli* has been described to be associated with several surface structures (Johnson, 1991). Studies on survival rates of UPEC strain 536 and its mutants in human serum, however, revealed no significant differences (data not shown). Therefore, alterations of any of the surface structures by the lack of histone-like proteins did not seem to affect serum resistance.

In summary, classical physiological tests confirmed the data obtained by expression profiling. It was shown that H-NS has a huge impact on the expression of most virulence factors of UPEC strain 536, acting mainly as a repressor. Therefore, mutants deficient for H-NS were highly hemolytic, hyper-fimbriated, very stress resistant but non-motile. Furthermore, *hns* mutants exhibited a different siderophore expression kinetic and capsule gene expression, as well as differences in lipopolysaccharide core phosphorylation.

Since most of the known virulence factors of UPEC strain 536 are affected by H-NS, the combined effect for urovirulence of a strain lacking the global regulator cannot be predicted easily. Therefore, the pathogenic potential of the mutants was tested in the animal model.

5.3.3 Effect of H-NS on in vivo *virulence*

The effects of a mutation of *hns* on *in vivo* virulence were studied in the mouse model. All experiments were performed by Gabor Nagy and György Schneider at the Institute of Medical Microbiology and Immunology of the University Medical School in Pécs, Hungary.

Fig. 43 depicts the survival rates of mice infected intravenously at different dose rates; Fig. 44 represents the results of a lung toxicity assay testing for α-hemolysin production.

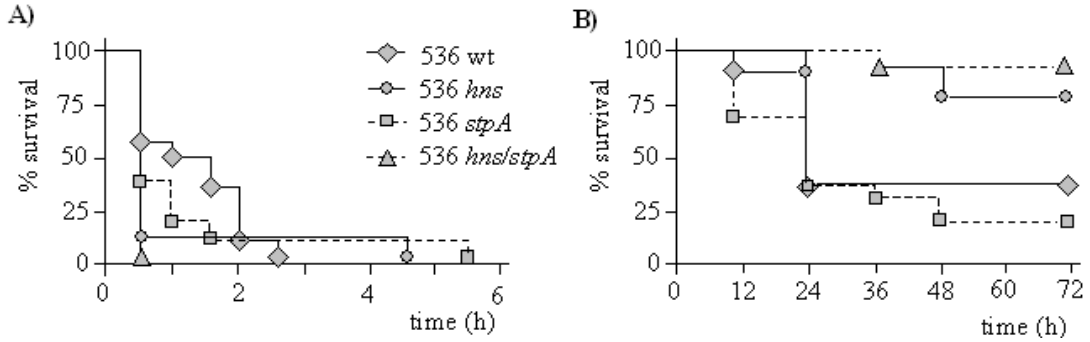

Fig. 43: Survival rates of mice infected with H-NS deficient strains. Groups of 10 mice were infected intravenously with UPEC strain 536 or its isogenic mutants in a dosis of either 10^9 CFU (A) or 10^8 CFU (B) (performed by G. Nagy; Pécs, Hungary).

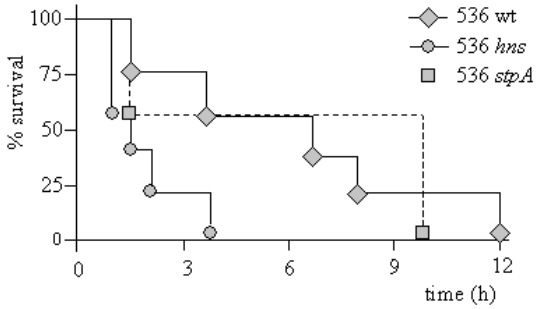

Fig. 44: Time course of lethality induced by H-NS deficient strains. Mouse lung toxicity assay. Groups of 5 mice were infected intranasally with UPEC strain 536 and isogenic mutants (performed by G. Nagy; Pécs, Hungary)

To summarize, H-NS deficient strains accelerated lethality when administered at a high infection dosis, which was a result of their increased acute toxicity in murine UTI and sepsis models. At lower infectious dose, however, the *hns* mutants were attenuated, probably due to their impaired growth rates.

5.3.4. Role of H-NS and its paralogs at different temperatures

So far, only minor effects on gene expression were identified for the H-NS paralogs StpA and Hlp. Both proteins seem to modify the repressive effect of H-NS on expression of fimbriae. Furthermore, a distinct role of an H-NS/Hlp regulatory complex seems to exist for the expression of the K15 capsule determinant.

Since expression levels of both *hns* and *stpA* were shown to be temperature-dependent, and since H-NS often mediates thermoregulation of some target genes, we also analyzed our mutants at different temperatures. Therefore, growth rates were assessed at a temperature range from 25 °C to 45 °C.

Growth rates of the mutants at different temperatures

Growth deficiencies of *hns* and *hns/stpA* mutants have been reported before (Sonden and Uhlin, 1996; Zhang *et al.*, 1996). In UPEC strain 536, a similar growth rate of the *hns* and *hlp/hns* mutant was found compared to the wild type, despite a prolonged lag phase at 37 °C. The *hns/stpA* as well as the triple mutant exhibited a much longer generation time compared to the wild type (Table 12; section 5.3.5.). To study growth differences at various temperatures, mutants were grown on agar plates at 25 °C, 30 °C, 37 °C, and 45 °C.

As expected, all H-NS-deficient strains formed smaller colonies than the wild type at every temperature (Fig. 45).

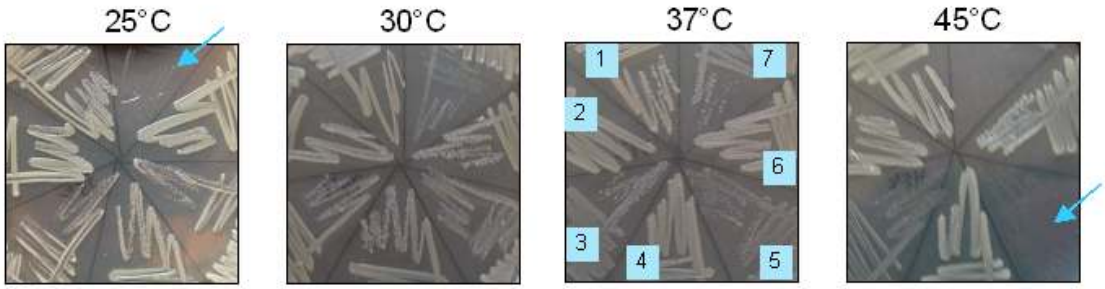

Fig. 45: Growth of wild type UPEC strain 536 and its isogenic mutants at various temperatures.
1 = 536 wt; 2 = 536 *stpA*; 3 = 536 *hns*; 4 = 536 *hlp*; 5 = 536 *hns/stpA*; 6 = 536 *hlp/stpA*; 7 = 536 *hns/hlp*

At low temperatures, both the *hns* and the *hns/stpA* mutant exhibited a mucoid phenotype. The most interesting results, however, were obtained with the *hns/stpA* and *hns/hlp* double mutants. So far, both mutants behaved very similar for all factors tested.

Here, we found a clear difference in growth: the *hns/stpA* mutant had a severe growth defect at 45 °C, whereas the *hns/hlp* mutant still grew on plate, though in very tiny colonies. The opposite was true at 25 °C, where the *hns/hlp* mutant did not grow at all, but the *hns/stpA* mutant displayed a mucoid growth phenotype. The growth experiments were repeated using liquid cultures. The generation times determined from the growth curves confirmed the results obtained on agar plates (see Table 12 in section 5.3.5. and Fig. 53 in the appendix). Therefore, the influence of the H-NS homologs StpA or Hlp seems to vary with temperature.

Expression of hns, hlp, and stpA at different temperatures

To test, whether this influence of temperature is reflected in expression rates, RNA was extracted from 536 wild type cultures grown to mid-log phase at four different temperatures, and expression of *hlp, hns*, and *stpA* was determined by semi-quantitative RT-PCR (Fig. 46). As expected, expression of *hns* was cold-shock induced, resulting in higher transcript amounts at 30 °C compared to temperatures above 37 °C. However, at temperatures below 30 °C, *hns* expression was decreased again, therefore resulting in a clear peak at 30 °C.

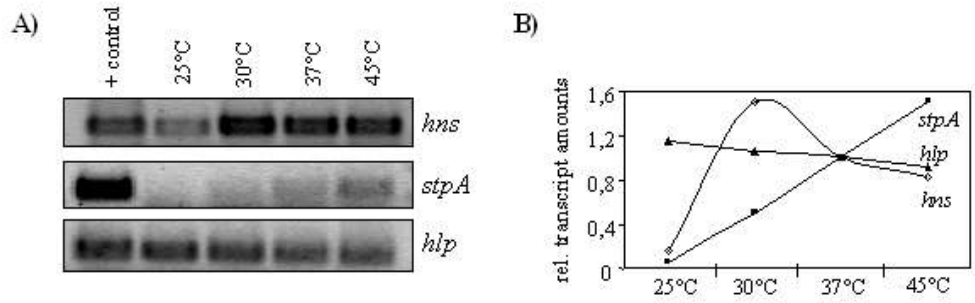

Fig. 46: Effect of temperature on transcript levels of *hns*, *stpA*, and *hlp*. (A) semi-quantitative RT-PCR for *hns*, *stpA*, and *hlp* transcripts; (B) quantitation of transcript amounts from the gel (relative to 37 °C).

Expression of *stpA* increases upon temperature upshift (Sonden and Uhlin, 1996). We also found an increase in transcript amounts with increasing temperatures, resulting in highest *stpA*-mRNA levels at 45 °C. Finally, expression of *hlp* does not seem to change with temperature.

Taken together, evidence was provided that the expression levels of *hns*, *hlp* and *stpA* strongly depend on growth temperature. Furthermore, the results obtained suggest that, due to these differences in expression levels, the composition of the nucleoid-associated protein pool might vary with changing temperature.

5.3.5. Summary – phenotypic characterization

The results of all phenotypic tests for the expression of the major virulence factors of UPEC strain 536, as well as the results on growth rates are summarized in Table 12.

Table 12: Summary of the phenotypic characterization of UPEC strain 536 and its isogenic mutants

	536 wt	536 *stpA*	536 *hns*	536 *hlp*	536 *hns/stpA*	536 *hlp/stpA*	536 *hns/hlp*	*536 hns /stpA/hlp*
Generation time at 37 °C	24	24	29	25	47	24	27	53
(min) at 25 °C	51	50	55	50	62	49	111	83
at 45 °C	30	28	27	29	103	29	29	145
bgl phenotype	white	white	blue	white	blue	white	blue	blue
Motility	+	+	-	+	-	+	-	-
Fimbriation - P-pili	+	+	+++	+	++	+	+++	++
- S-pili	+	+	++	+	+++	+	++	+++
Hemolytic activity (units)	14	15	85	14	76	18	127	70
Siderophore kinetic	slow	slow	fast	slow	fast	slow	fast	fast
Autoaggregation	-	-	+	-	++	-	+++	+++
Curli expression at 37 °C	-	-	-	-	-	-	++	++
- at RT	+	+	-	+	-	+	-	-
Cellulose expression	+	+	+	+	+	+	++	++
K15 capsule expression	+	+	+	+	+	+	++	++
LPS core	normal	normal	mod.	normal	mod.	normal	mod.	not tested
Serum resistance	+	+	+	+	+	+	+	+

To summarize, UPEC strain 536 encodes three histone-like proteins, namely the global regulator H-NS, its paralog StpA, as well as the newly identified protein Hlp. Using expression profiling and classical phenotypic assays, H-NS was shown to affect expression of all major virulence factors of UPEC strain 536, acting mainly as a repressor. However, its role for *in vivo* virulence remains ambiguous. The H-NS paralogs on the other hand play only a minor role in this regulation, probably only by modifying H-NS function. Nevertheless, a distinct requirement for Hlp or StpA at low or high temperatures could be identified, which is reflected in their temperature-dependent expression rates.

Therefore, these results propose that the biological role of Hlp (and StpA) does not rely on distinct function of the single protein, but rather on its interactions with the global regulator H-NS in a highly flexible pool of histone-like proteins.

6. Discussion

In this study, the role of histone-like proteins on virulence of uropathogenic *Escherichia coli* was explored. The central question of this work was, whether regulatory cross-talk does exist between horizontally acquired pathogenicity islands, which encode many virulence factors as well as regulatory proteins, and the "core" chromosome, which is controlled by a well established cellular regulatory network.

Since pathogenicity islands represent upon their acquisition "foreign" DNA to the cell, a functional regulation of the encoded gene products is a prerequisite for a stable maintenance in the chromosome. Moreover, especially virulence-associated genes are usually tightly regulated. The focus of the first part of the Discussion will be on the effects of the global regulatory protein H-NS, whose unique structure and effects on the architecture of the chromosome – all of which are exerted by relatively sequence-unspecific DNA-binding – render it a possible candidate for regulation of pathogenicity island-encoded genes.

6.1. H-NS and virulence

The role of the histone-like nucleoid structuring protein H-NS for virulence was assessed by using expression profiling, as well as classical phenotypic tests and *in vivo* experiments. It was the first time that a pathogenic *E. coli* strain was subjected to such a large scale monitoring including all its known virulence factors. Furthermore, the use of a specific pathoarray enabled the identifcation of some previously unknown members of the H-NS regulon encoded on the pathogenicity islands of UPEC strain 536. Thus, it was proven that H-NS is playing a major role in the regulation of this extragenetic material, thereby linking PAI-encoded gene expression to the cellular regulatory network.

H-NS was found to be a global regulator in UPEC strain 536, affecting transcription of more than 500 genes, among them all classical virulence factors tested. Mutants deficient for H-NS expressed more fimbriae and hemolysin and differed in their siderophore expression kinetic. Furthermore, these mutants were non-motile and showed increased resistance to high osmolarity. These results suggested some benefits for the *hns* mutant for *in vivo* virulence:

Increased production of adhesins has undoubtable effects inside the host. For instance type 1 fimbriae were shown to play a major role in the *in vivo* colonization process of the mouse urinary tract (Snyder *et al.*, 2004). In our strain, however, we could not find an upregulation of the *fim* operon. This is probably due to the shaking growth conditions *in vitro*. Nevertheless, H-NS affected expression of both recombinases *fimB* and *fimE*, thereby leading to a rapid phase switching in the mutants, as described by Olsen and Klemm (1994). The consequences for the *in vivo* situation still need to be assessed.

For the other two major fimbrial adhesins, the effects of H-NS were more clear. Using the *E. coli* pathoarray, the mechanism of regulation of the *sfa* determinat could be analyzed: Repression by H-NS acts on the transcription directed by both the *sfaB* and *sfaA* promoter, resulting in derepression of the activator SfaB and the structural genes in the *hns* mutant. The SfaB protein itself is activating both the *sfaC* and *sfaB* promoter, thereby further enhancing transcription of the structural genes. For the P-related fimbriae, we could not demonstrate an increased transcription of the structural genes on the array, even though the protein levels were strongly increased in the mutant. Interestingly, only the *prfX* gene, which encodes a putative regulator of the *prf* operon, was significantly upregulated at the transcriptional level. Therefore, one could speculate, that one of the effects exerted by H-NS might be indirect by decreasing the expression of PrfX, which then would activate the *prf* structural genes.

Moreover, regulatory cross-talk between both types of fimbriae exists: the regulators of both gene clusters, SfaC, SfaB, PrfB, and PrfI are highly homologous and can complement each other (Morschhäuser *et al.*, 1994). Therefore, upregulation *sfaB* in the *hns* mutant might also indirectly result in activation of the *prf* operon. Despite all speculation about the mechanism, increased amounts of fimbrial protein on the cells, as seen by AFM, presumably contributed during the first stages of infection by virtue of increased adhesion to the urothelium.

Another important factor for colonization is the acquisition of iron. To date, no H-NS-dependent regulation of iron-uptake systems has been reported. In this study, we now demonstrate that the effects on the five iron-uptake systems of UPEC strain 536 are divergent: H-NS is playing both an activating and a repressing role, as seen e.g. for the *chuA* and *iroN* genes encoding the hemin receptor and the salmochelin receptor, respectively. Furthermore, the regulatory effects seem to be restricted to the receptor-encoding genes and do not include other genes of the clusters.

Under inducing conditions, the total amount of secreted siderophores was the same in the wild type and the mutants. Because of the altered kinetic in the mutant, however, one could speculate that the composition of siderophores differs from the wild type. For instance, the upregulation of a siderophore with a high affinity for iron in the *hns* mutant could explain the faster decrease in absorbance due to siderophore-mediated iron sequestration as detected in the photometric assay. This hypothesis is supported by the finding that both yersiniabactin and salmochelin, the siderophores with the highest binding constants, are the ones which were produced in higher amounts in the mutants.

Finally, another aspect of the role of H-NS on virulence and fitness of UPEC strain 536 is stress resistance. Numerous genes involved in osmoprotection and acid resistance, as well as multidrug resistance, were upregulated in the *hns* mutant. The array data obtained in this study could be confirmed by demonstrating a more than 10 times higher survival rate of the mutant at high osmolarity, as it has already been described in *E. coli* K-12 (Hommais *et al.*, 2001). These results suggest that H-NS plays a major role in the adaptation to various stress situations like high osmolarity and low pH. Since uropathogenic bacteria are even more likely to be confronted with these stress conditions during colonization of the urinary tract than commensal variants living in the gut, these findings are of particular importance.

Despite all these assumed advantages of *hns* mutants, an ambiguous role of H-NS in uropathogenesis was revelaed by experimental animal models of UTI and sepsis: At an infective dose highly exceeding the LD_{50} values, lack of H-NS resulted in accelerated lethality in both the UTI and the sepsis model. This was probably due to the increased α-hemolysin production in the *hns* mutants. An increased production of α-hemolysin in strains deficient for H-NS is already described in *E. coli* K-12 (Nieto *et al.*, 2000). These results could also be confirmed in UPEC strain 536 by both RT-PCR and a liquid assay. Interestingly, an upregulated expression of the hemolysin repressor Hha was found as well. This protein exhibits a similar structure to H-NS and is therefore able to form heteromers. This result confirms that Hha alone is not able to mediate repression of the hemolysin operon, but in contrast, a functional H-NS/Hha complex is required (Nieto *et al.*, 2000). Supporting this hypothesis, inactivation of *hns* resulted in a significantly higher *in vivo* toxicity in the α-hemolysin-dependent mouse lung assay. This emphasizes the importance of cytotoxicity for urovirulence and is also reflected in the finding that more than 50 % of all extraintestinal pathogens are hemolytic (Ludwig and Goebel, 1991).

In addition to α-hemolysin, some enterobacteria express another type of pore-forming toxin, namely ClyA (also known as SheA or HlyE), which could also contribute to the hemolytic phenotype (Oscarsson *et al.*, 1999).. This hemolysin determinant even can be found in non-pathogenic *E. coli* K-12. Here, it remains phenotypically silent under most tested laboratory conditions. On the other hand, expression of the *clyA* gene can be induced for instance in *hns* mutant strains (Gomez-Gomez *et al.*, 1996; Uhlin and Mizunoe, 1994), thereby indicating, that H-NS is one of the factors that keeps the gene silent in *E. coli* K-12. However, in UPEC strain 536 as well as in most other uropathogenic isolates, a large portion (217-bp) of the *clyA* gene was found to be deleted (Kerenyi *et al.*, 2005; Ludwig *et al.*, 2004). Therefore, we assume that the α-hemolysin is solely mediating the hyperhemolytic phenotype of the *hns* mutants.

Coming back to the urovirulence data, no significant difference in the virulence of *hns* mutants in the UTI model could be shown in comparison to the wild type strain. Moreover, when injected intravenously, lack of H-NS significantly reduced lethality in mice. This attenuation could have several reasons. The first is the complete loss of motility in H-NS-deficient strains. However, in a recent study, Snyder and co-workers (2004) demonstrated for the UPEC isolate CFT073, that flagella is not needed for a successful colonization of the murine urinary tract. Therefore, the lack of motility does not imply a disadvantage for the mutants during infection in this model.

Secondly, and even more important, one has to take into account the impaired growth rates of *hns* mutants. Although usually not considered to be a classical virulence characteristic, the optimal rate of bacterial replication *in vivo* might highly influence the outcome of an infection. It is hypothesized that slower growth of the *hns* mutants could be compensated by upregulation of various “classical” virulence factors. Reaching the blood stream, however, bacteria have to face the defence mechanisms of the immune system, which could only be overcome through rapid bacterial growth. Since the role of the upregulated virulence factors seems to be minor within the blood stream, *hns* mutants become attenuated compared to their wild type strain. These observations emphasize the role of house-keeping genes in bacterial fitness, which is a prerequisite for virulence. The impact of H-NS on virulence appears to be divergent along the infectious process. Nevertheless, a role for H-NS in virulence regulation is without doubt.

Another aspect of the influence of H-NS on virulence traits, which has not been reported so far, is the effect on the lipopolysaccharide. When analyzing lipopolysaccharide, modifications of the core fragments were detected in the LPS preparations of H-NS deficient strains as seen on polyacrylamide gels. In some preparations, these fragments were also found in the wild type, but never to the same extent as in the mutants. This suggested, that the LPS core might be chemically modified in absence of H-NS.

When searching the literature for known mechanisms of LPS modifications, several scenarios can be imagined. The first scenario involves the alternative acyltransferase LpxP. During synthesis of "normal" lipid A, the lauroyl-acyltransferase LpxL catalyzes the addition of laureate to Kdo_2-Lipid IV_A precursors. At low temperatures, however, the acyltransferase LpxP is induced, which uses the same substrate as LpxL, but catalyzes incorporation of the unsaturated fatty acid palmitoleate instead of laureate (Carty *et al.*, 1999). The resulting "cold-adapted" lipid A helps to maintain membrane fluidity at low temperatures, and also exhibits decreased permeability to antibiotics such as rifampicin and vancomycin (Vorachek-Warren *et al.*, 2002). Since H-NS itself is part of the cold-shock regulon, a role in regulation of *lpxP* would not be too unlikely. According to the data from expression profiling, however, expression of *lpxP* was only mildly induced in the *hns/stpA* mutant.

The second scenario involves the PhoP-PhoQ two-component system. In *Salmonella typhimurium*, this system was shown to affect more than 40 genes, including some genes involved in lipid A modifications (Guo et al., 1997). Among them, the *pagP* gene, also known as *crcA*, was identified. The PagP protein catalyzes transfer of an additional palmitate from a phospholipid to lipid A, thereby resulting in hepta-acylated lipidA instead of the "normal" hexa-acylted lipid A (Gronow and Brade, 2001; Guo *et al.*, 1998). This modification increases the resistance to cationic antimicrobial peptides such as polymyxin, probably by decreasing membrane fluidity. Activation of the PhoP-PhoQ system also induces another two-component system involved in polymyxin resistance, PmrA-PmrB, which in turn activates genes of the *yfb* or *pmr* operon, encoding a 4-amino-4-deoxy-L-arabinose (L-Ara4N) transferase YfbF, as well as the *ugd* (also known as *pagA* or *pmrE*) gene (Gunn *et al.*, 1998). The latter encodes a UDP-glucose-dehydrogenase, which, like YfbF, induces addition of aminoarabinose or ethanolamide to the lipid A moiety, thereby also increasing polymyxin resistance.

In UPEC strain 536, the expression pattern of *hns* mutants revealed increased expression of *pagP*, *udg*, as well as the *yfb* operon. When analyzing LPS preparations of *pagP*, *ugd*, and *yfbF* mutants, respectively, in an *hns*$^{+}$ and *hns*$^{-}$ background, however, no differences in presence or absence of H-NS could be observed (data not shown). All possible pathways for lipid A modifications are summarized in Figure 47.

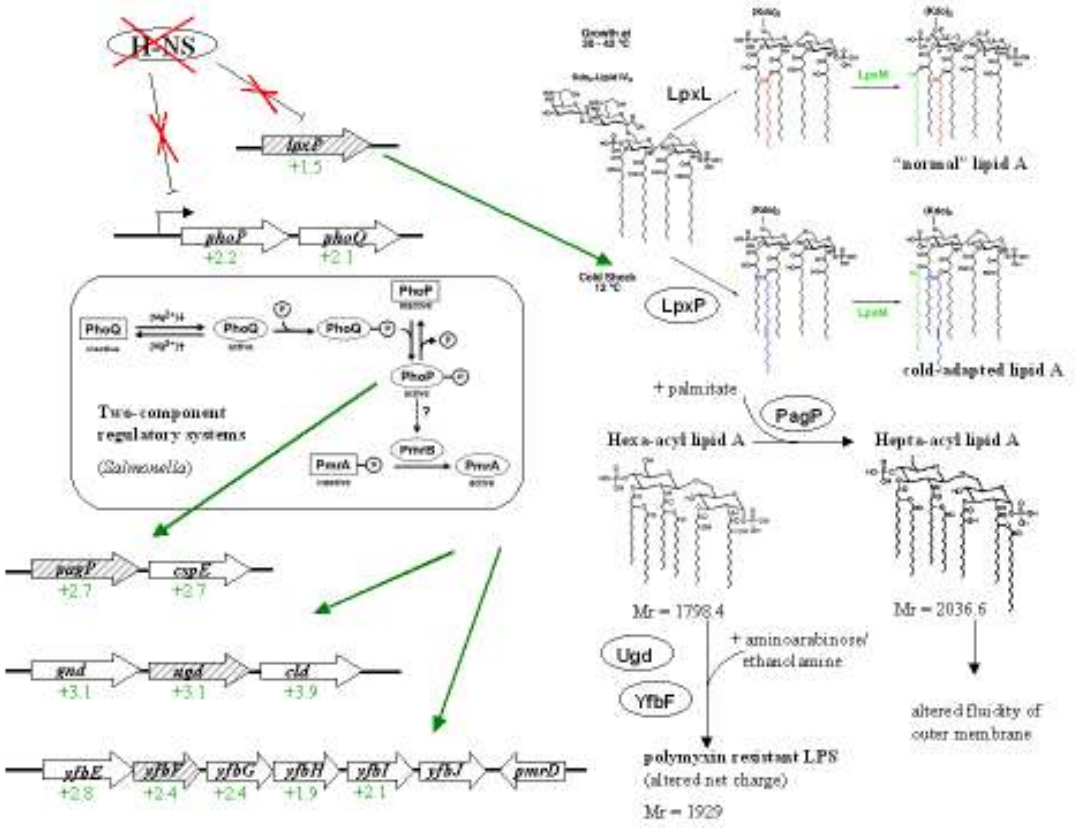

Fig. 47: Model for PhoP-PhoQ induced lipid A modifications due to lack of H-NS. All genes and operons known to be involved in modification of lipid A, as well as the expression ratios in the *hns* mutant of UPEC strain 536 derived from expression profiling are summarized in the graph.

Analysis of the LPS composition in Borstel also did not confirm any of the lipid A modifications mentioned before. Instead, the LPS of the *hns* mutant differed from the wild type only in the number of phosphate residues. This could be the result of either increased expression of a specific phosphatase or decreased expression of a kinase in the mutant. When screening the array data, expression of several kinases/phosphatases was deregulated in *hns* mutants. However, none of them was known to be involved in LPS phosphorylation.

Lipopolysaccharide, together with other factors, also affect survival rates of bacteria in human serum. However, significant changes in serum resistance of UPEC strain 536 after mutation of any of the histone-like proteins could not be detected.

6.2. Identification of H-NS and H-NS/StpA dependent regulons

So far, all changes in expression of virulence-associated genes seemed to be solely dependent upon the lack of H-NS. The paralogous protein StpA did not seem to be important in the context of virulence. However, the expression patterns of the *hns* single mutant and the *hns/stpA* mutant differed in many other genes, especially those of the core genome. Therefore, the data obtained suggest the existence of two different regulons: one subset of genes is regulated by the H-NS protein alone, whereas a second group seems to be regulated by a concerted action of H-NS and StpA.

It has been shown earlier that H-NS can exist as homodimers or as a heteromer together with StpA (Johansson *et al.*, 2001; Sonden and Uhlin, 1996), and a distinct function for each complex has been proposed. By using DNA arrays, it was possible to identify some of the target genes of the two types of DNA binding complexes. In keeping with the above mentioned hypothesis, three different scenarios could be expected:

First, there are those genes, which are commonly regulated in both mutants, i.e. 248 genes of the *E. coli* K-12 core-genome as well as the virulence-associated genes on the *E. coli* pathoarray, which are regulated by a H-NS/StpA heteromeric complex. This group also contains genes, which are repressed by H-NS, and where StpA cannot substitute for this function in absence of H-NS.

The second group comprises genes, which were only deregulated in the *hns/stpA* double mutant. These genes, again, are normally regulated by the H-NS protein alone, but on such cases, StpA might complement for H-NS function in the *hns* single mutant.

Finally, there are those genes, which are deregulated in the *hns* single mutant only. This cannot be explained by a regulation at the transcriptional level. Regulation by StpA, which is complemented by H-NS in the *stpA* single mutant, is not a very likely explanation. The expression level of *stpA* is too low to repress all 303 genes at the same time, even if they are part of an operon, such as genes encoding ribosomal proteins. Furthermore, these genes are proven to be regulated by H-NS and not StpA, as described by several authors (Afflerbach *et al.*, 1998; Tippner *et al.*, 1994). One possible explanation for this phenomenon is StpA acting at the post-transcriptional level due to RNA chaperon activity. In this context, Zhang and co-workers (1996) suggested a role of StpA for mRNA folding.

If some transcripts of other regulators (for instance the small RNA DsrA, wich was shown to counteract H-NS) are affected by StpA in their conformation and activity, absence of StpA could have indirect effects on H-NS regulated genes. Possible regulatory loops are summarized in Fig. 47. A similar classification was proposed by Zhang *et al*. (1996), who could also detect distinct protein pattern of *hns* and *hns/stpA* mutants of strain M182 by two-dimensional gelelectrophoresis. However, the differentially regulated proteins were not characterized.

Altogether, it demonstrates the variety of possible interactions between the two DNA-binding proteins and the complexity of the regulatory network.

6.3. Characteristics of the novel H-NS-like protein Hlp

In this study, evidence was provided that uropathogenic *Escherichia coli* strain 536, in addition to the nucleoid-associated proteins H-NS and StpA, encodes a third member of the H-NS-like protein family, designated Hlp. The gene coding for Hlp and its correspondent product have been characterized.

6.3.1. The hlp *gene*

The gene coding for Hlp is located on a putative genomic island inserted into the *serU* locus. The insertion is about 23-kb in size and encodes 27 putative ORFs. A highly homologous *serU*-island has been characterized in UPEC strain CFT073 by Williamson and Free (2005). In addition to the Hlp protein (or H-NSB in UPEC strain CFT073), a truncated H-NS protein termed H-NST is present on the island. Unlike in EPEC strain E2348/69, where this truncated form is able to inhibit the repressive function of H-NS, the truncated H-NST protein of uropathogenic *E. coli* does not exhibit any anti-H-NS function (Williamson and Free, 2005).

Nevertheless, it is a proof of principle that many regulatory proteins are encoded on mobile DNA, which can be acquired by horizontal gene transfer. There are many examples for members of the H-NS-like family encoded on such acquired genetic material. For instance, the Ler protein is encoded on the LEE pathogenicity island of enteropathogenic *E. coli* (Haack *et al.*, 2003), whereas the Sfh protein of *Shigella* is located on a large plasmid (Beloin *et al.*, 2003). All these proteins, including Hlp, are believed to fulfill a major role in the interplay between factors involved in regulation of genes present on the core genome and on the horizontally acquired DNA, therefore being of special importance for gene regulation in these bacteria.

When screening other pathogenic *E. coli* variants for the presence of the *hlp* gene, it was mainly present in extraintestinal pathogenic isolates from urinary tract infections, sepsis or newborn meningitis, but also in many faecal isolates. Since the faecal flora is considered to be the main reservoir for uropathogenic *E. coli*, tight associations and even gene transfer events between the pathogens and the faecal strains are very likely. However, no correlation with a specific serotype could be made. Therefore, the origin of the *hlp* gene still remains unclear. Nevertheless, the presence of the gene in so many different pathotypes suggests, that the acquisition of the *hlp* gene was not a recent event. On the other hand, the occurence of Hlp in non-pathogenic faecal isolates would imply, that the protein is not associated with virulence. However, the presence of the gene itself in the PCR-positive strains does not infer a functional protein. In the fecal *E. coli* isolate Nissle 1917 (EcN), for instance, sequence analysis of an unaligned contig revealed, that the hlp_{EcN} gene carries two single base deletions of alanine residues at positions 61 and 96, resulting in frameshift mutation relative to UPEC strains 536 or CFT073, and thereby in a non-functional protein.

6.3.2. The Hlp protein

The Hlp protein of UPEC strain 536 is predicted to be very similar to the H-NS protein, both in size and in charge. Unlike StpA, which is much more basic, the theoretical pI of Hlp and H-NS are almost identical. The N-terminus of all three proteins is predicted to be mostly α-helical. For the H-NS protein, this prediction was confirmed by NMR spectoscropy (Bloch *et al.*, 2003; Esposito *et al.*, 2002), and was shown to mediate oligomerization by coiled-coil formation (Renzoni *et al.*, 2001). The linker region (residues 63 to 79) is not conserved and shows a variable structure. The C-terminus, on the other hand, is supposed to be highly conserved between H-NS-like proteins. DNA-binding, however, happens at two loop structures at residues 80 to 96, and 110 to 117, which can not be accurately predicted in the Hlp protein.

Nevertheless, a similar two-domain structure of Hlp can be proposed, with a C-terminal DNA-binding domain and an N-terminal oligomerization domain, connected by a flexible linker. The C-terminus of Hlp also contained the proposed core DNA-binding motif TWTGQGRTP (Dorman *et al.*, 1999), and gel shift experiments confirmed, that Hlp has DNA binding capacity. Any additional RNA binding activity, as seen for StpA, and to a lesser extend also for H-NS, was not assessed in this study, but cannot be excluded.

Homology between Hlp and H-NS is highest in the N-terminal oligomerization domain, even higher than between H-NS and StpA. Thus, it was not very surprising to find Hlp in heteromers with H-NS. For StpA, it was even shown that the heteromer is the biological relevant form of the protein (Johansson *et al.*, 2001). This is corroborated by the instability of homomeric StpA due to proteolytic degradation by the Lon protease (Johansson and Uhlin, 1999). In the presence of H-NS, both proteins interact via two distinct domains of the H-NS protein, thus masking the proteolytic site of StpA. Degradation is inhibited by a single amino acid exchange from phenylalanine to cysteine at position 21 of the StpA protein. In contrast to StpA, the residue at position 21 in Hlp is threonine, thereby resulting in a more hydrophilic "area". This might also be the reason for the unsusceptibility of Hlp to the protease, since no degradation of Hlp was observed in the absence of H-NS.

6.3.3. Hlp activity

Histone-like proteins are not only interacting at the protein level, but also at the transcriptional level. It has been described that both H-NS and StpA are subject to negative auto- and cross-regulation (Falconi *et al.*, 1993; Sonden and Uhlin, 1996; Ueguchi *et al.*, 1993). The results obtained in this study from semi-quantitative RT-PCR confirmed this finding as derepression of *hns* transcription was detected in the *stpA* mutant and vice versa. Furthermore, electrophoretic mobility shift assays provided evidence, that this repressive effect relies on specific binding of the protein to the promoter sequences.

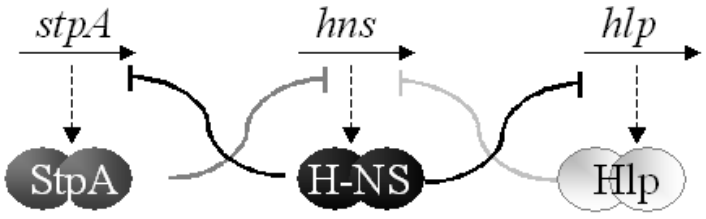

Fig. 48: Model for network of negative cross-regulation by histone-like proteins.
Current model based on the results of both semi-quantitative RT-PCR and promoter-binding studies, not including negative auto-regulation of *hns*, *stpA*, and *hlp*.

When analyzing cross-regulatory activity of the Hlp protein, strong binding to its own and also to the *hns* promoter was found, thus confirming auto- and cross-regulatory activity. This was also reflected in the predicted curvature of the *hlp* upstream region, which is AT-rich and intrinsically curved, thus rendering it a potential target for H-NS binding. Binding of Hlp to the *stpA* promoter, on the other hand, only occurred at high protein concentrations.

Together with the finding, that *stpA* and *hlp* expression was not induced in *hlp* and *stpA* mutants, respectively, these results suggest that no or only weak cross-regulation between the two H-NS homologs exists. Therefore, a cross-regulatory network of histone-like proteins can be proposed as presented in Figue 48.

Complementation studies with Hlp of UPEC strain 536 expressed from a low copy number vector in *E. coli* K-12 also served to prove the *in vivo* activity of Hlp. It restored motility of an *hns* mutant and was able to repress the hemolysin *clyA*, as well as the *bgl* and *proU* operons. When monitoring binding activities of Hlp to *clyA* by electrophoretic mobility shift assay as described by Westermark *et al.* (2000), no specific binding could be detected with the Hlp protein alone. On the other hand, addition of small amounts of H-NS resulted in specific DNA-protein complexes, thereby suggesting possible effects of Hlp on *clyA*. However, since no functional ClyA protein is expressed in UPEC strain 536, this effect is of less significance in wild type cells.

Repressive effects of H-NS homologs on the *bgl* and *proU* operons have been reported before. Sonden and Uhlin (1996) showed that over-expressed StpA is able to repress both operons in absence of H-NS. In the experiments performed in this study, Hlp was acting as a repressor even when expressed from a low-copy number plasmid only. In case of the *bgl* operon, this repressive effect was independent from the presence or absence of StpA, since both *hns* single and *hns/stpA* double mutants, when complemented with Hlp, were white on X-Glu plates (data not shown). However, since an *hns*$^{-}$ *hlp*$^{+}$ mutant of UPEC strain 536 still was blue on this plates, it can be assumed, that Hlp in its normal abundance in the cell is not sufficient for repression of the *bgl* operon.

Interestingly, *proU* expression was also derepressed in the *hns*$^{+}$ wild type strain harbouring the *hlp*-plasmid. The level of derepression was the same as seen for the *hns* mutant transformed with the vector control. One possible explanation for this observation would be an inhibition of H-NS-mediated repression in presence of the recombinant Hlp protein. Anti-H-NS factors are not uncommon. The effects of cAMP-CRP on H-NS-mediated silencing of the *bgl* operon have already been described in the introduction. Moreover, recombinant expression of the recently identified truncated H-NS protein encoded on the *serU*-island in enteropathogenic *E. coli* resulted in the same derepression of *proU* in presence of H-NS (Williamson and Free; 2005).

This truncated version consists only of the oligomerization domain of H-NS, therefore lacking DNA-binding activity. It is believed, that such truncated proteins interact with the oligomerization domain of H-NS, thereby preventing any higher order multimerization, which is for instance required for transcriptional silencing (see section 2.3.2.). Therefore, such "oligomerization-inhibitors" can act in a dominant-negative manner on H-NS repression.

Lastly, a positive effect of Hlp was observed on growth of an *hns/stpA* double mutant, which normally grows only slowly compared to the wild type. However, the growth curve of the complemented strain resembled more that of an *hns* mutant, and no complementation was observed in the *hns* single mutant. These results suggest, that, in terms of growth, the Hlp protein is complementing the lack of the StpA protein rather than of H-NS, and that the presence of StpA is already mediating all feasible growth restoration in an *hns* mutant.

6.4. Biological function of the H-NS paralogs

Despite the observed ability of the Hlp protein to repress its own transcription and that of *hns*, as well as the ability to complement for the lack of H-NS in *E. coli* K-12, a clear phenotype of an *hlp* mutant in UPEC strain 536 could not be identified. Like the *stpA* single mutant, an *hlp* mutant did not differ from the wild type in all classical phenotypic tests. These results suggest that both Hlp and StpA are dispensible under this growth condition. However, the differences in the expression pattern of the *hns/stpA* mutant relative to that of the *hns* single mutant corroborate a biological activity of the H-NS/StpA heteromeric complex and suggest the existence of distinct target genes for H-NS and H-NS/StpA (see Fig. 50).

Moreover, some obvious differences between the *hns/stpA* and the *hns/hlp* mutants were found, which will now be discussed in detail.

6.4.1. Fine-tuning of fimbrial gene expression

The presence or absence of StpA seemed to have a modulating effect on derepression of S and P pili in *hns* mutants. The upregulation of S pili in absence of H-NS was more pronounced in strains also lacking StpA, whereas the opposite was true for the P pili. One possible explanation would be that StpA might assume some repressive activity on the *sfa* determinant when H-NS is absent. Therefore, maximal expression of S pili would only occur in strains lacking both repressors H-NS and StpA. Since P and S pili are oppositely expressed due to regulatory cross-talk (Morschhäuser *et al.*, 1994), this assumption might also account for the

decreased expression of P pili in the same mutants. Despite the speculation about the exact mechanism, we propose that StpA and/or Hlp have a modulating function on the effect of H-NS, e.g. resulting in fine-tuned cross-regulation of fimbrial adhesins

6.4.2. Alteration in surface structure and extracellular substances

One striking phenotype of *hns/hlp* double mutants is their mucoid colony morphology on plate. There are various possible factors, which could account for this finding:

Capsular polysaccharide. A distinct role of an H-NS/Hlp complex in the regulation of the K15 capsule determinant was found in strains lacking H-NS and Hlp. Both proteins were binding to upstream sequences of all three regions of the K15 capsule determinant, but only binding to region 1 seemed to be cooperative. Mixtures of H-NS and Hlp had a much higher binding affinity to the *kpsF* promoter than had the single proteins. Furthermore, comparison of relative transcript amounts in various mutants by semi-quantitative RT-PCR revealed that expression of region 1 genes only was upregulated in mutants lacking both H-NS and Hlp. Transcription of region 2 and 3 genes, on the other hand, seemed to be slightly downregulated in these strains. This might be due to different functions of the Hlp protein: Regarding region 1 genes, the results from gel shift analysis strongly suggest, that a heteromeric complex of H-NS and Hlp is the active repressor, resulting in an upregulated expression of these genes in *hns/hlp* mutants. However, since both proteins are also able to bind in absence of its interaction partner – even though at lower affinities – this might indicate that H-NS, as well as Hlp, can act as a repressor of their own, thereby resulting in similar expression levels in the single mutants as in the wild type. For region 2 and 3 genes, no cooperative binding of H-NS and Hlp was detected, but still, both proteins interacted with the promoter regions. Therefore, the mechanism that leads to a downregulated expression in the *hns/hlp* mutants only is still not clear and needs further investigation.

To date, only little data on the effects of H-NS on capsule biosynthesis is available. Rowe et al. (2000) reported, that H-NS is required for maximal expression of the K5 capsule determinant at 37 °C, whereas at 20 °C, H-NS acts as a repressor. For the K15 capsule, no such effect of H-NS could be detected. The *hns* single mutant did not differ from the wild type at 37 °C, which might be the result of compensatory effects of Hlp in the pathogenic strain. However, regulation of the K15 determinant seems to be more complex, depending on both regulators H-NS and Hlp.

Outer membrane proteins. Theoretically, most changes in the amount of extracellular substances should also require changes in their transport systems, as seen for the hemolysin transporters HlyB and HlyD, or for the capsule transporter KpsE and KpsF. Therefore, alterations in the composition of other outer membrane components can not be excluded.

Landini and Zehnder (2002) found drastic differences in the composition of outer membrane proteins in an *hns* mutant compared to the wild type. For instance, the porins LamB, OmpF, Tsx, and OmpX were present in lower amounts in the mutant, while two other porins, OmpN and OmpA, were more abundant. According to the array data obtained in this study, we could confirm a significantly downregulated expression of *lamB* and *tsx* in both the *hns* and the *hns/stpA* mutants, whereas *ompX* expression turned out to be elevated in our strain background. The gene coding for the porin OmpT exhibited the strongest upregulation in the *hns* mutant, with an 30-fold increased expression compared to the wild type. In total, expression of more than 100 genes assigned to the functional group of transport and membrane proteins was altered in the *hns* mutants.

Curli and cellulose production. There are indications for alterations of other surface structures than porins. As observed in the Congo Red-binding assay, *hns/hlp* mutants were dark brown even at 37 °C, where no curli fimbriae are produced in the wild type. Relieved expression of curli fimbriae in *hns* mutants grown at 26 °C has been described before (Olsen *et al.*, 1993a; 1993b). In UPEC strain 536, however, both Hlp and H-NS seem to be able to repress curli expression. Semi-quantitative RT-PCR for the major curli subunit gene *csgA* confirmed this result, and at the same time indicated an increased expression of the cellulose synthesis activator-encoding gene *yaiC* in these mutants. Therefore, the production of curli fimbriae and cellulose might also contribute to the mucoid phenotype of strains lacking both H-NS and Hlp.

6.4.3. Effect on growth rates

Finally, we found differences in the requirement for the H-NS paralogs for normal growth depending on temperature. H-NS and StpA seemed to be indispensable at elevated temperatures, whereas the presence of H-NS together with Hlp was required at low temperatures. This differences in requirement for growth was reflected in the expression levels of the various nucleoid-associated proteins, which will be discussed in the next section.

6.5. Temperature-dependent expression of histone-like proteins

When comparing transcript amounts of *hlp*, *hns*, and *stpA* at various growth conditions, a clear difference in temperature-dependent expression was found. Expression of *hns* is cold-shock induced, due to the action of the major cold-shock protein CspA (La Teana *et al.*, 1991). Elevated *hns* transcript amounts could be detected at 30 °C compared to 37 °C. However, at temperatures below 30 °C, *hns* expression was decreased again, which has to be explained by additional factors not present in *E. coli* K-12. Expression of *stpA* increases upon temperature upshift (Sonden and Uhlin, 1996). In UPEC strain 536, almost any *stpA* transcript could be detected at low temperatures. However, the increase in expression level with increasing temperatures was clearly visible, resulting in fairly high *stpA*-mRNA levels at 45 °C. Finally, expression of *hlp* does not seem to change with temperature, or might, to a low extent, be reciprocally regulated to *stpA*. This could also be the missing factor for decreased expression of *hns* at 25 °C compared to 30 °C, since the elevated levels of Hlp at low temperatures would result in increased repression of H-NS by Hlp.

Referring now to the relative expression levels of each of the proteins, and assuming H-NS/Hlp or H-NS/StpA heteromers only, the following model of a temperature-dependent composition of the nucleoid-associated protein pool is proposed (Fig. 49).

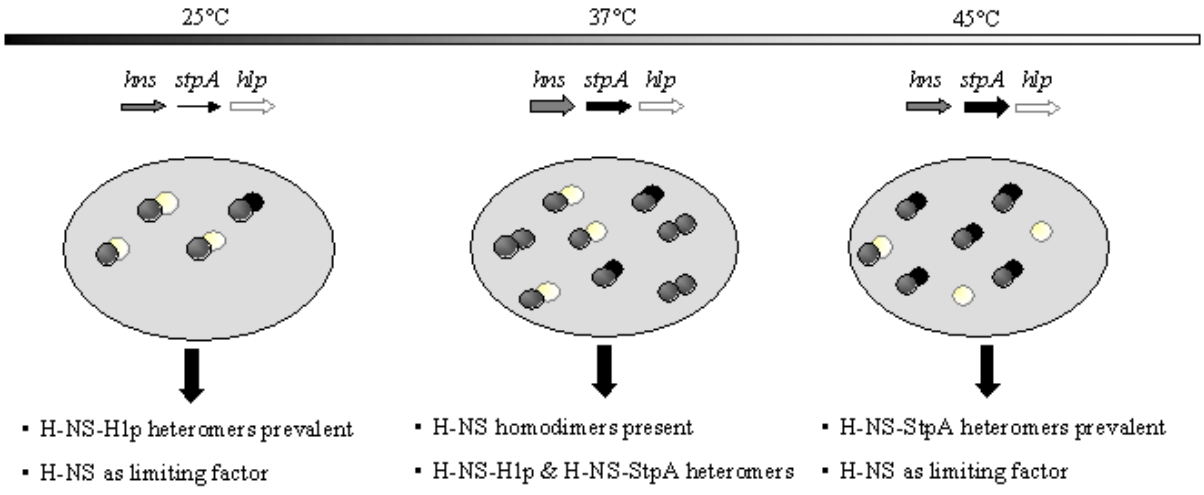

Fig. 49: Model for temperature-dependent composition of the pool of H-NS-like proteins. The model results from studies on expression levels of *hns*, *stpA*, and *hlp* at various temperatures, and assumes only H-NS /StpA or H-NS/Hlp heteromers. See text for further details.

At lower temperatures (25 °C), only little H-NS protein is present, and even lower levels of StpA. Therefore, Hlp will be preferentially found in heteromers with H-NS, which is the limiting factor in formation of stable complexes. Thus, H-NS/Hlp heteromers would be the biological active form required for normal state of the cell at low temperatures. Therefore, an *hns/hlp* double mutant would grow only poorly at 25 °C, as it was observed on agar plates and in liquid broth (Fig. 53; Table 12).

At normal temperature of 37 °C, expression of both *hns* and *stpA* is elevated compared to 25 °C, while the amount of *hlp* stays the same. As a consequence, the occurrence of H-NS/StpA heteromers in addition to the H-NS/Hlp complexes would be expected first, and secondly, free H-NS homodimers would occur due to an excess of H-NS protein. Here, the H-NS dimers would be of biological relevance. However, as seen in *hns* mutants, StpA (and/or Hlp) can substitute for some of the functions of the absent H-NS dimers.

Finally, at even higher temperatures of 45 °C, *stpA* expression reaches high enough levels to render H-NS/StpA heteromers the prevalent form (maybe even dislodging Hlp from the H-NS N-terminus). Again, H-NS is the limiting factor for heteromeric interactions, and here, an *hns/stpA* double mutant is supposed to grow slowly.

Of course, this model is only speculative. Other factors like compensating abilities of each paralog, degradation of free monomers by proteases, and differences in oligomerization abilities have to be taken into account. However, the model illustrates, how differential expression of only three genes can result in a variable outcome of regulatory complexes and expression of their target genes.

6.6. Implications and Outlook

In this study, the question was addressed, whether there is regulatory cross-talk between pathogenicity island-encoded virulence factors or regulatory proteins, and the core chromosome, which is controlled by a pre-established regulatory network. The global regulator H-NS was found to affect the expression of many PAI-encoded virulence-associated genes in uropathogenic *E. coli* strain 536, thereby linking PAIs to the cellular regulatory network. Moreover, a third member of the H-NS-family, the Hlp protein, which is encoded on a putative genomic island, was found to be able to interact with H-NS both at the transcriptional, as well as at the protein level, thereby having successfully insituated itself into the cellular regulatory network.

Thus, the answer to the central question of this thesis is positive, in the meaning that there indeed is regulatory cross-talk between pathogenicity islands and the core chromosome.

This suggests, that acquisition of novel global regulators alter the entire global regulatory programm of the cell. However, the exact mechanisms of this modulation remains unclear. Johansson *et al*. (2001) proposed, that C-terminal interactions between histone-like proteins might alter their DNA-binding ability and cause a change in the DNA motif that is recognized. Thus, H-NS/StpA or H-NS/Hlp heteromeric complexes would affect different target genes than H-NS homomers. Moreover, as seen for anti-H-NS factors, interactions of the N-terminus could interfere with higher-order polymerization of H-NS along the DNA and with the process of transcriptional silencing. Therefore, interactions between H-NS-like proteins can have both a positive or negative outcome.

Finally, the H-NS homologs can also act independently of H-NS and heteromeric complex formation. For some genes, both Hlp or StpA are able to complement for the lack of H-NS, thereby acting as molecular backups. This effects is further enhanced by the negative cross-regulation between the histone-like proteins, since a lack of one of the proteins automatically results in increased expression of one of its homologs, which then can assume the function of the missing regulator.

Possible regulatory loops of histone-like proteins are summarized in Figure 50.

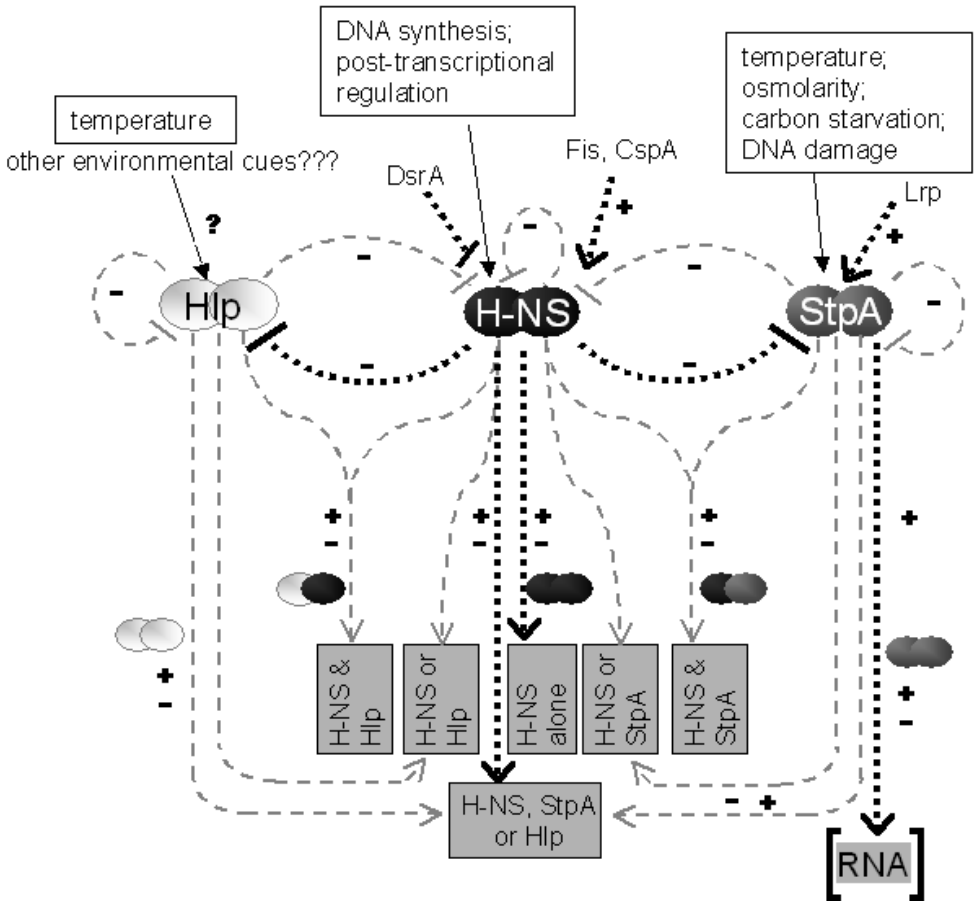

Fig. 50: Regulatory loops. Dominant regulatory circuits are indicated in bold; + positve regulation; - negative regulation; grey boxes indicate the different classes of genes regulated either by H-NS alone, by H-NS or StpA, and H-NS/StpA or H-NS/Hlp comlexes, respectively. RNA mediated (indirect) regulation by StpA has been taken into account. Modified after Zhang *et al.* (1996).

These regulatory loops include both auto- and cross-regulation of the H-NS-like proteins, as well as known environmental stimuli that affect their expression. Interestingly, each protein is subject to different stimuli. Therefore, any specific growth condition will produce a certain profile of nucleoid-associated proteins. As a consequence, the effects on expression of the distinct classes of target genes also vary with the external conditions.

Taken together, all those variable interactions result in a very complex network between the histone-like proteins, and this complexity is even increased after acquisition of a novel H-NS-like protein such as Hlp. However, since such global regulators are also subject to strong selective pressure, it can be assumed, that a diversification of the regulatory circuits offers some advantages for bacterial lifestyle.

Despite all speculations, the identification and characterization of Hlp also offers some practical possibilities. Even if sequence aligment of all H-NS-like proteins proteins results in only dispersed regions of complete identity, identification of any conserved region might provide information about features, which are crucial for function (i.e. DNA binding and oligomerization). For instance, by comparing the amino-acid sequences of ten different H-NS-related proteins of different bacterial species, Dorman *et al*. (1999) were able to deduce a consensus sequence, from which Hlp differed only in 29 out of 109 residues. Therefore, discovery and analysis of more H-NS homologs like Hlp can be very helpful for understanding the exact mode of action of these proteins. Future studies with mutagenized and truncated Hlp protein is another possibility to answer this question.

In summary, it can be proposed that the biological role of Hlp (and StpA) does not rely on a distinct function of the single protein, but rather on its interactions with H-NS, modulating its regulatory activity. Therefore, the presence of several nucleoid-associated proteins in strains like UPEC strain 536 accounts for a highly flexible and fine tuned network of gene regulation.

7. References

Afflerbach, H., Schröder, O., and Wagner, R. (1998) Effects of the *Escherichia coli* DNA-binding protein H-NS on rRNA synthesis *in vivo*. *Mol. Microbiol.* **28**: 641-653.

Allison, C., Emödy, L., Coleman, N., and Hughes, C. (1994) The role of swarm cell differentiation and multicellular migration in the uropathogenicity of *Proteus mirabilis*. *J. Infect. Dis.* **169**: 1155-1158.

Asscher, A.W., Sussman, M., Waters, W.E., Davis, R.H., and Chick, S. (1966) Urine as a medium for bacterial growth. *Lancet* **2**: 1037-1041.

Atlung, T., and Ingmer, H. (1997) H-NS: a modulator of environmentally regulated gene expression. *Mol. Microbiol.* **24**: 7-17.

Barth, M., Marschall, C., Muffler, A., Fischer, D., and Hengge-Aronis, R. (1995) Role for the histone-like protein H-NS in growth phase-dependent and osmotic regulation of sigma S and many sigma S-dependent genes in *Escherichia coli*. *J. Bacteriol.* **177**: 3455-3464.

Beloin, C., Deighan, P., Doyle, M., and Dorman, C.J. (2003) *Shigella flexneri* 2a strain 2457T expresses three members of the H-NS-like protein family: characterization of the Sfh protein. *Mol. Gen. Genomics* **270**: 66-77.

Beloin, C., and Dorman, C.J. (2003) An extended role for the nucleoid structuring protein H-NS in the virulence gene regulatory cascade of *Shigella flexneri*. *Mol. Microbiol.* **47**: 825-838.

Berger, H., Hacker, J., Juarez, A., Hughes, C., and Goebel, W. (1982) Cloning of the Chromosomal Determinants Encoding Hemolysin Production and Mannose-Resistant Hemagglutination in *Escherichia coli*. *J. Bacteriol.* **152**: 1241-1247.

Bertin, P., Lejeune, P., Laurent-Winter, C., and Danchin, A. (1990) Mutations in bglY, the structural gene for the DNA-binding protein H1, affect expression of several *Escherichia coli* genes. *Biochimie* **72**: 889-891.

Bertin, P., Benhabiles, N., Krin, E., Laurent-Winter, C., Tendeng, C., Turlin, E., Thomas, A., Danchin, A., and Brasseur, R. (1999) The structural and functional organization of H-NS-like proteins is evolutionarily conserved in gram-negative bacteria. *Mol. Microbiol.* **31**: 319-329.

Bertin, P., Hommais, F., Krin, E., Soutourina, O., Tendeng, C., Derzelle, S., and Danchin, A. (2001) H-NS and H-NS-like proteins in Gram-negative bacteria and their multiple role in the regulation of bacterial metabolism. *Biochimie* **83**: 235-241.

Bertoni, G., Fujita, N., Ishihama, A., and de Lorenzo, V. (1998) Active recruitment of sigma54-RNA polymerase to the *Pu* promoter of *Pseudomonas putida*: role of IHF and alphaCTD. *EMBO J.* **17**: 5120-5128.

Blattner, F.R., Plunkett, G., Bloch, C.A., Perna, N.T., Burland, V., Riley, M., Collado-Vides, J., Glasner, J.D., Rode, C.K., Mayhew, G.F., Gregor, J., Davis, N.W., Kirkpatrick, H.A., Goeden, M.A., Rose, D.J., Mau, B., and Shao, Y. (1997) The Complete Genome Sequence of *Escherichia coli* K-12. *Science* **277**: 1453-1462.

Bloch, V., Yang, Y., Margeat, E., Chavanieu, A., Auge, M.T., Robert, B., Arold, S., Rimsky, S., and Kochoyan, M. (2003) The H-NS dimerization domain defines a new fold contributing to DNA recognition. *Nat. Struct. Biol.* **10**: 212-218.

Blomfield, I. (2001) The regulation of pap and type 1 fimbriation in *Escherichia coli*. *Adv. Microb. Physiol.* **45**: 1-49.

Blum, G., Ott, M., Lischewski, A., Ritter, A., Imrich, H., Tschäpe, H., and Hacker, J. (1994) Excision of large DNA regions termed pathogenicity islands from tRNA-specific loci in the chromosome of an *Escherichia coli* wild-type pathogen. *Infect. Immun.* **62**: 606-614.

Bokal, A., Ross, W., Gaal, T., Johnson, R., and Gourse, R. (1997) Molecular anatomy of a transcription activation patch: FIS-RNA polymerase interactions at the *Escherichia coli rrnB* P1 promoter. *EMBO J.* **16**: 154-162.

Caramel, A., and Schnetz, K. (2000) Antagonistic control of the *Escherichia coli bgl* promoter by FIS and CAP *in vitro*. *Mol. Microbiol.* **36**: 85-92.

Carniel, E. (2001) The *Yersinia* high-pathogenicity island: an iron-uptake island. *Microbes Infect.* **3**: 561-569.

Carty, S., Sreekumar, K., and Raetz, C. (1999) Effect of Cold Shock on Lipid A Biosynthesis in *Escherichia coli*. Induction at 12 °C of an acyltransferase specific for palmitoloyl-acyl carrier protein. *J. Biol. Chem.* **274**: 9677-9685.

Ceschini, S., Lupidi, G., Coletta, M., Pon, C., Fioretti, E., and Angeletti, M. (2000) Multimeric Self-assembly Equilibria Involving the Histone-like Protein H-NS. A Thermodynamic Study. *J. Biol. Chem.* **275**: 729-734.

Chuang, S.E., Daniels, D.L., and Blattner, F.R. (1993) Global regulation of gene expression in *Escherichia coli. J. Bacteriol.* **175**: 2026-2036.

Cornelis, G.R., Sluiters, C., Delor, I., Geib, D., Kaniga, K., Lambert de Rouvroit, C., Sory, M.P., Vanooteghem, J.C., and Michiels, T. (1991) *ymoA*, a *Yersinia enterocolitica* chromosomal gene modulating the expression of virulence functions. *Mol. Microbiol.* **5**: 1023-1034.

Costerton, J.W., Stewart, P.S., and Greenberg, E.P. (1999) Bacterial Biofilms: A Common Cause of Persistent Infections. *Science* **284**: 1318-1322.

Cusick, M., and Belfort, M. (1998) Domain structure and RNA annealing activity of the *Escherichia coli* regulatory protein StpA. *Mol. Microbiol.* **28**: 847-857.

Dagberg, B., and Uhlin, B.E. (1992) Regulation of virulence-associated plasmid genes in enteroinvasive *Escherichia coli. J. Bacteriol.* **174**: 7606-7612.

Dai, X., and Rothman-Denes, L.B. (1999) DNA structure and transcription. *Curr. Opin. Microbiol.* **2**: 126-130.

Dame, R., Wyman, C., and Goosen, N. (2001) Structural basis for preferential binding of H-NS to curved DNA. *Biochimie* **83**: 231-234.

Dame, R. (2005) The role of nucleoid-associated proteins in the organization and compaction of bacterial chromatin. *Mol. Microbiol.* **56**: 858-870.

Dame, R., Luijsterburg, M., Krin, E., Bertin, P., Wagner, R., and Wuite, G. (2005) DNA Bridging: a Property Shared among H-NS-Like Proteins. *J. Bacteriol.* **187**: 1845-1848.

Danese, P.N., Pratt, L.A., Dove, S.L., and Kolter, R. (2000) The outer membrane protein, Antigen 43, mediates cell-to-cell interactions within *Escherichia coli* biofilms. *Mol. Microbiol.* **37**: 424-432.

Datsenko, K., and Wanner, B. (2000) One-step inactivation of chromosomal genes in *Escherichia coli* K-12 using PCR products. *Proc. Natl. Acad. Sci. USA* **97**: 6640-6645.

Defez, R., and De Felice, M. (1981) Cryptic operon for beta-glucoside metabolism in *Escherichia coli* K12: genetic evidence for a regulatory protein. *Genetics* **97**: 11-25.

Deighan, P., Free, A., and Dorman, C. (2000) A role for the *Escherichia coli* H-NS-like protein StpA in OmpF porin expression through modulation of *micF* RNA stability. *Mol. Microbiol.* **38**: 126-139.

Deighan, P., Beloin, C., and Dorman, C.J. (2003) Three-way interactions among the Sfh, StpA and H-NS nucleoid-structuring proteins of *Shigella flexneri* 2a strain 2457T. *Mol. Microbiol.* **48**: 1401-1416.

Dersch, P., Kneip, S., and Bremer, E. (1994) The nucleoid-associated DNA-binding protein H-NS is required for the efficient adaptation of *Escherichia coli* K-12 to a cold environment. *Mol. Gen. Genet.* **245**: 255-259.

Dobrindt, U., and Hacker, J. (2001) Whole genome plasticity in pathogenic bacteria. *Curr. Opin. Microbiol.* **4**: 550-557.

Dobrindt, U., Blum-Oehler, G., Nagy, G., Schneider, G., Johann, A., Gottschalk, G., and Hacker, J. (2002a) Genetic structure and distribution of four pathogenicity islands (PAI I(536) to PAI IV(536)) of uropathogenic *Escherichia coli* strain 536. *Infect. Immun.* **70**: 6365-6372.

Dobrindt, U., Emödy, L., Gentschev, I., Goebel, W., and Hacker, J. (2002b) Efficient expression of the alpha-haemolysin determinant in the uropathogenic *Escherichia coli* strain 536 requires the *leuX*-encoded tRNA(5)(Leu). *Mol. Gen. Genomics* **267**: 370-379.

Dobrindt, U., Agerer, F., Michaelis, K., Janka, A., Buchrieser, C., Samuelson, M., Svanborg, C., Gottschalk, G., Karch, H., and Hacker, J. (2003) Analysis of genome plasticity in pathogenic and commensal *Escherichia coli* isolates by use of DNA arrays. *J. Bacteriol.* **185**: 1831-1840.

Dobrindt, U., Hochhut, B., Hentschel, U., and Hacker, J. (2004) Genomic islands in pathogenic and environmental microorganisms. *Nat. Rev. Micro.* **2**: 414-424.

Dorman, C. (1994) Genetics of Bacterial Virulence. *Blackwell scientific publications, Oxford*.

Dorman, C., Hinton, J., and Free, A. (1999) Domain organization and oligomerization among H-NS-like nucleoid-associated proteins in bacteria. *Trends Microbiol.* **7**: 124-128.

Dorman, C., and Deighan, P. (2003) Regulation of gene expression by histone-like proteins in bacteria. *Curr. Opin. Genet. Dev.* **13**: 179-184.

Dorman, C. (2004) H-NS: a universal regulator for a dynamic genome. *Nat. Rev. Microbiol.* **2**: 391-400.

Dorman, C.J., Bhriain, N.N., and Higgins, C.F. (1990) DNA supercoiling and environmental regulation of virulence gene expression in *Shigella flexneri*. *Nature* **344**: 789-792.

Escolar, L., Perez-Martin, J., and de Lorenzo, V. (1998) Coordinated Repression In Vitro of the Divergent *fepA-fes* Promoters of *Escherichia coli* by the Iron Uptake Regulation (Fur) Protein. *J. Bacteriol.* **180**: 2579-2582.

Esposito, D., Petrovic, A., Harris, R., Ono, S., Eccleston, J.F., Mbabaali, A., Haq, I., Higgins, C.F., Hinton, J.C.D., Driscoll, P.C., and Ladbury, J.E. (2002) H-NS Oligomerization Domain Structure Reveals the Mechanism for High Order Self-association of the Intact Protein. *J. Mol. Biol.* **324**: 841-850.

Falconi, M., McGovern, V., Hillyard, D., and Higgins, N. (1991) Mutations altering chromosomal protein H-NS induce mini-Mu transposition. *New Biol.* **3**: 615-625.

Falconi, M., Higgins, N., Spurio, R., Pon, C., and Gualerzi, C. (1993) Expression of the gene encoding the major bacterial nucleotide protein H-NS is subject to transcriptional auto-repression. *Mol. Microbiol.* **10**: 273-282.

Falconi, M., Colonna, B., Prosseda, G., Micheli, G., and Gualerzi, C.O. (1998) Thermoregulation of *Shigella* and *Escherichia coli* EIEC pathogenicity. A temperature-dependent structural transition of DNA modulates accessibility of *virF* promoter to transcriptional repressor H-NS. *Embo J.* **17**: 7033-7043.

Finkel, S.E., and Johnson, R.C. (1992) The Fis protein: it's not just for DNA inversion anymore. *Mol. Microbiol.* **6**: 3257-3265.

Finlay, B., and Falkow, S. (1997) Common themes in microbial pathogenicity revisited. *Microbiol. Mol. Biol. Rev.* **61**: 136-169.

Free, A., and Dorman, C. (1995) Coupling of *Escherichia coli hns* mRNA levels to DNA synthesis by autoregulation: implications for growth phase control. *Mol. Microbiol.* **18**: 101-113.

Free, A., and Dorman, C. (1997) The Escherichia coli *stpA* gene is transiently expressed during growth in rich medium and is induced in minimal medium and by stress conditions. *J. Bacteriol.* **179**: 909-918.

Free, A., Williams, R., and Dorman, C. (1998) The StpA Protein Functions as a Molecular Adapter To Mediate Repression of the *bgl* Operon by Truncated H-NS in *Escherichia coli*. *J. Bacteriol.* **180**: 994-997.

Gerstel, U., Park, C., and Römling, U. (2003) Complex regulation of *csgD* promoter activity by global regulatory proteins. *Mol. Microbiol.* **49**: 639-654.

Gomez-Gomez, J., Blazquez, J., Baquero, F., and Martinez, J. (1996) *hns* mutant unveils the presence of a latent haemolytic activity in *Escherichia coli* K-12. *Mol. Microbiol.* **19**: 909-910.

Göransson, M., Sonden, B., Nilsson, P., Dagberg, B., Forsman, K., Emanuelsson, K., and Uhlin, B.E. (1990) Transcriptional silencing and thermoregulation of gene expression in *Escherichia coli*. *Nature* **344**: 682-685.

Gottesman, S., and Stout, V. (1991) Regulation of capsular polysaccharide synthesis in *Escherichia coli* K12. *Mol. Microbiol.* **5**: 1599-1606.

Grimberg, J., Maguire, S., and Belluscio, L. (1989) A simple method for the preparation of plasmid and chromosomal DNA. *Nucl. Acids. Res.* **21**: 8893.

Gronow, S., and Brade, H. (2001) Lipopolysaccharide biosynthesis: which steps do bacteria need to survive? *J. Endotoxin Res.* **7**: 3-23.

Gross, R. (1993) Signal transduction and virulence regulation in human and animal pathogens. *FEMS Microbiol. Rev.* **10**: 301-326.

Gunn, J.S., Lim, K.B., Krueger, J., Kim, K., Guo, L., Hackett, M., and Miller, S.I. (1998) PmrA-PmrB-regulated genes necessary for 4-aminoarabinose lipid A modification and polymyxin resistance. *Mol. Microbiol.* **27**: 1171-1182.

Guo, L., Lim, K.B., Gunn, J.S., Bainbridge, B., Darveau, R.P., Hackett, M., and Miller, S.I. (1997) Regulation of Lipid A Modifications by *Salmonella typhimurium* Virulence Genes *phoP-phoQ*. *Science* **276**: 250-253.

Guo, L., Lim, K.B., Poduje, C.M., Daniel, M., Gunn, J.S., Hackett, M., and Miller, S.I. (1998) Lipid A Acylation and Bacterial Resistance against Vertebrate Antimicrobial Peptides. *Cell* **95**: 189-198.

Haack, K., Robinson, C., Miller, K., Fowlkes, J., and Mellies, J. (2003) Interaction of Ler at the LEE5 (tir) operon of enteropathogenic *Escherichia coli*. *Infect. Immun.* **71**: 384-392.

Hacker, J., Hof, H., Emödy, L., and Goebel, W. (1986) Influence of cloned *Escherichia coli* hemolysin genes, S-fimbriae and serum resistance on pathogenicity in different animal models. *Microb. Pathog.* **1**: 533-547.

Hacker, J., Blum-Oehler, G., Mühldorfer, I., and Tschäpe, H. (1997) Pathogenicity islands of virulent bacteria: structure, function and impact on microbialevolution. *Mol. Microbiol.* **23**: 1089-1097.

Hacker, J., and Kaper, J.B. (2000) Pathogenicity islands and the evolution of microbes. *Ann. Rev. Microbiol.* **54**: 641-679.

Hacker, J., and Carniel, E. (2001) Ecological fitness, genomic islands and bacterial pathogenicity: A Darwinian view of the evolution of microbes. *EMBO Reports* **2**: 376-381.

Hacker, J., Hentschel, U., and Dobrindt, U. (2003) Prokaryotic Chromosomes and Disease. *Science* **301**: 790-793.

Hall, T. (1999) BioEdit: a user-friendly biological sequence alignment editor and analysis program for Windows 95/98/NT. *Nucl. Acids. Symp. Ser.* **41**: 95-98.

Hardy, C.D., and Cozzarelli, N.R. (2005) A genetic selection for supercoiling mutants of *Escherichia coli* reveals proteins implicated in chromosome structure. *Mol. Microbiol.* **57**: 1636-1652.

Higgins, C., Dorman, C., Stirling, D., Waddell, L., Booth, I., May, G., and Bremer, E. (1988) A physiological role for DNA supercoiling in the osmotic regulation of gene expression in *S. typhimurium* and *E. coli*. *Cell* **52**: 569-584.

Hommais, F., Krin, E., Laurent-Winter, C., Soutourina, O., Malpertuy, A., Le Caer, J., Danchin, A., and Bertin, P. (2001) Large-scale monitoring of pleiotropic regulation of gene expression by the prokaryotic nucleoid-associated protein, H-NS. *Mol. Microbiol.* **40**: 20-36.

Hooton, T.M., and Stamm, W.E. (1997) Diagnosis and treatment of uncomplicated urinary tract infection. *Infect. Dis. Clin. North. Am.* **11**: 551-581.

Ishihama, A. (1993) Protein-protein communication within the transcription apparatus. *J Bacteriol* **175**: 2483-2489.

Jacob, F., and Monod, J. (1961) Genetic regulatory mechanisms in the synthesis of proteins. *J. Mol. Biol.* **3**: 318-356.

Johansson, J., and Uhlin, B.E. (1999) Differential protease-mediated turnover of H-NS and StpA revealed by a mutation altering protein stability and stationary-phase survival of *Escherichia coli*. *Proc. Natl. Acad. Sci. USA* **96**: 10776-10781.

Johansson, J., Eriksson, S., Sonden, B., Wai, S., and Uhlin, B.E. (2001) Heteromeric interactions among nucleoid-associated bacterial proteins: localization of StpA-stabilizing regions in H-NS of *Escherichia coli*. *J. Bacteriol.* **183**: 2343-2347.

Johnson, J.R. (1991) Virulence factors in *Escherichia coli* urinary tract infection. *Clin. Microbiol. Rev.* **4**: 80-128.

Kalinowski, B., KLiermann, L., Givens, S., and Brantley, S. (2000) Rates of bacteria-promoted solubilization of Fe from minerals: a review of problems and approaches. *Chem. Geol.* **169**: 357-370.

Kawula, T., and Orndorff, P. (1991) Rapid site-specific DNA inversion in *Escherichia coli* mutants lacking the histone-like protein H-NS. *J. Bacteriol.* **173**: 4116-4123.

Kerenyi, M., Allison, H.E., Batai, I., Sonnevend, A., Emödy, L., Plaveczky, N., and Pal, T. (2005) Occurrence of *hlyA* and *sheA* genes in extraintestinal *Escherichia coli* strains. *J. Clin. Microbiol.* **43**: 2965-2968.

Knapp, S., Hacker, J., Jarchau, T., and Goebel, W. (1986) Large, unstable inserts in the chromosome affect virulence properties of uropathogenic *Escherichia coli* O6 strain 536. *J. Bacteriol.* **168**: 22-30.

La Teana, A., Falconi, M., Scarlato, V., Lammi, M., and Pon, C. (1989) Characterization of the structural genes for the DNA-binding protein H-NS in *Enterobacteriaceae*. *FEBS Lett.* **244**: 34-38.

La Teana, A., Brandi, A., Falconi, M., Spurio, R., Pon, C., and Gualerzi, C. (1991) Identification of a cold shock transcriptional enhancer of the *Escherichia coli* gene encoding nucleoid protein H-NS. *Proc. Natl. Acad. Sci. USA* **88**: 10907-10911.

Laemmli, U.K. (1970) Cleavage of structural proteins during assembly of the head of bacteriophage T4. *Nature* **227**: 680-685.

Lammi, M., Paci, M., Pon, C.L., Losso, M.A., Miano, A., Pawlik, R.T., Gianfranceschi, G.L., and Gualerzi, C.O. (1984) Proteins from the prokaryotic nucleoid: biochemical and 1H NMR studies on three bacterial histone-like proteins. *Adv. Exp. Med. Biol.* **179**: 467-477.

Landini, P., and Zehnder, A. (2002) The global regulatory hns gene negatively affects adhesion to solid surfaces by anaerobically grown *Escherichia coli* by modulating expression of flagellar genes and lipopolysaccharide production. *J. Bacteriol.* **184**: 1522-1529.

Laurent-Winter, C., Lejeune, P., and Danchin, A. (1995) The *Escherichia coli* DNA-binding protein H-NS is one of the first proteins to be synthesized after a nutritional upshift. *Res. Microbiol.* **146**: 5-16.

Lewin, B. (2002) Molekularbiologie der Gene. *6. Auflage, Spektrum Akademischer Verlag, Heidelberg-Berlin*.

Lucht, J., Dersch, P., Kempf, B., and Bremer, E. (1994) Interactions of the nucleoid-associated DNA-binding protein H-NS with the regulatory region of the osmotically controlled *proU* operon of *Escherichia coli*. *J. Biol. Chem.* **269**: 6578-.

Lucht, J.M., and Bremer, E. (1994) Adaptation of *Escherichia coli* to high osmolarity environments: osmoregulation of the high-affinity glycine betaine transport system *proU*. *FEMS Microbiol. Rev.* **14**: 3-20.

Ludwig, A., and Goebel, W. (1991) Genetic determinants of cytolytic toxins from gram-negative bacteria. In: Alouf, J.E., Freer, J.H. (eds). Sourcebook of Bacterial Protein Toxins. London. Acadenic Press.: 117-146.

Ludwig, A., von Rhein, C., Bauer, S., Huttinger, C., and Goebel, W. (2004) Molecular analysis of cytolysin A (ClyA) in pathogenic *Escherichia coli* strains. *J. Bacteriol.* **186**: 5311-5320.

Mademidis, A., and Koster, W. (1998) Transport activity of FhuA, FhuC, FhuD, and FhuB derivatives in a system free of polar effects, and stoichiometry of components involved in ferrichrome uptake. *Mol. Genet. Genomics* **258**: 156-165.

Madrid, C., Nieto, J., Paytubi, S., Falconi, M., Gualerzi, C., and Juarez, A. (2002) Temperature- and H-NS-dependent regulation of a plasmid-encoded virulence operon expressing *Escherichia coli* hemolysin. *J. Bacteriol.* **184**: 5058-5066.

McLeod, S., and Johnson, R. (2001) Control of transcription by nucleoid proteins. *Curr. Opin. Microbiol.* **4**: 152-159.

Miller, J. (1972) Experiments in Molecular Genetics. *Cold Spring Harbor Laboratory Press, Cold Spring Harbor, NY*.

Morschhäuser, J., Uhlin, B.E., and Hacker, J. (1993) Transcriptional analysis and regulation of the *sfa* determinant coding for S fimbriae of pathogenic *Escherichia coli* strains. *Mol. Gen. Gent.* **238**: 97-105.

Morschhäuser, J., Vetter, V., Emödy, L., and Hacker, J. (1994) Adehsin regulatory genes within large, unstable DNA regions of pathogenic *Escherichia coli*: cross-talk between different adhesin gene clusters. *Mol. Microbiol.* **11**: 555-566.

Mühldorfer, I., Ziebuhr, W., and Hacker, J. (2001) *Escherichia coli* in urinary tract infections. In Sussmann, M. *edt.* Molecular Medical Microbiology. Academic Press: Chapt. 81.

Mukerji, M., and Mahadevan, S. (1997) Characterization of the negative elements involved in silencing the *bgl* operon of *Escherichia coli*: possible roles for DNA gyrase, H-NS, and CRP-cAMP in regulation. *Mol. Microbiol.* **24**: 617-627.

Nagy, G., Dobrindt, U., Kupfer, M., Emödy, L., Karch, H., and Hacker, J. (2001) Expression of hemin receptor molecule ChuA is influenced by RfaH in uropathogenic *Escherichia coli* strain 536. *Infect. Immun.* **69**: 1924-1928.

Nagy, G., Dobrindt, U., Schneider, G., Khan, A., Hacker, J., and Emödy, L. (2002) Loss of Regulatory Protein RfaH Attenuates Virulence of Uropathogenic *Escherichia coli*. *Infect. Immun.* **70**: 4406-4413.

Nieto, J., Madrid, C., Prenafeta, A., Miquelay, E., Balsalobre, C., Carrascal, M., and Juarez, A. (2000) Expression of the hemolysin operon in *Escherichia coli* is modulated by a nucleoid-protein complex that includes the proteins Hha and H-NS. *Mol. Gen. Genet.* **263**: 349-358.

Nieto, J.M., Madrid, C., Miquelay, E., Parra, J.L., Rodriguez, S., and Juarez, A. (2002) Evidence for Direct Protein-Protein Interaction between Members of the Enterobacterial Hha/YmoA and H-NS Families of Proteins. *J. Bacteriol.* **184**: 629-635.

Nishino, K., and Yamaguchi, A. (2004) Role of Histone-Like Protein H-NS in Multidrug Resistance of *Escherichia coli*. *J. Bacteriol.* **186**: 1423-1429.

O'Byrne, C.P., and Dorman, C.J. (1994) Transcription of the *Salmonella typhimurium spv* virulence locus is regulated negatively by the nucleoid-associated protein H-NS. *FEMS Microbiol. Lett.* **121**: 99-105.

Oelschlaeger, T.A., Dobrindt, U., and Hacker, J. (2002) Virulence factors of uropathogens. *Curr. Opin. Urol.* **12**: 33-38.

Olsen, A., Arnqvist, A., Hammar, M., and Normark, S. (1993a) Environmental regulation of curli production in *Escherichia coli*. *Infect. Agents Dis.* **2**: 272-274.

Olsen, A., Arnqvist, A., Hammar, M., Sukupolvi, S., and Normark, S. (1993b) The RpoS sigma factor relieves H-NS-mediated transcriptional repression of *csgA*, the subunit gene of fibronectin-binding curli in *Escherichia coli*. *Mol. Microbiol.* **7**: 523-536.

Olsen, P., and Klemm, P. (1994) Localization of promoters in the *fim* gene cluster and the effect of H-NS on the transcription of *fimB* and *fimE*. *FEMS Microbiol. Lett.* **116**: 95-100.

Oscarsson, J., Mizunoe, Y., Li, L., Lai, X.H., Wieslander, A., and Uhlin, B.E. (1999) Molecular analysis of the cytolytic protein ClyA (SheA) from *Escherichia coli*. *Mol. Microbiol.* **32**: 1226-1238.

O'Toole, G., and Kolter, R. (1998) Initiation of biofilm formation in *Pseudomonas fluorescens* WCS365 proceeds via multiple, convergent signalling pathways: a genetic analysis. *Mol. Microbiol.* **28**: 449-461.

Ozenberger, B.A., Nahlik, M.S., and McIntosh, M.A. (1987) Genetic organization of multiple fep genes encoding ferric enterobactin transport functions in *Escherichia coli*. *J. Bacteriol.* **169**: 3638-3646.

Paytubi, S., Madrid, C., Forns, N., Nieto, J.M., Balsalobre, C., Uhlin, B.E., and Juarez, A. (2004) YdgT, the Hha paralogue in *Escherichia coli*, forms heteromeric complexes with H-NS and StpA. *Mol. Microbiol.* **54**: 251-263.

Perez-Martin, J., Rojo, F., and de Lorenzo, V. (1994) Promoters responsive to DNA bending: a common theme in prokaryotic gene expression. *Microbiol. Rev.* **58**: 268-290.

Pon, C.L., Calogero, R.A., and Gualerzi, C.O. (1988) Identification, cloning, nucleotide sequence and chromosomal map location of *hns*, the structural gene for Escherichia coli DNA-binding protein H-NS. *Mol. Gen. Genet.* **212**: 199-202.

Record, M.J., Reznikoff, W., Craig, M., McQuade, K., and Schlax, P. (1996) In: Escherichia coli and Salmonella. Cellular and Molecular Biology. 2nd edition. Neidhardt, F.C., Curtis, R.III., Ingraham, J.L., Lin, E.C.C., Low, K.B., Magasanik, B., Reznikoff, W.S., Riley, M., Schaechter, M., and Umbarger, H.E. *American Society for Microbiology, Washington DC*: 792-821.

Renzoni, D., Esposito, D., Pfuhl, M., Hinton, J., Higgins, C., Driscoll, P., and Ladbury, J. (2001) Structural Characterization of the N-terminal Oligomerization Domain of the Bacterial Chromatin-structuring Protein, H-NS,. *J. Mol. Biol.* **306**: 1127-1137.

Rimsky, S., Zuber, F., Buckle, M., and Buc, H. (2001) A molecular mechanism for the repression of transcription by the H-NS protein. *Mol. Microbiol.* **42**: 1311-1323.

Rine, J. (1999) On the mechanism of silencing in *Escherichia coli*. *Proc. Natl. Acad. Sci. USA* **96**: 8309-8311.

Rouquette, C., Serre, M., and Lane, D. (2004) Protective Role for H-NS Protein in IS1 Transposition. *J. Bacteriol.* **186**: 2091-2098.

Rowe, S., Hodson, N., Griffiths, G., and Roberts, I. (2000) Regulation of the *Escherichia coli* K5 capsule gene cluster: evidence for the roles of H-NS, BipA, and integration host factor in regulation of group 2 capsule gene clusters in pathogenic *E. coli*. *J. Bacteriol.* **182**: 2741-2745.

Russo, T.A., McFadden, C.D., Carlino-MacDonald, U.B., Beanan, J.M., Barnard, T.J., and Johnson, J.R. (2002) IroN Functions as a Siderophore Receptor and Is a Urovirulence

Factor in an Extraintestinal Pathogenic Isolate of *Escherichia coli*. *Infect. Immun.* **70**: 7156-7160.

Sambrook, J., Fritsch, E., and Maniatis, T. (1989) Molecular cloning. A Laboratory Manual, 2nd ed. *Cold Spring Harbor Laboratory Press* **Cold Spring Harbor**.

Schechter, L., Jain, S., Akbar, S., and Lee, C. (2003) The Small Nucleoid-Binding Proteins H-NS, HU, and Fis Affect hilA Expression in *Salmonella enterica* Serovar *Typhimurium. Infect. Immun.* **71**: 5432-5435.

Schembri, M.A., Hjerrild, L., Gjermansen, M., and Klemm, P. (2003) Differential Expression of the *Escherichia coli* Autoaggregation Factor Antigen 43. *J. Bacteriol.* **185**: 2236-2242.

Schneider, G., Dobrindt, U., Bruggemann, H., Nagy, G., Janke, B., Blum-Oehler, G., Buchrieser, C., Gottschalk, G., Emödy, L., and Hacker, J. (2004) The Pathogenicity Island-Associated K15 Capsule Determinant Exhibits a Novel Genetic Structure and Correlates with Virulence in Uropathogenic *Escherichia coli* Strain 536. *Infect. Immun.* **72**: 5993-6001.

Schneider, G. (2005) Studies on the architecture and on transferability of pathogenicity islands of uropathogenic *Escherichia coli* strain 536. *PhD-thesis of the University Würzburg*.

Schröder, O., and Wagner, R. (2002) The bacterial regulatory protein H-NS--a versatile modulator of nucleic acid structures. *Biol. Chem.* **383**: 945-960.

Schwyn, B., and Neilands, J.B. (1987) Universal chemical assay for the detection and determination of siderophores. *Analyt. Biochem.* **160**: 47-56.

Shi, X., and Bennett, G. (1994) Plasmids bearing hfq and the hns-like gene stpA complement hns mutants in modulating arginine decarboxylase gene expression in *Escherichia coli*. *J. Bacteriol.* **176**: 6769-6775.

Shiga, Y., Sekine, Y., Kano, Y., and Ohtsubo, E. (2001) Involvement of H-NS in transpositional recombination mediated by IS1. *J. Bacteriol.* **183**: 2476-2484.

Shindo, H., Iwaki, T., Ieda, R., Kurumizaka, H., Ueguchi, C., Mizuno, T., Morikawa, S., Nakamura, H., and Kuboniwa, H. (1995) Solution structure of the DNA binding domain of a nucleoid-associated protein, H-NS, from *Escherichia coli*. *FEBS Lett.* **360**: 125-131.

Shindo, H., Ohnuki, A., Ginba, H., Katoh, E., Ueguchi, C., Mizuno, T., and Yamazaki, T. (1999) Identification of the DNA binding surface of H-NS protein from *Escherichia coli* by heteronuclear NMR spectroscopy. *FEBS Lett.* **455**: 63-69.

Silhavy, T., Berman, M., and Enquist, L. (1984) Experiments with Gene Fusions. *Cold Spring Harbor Laboratory Press, Cold Spring Harbor, NY*.

Skerra, A. (1994) Use of the tetracycline promoter for the tightly regulated production of a murine antibody fragment in *Escherichia coli*. *Gene* **151**: 131-135.

Sledjeski, D., and Gottesman, S. (1995) A Small RNA Acts as an Antisilencer of the H-NS-Silenced *rcsA* Gene of *Escherichia coli*. *PNAS* **92**: 2003-2007.

Smyth, C., Lundback, T., Renzoni, D., Siligardi, G., Beavil, R., Layton, M., Sidebotham, J., Hinton, J., Driscoll, P., Higgins, C., and Ladbury, J. (2000) Oligomerization of the chromatin-structuring protein H-NS. *Mol. Microbiol.* **36**: 962-972.

Snyder, J., Haugen, B., Buckles, E., Lockatell, C., Johnson, D., Donnenberg, M., Welch, R., and Mobley, H. (2004) Transcriptome of Uropathogenic *Escherichia coli* during Urinary Tract Infection. *Infect. Immun.* **72**: 6373-6381.

Solano, C., Garcia, B., Valle, J., Berasain, C., Ghigo, J., Gamazo, C., and Lasa, I. (2002) Genetic analysis of *Salmonella enteritidis* biofilm formation: critical role of cellulose. *Mol. Microbiol.* **43**: 793-808.

Sonden, B., and Uhlin, B.E. (1996) Coordinated and differential expression of histone-like proteins in *Escherichia coli*: regulation and function of the H-NS analog StpA. *EMBO J.* **15**: 4970-4980.

Sonnenfield, J., Burns, C., Higgins, C., and Hinton, J. (2001) The nucleoid-associated protein StpA binds curved DNA, has a greater DNA-binding affinity than H-NS and is present in significant levels in *hns* mutants. *Biochimie* **83**: 243-249.

Soutourina, O., Kolb, A., Krin, E., Laurent-Winter, C., Rimsky, S., Danchin, A., and Bertin, P. (1999) Multiple control of flagellum biosynthesis in *Escherichia coli:* role of H-NS protein and the cyclic AMP-catabolite activator protein complex in transcription of the *flhDC* master operon. *J. Bacteriol.* **181**: 7500-7508.

Soutourina, O.A., and Bertin, P.N. (2003) Regulation cascade of flagellar expression in Gram-negative bacteria. *FEMS Microbiol. Rev.* **27**: 505-523.

Spassky, A., Rimsky, S., Garreau, H., and Buc, H. (1984) H1a, an *E. coli* DNA-binding protein which accumulates in stationary phase, strongly compacts DNA *in vitro*. *Nucl. Acids Res.* **12**: 5321-5340.

Spurio, R., Dürrenberger, M., Falconi, M., La Teana, A., Pon, C., and Gualerzi, C. (1992) Lethal overproduction of the *Escherichia coli* nucleoid protein H-NS: ultramicroscopic and molecular autopsy. *Mol. Gen. Gent.* **231**: 201-211.

Stella, S., Spurio, R., Falconi, M., Pon, C., and Gualerzi, C. (2005) Nature and mechanism of the *in vivo* oligomerization of nucleoid protein H-NS. *EMBO J.* **24**: 2896–2905.

Stevenson, G., Andrianopoulos, K., Hobbs, M., and Reeves, P. (1996) Organization of the *Escherichia coli* K-12 gene cluster responsible for production of the extracellular polysaccharide colanic acid. *J. Bacteriol.* **178**: 4885-4893.

Straus, D.B., Walter, W.A., and Gross, C.A. (1987) The heat shock response of *E. coli* is regulated by changes in the concentration of sigma32. *Nature* **329**: 348-351.

Svanborg, C., and Godaly, G. (1997) Bacterial virulence in urinary tract infection. *Infect. Dis. Clin. North. Am.* **11**: 513-529.

Talukder, A., and Ishihama, A. (1999) Twelve Species of the Nucleoid-associated Protein from *Escherichia coli*. Sequence recognition specificity and DNA bining affinity. *J. Biol. Chem.* **274**: 33105-33113.

Talukder, A., Iwata, A., Nishimura, A., Ueda, S., and Ishihama, A. (1999) Growth Phase-Dependent Variation in Protein Composition of the *Escherichia coli* Nucleoid. *J. Bacteriol.* **181**: 6361-6370.

Tendeng, C., and Bertin, P. (2003) H-NS in Gram-negative bacteria: a family of multifaceted proteins. *Trends Microbiol.* **11**: 511-518.

Tendeng, C., Krin, E., Soutourina, O., Marin, A., Danchin, A., and Bertin, P. (2003a) A Novel H-NS-like Protein from an Antarctic Psychrophilic Bacterium Reveals a Crucial Role for the N-terminal Domain in Thermal Stability. *J. Biol. Chem.* **278**: 18754-18760.

Tendeng, C., Soutourina, O.A., Danchin, A., and Bertin, P.N. (2003b) MvaT proteins in *Pseudomonas* spp.: a novel class of H-NS-like proteins. *Microbiology* **149**: 3047-3050.

Tippner, D., Afflerbach, H., Bradaczek, C., and Wagner, R. (1994) Evidence for a regulatory function of the histone-like *Escherichia coli* protein H-NS in ribosomal RNA synthesis. *Mol. Microbiol.* **11**: 589-604.

Torres, A.G., and Payne, S.M. (1997) Haem iron-transport system in enterohaemorrhagic *Escherichia coli* O157:H7. *Mol. Microbiol.* **23**: 825-833.

Trachman, J.D., and Maas, W.K. (1998) Temperature Regulation of Heat-Labile Enterotoxin (LT) Synthesis in *Escherichia coli* Is Mediated by an Interaction of H-NS Protein with the LT A-Subunit DNA. *J. Bacteriol.* **180**: 3715-3718.

Travers, A., and Muskhelishvili, G. (2005) DNA supercoiling - a global transcriptional regulator for enterobacterial growth? *Nat. Rev. Micro.* **3**: 157-169.

Tsai, C.M., and Frasch, C.E. (1982) A sensitive silver stain for detecting lipopolysaccharides in polyacrylamide gels. *Anal. Biochem.* **119**: 115-119.

Ueguchi, C., Kakeda, M., and Mizuno, T. (1993) Autoregulatory expression of the *Escherichia coli hns* gene encoding a nucleoid protein: H-NS functions as a repressor of its own transcription. *Mol. Gen. Genet.* **236**: 171-178.

Ueguchi, C., Suzuki, T., Yoshida, T., Tanaka, K., and Mizuno, T. (1996) Systematic mutational analysis revealing the functional domain organization of *Escherichia coli* nucleoid protein H-NS. *J. Mol. Biol.* **263**: 149-162.

Ueguchi, C., Seto, C., Suzuki, T., and Mizuno, T. (1997) Clarification of the Dimerization Domain and its Functional Significance for the *Escherichia coli* Nucleoid Protein H-NS. *J. Mol. Biol.* **274**: 145-151.

Uhlin, B.E., and Mizunoe, Y. (1994) Expression of a novel contact-hemolytic activity by *E. coli*. *J. Cell. Biochem.* **18A**: 71-73.

Ussery, D., Hinton, J., Jordi, B., Granum, P., Seirafi, A., Stephen, R., Tupper, A., Berridge, G., Sidebotham, J., and Higgins, C. (1994) The chromatin associated protein H-NS. *Biochimie* **76**: 968-980.

Varshavsky, A.J., Nedospasov, S.A., Bakayev, V.V., Bakayeva, T.G., and Georgiev, G.P. (1977) Histone-like proteins in the purified *Escherichia coli* deoxyribonucleoprotein. *Nucleic Acids Res.* **4**: 2725-2745.

Vorachek-Warren, M.K., Carty, S.M., Lin, S., Cotter, R.J., and Raetz, C.R. (2002) An *Escherichia coli* mutant lacking the cold shock-induced palmitoleoyltransferase of lipid A biosynthesis: absence of unsaturated acyl chains and antibiotic hypersensitivity at 12 degrees C. *J. Biol. Chem.* **277**: 14186-14193.

Wang, R., and Kushner, S. (1991) Construction of versatile low-copy-number vectors for cloning, sequencing and gene expression in *Escherichia coli*. *Gene* **100**: 195-159.

Warren, J. (1996) Clinical presentations and epidemiology of urinary tract infections. In: Mobley HL, Warren JW, eds. Urinary Tract Infections: Molecular Pathogenesis and Clinical Management. Washington, DC, ASM Press: 3-27.

Westermark, M., Oscarsson, J., Mizunoe, Y., Urbonaviciene, J., and Uhlin, B.E. (2000) Silencing and Activation of ClyA Cytotoxin Expression in *Escherichia coli*. *J. Bacteriol.* **182**: 6347-6357.

White-Ziegler, C., Villapakkam, A., Ronaszeki, K., and Young, S. (2000) H-NS controls pap and daa fimbrial transcription in *Escherichia coli* in response to multiple environmental cues. *J. Bacteriol.* **182**: 6391-6400.

Whitfield, C., and Roberts, I.S. (1999) Structure, assembly and regulation of expression of capsules in *Escherichia coli*. *Mol. Microbiol.* **31**: 1307-1319.

Williams, R., Rimsky, S., and Buc, H. (1996) Probing the structure, function, and interactions of the *Escherichia coli* H-NS and StpA proteins by using dominant negative derivatives. *J. Bacteriol.* **178**: 4335-4343.

Williams, R., and Rimsky, S. (1997) Molecular aspects of the *E. coli* nucleoid protein, H-NS: a central controller of gene regulatory networks. *FEMS Microbiol. Lett.* **156**: 175-185.

Williamson, H., and Free, A. (2005) A truncated H-NS-like protein from enteropathogenic *Escherichia coli* acts as an H-NS antagonist. *Mol. Microbiol.* **55**: 808-827.

Yamada, H., Yoshida, T., Tanaka, K., Sasakawa, C., and Mizuno, T. (1991) Molecular analysis of the Escherichia coli *hns* gene encoding a DNA-binding protein, which preferentially recognizes curved DNA sequences. *Mol. Gen. Genet.* **230**: 332-336.

Yamashino, T., Ueguchi, C., and Mizuno, T. (1995) Quantitative control of the stationary phase-specific sigma factor, sigma S, in *Escherichia coli*: involvement of the nucleoid protein H-NS. *EMBO J.* **14**: 594-602.

Yarmolinsky, M. (2000) Transcriptional silencing in bacteria. *Curr. Opin. Microbiol.* **3**: 138-143.

Zhang, A., and Belfort, M. (1992) Nucleotide sequence of a newly-identified *Escherichia coli* gene, *stpA*, encoding an H-NS-like protein. *Nucleic Acids Res.* **20**: 6735.

Zhang, A., Derbyshire, V., Salvo, J.L., and Belfort, M. (1995) Escherichia coli protein StpA stimulates self-splicing by promoting RNA assembly in vitro. *Rna* **1**: 783-793.

Zhang, A., Rimsky, S., Reaban, M., Buc, H., and Belfort, M. (1996) *Escherichia coli* protein analogs StpA and H-NS: regulatory loops, similar and disparate effects on nucleic acid dynamics. *EMBO J.* **15**: 1340-1349.

8. Appendix

8.1. Legends to figures and tables:

Table 1: Molecular properties of *E. coli* histone-like proteins.....p.20
Table 2: Virulence and fitness factors of uropathogenic *E. coli* isolate 536.....p.37
Table 3: Bacterial strains used in this study.....p.40
Table 4: Plasmids used in this study.....p.41
Table 5: Oligonucleotides used in this study.....p.41
Table 6: Antibiotic substances used in this study.....p.48
Table 7: Parameters of Arrayvision pre-set protocols.....p.68
Table 8: Total numbers of deregulated genes in the *hns* and *stpA* mutants.....p.84
Table 9: Predicted protein parameters of the three histone-like proteins of strain 536.....p.90
Table 10: Occurrence of the *hlp* gene in other *E. coli* variants.....p.91
Table 11: LPS-composition of UPEC strain 536 wild type and isogenic *hns* mutant.....p.119
Table 12: Summary - phenotypic characterization of UPEC strain 536 and mutants.....p.124
App-Table 13: Top50 genes with upregulated expression in *hns* mutant.....p.158
App-Table 14: Top50 genes with upregulated expression in *hns/stpA* mutant.....p.159
App-Table 15: Top37 genes with downregulated expression in *hns* mutant.....p.160
App-Table 16: Top37 genes with downregulated expression in *hns/stpA* mutant.....p.161
App-Table 17: Most abundant transcripts in wild type UPEC 536.....p.162
App-Table 18: Significantly deregulated genes involved in motility and chemotaxis.....p.163
App-Table 19: Significantly deregulated genes of the hemolysin operon.....p.163
App-Table 20: Significantly deregulated genes involved in iron uptake.....p.163
App-Table 21: Significantly deregulated genes involved in adhesion.....p.164
App-Table 22: Significantly deregulated genes involved in generegulation.....p.164
App-Table 23: Significantly deregulated genes involved in resistance/adaptation.....p.165
App-Table 24: Significantly deregulated genes involved in synthesis of extracellular components.....p.166
App-Table 25: *E. coli* strains used for PCR screening and detailed results on the occurrence of the *hlp* gene.....p.167

Fig. 1: Schematic representation of the bacterial nucleoid.....p.23
Fig. 2: Predicted Structure of the H-NS protein.....p.24
Fig. 3: Shematic models for H-NS dimerization and tetramerization.....p.26
Fig. 4: Mechanisms of repression by the H-NS protein.....p.27
Fig. 5: Cladogramm of H-NS homologs in various bacterial species.....p.33
Fig. 6: Chromosomal map of uropathogenic *E. coli* strain 536.....p.38
Fig. 7: DNA and protein markers used in electrophoresis.....p.48
Fig. 8: Strategy for inactivation of chromosomal genes using PCR products.....p.56
Fig. 9: Verification of the *hns* and *stpA* mutations p.81
Fig. 10: Example of hybridization signals obtained with cDNA of wild type 536 and its isogenic *stpA/hns* mutant.....p.82
Fig. 11: Scatterplots and trendlines for linear regression between different experiments..p.83
Fig. 12: Distribution of deregulated genes of the core genome into functional groups.....p.85
Fig. 13: Cluster analysis of expression profiles.....p.86
Fig. 14: Expression levels of major virulence-associated genes in UPEC 536 and isogenic mutants.....p.87
Fig. 15: Sequence alignment of the three nucleoid-associated proteins of UPEC strain 536.....p.89

Fig. 16: Secondary structure prediction for H-NS, StpA, and Hlp.....p.90
Fig. 17: Analysis of the chromosomal location of the gene coding for Hlp.....p.92
Fig. 18: Analysis of *hlp* transcription.....p.94
Fig. 19: Influence of histone-like proteins on *hlp*, *hns*, and *stpA* transcript amounts.....p.95
Fig. 20: Analysis of binding capacities of histone-like proteins to their own promoter regions.....p.95
Fig. 21: Analysis of fractions during purification of His-tagged Hlp protein.....p.96
Fig. 22: Analysis of the nature of the interactions between Hlp and H-NS.....p.97
Fig. 23: Analysis of native Hlp by gel filtration.....p.98
Fig. 24: Analysis of *in vitro* oligomerization by chemical crosslinking.....p.99
Fig. 25: Alternative strategies for purification of recombinant Hlp protein.....p.100
Fig. 26: Analysis of Hlp stabilty.....p.100
Fig. 27: Analysis of complementing activity of Hlp in strains lacking H-NS.....p.102
Fig. 28: Effects of Hlp on transcription levels and growth rates of *hns* mutants.....p.103
Fig. 29: Verification of the *hlp* mutations.....p.105
Fig. 30: Swarming abilities of H-NS deficient strains on swarming agar plates.....p.106
Fig. 31: Effects of histone-like proteins on production of fimbrial adhesins.....p.107
Fig. 32: Analysis of fimbriae expression in wild type strain 536 and its isogenic mutants by AFM.....p.108
Fig. 33: Effects of histone-like proteins on hemolytic activity.....p.110
Fig. 34: Effects of histone-like proteins on the production of siderophores.....p.111
Fig. 35: Effects of histone-like proteins on autoaggregative behavior.....p.113
Fig. 36: Effects of histone-like proteins on multicellular behaviour.....p.114
Fig. 37: Effects of H-NS and Hlp on the production of curli adhesin and cellulose.....p.115
Fig. 38: Effects of histone-like proteins on utilization of ß-glucosides.....p.115
Fig. 39: Effect of Hlp and H-NS on expression of the K15 capsule determinant.....p.116
Fig. 40: Analysis of binding capacities of H-NS and Hlp to promoter regions of the K15 determinant.....p.117
Fig. 41: Effect of lack of H-NS on colanic acid synthesis.....p.118
Fig. 42: Analysis of lipopolysaccharide composition in strains deficient for histone-like proteins.....p.119
Fig. 43: Survival rates of mice infected with H-NS deficient strains p.121
Fig. 44: Time course of lethality induced by H-NS deficient strains.....p.121
Fig. 45: Growth of wild type UPEC strain 536 and its isogenic mutants at various temperatures.....p.122
Fig. 46: Effect of temperature on transcript levels of *hns*, *stpA*, and *hlp*.....p.123
Fig. 47: Model for PhoP-PhoQ induced lipid A modifications due to lack of H-NS.....p.130
Fig. 48: Model for network of cross-regulation by histone-like proteins.....p.134
Fig. 49: Model for temperature-dependent composition of the pool of H-NS-like proteins.....p.139
Fig. 50: Regulatory loops.....p.142
App-Fig. 51: Cell morphology of UPEC strain 536 and isogenic mutants visualized by Atomic Force Microscopy.....p.168
App-Fig. 52: Predicted curvature of promoter regions.....p.171
App-Fig. 53: Growth curves of UPEC strain 536 and isogenic mutants at different temperatures.....p.172
App-Fig. 54: Plasmid maps.....p.173

8.2. Nucleotide and amino-acid sequence of histone-like proteins in UPEC strain 536

(ORF numbers as in ERGO database; start and stopp codons are indicated in the sequence)

>RECP01273 ***hns*** - *Escherichia coli* 536, chromosome_1315557_1315147 (n=414)

CAATTTTGAATTCCTTACATTCCTGGCTATTGCACAACTGAATTTAAGGCTCTATTATTACCTCAACAAACCACCCCAATATAAGTTTGAGATT
ACTACA**ATG**AGCGAAGCACTTAAAATTCTGAACAACATCCGTACTCTTCGTGCGCAGGCAAGAGAATGTACACTTGAAACGCTGGAAGAAATGC
TGGAAAAATTAGAAGTTGTTGTTAACGAACGTCGCGAAGAAGAAAGCGCGGCTGCTGCTGAAGTTGAAGAGCGCACTCGTAAACTGCAGCAATA
TCGCGAAATGCTGATCGCTGACGGTATTGACCCGAACGAACTGCTGAATAGCCTTGCTGCCGTTAAATCTGGCACCAAAGCTAAGCGTGCTCAG
CGTCCGGCAAAATATAGCTACGTTGACGAAAACGGCGAAACTAAAACCTGGACTGGCCAGGGCCGTACTCCAGCTGTAATCAAAAAAGCAATGG
ATGAGCAAGGTAAATCCCTCGACGATTTCCTGATCAAGCAA**TAA**TCTTTTGTAGATTGCACATGCTAAAAATCCCGCCATCGGCGGGATTTTTT
ATTGTCCGGTTTAAGACAATATAATAAGAATAAGCTATAAAAAAACG

M S E A L K I L N N I R T L R A Q A R E C T L E T L E E M L E K L E V V V N E R R E E E S A A
A A E V E E R T R K L Q Q Y R E M L I A D G I D P N E L L N S L A A V K S G T K A K R A Q R P
A K Y S Y V D E N G E T K T W T G Q G R T P A V I K K A M D E Q G K S L D D F L I K Q

>RECP02600 ***stpA*** - *Escherichia coli* 536, chromosome_2773901_2773500 (n=405)

GGACTGTAAATAGATTAAATTTTGTGGAAATATAATAAGTGATCGCTTACACTACGCG**A**CGAAATACTTTTTTGTTTTGGGTTAAAAGGTTTT
CTTTATT**ATG**TCCGTAATGTTACAAAGTTTAAATAACATTCGCACCCTCCGTGCGATGGCTCGCGAATTCTCCATTGACGTTCTTGAAGAAATG
CTCGAAAAATTCAGGGTTGTCACTAAAGAAAGACGTGAAGAAGAAGAACAACAGCAGCGTGAACTGGCAGAGCGCCAGGAAAAAATTAGCACCT
GGCTGGAGCTGATGAAAGCTGACGGAATTAACCCGGAAGAGTTATTGGGTAATAGCTCTGCTGCGGCACCACGCGCTGGTAAAAAACGCCAGCC
GCGTCCGGCGAAATATAAATTCATCGATGTTAACGGTGAAACTAAAACCTGGACCGGTCAGGGCCGTACACCGAAGCCAATCGCTCAGGCGCTG
GCAGAAGGTAAATCTCTCGACGATTTCCTGATC**TAA**TTACTGAGGCCGGATGTCGCTGCTATGGCGCGTCCGGCGTCGCTTCTCAAGCTCGTTG
GTTCCACGGCATCTTATCTAACAACCTTGCCATTCCACA

M S V M L Q S L N N I R T L R A M A R E F S I D V L E E M L E K F R V V T K E R R E E E E Q Q
Q R E L A E R Q E K I S T W L E L M K A D G I N P E E L L G N S S A A A P R A G K K R Q P R P
A K Y K F I D V N G E T K T W T G Q G R T P K P I A Q A L A E G K S L D D F L I

>RECP01911: ***hlp*** - *Escherichia coli* 536, chromosome_1966487_1966888 (n=405)

ACTATATTATTTACTGACTGTTTTTTTTTTTGATTTTTCCAACAGCACCGTAAGCATTATTTTTA**T**TAATCGCCTATTTTAAAACACCGGATG
ACATACT**ATG**AGTGAAGCTCTTAAGGCACTGAACAATATTCGTACACTTCGCGCACAGGCTCGTGAAACAGATCTGGCAACTCTGGAAGAGATG
CTGGAAAAACTCACCACAATCGTTGAAGATCGCCGTGAGGAAGAAAATTCAGCCCGTAAAGAACAAGAAGAACGTCAGGCTAAACTGGAAGCCT
TCCGCCAGAAATTGTTAGAAGACGGTATCGATCCTACAGAACTACTCGCTTCAGTTGGTTCATCCCAGCCTAAAACCAAATCAACTCGTGCTCC
TCGTCCTGCTAAATACAAATATACAGATGAAAACGGTAATGAGCAGACTTGGACGGGTCAGGGCCGTACTCCTAAAGCAATCGCCGCTGCTATC
GAAGCTGGTAAGACACTGGAAGACTTTGCTATC**TAA**CCGCTACAGCATATCCGGGCTTCACTGTTCTCAAGATAACAGGCCCGGAAAATATTCG
ATTATTCATCCAAGACTATCCCAGTCTGGCAGGTTGTTA

M S E A L K A L N N I R T L R A Q A R E T D L A T L E E M L E K L T T I V E D R R E E E E N S A
R K E Q E E R Q A K L E A F R Q K L L E D G I D P T E L L A S V G S S Q P K T K S T R A P R P
A K Y K Y T D E N G N E Q T W T G Q G R T P K A I A A A I E A G K T L E D F A I

8.3. Expression profile of hns *and* hns/stpA *mutants*

Data derived from expression profiling using both the *E. coli* K-12 Panorama-array and the *E. coli* pathoarray, sorted according to their level of upregulation compared to the wild type

Table 13. Top50 genes with upregulated expression in *hns* mutant

gene	Function	ratio[b]	Top 50 *hns/stpA*[c]
ompT	outer membrane protein 3b (porin)	29.67	++
III sfaA	S-fimbrial adhesin	27.31	++
hdeB	cons. hyp. protein	17.21	++
proV	glycine betaine/proline transport protein	16.72	++
hdeA	cons. protein with protein HNS-dependent expression A	16.57	++
yagY	cons. hyp. protein	13.68	++
yagZ	cons. hyp. protein	11.43	++
yahA	put. transcriptional repressor (LuxR/UhpA family)	9.80	+
I ORF1[a]	unknown	9.36	++
yicP	adenine deaminase	8.62	+
III sfaE[a]	S-fimbrial adhesin	8.48	++
yddC	redox cofactor for pyrroloquinoline quinone synthesis (cryptic in K-12)	7.86	
b1785	put. membrane protein	7.32	++
cadA	lysine decarboxylase 1	7.29	++
proX	glycine betaine/proline transport protein	7.15	+
b3060	put. transcriptional regulator (LysR family)	6.63	
III sfaB[a]	S-fimbrial adhesin	6.34	++
tnaA	tryptophan deaminase, PLP-dependent	6.33	
b1983	cons. protein with YebC-like domain	5.87	++
hlyD-I[a]	alpha-hemolysin	5.78	++
II 17-kDa[a]	unknown	5.74	++
yhaP	L-serine dehydratase 3, part 2, fuses with b3112, one orf	5.67	++
ydbA_1	split CDS, fragment 1	5.64	++
b2774	put. deoxygluconate dehydrogenase with NAD(P)-binding domain	5.56	
nmpC	DLP12 prophage; outer membrane porin	5.28	
ftn	cytoplasmic ferritin (iron storage protein)	5.21	
dapE	N-succinyl-diaminopimelate deacylase	5.17	+
ygiH	put. tRNA synthetase	5.16	
rplX	50S ribosomal subunit protein L24	5.08	
I ORF32[a]	unknown	4.82	++
b2877	cons. protein with nucleotide-diphospho-sugar transferase domain	4.79	
rpsU	30S ribosomal subunit protein S21	4.71	
hha	hemolysin expression modulator	4.70	
yjeJ	cons. protein	4.54	
cyoA	cytochrome o ubiquinol oxidase, subunit II	4.52	
treB	PTS family enzyme IIBC, trehalose(maltose)-specific	4.51	
rplM	50S ribosomal subunit protein L13	4.47	
stpA	DNA-bending protein with chaperone activity	4.44	
cyoB	cytochrome o ubiquinol oxidase, subunit I	4.30	
rpsO	30S ribosomal subunit protein S15	4.30	
ykgG	cons. hyp. protein	4.27	
cynS	cyanate aminohydrolase (cyanase)	4.25	+
b0294	put. transcriptional regulator	4.24	
17.3 kD[a]	unknown	4.23	+
b1673	put. aldehyde ferridoxin oxidoreductase	4.22	
ykgF	put. amino acid dehydrogenase with NAD(P)-binding and ferridoxin-like domain	4.22	
rpsT	30S ribosomal subunit protein S20	4.20	
glpT	sn-glycerol-3-phosphate transport protein (MFS family)	4.18	
rplU	50S ribosomal subunit protein L21	4.17	
ydiF	put. acetyl-CoA:acetoacetyl-CoA transferase	4.17	

[a] spotted on pathochip

[b] Ratio corresponds to spot intensity-mutant / spot intensity-wt

[c] A double plus indicates the presence of gene among the 50 most upregulated genes in the *hns/stpA* mutant; a single plus refers to the Top100 genes in this mutant

Table 14. Top50 genes with upregulated expression in *hns/stpA* mutant

gene	Function	ratio[b]	Top50 *hns*[c]
b2373	cons. hyp. protein with UBA-like domain	42.45	
b2374	unknown CDS	40.92	
b2372	cons. protein	38.76	
b2375	unknown CDS with UBA-like domain	28.43	
yciG	cons. hyp. protein	19.60	+
hdeB	cons. hyp. protein	19.02	++
b2371	put. peptidase with Zn-dependent exopeptidase domain	17.70	
asr	acid shock protein	16.67	
ydbA_1	split CDS, fragment 1	16.53	++
hdeA	cons. protein with protein HNS-dependent expression A	15.97	++
III sfaA[a]	S-fimbrial adhesin	12.64	++
I ORF32[a]	unknown	12.14	++
b1501	put. formate dehydrogenase, related to acid resistance	11.95	
ompT	outer membrane protein 3b (porin)	10.77	+
proV	glycine betaine/proline transport protein	10.77	+
I ORF1[a]	unkown	10.58	+
b0511	put. allantoin transport protein (NCS1 family)	10.14	+
b1983	cons. protein with YebC-like domain	10.09	++
yhaP	L-serine dehydratase 3	10.02	++
I ORF26[a]	unknown	9.41	
yagY	cons. hyp. protein	8.01	++
yciF	cons. protein	7.86	
III ORF22[a]	unknown	7.71	
hlyD I[a]	alpha-hemolysin	7.32	++
gadA	glutamate decarboxylase A, isozyme, PLP-dependent	7.15	
emrY	multidrug resistance protein Y (MFS family)	7.13	
b1504	put. fimbrial-like adhesin protein	6.47	
yhiE	put. transport protein (MFS family)	6.40	
III sfaE[a]	S-fimbrial adhesin	6.27	++
b2028	UDP-glucose 6-dehydrogenase	5.83	
appC	cytochrome oxidase bd-II, subunit I	5.81	
hlyB I[a]	alpha-hemolysin	5.44	+
gadB	glutamate decarboxylase, PLP-dependent, isozyme beta	5.44	
b1499	put. transcriptional regulator (AraC/XylS family)	5.35	
III sfaB[a]	S-fimbrial adhesin	5.24	++
III ORF23[a]	unknown	5.03	
b1785	put. membrane protein	5.01	++
b1388	put. subunit of multicomponent oxygenase,	4.96	
fimB	tyrosine recombinase, regulator of fimA	4.79	+
I ORF31	unknown	4.69	
cadA	lysine decarboxylase 1	4.68	++
yhhI	cons. protein, similar to H-repeat-associated proteins	4.55	
III sfaG	S-fimbrial adhesin	4.42	+
xasA	put. glutamate:gamma-aminobutyric acid antiporter (APC family)	4.37	
III sfaH	S-fimbrial adhesin	4.35	+
emrK	multidrug resistance protein K with single hybrid motif	4.02	
II 17-kDa	unknown	4.01	++
slp	outer membrane protein, induced after carbon starvation	4.01	
b0905	cons. hyp. protein	4.00	
yagZ	cons. hyp. protein	3.98	++

[a] spotted on pathochip

[b] Ratio corresponds to spot intensity-mutant / spot intensity-wt

[c] A double plus indicates the presence of gene among the 50 most upregulated genes in the *hns* mutant; a single plus refers to the Top100 genes in this mutant

Table 15: Top37 genes with downregulated expression in *hns* mutant

gene	Function	ratio[b]	Top37 *hns/stpA*[c]
fliC	flagellar biosynthesis; flagellin, filament structural protein	-12,61	++
flgG	flagellar biosynthesis; cell-distal portion of basal-body rod	-9,29	++
fliD	flagellar biosynthesis; filament capping protein, enables filament assembly	-8,12	++
flgN	flagellar biosynthesis; believed to be export chaperone for FlgK and FlgL	-7,74	++
flgK	flagellar biosynthesis; hook-filament junction protein 1	-7,65	++
tsr	methyl-accepting chemotaxis protein I, serine sensor receptor	-5,48	++
cheW	purine-binding chemotaxis protein; regulation	-5,19	++
cheA	chemotactic sensory histidine kinase (soluble) in two-component regulatory system	-5,09	++
flgF	flagellar biosynthesis; cell-proximal portion of basal-body rod	-5,07	++
flgJ	flagellar biosynthesis	-3,96	++
flgM	anti-FliA (anti-sigma) factor; also known as RflB protein	-3,80	++
tar	methyl-accepting chemotaxis protein II, aspartate sensor receptor	-3,68	++
fliK	flagellar hook-length control protein	-3,33	++
flgC	flagellar biosynthesis; cell-proximal portion of basal-body rod	-3,15	+
motA	proton conductor component of motor, torque generator	-2,87	++
yhjH	conserved protein	-2,75	++
fliG	flagellar biosynthesis; component of motor switching and energizing	-2,61	++
fliA	sigma F (sigma 28) factor of RNA polymerase, transcription of late flagellar genes	-2,57	+
cheY	chemotactic response regulator in two-component regulatory system with CheA	-2,49	++
fliT	flagellar biosynthesis; putative export chaperone for FliD	-2,47	++
fliM	flagellar biosynthesis; component of motor switch and energizing	-2,41	+
fliZ	putative regulator of FliA	-2,34	+
motB	enables flagellar motor rotation, linking torque machinery to cell wall	-2,29	+
fliI	flagellum-specific ATP synthase	-2,29	+
flgL	flagellar biosynthesis; hook-filament junction protein	-2,25	++
ExPEC sap[a]	autotranporter	-2,21	
flgI	putative flagella basal body protein	-2,10	+
flgD	flagellar biosynthesis; initiation of hook assembly	-2,08	++
cheZ	chemotactic response, CheY protein phophatase	-2,00	++
III ORF28[a]	unknown	-1,93	
mviN	putative virulence factor	-1,87	
air	aerotaxis sensor receptor, senses cellular redox state or proton motive force	-1,83	
guaC	GMP reductase	-1,69	+
fliH	flagellar biosynthesis; putative export of flagellar proteins	-1,69	
flhD	transcriptional regulator of flagellar class II biosynthesis	-1,64	+
flgA	flagellar biosynthesis; assembly of basal-body periplasmic P ring	-1,56	
flgE	flagellar biosynthesis; hook protein	-1,26	++

[a] spotted on pathochip

[b] Ratio corresponds to spot intensity-mutant / spot intensity-wt

[c] A double plus indicates the presence of gene among the 37 most downregulated genes in the *hns/stpA* mutant; a single plus refers to the Top100 genes in this mutant

Table 16. Top37 with downregulated expression in *hns/stpA* mutant

gene	Function	ratio[b]	Top37 *hns*[c]
flgE	flagellar biosynthesis; hook protein	-9,32	++
fliC	flagellar biosynthesis; flagellin, filament structural protein	-9,25	++
flgG	flagellar biosynthesis; cell-distal portion of basal-body rod	-7,29	++
fliD	flagellar biosynthesis; filament capping protein, enables filament assembly	-6,33	++
flgK	flagellar biosynthesis; hook-filament junction protein 1	-5,20	++
flgN	flagellar biosynthesis; believed to be export chaperone for FlgK and FlgL	-5,02	++
tsr	methyl-accepting chemotaxis protein I, serine sensor receptor	-4,85	++
cheA	chemotactic sensory histidine kinase (soluble) in two-component regulatory system	-4,03	++
lamB	maltoporin, high-affinity receptor for maltose; phage lambda receptor	-3,72	
cheW	purine-binding chemotaxis protein; regulation	-3,50	++
frdA	fumarate reductase, anaerobic, catalytic and NAD/flavoprotein subunit	-3,23	
nirB	nitrite reductase, large subunit, nucleotide-binding	-3,05	
flgF	flagellar biosynthesis; cell-proximal portion of basal-body rod	-3,05	++
tar	methyl-accepting chemotaxis protein II, aspartate sensor receptor	-3,02	++
yhjH	conserved protein	-3,01	
flgJ	flagellar biosynthesis	-2,82	++
glnH	high-affinity glutamine transport protein (ABC superfamily, peri_bind)	-2,80	
flgD	flagellar biosynthesis; initiation of hook assembly	-2,60	++
frdB	fumarate reductase, anaerobic, Fe-S subunit	-2,56	
flgL	flagellar biosynthesis; hook-filament junction protein	-2,49	++
glnA	glutamine synthetase	-2,47	
flgM	anti-FliA (anti-sigma) factor; also known as RflB protein	-2,44	++
motA	proton conductor component of motor, torque generator	-2,40	++
fliK	flagellar hook-length control protein	-2,40	++
nikA	nickel transport protein (ABC superfamily, peri_bind)	-2,24	
ptsI	PTS family enzyme I and Hpr components, PEP-protein phosphotransferase	-2,12	
pfkA	6-phosphofructokinase I	-2,05	
manX	PTS family enzyme IIA (N-terminal); enzyme IIB (C-terminal), mannose-specific	-2,03	
cheY	chemotactic response regulator in two-component regulatory system with CheA	-2,02	++
narG	nitrate reductase 1, alpha subunit	-2,00	
cheZ	chemotactic response, CheY protein phophatase	-2,00	++
malM	periplasmic protein of mal regulon	-2,00	
yibO	phosphoglycerate mutase III, cofactor-independent	-1,99	
fliG	flagellar biosynthesis; component of motor switching and energizing	-1,94	++
fliT	flagellar biosynthesis; putative export chaperone for FliD	-1,93	++
narH	nitrate reductase 1, Fe-S (beta) subunit	-1,91	
dmsA	anaerobic dimethyl sulfoxide (DMSO) reductase, subunit A	-1,87	

[a] spotted on pathochip

[b] Ratio corresponds to spot intensity-mutant / spot intensity-wt

[c] A double plus indicates the presence of gene among the 37 most downregulated genes in the *hns* mutant; a single plus refers to the Top100 genes in this mutant

Table 17: The 50 most abundant transcripts in wild type UPEC strain 536 from mid-log LB cultures. Average signal intensities were calculated from 12 data sets (4 wild type co-hybridizations per mutant; 3 mutants) and sorted in decreasing order. The position of each gene within the top-50 list of the three mutants is indicated in the list (bold: among top-50 genes, normal: among top-100 genes; na: not among top-100 genes).

#	gene name	gene description	functional group	signal intensities	rel. SD	# in *hns*	# in *hns/stpA*	# in *stpA*
1	*rpsD*	30S ribosomal subunit protein S4	14	950	0.57	**1**	**2**	**1**
2	*ompC*	outer membrane protein C precursor	4	757	0.54	**9**	**9**	**2**
3	*tufA*	elongation factor EF-Tu	14	689	0.56	**2**	**11**	**3**
4	*rpsA*	30S ribosomal protein S1	14	531	0.31	**4**	**6**	**4**
5	*tufB*	elongation factor EF-Tu (duplicate gene)	14	500	0.28	**7**	**20**	**5**
6	*rplF*	50S ribosomal subunit protein L6	14	439	0.59	**5**	**14**	**8**
7	*sucA*	2-oxoglutarate dehydrogenase E1 component	5	430	0.45	**13**	**7**	**6**
8	*prlA*	preprotein translocase secy subunit	12	422	0.51	**6**	**12**	**10**
9	*fusA*	elongation factor EF-G	14	410	0.42	**8**	**17**	**7**
10	*rplL*	50S ribosomal subunit protein L7/L12	14	337	0.06	**37**	**33**	**9**
11	*slyD*	fkbP-type peptidyl-prolyl cis-trans isomerase	14	337	0.44	**23**	**32**	**11**
12	*trmD*	tRNA(guanine-7)methyltransferase	14	307	0.51	**15**	**37**	**25**
13	*rplC*	50S ribosomal subunit protein L3	14	302	0.59	**10**	**23**	**17**
14	*tsf*	elongation factor Ts	14	291	0.46	**20**	51	**14**
15	*narG*	respiratory nitrate reductase 1 alpha chain	5	290	0.71	51	na	**22**
16	*rpsS*	30S ribosomal subunit protein S19	14	287	0.51	**11**	**36**	**18**
17	*rplB*	50S ribosomal subunit protein L2	14	285	0.44	**16**	**35**	**26**
18	*fdoG*	formate dehydrogenase-O alpha subunit	5	270	0.49	**29**	**48**	**24**
19	*kdgK*	2-dehydro-3-deoxygluconokinase	1	267	0.18	na	**13**	**19**
20	*cspC*	cold shock-like protein CspC	10	253	0.40	**14**	**10**	**12**
21	*sodA*	manganese superoxide dismutase	3	252	0.57	**22**	92	**38**
22	*nuoE*	NADH dehydrogenase I chain E	5	251	0.36	**25**	**34**	**21**
23	*nrdD*	anaerobic ribonucleoside-triphosphate reductase	9	242	0.24	54	**28**	**13**
24	*rplV*	50S ribosomal subunit protein L22	14	241	0.34	**35**	54	**16**
25	*rpmI*	50S ribosomal subunit protein L35	14	235	0.59	**12**	**16**	**34**
26	*sucB*	dihydrolipoamide succinyltransferase component	5	230	0.41	**50**	**40**	**31**
27	*fabB*	3-oxoacyl-[acyl-carrier-protein] synthase I	6	228	0.29	65	59	**15**
28	*rpoA*	RNA polymerase, alpha subunit	13	228	0.44	**17**	**43**	**29**
29	*hlpA*	histone-like protein Hlp-1 precursor	4	227	0.29	56	**44**	**28**
30	*cspA*	cold shock protein CspA	3	218	0.74	**18**	**18**	**32**
31	*yghJ*	putative lipoprotein (b2974)	11	218	0.31	97	**38**	**27**
32	*nlpD*	lipoprotein NlpD precursor	8	215	0.23	58	**41**	**23**
33	*thrS*	threonyl-tRNA synthetase	14	214	0.45	**40**	**46**	**30**
34	*rnr*	RNase R (VacB)	7	214	0.44	80	53	**20**
35	*narH*	respiratory nitrate reductase 1 beta chain	5	211	0.60	98	na	**36**
36	*rplO*	50S ribosomal subunit protein L15	14	210	0.70	**19**	58	**35**
37	*rpsB*	30S ribosomal protein S2	14	207	0.64	**24**	81	52
38	*lpdA*	dihydrolipoamide dehydrogenase	5	201	0.31	**33**	**24**	**33**
39	*ompA*	outer membrane protein A	4	197	0.76	**45**	62	64
40	*rpoB*	DNA-directed RNA polymerase, beta-subunit	13	186	0.38	**42**	60	**41**
41	*lamB*	phage lambda receptor protein	15	182	0.58	61	na	**47**
42	*cpsG*	phosphomannomutase	2	179	0.57	**26**	**19**	**37**
43	*pflB*	formate acetyltransferase 1	5	177	0.58	**34**	63	56
44	*rplQ*	50S ribosomal subunit protein L17	14	174	0.56	**31**	74	60
45	*cyoC*	cytochrome o ubiquinol oxidase subunit III	5	170	0.39	**45**	**42**	**44**
46	*atpA*	ATP synthase F1 alpha subunit	5	169	0.51	**32**	70	**40**
47	*sucD*	succinyl-coA synthetase alpha chain	5	164	0.35	**49**	57	53
48	*radC*	DNA repair protein radc	3	164	0.71	**30**	**25**	59
49	*fdoH*	formate dehydrogenase-O beta subunit	5	163	0.37	72	79	**50**
50	*infC*	initiation factor IF-3	14	163	0.51	**47**	52	**43**

Functional groups: 1 Carbon compound catabolism; 2 Cell processes (incl. adaptation, protection); 3 Cell structure; 4 Central intermediary metabolism; 5 Energy metabolism; 6 Fatty acid and phospholipid metabolism; 7 Hypothetical, unclassified, unknown; 8 Membrane proteins, 9 Nucleotide biosynthesis and metabolism, 10 Other known genes, 11 Putative enzyme; 12 Putative transport proteins; 13 Transcription, RNA processing and degradation; 14 Translation, post-translational modification, 15 Transport and binding proteins.

8.4. Expression ratios of major virulence-associated genes

Expression ratios of *hns* and *hns/stpA* mutants relative to expression in the wild type.
ns = not significant; na = not available; FDR = false discovery rate

Table 18: Significantly deregulated genes involved in motility and chemotaxis

gene name	gene description	ratio *hns*	FDR	ratio *hns/stpA*	FDR
cheA	sensory histidine kinase in two-component regulatory system	-5,09	*3,35*	-4,03	*0,43*
cheW	purine-binding chemotaxis protein; regulation	-5,19	*3,35*	-3,50	*0,43*
cheY	response regulator in two-component regulatory system with CheA	-2,49	*3,35*	-2,02	*0,43*
cheZ	chemotactic response, CheY protein phophatase	-2,00	*6,14*	-2,00	*0,43*
flgA	flagellar biosynthesis; assembly of basal-body periplasmic P ring	-1,56	*na*	ns	*na*
flgC	flagellar biosynthesis; cell-proximal portion of basal-body rod	-3,15	*3,35*	-1,70	*0,21*
flgD	flagellar biosynthesis; initiation of hook assembly	-2,08	*3,35*	-2,60	*0,43*
flgE	flagellar biosynthesis; hook protein	-1,26	*3,35*	-9,32	*0,43*
flgF	flagellar biosynthesis; cell-proximal portion of basal-body rod	-5,07	*3,35*	-3,05	*0,43*
flgG	flagellar biosynthesis; cell-distal portion of basal-body rod	-9,29	*3,35*	-7,29	*0,43*
flgI	putative flagella basal body protein	-2,10	*3,35*	-1,56	*0,21*
flgJ	flagellar biosynthesis	-3,96	*3,35*	-2,82	*0,43*
flgK	flagellar biosynthesis; hook-filament junction protein 1	-7,65	*3,35*	-5,20	*0,43*
flgL	flagellar biosynthesis; hook-filament junction protein	-2,25	*3,35*	-2,49	*0,43*
flgM	anti-FliA (anti-sigma) factor; also known as RflB protein	-3,80	*3,35*	-2,44	*0,43*
flgN	flagellar biosynthesis; export chaperone for FlgK and FlgL	-7,74	*3,35*	-5,02	*0,43*
flhD	transcriptional regulator of flagellar class II biosynthesis,	-1,64	*na*	-1,55	*0,21*
fliA	sigma F (sigma 28) factor of RNA polymerase	-2,57	*3,35*	-1,76	*0,21*
fliC	flagellar biosynthesis; flagellin, filament structural protein	-12,61	*3,35*	-9,25	*0,43*
fliD	flagellar biosynthesis; filament capping protein	-8,12	*3,35*	-6,33	*0,43*
fliF	flagellar biosynthesis; basal-body MS-ring and collar protein	4,21	*3,35*	2,05	*0,43*
fliG	flagellar biosynthesis; motor switching and energizing	-2,61	*3,35*	-1,94	*na*
fliI	flagellum-specific ATP synthase	-2,29	*3,35*	-1,78	*0,21*
fliK	flagellar hook-length control protein	-3,33	*3,35*	-2,40	*0,43*
fliM	flagellar biosynthesis; component of motor switch and energizing	-2,41	*3,35*	-1,85	*na*
fliS	flagellar biosynthesis; repressor of class 3a and 3b operons	ns	*na*	-1,61	*0,62*
fliT	flagellar biosynthesis; putative export chaperone for FliD	-2,47	*3,35*	-1,93	*0,21*
fliZ	putative regulator of FliA	-2,34	*3,35*	-1,59	*1,10*
motA	proton conductor component of motor, torque generator	-2,87	*3,35*	-2,40	*0,43*
motB	enables flagellar motor rotation	-2,29	*3,35*	-1,77	*2,07*
tar	methyl-accepting chemotaxis protein II, aspartate sensor receptor	-3,68	*3,35*	-3,02	*0,43*
tsr	methyl-accepting chemotaxis protein I, serine sensor receptor	-5,48	*3,35*	-4,85	*0,43*

Table 19: Significantly deregulated genes of hemolysin operon

gene name	gene description	ratio *hns*	FDR	ratio *hns/stpA*	FDR
hlyC	I ORF39	2,60	*2,32*	1,99	*na*
hlyD	I ORF40	5,78	*2,32*	7,32	*1,67*
hlyA		ns	*na*	ns	*na*
hlyB	I ORF41	4,04	*2,32*	5,44	*1,67*

Table 20: Significantly deregulated genes involved in iron uptake

gene name	gene description	ratio *hns*	FDR	ratio *hns/stpA*	FDR
iroN	III orf27; salmochelin receptor	3,40	*2,32*	3,54	*1,67*
IV ybtQ	yersiniabactin; transporter	1,74	*na*	1,98	*na*
IV ybtS	yersiniabactin	2,08	*2,32*	2,51	*1,67*
IV ybtX	yersiniabactin	2,09	*2,32*	2,39	*na*
fhuA	= *tonA*; ferrichrome receptor	2,18	*9,44*	1,54	*0,21*
tonB	energy transducer; uptake of iron, cyanocobalimin; sensitivity to phages, colicins	2,42	*3,35*	ns	*na*

Table 21: Significantly deregulated genes involved in adhesion

gene name	gene description	ratio *hns*	FDR	ratio *hns/stpA*	FDR
Type 1 fimbriae					
fimB	tyrosine recombinase, regulator of fimA	3,59	*3,35*	4,79	*0,43*
fimE	tyrosine recombinase, regulator of fimA	2,05	*3,35*	2,05	*0,43*
S-fimbrial adhesin					
sfaA	III orf19	27,31	*2,32*	12,64	*1,67*
sfaB	III orf18	6,34	*2,32*	5,24	*1,67*
sfaC	III orf17	1,66	*na*	2,45	*1,67*
sfaD	III orf20	2,58	*2,32*	2,29	*1,67*
sfaE	III orf21	8,48	*2,32*	6,27	*1,67*
sfaF	III orf22	3,50	*2,32*	3,54	*1,67*
sfaG	III orf23	3,79	*2,32*	4,42	*1,67*
sfaH	III orf25	3,62	*2,32*	4,35	*1,67*
sfaS	III orf24	3,05	*2,32*	2,80	*1,67*
P-related fimbriae					
prfX	II orf6	5,74	*2,32*	4,01	*1,67*
curli adhesin					
csgD	putative transcriptional regulator in curly assembly/transport,	2,14	*3,35*	1,76	*0,21*
putative adhesins					
I ORF26	putative CS12 fimbria-like major fimbrial protein subunit	2,08	*2,32*	9,41	*1,67*
I ORF29	FasD-like protein	1,63	*na*	2,61	*1,67*
I ORF30	FasE-like protein	1,62	*na*	3,39	*1,67*
I ORF31	FasF-like protein	2,59	*2,32*	4,69	*1,67*
I ORF32	FasG-like protein	4,82	*2,32*	12,14	*1,67*
I ORF6	putative F17-like fimbril adhesin subunit	3,11	*2,32*	2,56	*1,67*
II yjhW	= *hek*; involved in adhesion	ns	*na*	2,07	*1,67*
ydeS	putative fimbrial-like adhesin protein	ns	*na*	6,47	*0,43*
yehA	putative fimbrial-like adhesin protein	ns	*na*	2,28	*0,43*

Table 22: Significantly deregulated genes involved in generegulation

gene name	gene description	ratio *hns*	FDR	ratio *hns/stpA*	FDR
phoP	response regulator in two-component regulatory system with PhoQ, regulates gene expression at low [Mg+] (OmpR family)	2,20	*3,35*	2,15	*0,43*
phoQ	sensory histidine kinase in two-component regulatory system with PhoP, regulates gene expression at low [Mg+], senses Mg+	2,11	*3,46*	2,13	*0,43*
dpiA	response regulator in two-component regulatory system with DpiB, regulation of citrate fermentation and plasmid inheritance	ns	*na*	1,98	*0,21*
dpiB	sensory histidine kinase in two-component regulatory system with DpiA; senses citrate; OmpR-family	2,85	*3,35*	2,16	*0,43*
yahA	putative transcriptional repressor (LuxR/UhpA family)	9,80	*3,35*	3,41	*0,43*
yedV	putative sensory kinase in regulatory system	2,32	*3,35*	ns	*na*
yedW	putative response regulator in two-component regulatory system (OmpR family)	3,82	*3,35*	2,21	*0,43*
ygbI	putative transcriptional repressor with DNA-binding Winged helix domain (DeoR family)	2,33	*3,35*	2,03	*0,21*
ygeV	putative transcriptional regulator protein with GAF, PYP-like sensor, NTP hydrolysis, and FIS-like domains	2,81	*3,35*	ns	*na*
ygiP	putative transcriptional regulator with periplasmic binding protein domain (LysR family)	6,63	*3,35*	1,14	*na*
yidL	putative transcriptional regulator with homeodomain-like DNA binding domain (AraC/XylS family)	2,45	*3,35*	1,51	*0,21*
ykgK	putative transcriptional regulator	4,24	*3,35*	1,89	*0,21*

Table 23: Significantly deregulated genes involved in resistance/adaptation

gene name	gene description	ratio *hns*	FDR	ratio *hns/stpA*	FDR
low pH resistance					
asr	acid shock protein	2,19	*3,35*	16,67	*0,43*
gadA	glutamate decarboxylase A	2,27	*3,35*	7,15	*0,43*
gadB	glutamate decarboxylase	1,97	*na*	5,44	*0,43*
gadC	= *xasA*; glutamate:GABA ntiporter	ns	*na*	4,37	*0,43*
cadA	lysine decarboxylase 1	7,29	*3,35*	4,68	*0,43*
cadB	lysine/cadaverine transport protein	2,78	*3,35*	1,75	*na*
hdeA	acid chaperone	16,57	*3,35*	15,97	*0,43*
hdeB	acid chaperone	17,21	*3,35*	19,02	*0,43*
yhiQ	putative proteins encoded on 15kb „acid cluster“	2,08	*3,35*	ns	*na*
yhiD	putative proteins encoded on 15kb „acid cluster“	2,34	*3,35*	2,38	*0,43*
yhjH	putative proteins encoded on 15kb „acid cluster“	-2,75	*3,35*	-3,01	*0,43*
yhjJ	putative proteins encoded on 15kb „acid cluster“	3,37	*3,35*	ns	*na*
yhjK	putative proteins encoded on 15kb „acid cluster“	2,41	*3,35*	ns	*na*
yhjL	putative proteins encoded on 15kb „acid cluster“	2,76	*3,35*	ns	*na*
yhiM	putative proteins encoded on 15kb „acid cluster“	2,22	*3,35*	ns	*na*
gadE	= *yhjE*; activator	2,50	*3,35*	6,40	*0,43*
gadX	= *yhjX*; activator of *gadAB*	3,14	*3,35*	3,81	*0,43*
multidrug resistance					
mdtE	multidrug resistance protein	ns	*na*	1,80	*0,21*
mdtF	putative transport protein; multidrug resistance	ns	*na*	2,31	*0,43*
emrK	multidrug resistance protein K	ns	*na*	4,02	*0,43*
emrY	multidrug resistance protein Y	2,23	*3,35*	7,13	*0,43*
evgA	response regulator in two-component regulatory system for multidrug resistance	ns	*na*	1,61	*0,21*
evgS	sensory histidine kinase in two-component regulatory system for multidrug resistance	ns	*na*	2,36	*0,43*
osmoprotection					
proV	glycine betaine/proline transport protein	16,72	*3,35*	10,77	*0,43*
proW	glycine betaine/proline transport protein (ABC superfamily)	3,30	*3,35*	1,77	*0,21*
proX	glycine betaine/proline transport protein (ABC superfamily)	7,15	*3,35*	2,86	*0,43*
osmC	resistance protein, osmotically inducible	ns	*na*	1,79	*0,21*
osmB	lipoprotein, osmotically inducible	ns	*na*	1,71	*0,21*
osmY	hyperosmotically inducible periplasmic protein	2,01	*3,35*	1,56	*0,21*
danK	chaperone Hsp70; osmoprotection	2,64	*3,35*	2,18	*0,43*
dnaJ	heat shock protein (Hsp40), co-chaperone with DnaK	2,33	*3,35*	2,09	*0,43*
mdoB	periplasmic glucans biosynthesis protein	2,07	*3,35*	ns	*na*
mdoG	periplasmic glucans biosynthesis protein	2,07	*3,35*	ns	*na*
mdoH	periplasmic glucans biosynthesis protein	2,07	*3,35*	ns	*na*
tufA	protein chain elongation factor EF-Tu	2,11	*3,40*	ns	*na*
tufB	protein chain elongation factor EF-Tu	2,21	*3,72*	ns	*na*
ydcG	putative enzyme invlved in osmoprotection	2,89	*3,35*	1,68	*0,21*
betI	transcriptional repressor for the cellular response to osmotic stress	ns	*na*	1,64	*0,21*

Table 24: Significantly deregulated genes involved in synthesis of extracellular components

gene name	gene description	ratio *hns*	FDR	ratio *hns/stpA*	FDR
Cellulose					
yaiC	putative membrane protein	2,09	*3,35*	ns	*na*
bcsA	cellulose synthase, catalytic subunit	2,81	*3,35*	ns	*na*
bcsC	= *yhjL*; putative cellulose synthase with tetratricopeptide repeats	2,76	*3,35*	ns	*na*
M-antigen (colanic acid)					
cpsB	= *manC*; mannose-1-phosphate guanyltransferase	2,44	*3,35*	3,42	*0,43*
cpsG	= *manB*; phosphomannomutase	2,95	*3,35*	1,95	*0,21*
wcaE	putative transferase, colanic acid synthesis, with nucleotide-diphospho-sugar transferase domain	ns	*na*	2,36	*0,43*
wcaJ	putative UDP-glucose lipid carrier transferase	1,84	*na*	2,14	*0,43*
yefA	= *gmd*; GDP-D-mannose dehydratase	2,62	*3,35*	3,21	*0,43*
yefB	= *fcl*; bifunctional GDP-fucose synthetase;	2,54	*3,35*	2,79	*0,43*
yefC	= *wcaH*; GDP-mannose mannosyl hydrolase	ns	*na*	1,78	*0,21*
ugd	UDP-glucose 6-dehydrogenase	3,13	*3,35*	5,83	*0,43*
galU	UDP-glucose synthesis; TolC export	2,90	*3,35*	ns	*na*
galF	putative glucose-1-phosphate uridylyltransferase	2,78	*3,35*	ns	*na*
Lipopolysaccharide (LPS)					
cld	= *wzz*; regulator of length of O-antigen component of LPS chains	3,89	*3,35*	1,82	*0,21*
crcA	= *ybeG, pagP*; palmitoyl transferase for Lipid A	2,72	*3,35*	2,36	*0,43*
lpxD	UDP-3-O-(3-hydroxymyristoyl)-glucosamine N-acyltransferase	2,57	*3,35*	ns	*na*
tolA	required for outer membrane integrity, uptake of group A colicins, translocation of filamenous phage DNA to cytoplasm, role in surface expression of O-antigen	2,04	*3,35*	1,82	*0,71*
lpxP	palmitoleoyl-acyl carrier protein (ACP)-dependent acyltransferase, LPS modification, cold-induced gene	ns	*na*	1,50	*2,07*
K15 capsular polysaccharide					
kpsF	PAI V-region1	2,33	*2,32*	2,78	*1,67*
kpsE	PAI V-region1	2,38	*2,32*	2,66	*1,67*
kpsD	PAI V-region1	2,28	*2,32*	2,30	*1,67*
kpsU	PAI V-region1	1,82	*na*	1,90	*na*
kpsC	PAI V-region1	1,64	*na*	1,50	*na*
kpsS5	PAI V-region1	1,38	*na*	1,33	*na*
kpsS10	PAI V-region1	1,29	*na*	1,23	*na*
kpsT	PAI V-region3	ns	*na*	ns	*na*
kpsM	PAI V-region3	1,85	*na*	1,88	*na*
ORF1	PAI V-region2	1,36	*na*	1,22	*na*
ORF2	PAI V-region2	1,31	*na*	1,17	*na*
ORF3	PAI V-region2	1,29	*na*	1,10	*na*
ORF4	PAI V-region2	1,54	*na*	0,95	*na*
ORF5	PAI V-region2	1,94	*na*	2,61	*1,67*

8.5. Supplementary material (tables and figures)

More tables and figures such as more AFM micrographs, growth curves, and plasmid maps are following in this section.

Table 25: *E. coli* strains used for PCR screening and detailed results on the occurrence of the *hlp* gene.

Strain	Serotype	Group	*hlp*	Strain	Serotype	Group	*hlp*
536	O6:K15:H31	UPEC	+	764	O18:K5:H5/11	Faecal	+
CFT073	O6:K2:H1	UPEC	+	20A1	na	Faecal	+
RZ422	O6:K14:H-	UPEC	+	20A2	na	Faecal	+
RZ451	O6:K+:H31	UPEC	+	3D5	na	Faecal	-
RZ479	O6:K+:H-	UPEC	+	13A1	na	Faecal	-
RZ505	O6:K14:H-	UPEC	+	1H1	na	Faecal	+
RZ532	O6:K-:H31	UPEC	+	19A1	na	Faecal	+
RZ454	O6:K2:H-	UPEC	-	1G1	na	Faecal	-
J96	O4:K:H5	UPEC	+	8B1	na	Faecal	-
AD110	na	UPEC	+	AE5	na	Faecal	-
2980	O18ac:K5	UPEC	+	2A1	na	Faecal	+
E-B35	na	UPEC	+	2A2	na	Faecal	+
7521/94-1	na	UPEC	+	3B5	na	Faecal	+
RZ-439	O6:K5:H1	UPEC	+	3N5	na	Faecal	-
RZ-441	O6:K5:H1	UPEC	+	5A1	na	Faecal	-
RZ-443	O6:K5:H-	UPEC	+	8B2	na	Faecal	+
RZ-446	O6:K53:H1	UPEC	+	8F4	na	Faecal	-
RZ-468	O6:K5:H1	UPEC	+	16A3	na	Faecal	-
RZ-475	O6:K5:H1	UPEC	+	16B1	na	Faecal	-
RZ-495	O6:K5:H-	UPEC	+	19B1	na	Faecal	-
RZ-500	O6:K5:H1	UPEC	+	DSM6601	na	Faecal	+
RZ-525	O6:K5:H1	UPEC	+	EcoR-53	na	Faecal	+
RZ-526	O6:K5:H1	UPEC	+	EcoR-57	na	Faecal	+
EcoR-60	na	UPEC	+	EcoR-58	na	Faecal	+
4405/1	na	UPEC	-	EcoR-63	na	Faecal	+
S5	na	UPEC	-	EcoR-65	na	Faecal	-
EcoR62	na	UPEC	-	EcoR66	na	Faecal	-
EcoR50	na	UPEC	+	EcoR7	na	Faecal	-
RZ411	O6:K-:H1	UPEC	+	F18	na	Faecal	+
20A1U	na	UPEC	+	EcoR61	na	Faecal	-
22B2U	na	UPEC	+	EcoR-1	na	Faecal	-
1G1U	na	UPEC	+	EcoR-23	na	Faecal	-
1H1U	na	UPEC	+	EcoR-25	na	Faecal	-
2E1U	na	UPEC	-	EcoR-28	na	Faecal	-
16A2U	na	UPEC	+	EcoR-32	na	Faecal	-
5A1U	na	UPEC	-	EcoR-42	na	Faecal	-
A284	na	UPEC	+	EcoR-55	na	Faecal	-
EcoR-40	na	UPEC	-	EcoR-59	na	Faecal	-
EcoR-48	na	UPEC	-	E2348/69	O127:H6	EPEC	-
EcoR-56	na	UPEC	+	179/2	na	EPEC	-
EcoR-71	na	UPEC	-	156A	na	EPEC	-
BK658	na	NBM	+	37-4	na	EPEC	-
IHE3034	O18:K1:H7/9	NBM	-	933W	na	EHEC	-
IHE3036	na	NBM	-	86-24	na	EHEC	-
IHE3080	na	NBM	-	SF493/89	O157:H$^-$	EHEC	-
RS226	na	NBM	-	3574/92	na	EHEC	-
B13155	na	NBM	-	2907/97	na	EHEC	-
Ve1140	na	NBM	-	5720/96	na	EHEC	-
B10363	na	NBM(blood sample)	-	3697/97	na	EHEC	-
RS176	na	NBM	-	ED142	na	EHEC	-
Ve239	na	NBM	-	PIG E57	na	EHEC	-
HK8	na	Sepsis	+	2-45	na	EHEC	-
HK24	na	Sepsis	+	EDL 880	na	EHEC	-
AC/I	na	Avian Sepsis	-	5714/96	na	EHEC	-
E642	na	Sepsis	+	189	na	AAEC	-
HK54	na	Sepsis	-	DPA065	na	EAEC	-
B616	na	Sepsis	-	5477/94	na	EAEC	-
HK2	na	Sepsis	-	17-2	na	EAEC	-
HK1	na	Sepsis	-	042	na	EAEC	+
HK58	na	Sepsis	-	O149:K88	na	ETEC	-
E457	na	Sepsis	+	C9221a	O6:K15:H16	ETEC	-
HK4	na	Sepsis	+	258909-3	na	ETEC	-
HK17	na	Sepsis	-	H10407	na	ETEC	-
HK19	na	Sepsis	-	EDL-1284	O124:H$^-$	EIEC	-
HK25	na	Sepsis	-	76-5	na	EIEC	-
RB9	na	Sepsis	-	MG1655	OR:H48:K-	K-12	-

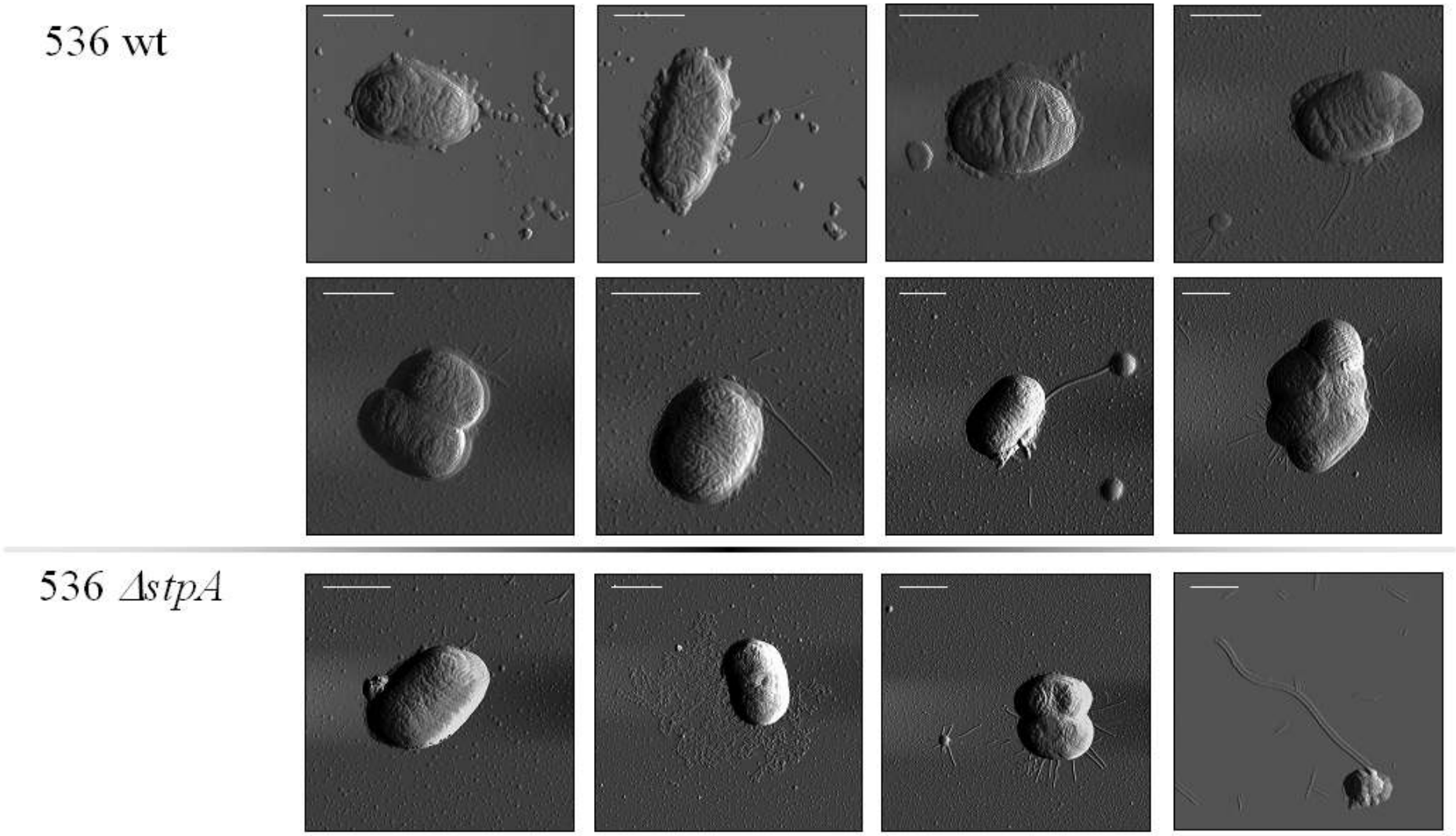

Fig. 51: Cell morphology of UPEC strain 536 and isogenic mutants visualized by AFM in tapping mode. (Bars represent 1 µm in length)

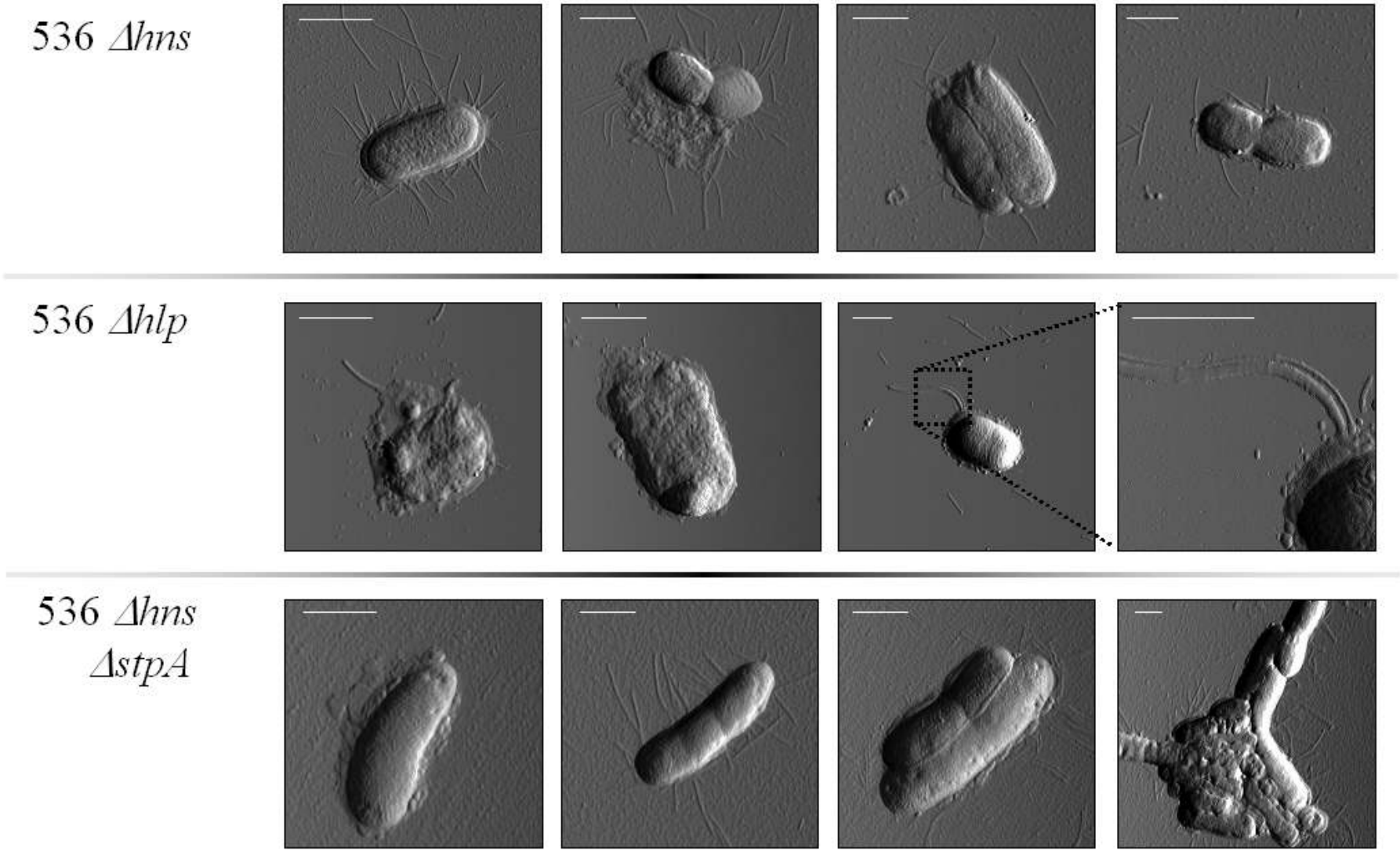

Fig. 51 – continued

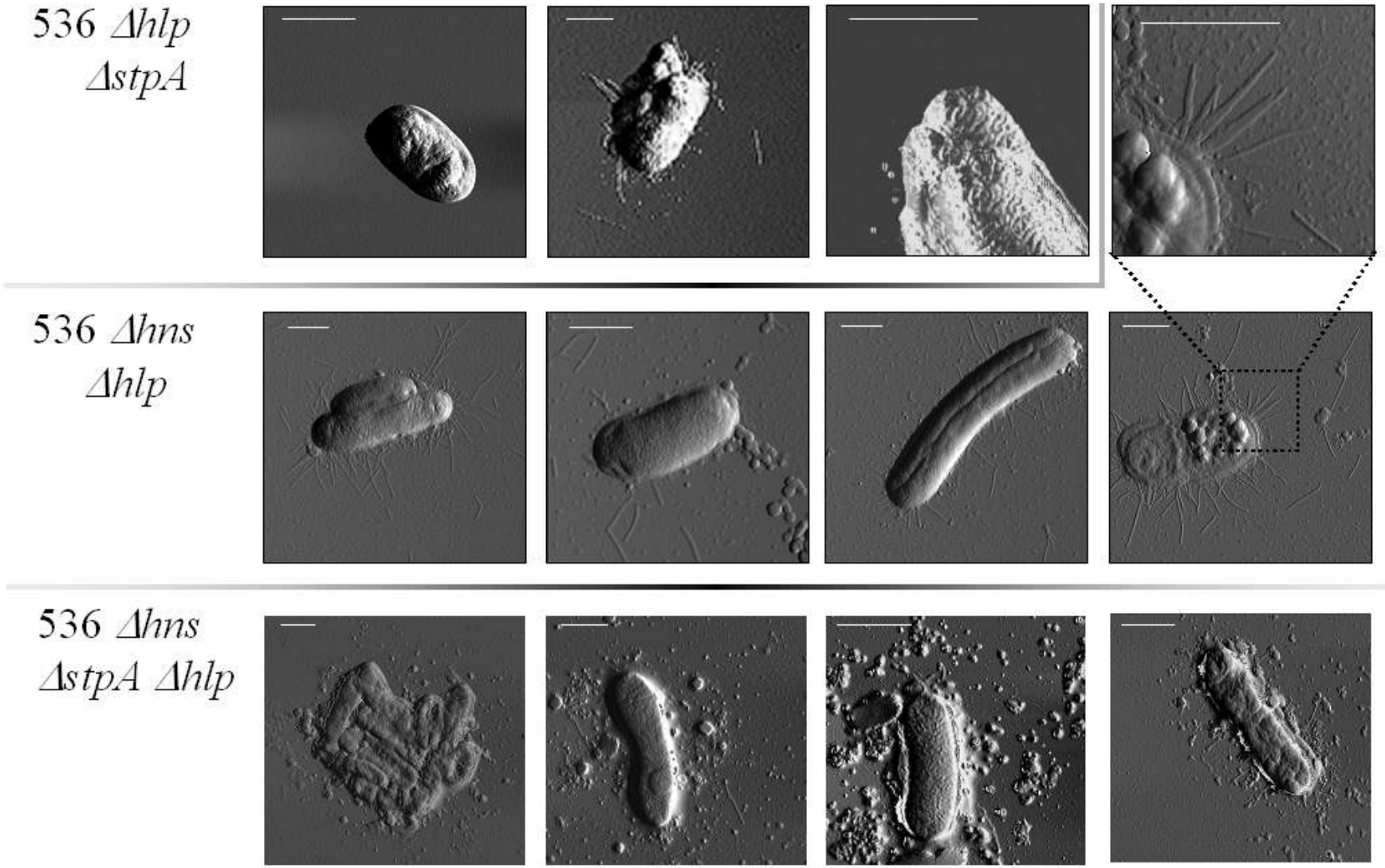

Fig. 51 - continued

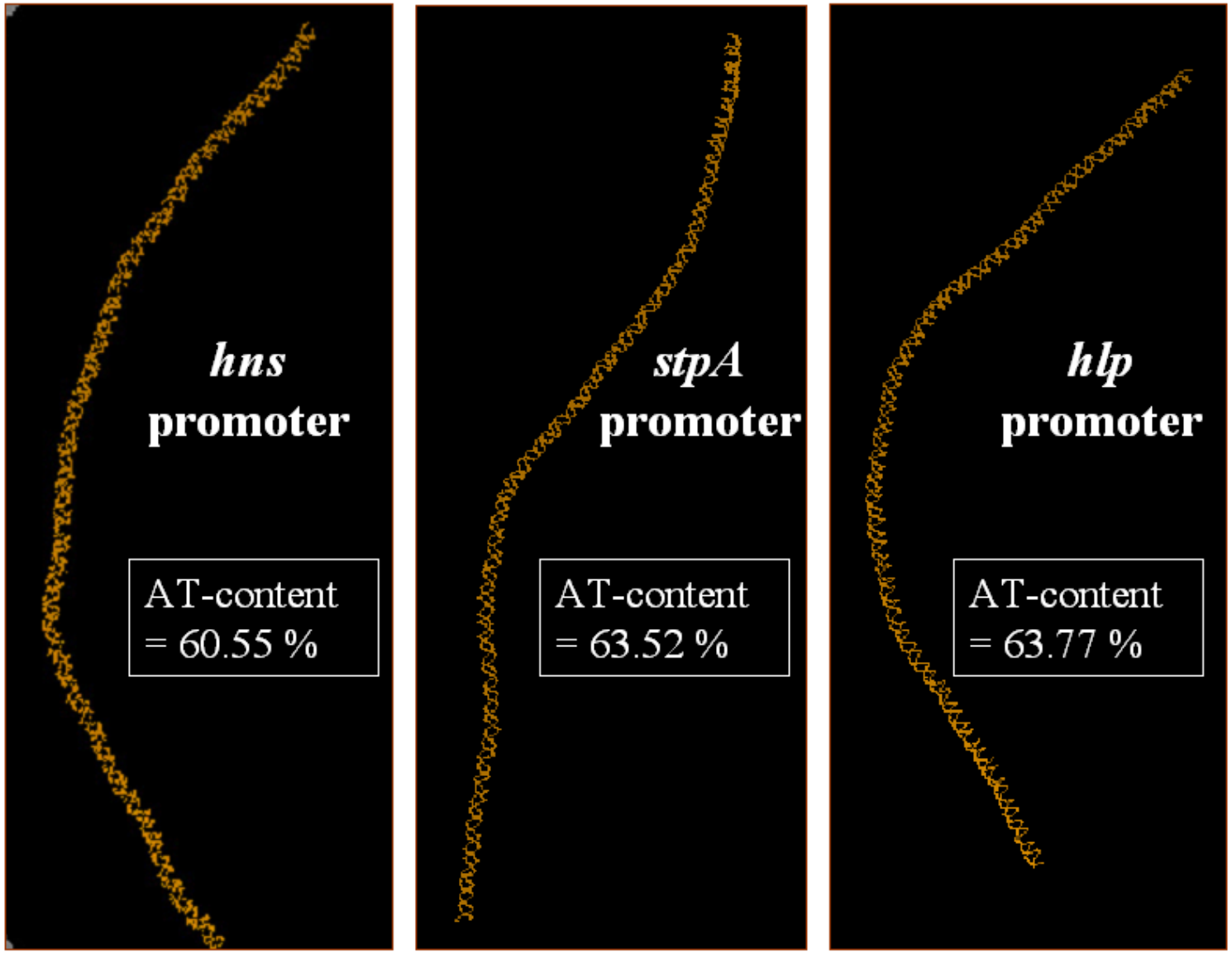

Fig. 52: Predicted curvature of promoter regions. 400-bp upstream of translation start codon were used for calculation of AT-content and curvature prediction (using the model.it software retrieved at http://hydra.icgeb.trieste.it/~kristian/dna/model_it.html)

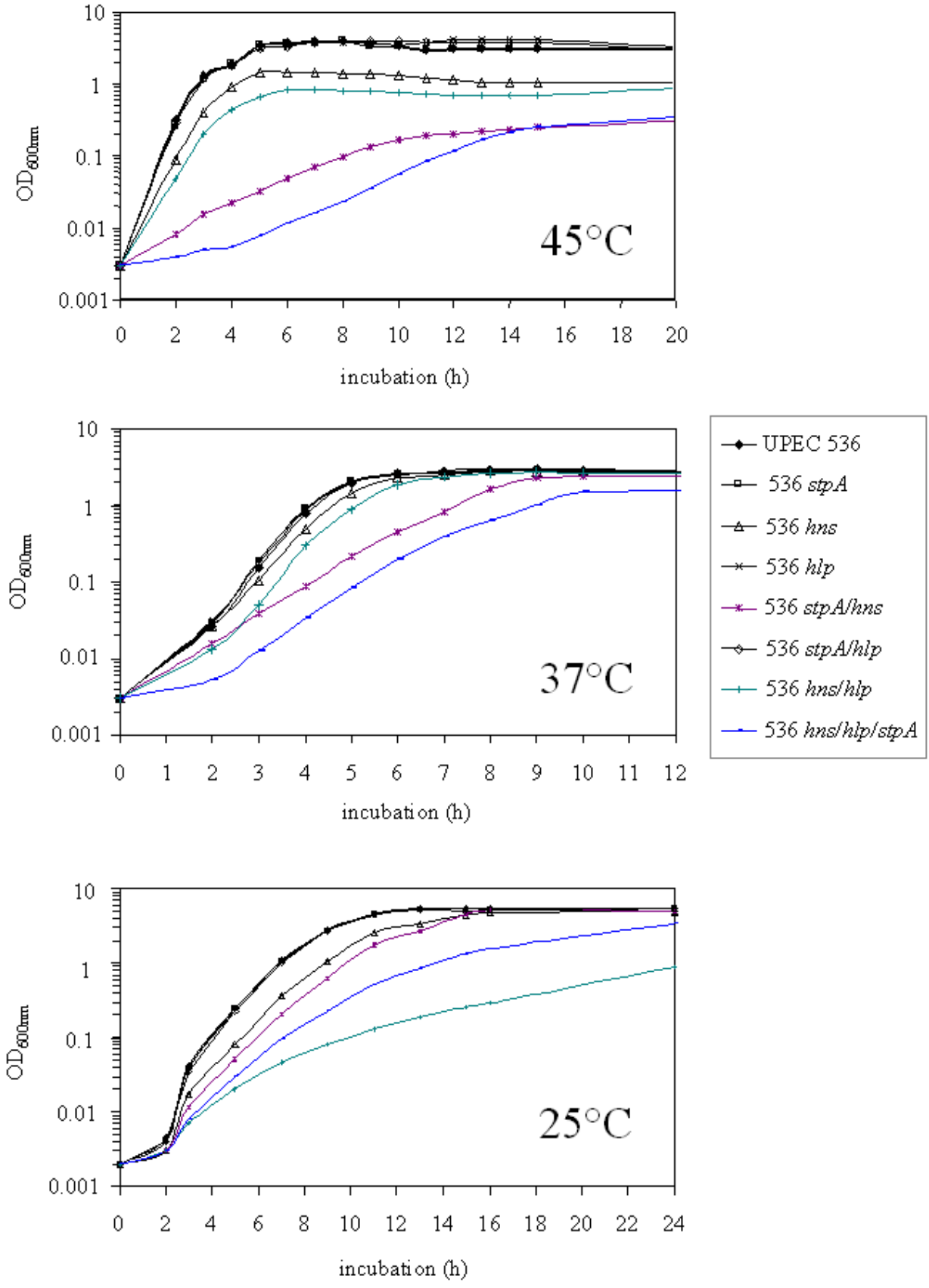

Fig. 53: Growth curves of UPEC strain 536 and isogenic mutants at different temperatures.

Three independent LB cultures of each strain were grown with aeration (200 rpm) at 45, 37, and 25 °C.

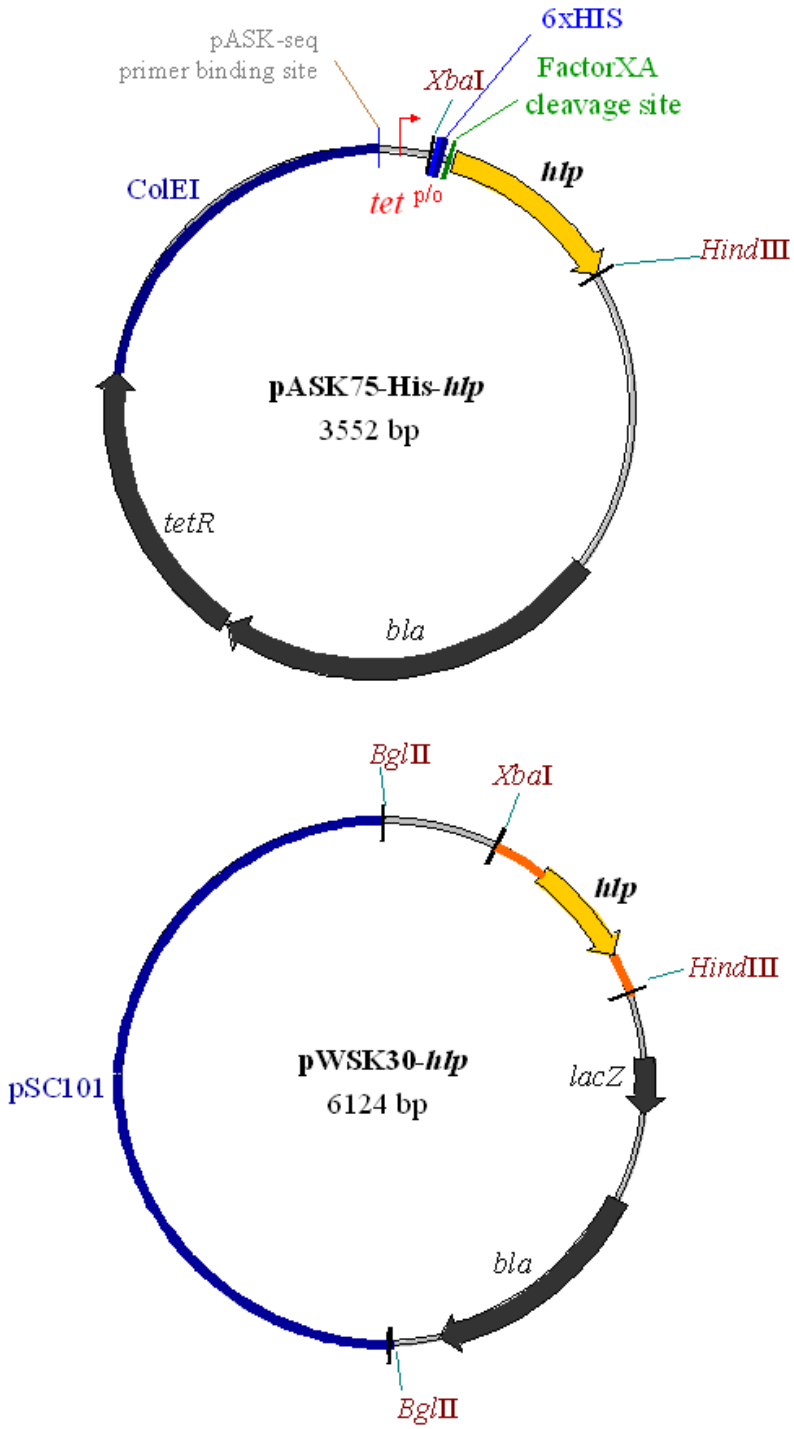

Fig. 54: Maps of plasmids constructed during this work.

Plasmid pASK75-His-*hlp* was constructed by cloning a PCR-generated fragment encoding a $(His)_6$ sequence followed by a factor X cleavage site and the CDS of the hlp_{536} gene into the *Xba*I/*Hind*III sites of the inducible expression vector pASK75.

Plasmid pWSK30-*hlp* was constructed by cloning a PCR-generated fragment containing the CDS ± 175-bp of the hlp_{536} gene into the *Xba*I/*Hind*III sites of the low copy number vector pWKS30.

8.6. Curriculum vitae

Persönliche Daten

Name	Claudia Maria Müller
Geburtsdatum	07.06.1979
Geburtsort	Sonthofen, Landkreis Oberallgäu

Studium und Ausbildung

1989-1998	Gymnasien Sonthofen (math. - nat.) und Oberstdorf (neusprachlich) Ablegung der Abiturprüfung am 26.06.98
1998-2001	Studium der Biologie (Diplom) an der Julius-Maximilians Universität Würzburg mit Hauptfach Mikrobiologie
2001-2002	Auslandsstudium an der Universität Umeå, Schweden, samt Anfertigung der Masterthesis am Institut für Molekularbiologie unter Anleitung der Arbeit durch Prof. Bernt Eric Uhlin und Dr. Carlos Balsalobre
Juni 2002	Erwerb des Abschlusses: “Magisterexamen med Molekylärbiologi som huvudämne” (Master of Science with a major in Molecular Biology) der Universität Umeå, Schweden
Seit Januar 2003	Anfertigung der Dissertation am Institut für Molekulare Infektionsbiologie der Universität Würzburg unter Anleitung der Arbeit durch Prof. Dr. Dr. h.c. J. Hacker und Dr. U. Dobrindt; Assoziertes Mitglied des Internationalen Graduiertenkollegs 587/2 und der Graduiertenschule – Klasse Biomedizin

Praktika

2002	Dreimonatiges Praktikum in der Abteilung für Forschung und Entwicklung des pharmazeutischen AG Orthogen in Düsseldorf

8.7. Publikationen

Publikationen

Müller, C.M., Dobrindt, U., Nagy,G., Emödy, L., Uhlin, B.E., and Hacker, J. (2005). Role of Histone-like Proteins H-NS and StpA in Expression of Virulence Determinants of uropathogenic *Escherichia coli*. *J. Bacteriol*. Submitted.

Müller, C.M., Dobrindt, U., Uhlin, B.E., and Hacker, J. (2005). Uropathogenic *Escherichia coli* strain 536 encodes three distinct histone-like proteins: Characterization of the H-NS homolog Hlp. In Preparation.

Präsentationen und Workshops

Müller, C.M., Dobrindt, U., and Hacker, J. (2003). Multiple effects of the nucleoid-associated protein H-NS on the expression of virulence factors in uropathogenic *E. coli* strain 536. Workshop "Molecular Microbial Pathogenesis" des Europäischen Graduiertenkollegs, Umeå (Sweden). Poster Präsentation

Müller, C.M., Dobrindt, U.,and Hacker, J. (2004). Regulation of pathogenicity-island encoded virulence traits in uropathogenic *Escherichia coli* strain 536: Role of two nucleoid-associated proteins H-NS and StpA. 56. Jahrestagung der Deutschen Gesellschaft für Hygiene und Mikrobiologie (DGHM), Münster. Poster Präsentation

Müller, C.M. (2005). Histone-like proteins affect expression of virulence-associated genes in uropathogenic *Escherichia coli*. Evaluierung des Internationalen Graduiertenkollegs durch die DFG, Würzburg. Vortrag

Müller, C.M., Dobrindt, U., Uhlin, B.E., and Hacker, J. (2005). Multiple effects of the nucleoid-associated protein H-NS on the expression of virulence factors in uropathogenic *E. coli* strain 536., Workshop "Molecular Microbial Pathogenesis" des Europäischen Graduiertenkollegs, Umeå (Sweden). Poster Präsentation

Müller, C.M. (2005) Characterization of a novel histone-like protein Hlp. 2. gemeinsame Jahrestagung der Deutschen Gesellschaft für Hygiene und Mikrobiologie (DGHM) und der Vereinigung für allgemeine und angewandte Mikrobiologie (VAAM), Göttingen. Vortrag

Würzburg, Dezember 2005

8.8. Abbreviations

µg = microgram
µl = microliter
µM = micromolar
µm = micrometer
A = adenine
a.a. = amino acid
ABU = asymptomatic bacteruria
AFM = atomic force microscope
Ap = Ampicillin
APS = ammonium persulfate
BLAST = Basic Local Alignment Search Tool
bp = base pairs
ß-ME = beta-mercaptoethanol
BSA = bovine serum albumin
C = cytosine
cAMP = cyclic adenosine monophosphate
CAS = chrome azurole S
cat = chloramphenicol acetyltransferase
CbpA/B = curved DNA-binding protein A/B
CDS = coding sequence
CFU = colony forming unit
Cm = chloramphenicol
cm = centimeter
CRP = cAMP receptor protein
dATP = desoxyadenosin-5'-triphosphate
DEPC = diethyl pyrocarbinate
DNA = desoxyribonucleic acid
DnaA = DNA-binding protein A
DNase = Desoxyribonuclease
Dps = DNA-binding protein of starved cells
DR = direct repeat
DRE = downstream regulatory element
EAEC = enteroaggregative *E. coli*
EDTA = Ethylendiamintertraacetat
EHEC = enterohemorrhagic *E. coli*
EIEC = enteroinvasive *E. coli*
EPEC = enteropathogenic *E. coli*
EPS = extracellulat polymeric substance
et al. = et altera (and others)
ETEC = enterotoxigenic *E. coli*
EtOH = ethanol
ExPEC = extraintestinal pathogenic *E. coli*
FDR = false discovery rate
Fig. = figure
Fis = factor for inversion stimulation
FPLC = Fast protein liquid chromatography
FRT = Flp recognition target
g = gram
G = guanine
GEI = genomic island
h = hour
HDTMA = hexadecyl-trimethyl-ammonium bromide
Hfq = host factor for phage $Q_ß$
Hlp = H-NS-like protein
H-NS = histone-like nucleoid structuring protein
HU = heat-unstable nucleoid protein
IciA = inhibitor of chromosome initiation A
i.e. = id est (this means)
IHF = integration host factor
IPEC = intestinal pathogenic *E. coli*
IRD = infrared fluorescence dye
IS = insertion sequence element
kb = kilo bases
kDa = kilo Dalton
Km = Kanamycin
l = liter
LB = lysogeny broth
Lrp = leucine-responsive regulatory protein
M = molar
mA = milliampere
mg = milligram
min = minute
ml = milliliter
mM = millimolar
mm = millimeter
MOPS =
NBM = newborn meningitis
ng = nanogramm
NMR = nuclear magnetic resonance
nt = nucleotides
OD = optical density
oligo = oligonucleotide
ONPG = o-Nitrophenyl-ß-galactopyranoside
ORF = open reading frame
PAI = pathogenicity island
PBS = Phosphate buffered saline
PCR = polymerase chain reaction
PIPES = 1,4-piperazine-diethane-sulfonic acid
RNA = ribonucleic acid
RNase = Ribonuclease
Rob = replication origin binding protein
rpm = rounds per minute
RT = reverse transcription
SD = standard deviation
SDS = sodium dodecyl sulfate
sec = second
Spec = Spectinomycin
SSC = standard saline citrate
StpA = suppressor of *td*$^-$ phenotype A
T = thymine
TAE = Tris-acetate-EDTA
TBS = Tris-buffered saline
TEMED = N,N,N`,N`-tetramethyldiamin
Tet = Tetracyclin
Tris = Trishydroxylmethylaminomethan
U = unit
UPEC = uropathogenic *Escherichia coli*
UTI = Urinary tract infection
V = Volt
wt = wild type